

**FUNGAL BIOTRANSFORMATION OF NOVEL
20(27)- OCTANOR CYCLOASTRAGENOL AND
BIOLOGICAL ACTIVITIES OF THE PURIFIED
METABOLITES**

**A Thesis Submitted to
The Graduate School of Engineering and Sciences of
İzmir Institute of Technology
in Partial Fulfilment of the Requirements for the Degree of**

**MASTER OF SCIENCE
in Biotechnology**

**by
Seda DUMAN**

July, 2019

İZMİR

We approve the thesis of **Seda DUMAN**

Examining Committee Members:

Prof. Dr. Erdal BEDİR

Department of Bioengineering, İzmir Institute of Technology

Prof. Dr. Ataç UZEL

Department of Biology, Ege University

Assist. Prof. Dr. Nur Başak SÜRMEİ

Department of Bioengineering, İzmir Institute of Technology

19 July 2019

Prof. Dr. Erdal BEDİR

Supervisor, Department of Bioengineering
İzmir Institute of Technology

Prof. Dr. Ali ÇAĞIR

Co-Supervisor, Department of Chemistry
İzmir Institute of Technology

Assoc. Prof. Dr. Engin ÖZÇİVİCİ

Head of the Department of Biotechnology

Prof. Dr. Aysun SOFUOĞLU

Dean of the Graduate School of
Engineering and Sciences

ACKNOWLEDGMENTS

I'm extremely grateful to Prof. Dr. Erdal BEDİR for his support and patience,

I want to thank to Sinem YILMAZ for biological activity studies; Salih GÜNNAZ and Hasan YUSUFOĞLU for assisting NMR studies,

I also want to thank all Bedir Group members,

I am grateful to Güner EKİZ and Özgür TAĞ for answering all my questions and sharing their knowledge,

I would like to thank to my friends and colleague, Dr. Özge ÖZÇINAR, Fadime AYDOĞAN, Eyüp BİLGİ, Özge GÜZEL for their encouragement, understanding and attitude throughout my study,

I would like to extend my sincere thanks to Çağlar ERSANLI, Seren ŞEN, Sibel DEĞER, Gürbüz DURSUN, Damla TAYKOZ and İrem PEHLİVANOĞLU, for their true friendships, being with me at good and bad time,

I must also thank, Ebru GÜZEL, Seden CİN, Neslihan DEMİR, Çiğdem KARAMAN, Oğuz AY, Bahadır AYAZ and Cem BAKKAL for valuable conversations, great times which made our friendships stronger, their support and motivation,

My special and deepest thanks are for my family; Necip DUMAN, Şükran DUMAN, Şahin DUMAN and Gizem DUMAN. They have supported me steadily and patiently during all my life.

This study was supported by the TUBITAK project “114Z958”, BAP Project “2017IYTE72” and Bionorm.

İzmir, July 2019

Seda DUMAN

ABSTRACT

FUNGAL BIOTRANSFORMATION OF NOVEL 20(27)- OCTANOR CYCLOASTRAGENOL AND BIOLOGICAL ACTIVITIES OF THE PURIFIED METABOLITES

Biotransformation is the chemical modifications performed by enzymes or living organisms. The difficulty and high cost of enzyme isolation and purification makes it more advantageous to use whole cell systems as biocatalysts. Microbial biocatalysts are particularly interesting in the modification of complex molecules such as steroids and triterpenoids, which can catalyze stereo- and regio- selective reactions that are difficult or impossible to perform with chemical reactions. Specially, ability of endophytic microorganisms to produce specific enzymes for adaptation to their environment by tolerating toxic defense metabolites, makes them interesting for biotransformation studies.

Telomeres are nucleotide structures located at the end of chromatids shortening with each cell division. Telomerase is a reverse transcriptase enzyme, and it helps to replenish telomere ends that are truncated by aging and stress factors. The telomerase activators (TA) with their potentials are suggested encouraging agents for healthy aging, and they are projected to generate a huge market in the future. Cycloastragenol is the only natural product in the sector marketed as a potent telomerase activator.

In this study, by using endophytic fungi, the biotransformation studies were performed on 20(27)-octanor cycloastragenol. As a result, 14 biotransformation products, were isolated by chromatographic studies, and the structures of the metabolites were established by spectral methods. Based on the literature survey, 13 compounds turned out to be new for nature. Seven metabolites were screened for telomerase activation. In these screenings, metabolites showed telomerase activation ranging from 5.43 to 12.36 fold at doses ranging from 0.1 to 30 nM compared to the control cells treated with DMSO.

ÖZET

ÖZGÜN 20(27)-OKTANOR SİKLOASTRAGENOL'ÜN FUNGAL BİYOTRANSFORMASYONU VE SAFLAŞTIRILMIŞ METABOLİTLERİNİN BİYOLOJİK AKTİVİTELERİ

Biyotransformasyon, enzimler ya da canlı organizmalar kullanılarak meydana getirilen kimyasal modifikasyonlardır. Enzimlerin izolasyonu ve saflaştırılmasının zor ve yüksek maliyetli olması, bütün hücre sistemlerinin biyokatalizör olarak kullanımını daha avantajlı kılmaktadır. Mikrobiyal biyokatalistler; steroidler ve triterpenoitler gibi kompleks moleküllerin modifikasyonunda, kimyasal reaksiyonlarla gerçekleştirilmesi zor ya da mümkün olmayan stereoselektif ve regioselektif reaksiyonlar katalizleyebilmeleriyle oldukça ilgi çekicidirler. Özellikle bitkinin toksik savunma metabolitlerini tolere ederek, yaşadıkları çevreye adaptasyon için spesifik enzimler üretebilme yetenekleri endofitik mikroorganizmaları biyotransformasyon çalışmaları için ilgi çekici kılmaktadır.

Telomerler, kromozomlarımızın sonunda bulunan ve hücre bölünmesiyle kısalan nükleotit yapılarıdır. Telomeraz ise, yaşa ve strese bağlı olarak kısalan telomer uçlarını onarmaya yardım eden revers transkriptaz bir enzimdir. Telomeraz enzimi aktivatörleri (TA) barındırdıkları potansiyel ile sağlıklı yaşlanma için ümit verici ajanlar olarak gösterilmektedir ve ileride büyük bir pazar oluşturacağı öngörülmektedir.

Bu çalışmada anti-aging etkilerinden dolayı son dönemde önemli hale gelmiş ve sadece *Astragalus* türlerinde bulunan sikloastragenol (CA) molekülünün türevlerinden biri olan 20(27)-oktanor sikloastragenol (SCG) üzerinde, *Astragalus* bitkisinden izole edilen endofitik funguslar kullanılarak biyotransformasyon çalışmaları gerçekleştirilmiş ve elde edilen yeni metabolitlerin biyolojik aktiviteleri taranmıştır. Sonuç olarak, kromatografik çalışmalar ile 14 biyotransformasyon ürünü izole edilmiş ve metabolitlerin yapıları spektral yöntemler kullanılarak belirlenmiştir. Literatür araştırması sonucunda, 13 bileşiğin doğa için yeni olduğu anlaşılmıştır. Endofitlerin enzim sistemleri; oksidasyon (çoğunlukla hidroksilasyon), halka açılması (metil göçü ve halka genişlemesi veren) ve dehidrojenasyon reaksiyonlarını katalizlemiştir. Biyotransformasyon ürünlerinin 7'si telomeraz enziminin aktivasyonuna yönelik taranmıştır. Bu taramalarda DMSO ile muamele edilen kontrol hücrelerine kıyasla metabolitler 0.1-30 nM doz aralığında 5.43 ile 12.36 kat arasında değişen telomeraz aktivasyonu göstermişlerdir.

to my nephew Necip Deniz DUMAN

TABLE OF CONTENTS

LIST OF FIGURES	x
LIST OF TABLES.....	xii
LIST OF SPECTRA	xiii
ABBREVIATIONS	xvi
CHAPTER 1. INTRODUCTION.....	1
1.1 Saponins	1
1.1.1 <i>Astragalus</i> species and cycloartanes	5
1.2 Telomere and Telomerase	6
1.3 Endophytic Fungi.....	9
1.4 Biotransformation	10
1.4.1 Enzymatic biotransformation.....	11
1.4.2 Whole cell microbial biotransformation.....	14
1.5 Microbial transformation of saponins	17
CHAPTER 2. MATERIALS AND METHODS	20
2.1 Materials.....	20
2.1.1 Endophytic Fungi.....	20
2.1.2 Substrate	21
2.1.3 Media.....	22
2.1.3.1 Medium 1: Potato Dextrose Agar (PDA)	22
2.1.3.2 Medium 2: Biotransformation Medium.....	22
2.1.3.3 Medium 3: Potato Dextrose Broth	22
2.1.3.4 Medium 4: Media components for growing of HEKN.....	23
2.1.4.2 Chemicals and Adsorbents used in extraction	24
2.1.5 Instruments	24
2.2 Methods.....	25

2.2.1 Biotransformation studies.....	25
2.2.1.1 Analytical Scale.....	25
2.1.2 Preparative Scale.....	25
2.2.2 Post-Biotransformation Procedures	26
2.2.2.1 Extraction, Isolation and Purification Studies.....	28
2.2.3 Bioactivity Screening Studies.....	37
CHAPTER 3. RESULTS AND DISCUSSION	40
3.1 Results of Biotransformation Studies	40
3.2.1 Pure Compounds Isolated from Biotransformation by <i>Alternaria eureka</i>	41
3.2.1.1 Structure Elucidation of A-SCG-01	41
3.2.1.2 Structure Elucidation of A-SCG-03	50
3.2.1.3 Structure Elucidation of A-SCG-06	58
3.2.1.4 Structure Elucidation of A-SCG-07	65
3.2.1.5 Structure Elucidation of A2-SCG-01	73
3.2.1.6 Structure Elucidation of A2-SCG-02	82
3.2.1.7 Structure Elucidation of A2-SCG-03	91
3.2.2 Pure Compounds Isolated from Biotransformation by <i>Camarosporium laburnicola</i>	94
3.2.2.1 Structure Elucidation of E-SCG-01.....	94
3.2.2.2 Structure Elucidation of E-SCG-02.....	101
3.2.3 Pure Compounds Isolated from Biotransformation by <i>Neosartorya hiratsukae</i>	108
3.2.3.1 Structure Elucidation of Neo-SCG-01.....	108
3.2.3.2 Structure Elucidation of Neo-SCG-02.....	116
3.2.3.3 Structure Elucidation of Neo-SCG-03.....	124
3.2.3.4 Structure Elucidation of Neo-SCG-04.....	131
3.2.3.5 Structure Elucidation of Neo-SCG-06.....	140

3.3 Biological Activity Studies	150
3.3.1 Telomerase Activation Screening	150
CHAPTER 4. CONCLUSION	153
REFERENCES	159

LIST OF FIGURES

<u>Figure</u>	<u>Page</u>
Figure 1.1 Structures of the major saponin aglycones	2
Figure 1.2 Mevalonate pathway	3
Figure 1.3 Biosynthesis of squalene	3
Figure 1.4 Formation of cycloartenol skeleton	4
Figure 1.5 Biosynthesis of main saponin skeletons	4
Figure 1.6 Chemical structures of astragalosides II and IV	6
Figure 2.1 Endophytic organisms for biotransformation studies	21
Figure 2.2 Structure of 20(27)- octanor cycloastragenol	21
Figure 2.3 Analytical scale biotransformation studies	26
Figure 2.4 Post-biotransformation processes	27
Figure 2.5 TLC chromatograms of the EtOAc extract obtained from preparative scale biotransformation study of <i>Alternaria eureka</i> biotransformation extracts	28
Figure 2.6 The TLC profile of EtOAc extract obtained after preparative scale biotransformation study of <i>Camarosporium laburnicola</i>	30
Figure 2.7 The TLC profile of EtOAc extract obtained after preparative scale biotransformation study of <i>Neosartorya hiratsukae</i>	31
Figure 2.8 Isolation scheme of <i>Alternaria eureka</i> EtOAc extract (BM)	32
Figure 2.9 Isolation scheme of <i>Alternaria eureka</i> EtOAc extract (PDB)	33
Figure 2.10 Isolation scheme of <i>Camarosporium laburnicola</i> EtOAc extract	34
Figure 2.11 Isolation scheme of <i>Neosartorya hiratsukae</i> EtOAc extract (Part 1)	35
Figure 2.12 Isolation scheme of <i>Neosartorya hiratsukae</i> EtOAc extract (Part 2)	36
Figure 2.13 TELOTAGGG Telomerase PCR ELISA ^{PLUS} kit steps	39
Figure 3.1 The metabolite profiles of screening biotransformation studies	40
Figure 3.2 Chemical structure of A-SCG-01	41
Figure 3.3 Chemical structure of A-SCG-03	50
Figure 3.4 Chemical structure of A-SCG-06	58
Figure 3.5 Chemical structure of A-SCG-07	65
Figure 3.6 Chemical structure of A2-SCG-01	73
Figure 3.7 Chemical structure of A2-SCG-02	82

<u>Figure</u>	<u>Page</u>
Figure 3.8 Chemical structure of A2-SCG-03	91
Figure 3.9 Chemical structure of E-SCG-01	94
Figure 3.10 Chemical structure of E-SCG-02	101
Figure 3.11 Chemical structure of Neo-SCG-01	108
Figure 3.12 Chemical structure of Neo-SCG-02	116
Figure 3.13 Chemical structure of Neo-SCG-03	124
Figure 3.14 Chemical structure of Neo-SCG-04	131
Figure 3.15 Chemical structure of Neo-SCG-06	140
Figure 3.16 Effects of E-SCG-01 and E-SCG-02 molecules on telomerase enzyme activity in HEKN cells.....	151
Figure 3.17 Effects of A-SCG-01, Neo-SCG-02, A2-SCG-02, Neo-SCG-03 and CA (CG) molecules on telomerase enzyme activity in HEKN cells.	151
Figure 3.18 Effects of Neo-SCG-01 and CA (CG) molecules on telomerase enzyme activity in HEKN cells.....	151
Figure 4.1 Metabolites derived from biotransformation of 20(27)-octanor cycloastragenol by <i>Alternaria eureka</i> (Biotransformation media)	154
Figure 4.2 Metabolites derived from biotransformation of 20(27)-octanor cycloastragenol by <i>Alternaria eureka</i> (Potato Dextrose Broth)	154
Figure 4.3 Metabolites derived from biotransformation of 20(27)-octanor cycloastragenol by <i>Neosartorya hiratsukae</i>	155
Figure 4.4 Metabolites derived from biotransformation of 20(27)-octanor cycloastragenol by <i>Camarosporium laburnicola</i>	156
Figure 4.5 The proposed biochemical reaction chain for modifications occurring in the A ring	156
Figure 4.6 Chemical structures and active dosages of bioactive biotransformation products.	158

LIST OF TABLES

<u>Table</u>	<u>Page</u>
Table 1.1 Enzyme classification	11
Table 1.2 Hydrolases actively used in the preparation of biologically active compounds.....	12
Table 1.3 Oxidative reactions catalyzed by whole cells in the preparation of biologically active compounds at industrial scale	16
Table 2.1 Phylogenetic analysis results of isolates based on ITS rDNA sequences	20
Table 2.2 Contents of the biotransformation medium.....	22
Table 2.3 Media components for Hekn Cells	23
Table 2.4 PCR program.....	38
Table 3.1 ¹ H and ¹³ C NMR data of A-SCG-01 (125/500 MHz, C ₅ D ₅ N)	42
Table 3.2 ¹ H and ¹³ C NMR data of A-SCG-03 (125/500 MHz, C ₅ D ₅ N)	51
Table 3.3 ¹ H and ¹³ C NMR data of A-SCG-06 (125/500 MHz, C ₅ D ₅ N)	59
Table 3.4 ¹ H and ¹³ C NMR data of A-SCG-07 (125/500 MHz, C ₅ D ₅ N).	66
Table 3.5 ¹ H and ¹³ C NMR data of A2-SCG-01(125/500 MHz, C ₅ D ₅ N)	74
Table 3.6 ¹ H and ¹³ C NMR data of A2-SCG-02 (125/500 MHz, C ₅ D ₅ N)	83
Table 3.7 ¹ H and ¹³ C NMR data of A2-SCG-03 (125/500 MHz, C ₅ D ₅ N)	91
Table 3.8 ¹³ C- ve ¹ H-NMR data of E-SCG-01 (100/400 MHz, C ₅ D ₅ N).....	95
Table 3.9 ¹³ C- ve ¹ H-NMR data of E-SCG-02 (100/400 MHz, C ₅ D ₅ N).....	102
Table 3.10 ¹³ C- ve ¹ H-NMR data of Neo-SCG-01 (125/500 MHz, C ₅ D ₅ N).....	109
Table 3.11 ¹³ C- ve ¹ H-NMR data of Neo-SCG-02 (125/500 MHz, C ₅ D ₅ N).....	117
Table 3.12 ¹ H and ¹³ C NMR data of Neo-SCG-03 (125/500 MHz, C ₅ D ₅ N).....	125
Table 3.13 ¹ H and ¹³ C NMR data of Neo-SCG-04 (125/500 MHz, C ₅ D ₅ N).....	132
Table 3.14 ¹ H and ¹³ C NMR data of Neo-SCG-06 (125/500 MHz, C ₅ D ₅ N).....	141
Table 3.15 Telomerase enzyme activation of selected compounds	152

LIST OF SPECTRA

<u>Spectrum</u>	<u>Page</u>
Spectrum 3.1 ^1H -NMR Spectrum of A-SCG-01	43
Spectrum 3.2 ^{13}C -NMR Spectrum of A-SCG-01	44
Spectrum 3.3 DEPT spectrum of A-SCG-01	45
Spectrum 3.4 HSQC spectrum of A-SCG-01	46
Spectrum 3.5 HMBC spectrum of A-SCG-01	47
Spectrum 3.6 COSY spectrum of A-SCG-01	48
Spectrum 3.7 ROESY spectrum of A-SCG-01	49
Spectrum 3.8 HR-ESI-MS spectrum of A-SCG-03 (negative mode)	52
Spectrum 3.9 ^1H -NMR Spectrum of A-SCG-03	53
Spectrum 3.10 HSQC spectrum of A-SCG-03	54
Spectrum 3.11 HMBC spectrum of A-SCG-03	55
Spectrum 3.12 COSY spectrum of A-SCG-03	56
Spectrum 3.13 ROESY spectrum of A-SCG-03	57
Spectrum 3.14 HR-ESI-MS spectrum of A-SCG-06 (negative mode)	59
Spectrum 3.15 ^1H -NMR Spectrum of A-SCG-06	60
Spectrum 3.16 HSQC spectrum of A-SCG-06	61
Spectrum 3.17 HMBC spectrum of A-SCG-06	62
Spectrum 3.18 COSY spectrum of A-SCG-06	63
Spectrum 3.19 ROESY spectrum of A-SCG-06	64
Spectrum 3.20 HR-ESI-MS spectrum of A-SCG-07 (negative mode)	66
Spectrum 3.21 ^1H -NMR Spectrum of A-SCG-07	67
Spectrum 3.22 ^{13}C -NMR Spectrum of A-SCG-07	68
Spectrum 3.23 HSQC spectrum of A-SCG-07	69
Spectrum 3.24 HMBC spectrum of A-SCG-07	70
Spectrum 3.25 COSY spectrum of A-SCG-07	71
Spectrum 3.26 ROESY spectrum of A-SCG-07	72
Spectrum 3.27 HR-ESI-MS spectrum of A2-SCG-01 (positive mode)	74
Spectrum 3.28 ^1H -NMR Spectrum of A2-SCG-01	75
Spectrum 3.29 ^{13}C -NMR Spectrum of A2-SCG-01	76
Spectrum 3.30 DEPT spectrum of A2-SCG-01	77

<u>Spectrum</u>	<u>Page</u>
Spectrum 3.31 HSQC spectrum of A2-SCG-01	78
Spectrum 3.32 HMBC spectrum of A2-SCG-01	79
Spectrum 3.33 COSY spectrum of A2-SCG-01	80
Spectrum 3.34 ROESY spectrum of A2-SCG-01	81
Spectrum 3.35 ¹ H-NMR Spectrum of A2-SCG-02.....	84
Spectrum 3.36 ¹³ C-NMR Spectrum of A2-SCG-02.....	85
Spectrum 3.37 DEPT spectrum of A2-SCG-02.....	86
Spectrum 3.38 HSQC spectrum of A2-SCG-02	87
Spectrum 3.39 HMBC spectrum of A2-SCG-02	88
Spectrum 3.40 COSY spectrum of A2-SCG-02	89
Spectrum 3.41 ROESY spectrum of A2-SCG-02	90
Spectrum 3.42 HR-ESI-MS spectrum of A2-SCG-02 (positive mode)	83
Spectrum 3.43 ¹ H-NMR Spectrum of A2-SCG-03.....	92
Spectrum 3.44 ¹³ C-NMR Spectrum of A2-SCG-03.....	93
Spectrum 3.45 HR-ESI-MS spectrum of E-SCG-01 (positive mode)	95
Spectrum 3.46 ¹ H-NMR Spectrum of E-SCG-01	96
Spectrum 3.47 ¹³ C-NMR Spectrum of E-SCG-01	97
Spectrum 3.48 HSQC spectrum of E-SCG-01.....	98
Spectrum 3.49 HMBC spectrum of E-SCG-01.....	99
Spectrum 3.50 COSY spectrum E-SCG-01	100
Spectrum 3.51 ¹ H-NMR Spectrum of E-SCG-02	103
Spectrum 3.52 ¹³ C-NMR Spectrum of E-SCG-02.....	104
Spectrum 3.53 HSQC spectrum of E-SCG-02.....	105
Spectrum 3.54 HMBC spectrum of E-SCG-02.....	106
Spectrum 3.55 COSY spectrum of E-SCG-02.....	107
Spectrum 3.56 ¹ H-NMR Spectrum of Neo-SCG-01	110
Spectrum 3.57 ¹³ C-NMR Spectrum of Neo-SCG-01	111
Spectrum 3.58 HSQC spectrum of Neo-SCG-01.....	112
Spectrum 3.59 HMBC spectrum of Neo-SCG-01	113
Spectrum 3.60 COSY spectrum of Neo-SCG-01.....	114
Spectrum 3.61 NOESY spectrum of Neo-SCG-01	115
Spectrum 3.62 HR-ESI-MS spectrum of Neo-SCG-02 (positive mode)	117
Spectrum 3.63 ¹ H-NMR Spectrum of Neo-SCG-02	118

<u>Spectrum</u>	<u>Page</u>
Spectrum 3.64 ¹³ C-NMR Spectrum of Neo-SCG-02	119
Spectrum 3.65 DEPT spectrum of Neo-SCG-02	120
Spectrum 3.66 HSQC spectrum of Neo-SCG-02.....	121
Spectrum 3.67 HMBC spectrum of Neo-SCG-02	122
Spectrum 3.68 COSY spectrum of Neo-SCG-02.....	123
Spectrum 3.69 HR-ESI-MS spectrum of Neo-SCG-03 (positive mode)	125
Spectrum 3.70 ¹ H-NMR Spectrum of Neo-SCG-03	126
Spectrum 3.71 ¹³ C-NMR Spectrum of Neo-SCG-03	127
Spectrum 3.72 HSQC spectrum of Neo-SCG-03.....	128
Spectrum 3.73 HMBC spectrum of Neo-SCG-03	129
Spectrum 3.74 COSY spectrum of Neo-SCG-03.....	130
Spectrum 3.75 HR-ESI-MS spectrum of Neo-SCG-04 (positive mode)	132
Spectrum 3.76 ¹ H-NMR Spectrum of Neo-SCG-04	133
Spectrum 3.77 ¹³ C-NMR Spectrum of Neo-SCG-04	134
Spectrum 3.78 DEPT spectrum of Neo-SCG-04	135
Spectrum 3.79 HSQC spectrum of Neo-SCG-04.....	136
Spectrum 3.80 HMBC spectrum of Neo-SCG-04	137
Spectrum 3.81 COSY spectrum of Neo-SCG-04.....	138
Spectrum 3.82 NOESY spectrum of Neo-SCG-04.....	139
Spectrum 3.83 HR-ESI-MS spectrum of Neo-SCG-06 (positive mode)	141
Spectrum 3.84 ¹ H-NMR Spectrum of Neo-SCG-06	142
Spectrum 3.85 ¹³ C-NMR Spectrum of Neo-SCG-06.....	143
Spectrum 3.86 DEPT spectrum of Neo-SCG-06	144
Spectrum 3.87 HSQC spectrum of Neo-SCG-06.....	145
Spectrum 3.88 HMBC spectrum of Neo-SCG-06	146
Spectrum 3.89 COSY spectrum of Neo-SCG-06.....	147
Spectrum 3.90 ¹ H-NMR spectrum of 20(27)-octanor cycloastragenol.....	148
Spectrum 3.91 ¹³ C-NMR spectrum of 20(27)-octanor cycloastragenol.....	149

ABBREVIATIONS

CHCl ₃	Chloroform
K ₂ HPO ₄	di-Potassium hydrogen phosphate
DMSO	Dimethyl sulfoxide
EtOAc	Ethyl acetate
MeOH	Methanol
Hex	n-Hexane
CH ₂ Cl ₂	Dichloromethane
H ₂ SO ₄	Sulfuric Acid
FA	Formic Acid
H ₂ O	Water
CDCl ₃	Deuterated chloroform
CD ₃ OD	Deuterated methanol
PDB	Potato Dextrose Broth
BM	Biotransformation Media
UV	Ultraviolet
CC	Column Chromatography
TLC	Thin Layer Chromatography
HPLC	High Performance Liquid Chromatography
VLC	Vacuum Liquid Chromatography
NMR	Nuclear Magnetic Resonance
1D-NMR	One-Dimensional Nuclear Magnetic Resonance
2D-NMR	Two-Dimensional Nuclear Magnetic Resonance
¹ H-NMR	Proton Nuclear Magnetic Resonance
¹³ C-NMR	Carbon Nuclear Magnetic Resonance
HSQC	Heteronuclear Single Quantum Coherence
HMBC	Heteronuclear Multiple Bond Coherence
COSY	Correlation Spectroscopy
NOESY	Nuclear Overhauser Enhancement Spectroscopy
ROESY	Nuclear Overhauser Enhancement in a Rotating Frame
<i>m</i>	Multiplet
<i>s</i>	Singlet

<i>d</i>	Doublet
<i>bs</i>	Broad singlet
<i>t</i>	Triplet
<i>dd</i>	doublet-doublet
HRTOFMS	High-Resolution Time of Flight Mass Spectrometry

CHAPTER 1

INTRODUCTION

1.1. Saponins

Saponins are secondary metabolites including one or more sugar residue(s) linked to a higher molecular weight aglycone. The aglycone part might be triterpenic with 30 carbon atoms or steroidal with 27 carbons in its backbone. They are widely distributed in higher plants, and can also be present in animal sources such as marine invertebrates.^{1, 2}

The biological roles of saponins are not fully elucidated. They are thought to be part of the defense system of plants due to their biological activities such as antimicrobial, fungicidal, allelopathic, insecticidal and molluscicidal.³ Saponin-rich plants (*Ginseng*, *Astragalus*, *Tribulus*, *Centella*, etc.) have been used in traditional folk medicine for several diseases since ancient times. Nowadays, many of them are marketed as dietary supplements and immune system boosters due to their tonic and adaptogenic effects. Additionally, saponins have a wide variety of pharmacological activities such as expectorant, anti-inflammatory, vasoprotective, hypocholesterolemic, immunomodulator, hypoglycemic, molluscicide, antifungal, antiparasitic, antimutagenic, antiviral, anti-HIV and analgesic.⁷ Saponins can also be used as adjuvants in vaccine formulations.⁴ Below three major groups of saponin aglycones are shown in Figure 1.1.⁵

Saponins are biosynthetically derived from isoprene units (C₅) combined in a head-to-tail fashion. However, the isoprene units are mainly synthesized from the mevalonate pathway (Figure 1.2), whereas they can also be derived from methylerythritol-phosphate (MEP) path. Figure 1.3 illustrates that; three isoprene units join to yield C₁₅ farnesyl pyrophosphate (FPP), and two FPP residues, in turn, couple with each other tail-to-tail linkage to form the squalene skeleton (C₃₀). Cyclization reactions commence with the oxidation of squalene to afford (3S) 2,3-oxidosqualene.^{6, 7}

As seen in Figure 1.4, cyclization requires a carbocation and π -electrons of a double bond nearby. This carbocation formation originates from the epoxide ring of (3S) 2,3-oxidosqualene. After protonation of the epoxide, a hydroxylation and/or methyl migration takes place subsequently. In the last stage, the intermediate is neutralized by proton elimination via generation of a double bond, a cyclopropane ring and/or a hydroxyl

group. This cyclization process occurs on the surface of enzymes such as cyclases (cycloartenol synthase, lanosterol synthase, β -amyrin synthase). The cyclization from 2,3-oxidosqualene to saponins can take place in two ways as chair-chair-chair or chair-boat-chair conformation leading to different conformational arrangements in the structure.⁵⁻⁷

Especially in plants, cycloartenol, in which a cyclopropane ring formed by carbon inclusion from the methyl at C10 exist, is one of the key precursors involved in the synthesis of saponins (Figure 1.5).⁶

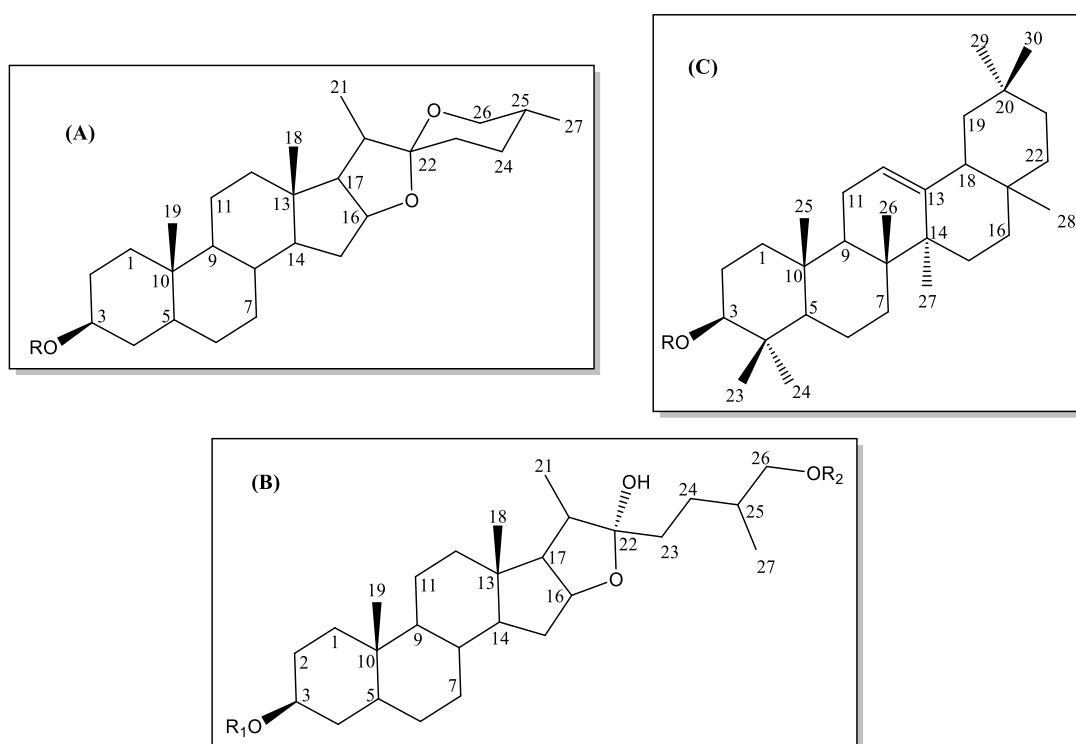


Figure 1.1 Structures of the major saponin aglycones; (A): Steroidal spirostanol (B): Steroidal furostanol, (C): Triterpenic (Olenane Skeleton), R: Sugar units.

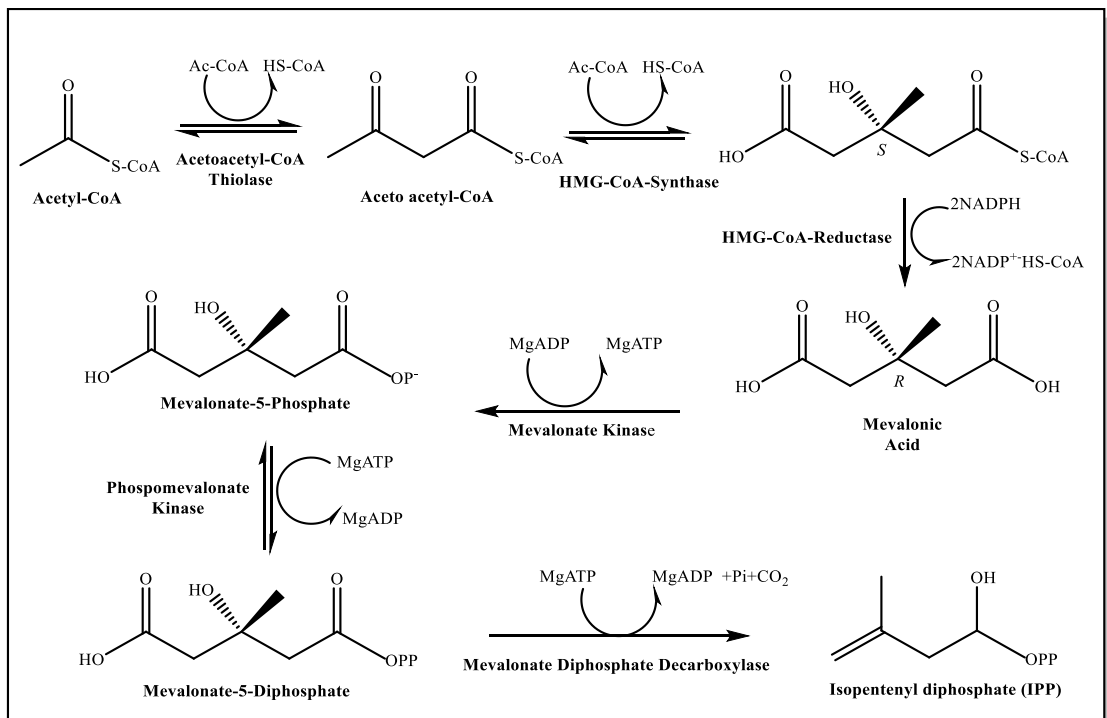


Figure 1.2 Mevalonate pathway

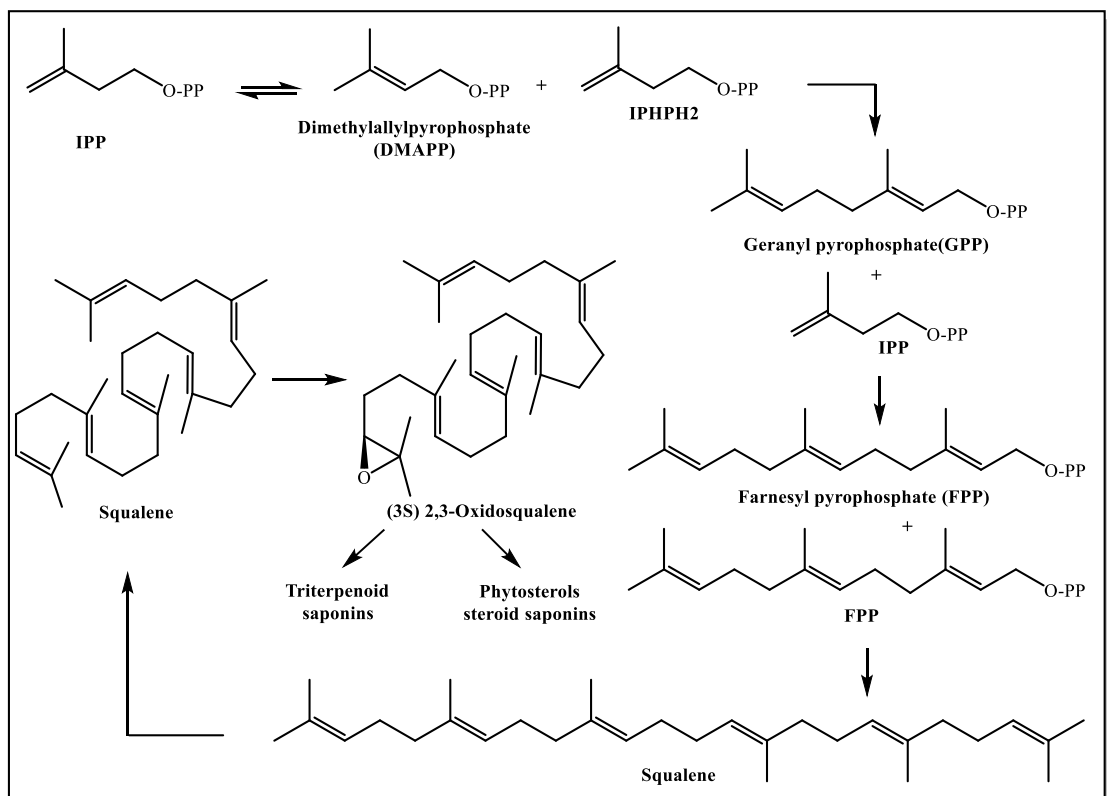


Figure 1.3 Biosynthesis of squalene

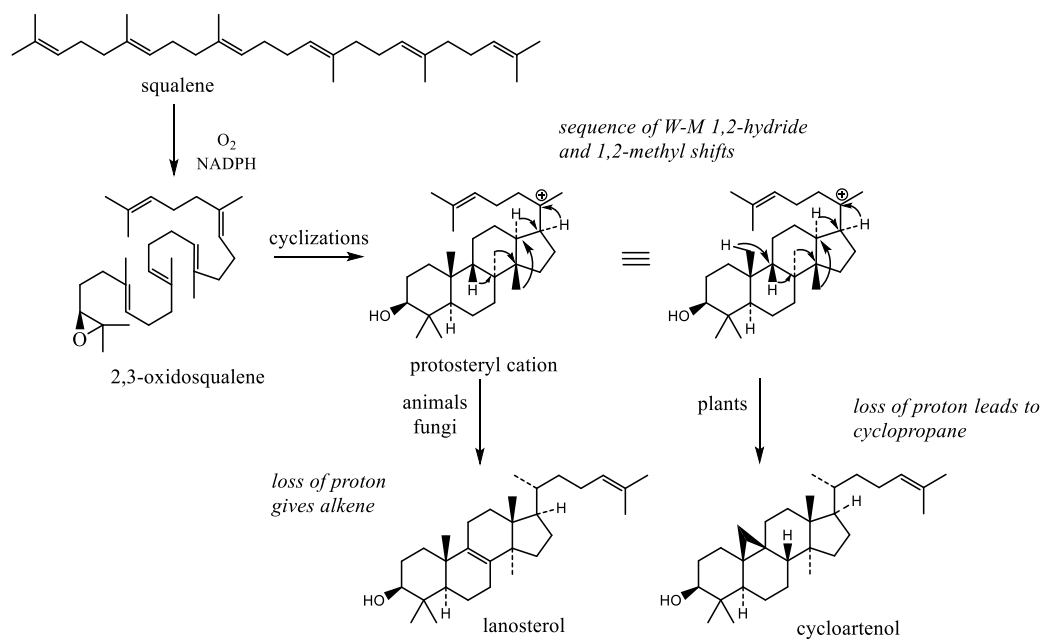


Figure 1.4 Formation of cycloartenol skeleton

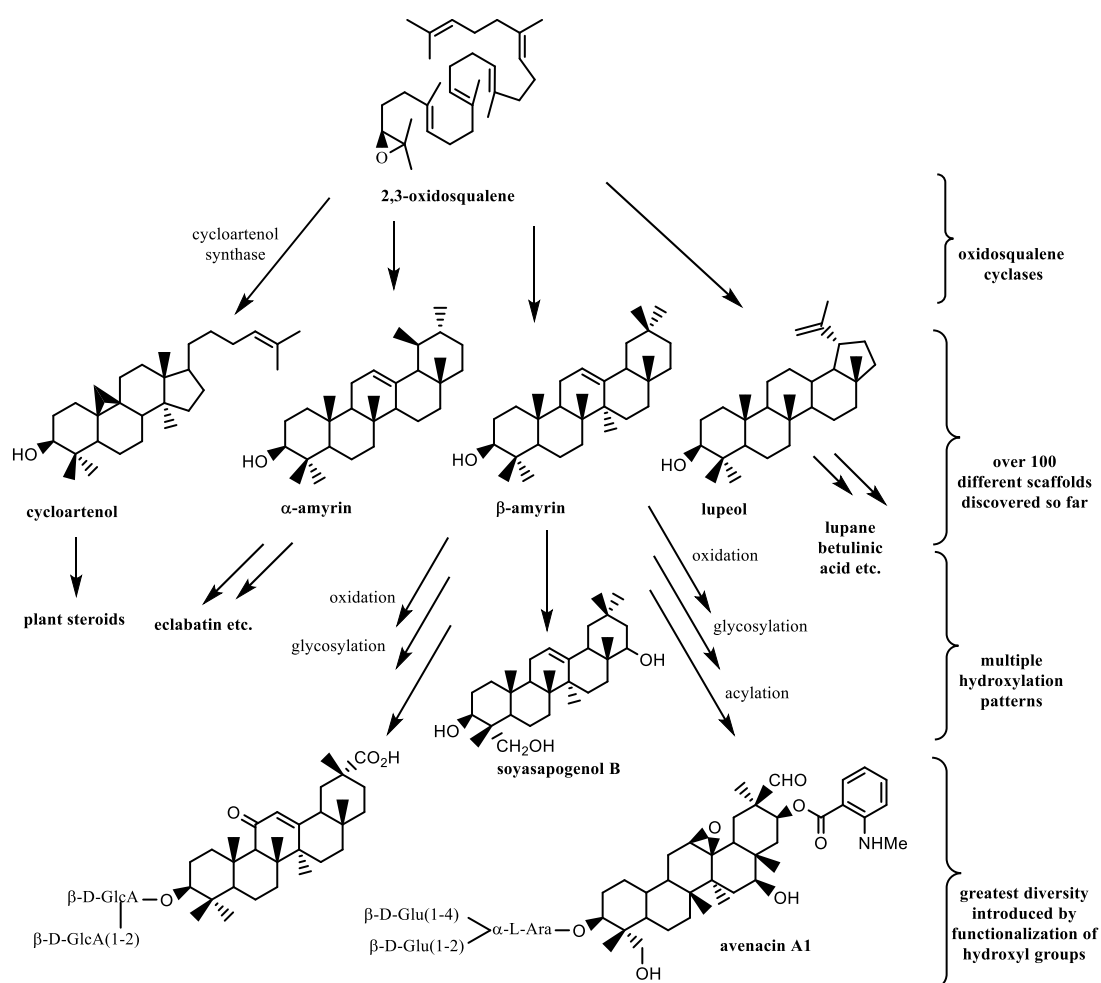


Figure 1.5 Biosynthesis of main saponin skeletons

1.1.1. *Astragalus* species and cycloartanes

Astragalus genus is a member of Fabaceae (Leguminosae)⁸ family represented by about 2398 species and 136 sections around the world. The genus has 63 sections and 457 taxa in Turkey and the endemism rate is about 51%. In 2013, Podlech et al. showed that *Astragalus* genus has 58 sections and 425 species in Turkey.⁹

Astragalus taxa consist variety of species being traditionally used to strengthen the immune system, and to treat health problems such as wounds, anemia, fever, viral infections, multiple allergies, chronic fatigue, loss of appetite, uterine bleeding and uterine prolapse in different countries.^{10, 11}

In recent years, many scientific studies on the pharmacological effects of *Astragalus* species have been reported such as anti-inflammatory, antihyperglycemic, antioxidant, antiviral, hepatoprotective, cardiovascular, diuretic, cytotoxic and immunomodulating activities.^{10, 12} To date, many compounds have been isolated and identified from *Astragalus* in order to benefit from their therapeutic efficacies. Phytochemical studies revealed that the main chemical groups of the genus *Astragalus* are cycloartane and oleanane type saponins, together with polysaccharides and flavonoids. In addition, *Astragalus* contains different secondary metabolites such as amino acid conjugates, alkaloids, anthraquinones.¹³

Cycloartane type triterpenoids (9,19-cyclolanostane), produced only by photosynthetic eukaryotes, were first defined in *Astragalus* plants. After the discovery of bioactivities of this group of triterpenoids, *Astragalus* species gained attention owing to their rich profiles.¹⁴ Bioactivities of cycloartanes and their semi-synthetic derivatives points out immunomodulating, cytotoxic and cholesterol lowering properties.^{15,16} Astragaloside II (Figure 1.6), a disaccharide of the aglycone cycloastragenol, prevented T-lymphocyte cells from cytopathic effects of HIV virus in vitro. Also, it inhibited the growth of HS294T melanoma cell lines.^{17,18}

Furthermore, astragaloside IV (Ast IV), the most common cycloartane glycoside isolated from *Astragalus* species, showed anti-inflammatory, immunoregulatory and antifibrotic properties in vitro and also had an important protection role in cardiovascular diseases.^{19, 20} A study performed by Liu et al., the results showed that Astragaloside IV delayed the formation of liver fibrosis and decrease the serum levels of hyaluronic acid (HA), procollagen type III (PCIII) and hydroxyproline (Hyp) content in liver. The levels

of transforming growth factor- β_1 (TGF- β_1) in serum and expression in liver were significantly decreased by astragaloside IV. Collagen synthesis and proliferation were significantly inhibited by astragaloside IV (1.5, 3.0, 6.0, 12.0 and 24.0 mg L⁻¹) in HSCs.²¹

From bioactivity point of view, the most important and commercially significant development in *Astragalus* studies has been the discovery of cycloastragenol, the main aglycone of *Astragalus* cycloartane glycosides, as a telomerase activator.²² This compound was licensed by TA Sciences and introduced into the food supplement market as an antiaging product under the brand name TA-65 in 2007.^{22, 23}

The detailed information on *Astragalus* chemistry and its bioactivities are not mentioned comprehensively in the scope of this thesis since it had been described in previous theses of our group.^{14, 24-26}

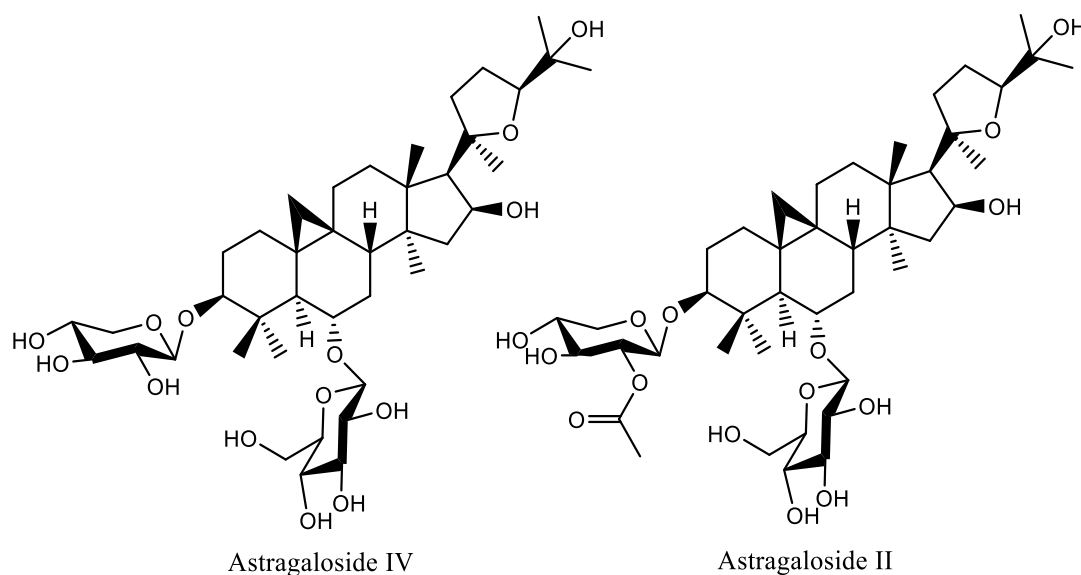


Figure 1.6 Chemical structures of astragalosides II and IV

1.2. Telomere and Telomerase

Telomeres are special structures, consisting of successive repeat sequences of TTAGGG located at the ends of chromosomes. They protect chromosome ends from fusion and degradation.²⁷⁻²⁹ Telomerase is a cellular reverse transcriptase (TERT, telomerase reverse transcriptase) enzyme that helps to repair the telomere ends by adding the corresponding RNA component and TTAGGG repeats.³⁰ The dynamic continuity of the telomeres, which are directly depending on telomerase activity, has been found to be

closely related to limited proliferative capacity of the somatic cells. To be specific, the somatic cells could replicate up to 50 cycles after which they stop dividing, and this phenomenon is known as Hayflick limit. On the other hand, the cancer cells are known with their everlasting proliferative capacity. Since both healthy and unhealthy (such as cancer) cells have to maintain their genomic integrity, studies on telomere and telomerase have become important in the investigation of various areas such as aging, cancer and pathogen-induced chronic degenerative diseases.³¹ In recent years, considering the ever-increasing aging population, the regenerative medicine has been focusing on developing strategies for the maintenance of telomere length.³²

In 2000, Geron Corporation reported that telomerase-based therapies were not only stop the aging process in humans, but also could reverse the aging process. The Geron team cultured human skin cells up to the replicative limit and then applied these cells to the immunodeficient mice. As expected, application of these cells showed characteristic properties such as skin thickness, subepidermal bubble formation that are related to “old skin”. Their study continued with culturing of telomerase added old skin cells for 25 more additional generations and these cells were seeded on mice. At last, they analyzed gene expression profile of these “telomerized” young and old skins. The skin was actually seen to be rejuvenated.³³

In 2003, the Richard Cawthon team worked on the blood samples from 143 people aged over 60 who donated bloods between 1982 and 1986. The telomere lengths were measured and relationship between telomere length and the mortality rate had been investigated. At the end of the study, it was found that mortality rate in individuals with short telomere was almost two times higher than the rate of death in long telomere individuals. Also, the deaths due to the heart diseases were found to be 3 times higher in individuals with short telomeres. These results provided evidence for the correlation between telomere shortening and aging-related deaths or diseases.³⁴

All these pioneering studies have raised the following question: Is it possible to activate telomerase in adult human somatic cells with natural and/or synthetic compounds? Geron has started screening of chemical libraries in terms of telomerase activation. In 2006, it was discovered that *Astragalus membranaceus* derived cycloastragenol had significant levels of telomerase activation. This molecule, licensed by TA Sciences, was launched in 2007 under the trade name TA-65. TA-65 is still the only natural product in the market as telomerase activator.

As emphasized before, telomerase activators have great importance for the development of novel anti-aging therapeutics. Nevertheless, one of the main reasons of their little exploitation is the speculation that they could lead to cancer development. The reason behind this speculation is the high expression of telomerase in more than 90% of human cancer cell lines.³⁵ However, studies in the last 10 years have refuted these thoughts.

In 2002; Harley, reviewed 86 publications about the relationship between cancer and telomerase, and stated that telomerase was not a cancer-causing oncogene. Additionally, he reported that the cells did not lose their growth control to cancer formation.³⁶ On the contrary, scientists have recently revealed that short telomeres are important risk factor for cancer. As a result of collaboration between Georgetown University and the National Cancer Institutes in 2009; it was concluded that short telomeres, telomere dysfunction and chromosomal arm led to the stimulus of cancer.³⁷ Thus, it is clear that long telomeres can eliminate the risk factors and prevent the onset of many cancers. In another study with 787 patients, telomere lengths in cancer patients were measured. It was found that patients with the shortest telomere length had a three-fold higher incidence of disease than patients with longer telomeres. Besides, the lethality of cancer was rather significant with patients having short telomeres, the mortality rate was doubled with shortening of the telomere length.³⁸ These results point out that telomeric length maintenance via telomerase activation can prevent cancer and/or may increase the chances of survival for cancer patients.

According to a research by Harvard Medical School, telomere prolongation via activation of telomerase in mice could reverse the signs of aging. In another experiment; instead of suppressing the telomerase gene as previously described by the Centro Nacional de Investigaciones Oncológicas (CNIO) team, DePinho's team managed a complete activation of telomerase utilizing the drug named 4-hydroxytamoxifen (4-OHT). A mouse line was constructed with this modified telomerase form and these mice were paired with each other for several generations until their telomere lengths reached a critical level. It was observed that these mice exhibit human-like aging symptoms in a way that was consistent with the results of CNIO. DePinho and his team increased the telomerase activity in the cells by giving 4-hydroxytamoxifen to the mice. This application resulted in a decrease in the number of telomeres reached in critical shortening in the cells. Cell proliferation was increased and the symptoms of degeneration in organs

such as testis, spleen, intestine were eliminated, new neuron cells were observed, and brain weights of animals were increased. Also, mice treated with 4-hydroxytamoxifen for more than 4 weeks did not show an increased risk of cancer.³⁹

1.3. Endophytic Fungi

Endophytic fungi are microorganisms that live at least one period of their life cycle without forming a visible disease in the internal tissues of plants.^{40, 41} The term endophyte was introduced by De Bary in 1866, and this term has been used for all organisms that cause asymptomatic infections without causing any disease symptoms in plant tissues.⁴²

Ascomycota phylum are the most common endophytic fungus, a very large polyphyletic group. Endophytes can live in intracellular or intercellular spaces and colonize in all tissues including stems, leaves, petioles and roots of plants.⁴²⁻⁴⁴

Endophytic fungi can develop a symbiotic relationship with plant hosts. Fungi-plant symbiosis life form is a widespread phenomenon in nature and represent a major role in structuring plant communities etc. colonization, competition, coexistence.⁴⁰ Endophytes are capable of producing the necessary enzymes in order to make colonization and use the components in plant tissues. Tolerating the toxic metabolites of the plant and producing specific enzymes for adaptation to their environment, make them popular for biotransformation studies. Endophytic fungi are promising biocatalysts in green chemistry applications, with a wide range of stereospecificity in the biotransformation of natural products and drugs.^{40, 45}

Recent advances have shown that it is possible to make endophytes produce secondary metabolites by modifying their biochemical pathways.^{40, 46} Right after the discovery of the production of secondary metabolites (such as paclitaxel (taxol), podophyllotoxin, deoxypodophyllotoxin, hypericin and emodin,) by endophytic microorganisms, they gathered more attention. For example; antitumor agent maytansinoid ansamitocin, first isolated from higher plants, was also obtained from a bacterial endophyte *Actinosynnema pretiosum* spp. *auranticum*. The similarity of maytansinoid structures to the ansamycin group microbial metabolites, unusual for higher plants, suggests that the actual biosynthetic source of the maytansinoid skeleton may be a bacterial endophyte.⁴⁷ Although the production of maytansinoids from plants can be

explained by horizontal gene transfer, these compounds are more likely to be produced by symbionts.⁴³

Considering that endophytes are in constant interaction with the host plant; the plant is thought to have very important effects on metabolic processes of endophytes.⁴³
⁴⁴ For example; plant homoserine and asparagine have been reported to act as host signals that activate the expression of a lethal gene in virulent species of the *Nectria hematococca* fungus.⁴⁸ In addition, although *Fusarium solani*, the camptothecin producer, used its own enzymes in the biosynthesis of the camptothecin precursors, it was shown that it needed a key plant enzyme (strictosidine) to complete the biosynthesis. This explains the main reason for the significant decrease of camptothecin production in subcultures under axenic conditions.^{43, 49, 50}

1.4. Biotransformation

Biotransformation is mainly enzyme-catalyzed reactions to modify molecules by cellular systems or organelles as well as isolated enzymes.⁵¹ Many metabolic processes in animals (drug metabolism), plants (secondary metabolism) and microorganisms are catalyzed by enzymes so, the biological systems are indeed utilize biotransformation efficiently.⁵²

In the food, animal feed stock and vitamin productions together with synthesis of chiral drugs and specialty chemicals, biotransformation plays a key role.⁵² Biotransformation based processes have been used by humankind for ages. As an example, the ethanol-acetic acid biotransformation (vinegar) by *Acetobacter* could be given that was developed alongside with ethanol production from fermentable sugars in Babylon (Mesopotamia), Egypt, Mexico, and the Sudan.⁵³

The most important advantages of biotransformation from the perspective of chemical and pharmaceutical industries are; i) catalysis of stereo-, regio- and enantioselective reactions; ii) activation of non-reactive sites of the substrates; iii) workability in mild conditions (optimum pH, non-toxic atmospheres, atmospheric pressure, etc.).^{40, 53-56}

Biotransformation processes are classified in two categories based on the biocatalyst used: enzymatic or whole cell systems (microorganisms, plant and mammalian cell cultures). Whole cell systems are more preferred in industrial

applications. The overriding reasons for this trend are: being able to produce and regenerate required cofactors, more proper folding of the enzymes in appropriate cellular conditions, presence of the optimum catalysis conditions, and more economic process opportunity.^{52, 57, 58} In the pharmaceutical industry, microbial biotransformation has begun to take place in enzymatic transformation in the synthesis of chiral intermediates and end products, and its industrial applications include the production of cortisone (*Rhizopus nigricans*), hydrocortisone (*Curvularia* sp.), compactine (*Mucor hiemalis*), where mainly P450 monooxygenases are involved.^{51, 55, 59}

1.4.1. Enzymatic biotransformation

All life forms require enzymes for the catalysis of metabolic biochemical reactions. These macromolecules assist reactions to last in a rapid manner and under mild environments, in a slight range of pH and temperature. Furthermore, enzymes can function continuously in in vitro conditions not proper for cell growth.⁶⁰ Enzymes can be isolated by extraction from cells or their exudates. Especially, microbial cells are exceptional factories of enzymes signifying *ca.* 90% of the total biotransformation market.^{56, 61, 62} Enzymes can be classified into six major groups based on reactions they catalyze (Table 1.1). It was projected that about 60% of biocatalysis currently depend on the use of hydrolases, followed by oxidoreductases with 20% slice.⁶¹

Table 1.1 Enzyme classification ⁶¹

Enzyme class	Examples	Reaction catalyzed
Hydrolases	lipase, protease, esterase nitrilase, nitrile hydratase glycosidase, phosphatase	hydrolysis reactions in H ₂ O
Oxidoreductases	dehydrogenase, oxidase oxygenase, peroxidase	oxidation or reduction
Transferases	transaminase, glycosyltransferase transaldolase	transfer of a group from one molecule to another
Lyases	decarboxylase, dehydratase, deoxyribose-phosphate aldolase	Non-hydrolytic bond cleavage
Isomerases	racemase, mutase	Intramolecular rearrangement
Ligases	DNA ligase	bond formation requiring triphosphate

In industry, almost 150 biocatalytic practices are in use, mainly utilizing isolated enzymes, in immobilized or free forms, rather than cells. Many plant and animal enzymes were replaced by microbial enzymes in the 1980s and 1990s, and were used commonly in many industries; viz. therapy, diagnostics, food, detergents, textiles, leather, pulp and paper.^{61, 63} Some industrially utilized hydrolases are summarized in Table 1.2.⁶⁴

Table 1.2 Hydrolases actively used in the preparation of biologically active compounds⁶⁴

Entry	Product	Biocatalyst	Production parameters	Drug	Company
1	(S)-1	<i>C. rugose</i> lipase	Multi kg	(S)-Ibuprofen (NSAID)	Pfizer
			90% yield		
			$ee_p = 99\%$		
2	(S)-2	CALB	200 kg	NK1/NK2 dual antagonists	Schering-Plough
			98% yield		
			$ee_p > 99\%$		
3	(S)-3	Immobilized CALB	Several hundred kg	Lotrafiban S-16 antithrombotic	GlaxoSmithkline Pharmaceuticals
			97% yield		
			$ee_p = 99\%$		
4	(1S,2R)-4	Novozyme 435®	98% yield	Chemokine receptor modulator	Bristol–Myers Squibb
			$ee_p > 99\%$		
5	(S)-5	CALB	220 g L ⁻¹	Saxagliptin (oral hypoglycemic)	Bristol–Myers Squibb
			81% yield		
			$ee_p > 99\%$		
6	(3R,4S)-6	<i>P. cepacia</i> lipase PS-30 BMS lipase	1.2 kg Batch ⁻¹	Paclitaxel (antimitotic agent)	Bristol–Myers Squibb
			96% yield		
			$ee_p > 99.5\%$		
7	(2S,3R)-8	<i>S. marcescens</i> lipase	40 kg	Diltiazem (calcium canal blocker)	Tanabe Pharmaceutical
			40–45% yield		
			$ee_p = 99.9\%$		
8	(S)-9	<i>P. fluorescens</i> lipase	Multi kg	Carbovir (antiviral agent)	Celltech Group
			22% yield		
			$ee_p > 92\%$		
9	(S)-10	Subtilisin Carlsberg	>100 kg	Remikiren & Ciprokiren (Renin inhibitor)	Hoffmann La-Roche
			50% yield		
			$ee_p > 99\%$		

A commonly used example of enzymatic reactions implying its greener side is the replacement of alkaline hydrolysis of esters with hydrolases. On the other hand, enzymes can be exploited in the cases of difficult or non-selective chemical transformations. The advantages and disadvantages of this group of reactions are briefly given below.⁶²

Advantages:

1. Rate enhancements as much as 10^{12} ,
2. Wide-range tolerance to structurally diverse substrates,
3. High regio-, stereo- and enantioselectivity,
4. Mild medium conditions,
5. Possibility of over-expression and directed evolution for improved efficiency and/or specificity,
6. Low operational cost,
7. “Green” conditions,
8. Lower waste component, higher reaction mass efficacy, E-value, or effective mass yields,
9. More suitable for waste streams for municipal sewers.⁶²

Disadvantages:

1. Instability in isolated state,
2. Cofactors requirement or cofactor recycling for oxidoreductases,
3. Commercial obtainability in competition with cost of isolation or over expression,
4. Cost of specific apparatus for fermentations,
5. Difficulty to displace conventional practices,
6. Training investment to adapt to new techniques.⁶²

Ligases and lyases are not as much of common in synthetic endeavors. As they do not require cofactors, the use of lipases or hydrolases offers the easiest experimental procedures. The other most frequently engaged enzymatic procedure is possibly reduction of carbonyl compounds by yeasts. The utilization of oxidoreductases is slightly more demanding, especially for the enzymes overexpressed in recombinant microorganisms.⁶²

Still, the isolation and purification of enzymes is quite costly and time intense, whereas the requirement of co-factors and their recycling may be challenging: In addition, if more than one enzyme is required for the complete process, it is more difficult to carry out the reactions compared to the whole microbial cell systems.⁶⁰

1.4.2. Whole cell microbial biotransformation

Regeneration of cofactors and production of multiple enzymes which allow multi-step chemistry can be supplied via whole-cells as an alternative *in situ* methodology. Moreover, whole-cell methods are cost-effective to implement upstream since there is no necessity for enzyme isolation.⁶⁵ Besides, biocatalyst that are used for organic reactions can fail to invade non-activated sites of molecules which hinders them participating reactions effectively such as lack of hydroxylation at aliphatic chains. Notably, instead of biocatalyst, the use of microorganisms in order to catalyze wide range of chemical reaction is promising approach with their high substrate tolerance and applicability to multiple compounds. Among this approach, endophytic fungi are not yet very examined source for microbial transformation. It is known that they have to deal with plant-originated defense compounds which are highly toxic since plant tissue is their host tissue. For that reason, it can be thought that these kind of microorganisms potentially must adapt to biodegradation and their certain enzymes must help them to maintain their living status under these harsh conditions.^{40, 66}

In this respect, in 2013, Luo et al., have reported the biotransformation study of the main saponins in *Panax notoginseng* (which also includes the ginsenosides Rg1, Rh1, Rb1, and Re) by employing endophytes that are isolated from *Panax notoginseng*. First, they have isolated 136 endophytes and their biotransformation abilities have screened. Accordingly, 5 of these isolated and screened endophytes were able to transform these saponins. After identification of their ITS or 16S rDNA sequence, these 5 strains were found that they related with *Fusarium*, *Nodulisporium*, *Brevundimonas*, and *Bacillus* genera. Afterwards, isolation and identification of 10 of transformed products including a new compound 6-O-[α -l-rhamnopyranosyl-(1-2)- β -d-glucopyranosyl]-20-O- β -d-glucopyranosyldammarane-3,6,12,20,24,25-hexaol and 9 known compounds (which are compound K, ginsenoside F2, vinaginsenoside R13, vinaginsenoside R22, pseudo-ginsenoside RT4, (20S)-protopanaxatriol, ginsenoside Rg1, vinaginsenoside R15 and (20S)-3-O- β -d-glucopyranosyl-6-O- β -d-glucopyranosylprotopanaxatriol) were completed with success. This reported study is the first study in literature about the biotransformation of chemical components in *Panax notoginseng* by employing endophytes isolated from the same plant.⁶⁷

It should be noted that microbial models which can mimic the mammalian metabolism can be categorized as alternative way to understand metabolic fate of drug instead of the use of animal models. Hence, the use of animals can be decreased in the early phases of related drug development. Microbial transformation has been investigated on mainly antibiotics and steroids for a long time.⁶⁸ In 1974, Smith and Rosazza have proposed microbial transformation system that can mimic Phase I transformation of a drug in mammals, after they have explored the possibility of similarity between microbial and mammalian cytochromes P450 (CYP) which are both structurally conserved and functionally diverse group of hemecontaining mixed function oxidase.⁶⁹ In order to reinforce their hypothesis, they have screened a number of bacteria and fungi to see if they have ability to transform model aromatic compounds that the pattern for mammalian transformation products were well-known. At the end, they were observed that both *in vitro* and *in vivo* mammalian systems have formed metabolites that are analogous to metabolites from microbial biotransformation system in most cases. With the other studies that continued after this first study, it was supported that certain microorganisms have ability to transform drugs and xenobiotics to mammalian metabolites efficiently.⁷⁰

There are lots of study that have been reported about microbial systems as an *in vitro* model that have ability to mimic mammalian P450 activation of drugs. According to recent reports, either native or designed forms of microbial P450s from microbial systems can be used for specific biotransformation reactions for drugs that have natural and/or synthetic origin (Table 1.3). Besides, particularly fungi and actinomycetes having catabolic P450s have been shown to degrade toxic environmental chemicals (persistent organic pollutants).⁷¹

In 2001, Parshikov et al., have investigated the metabolism of the fluoroquinolone drugs (ciprofloxacin and norfloxacin) by *Pestalotiopsis guepini* strain P-8. From each drug, 4 major metabolites (Ciprofloxacin metabolites: N-acetylciprofloxacin (52.0%), desethylene-N-acetylciprofloxacin (9.2%), N-formylciprofloxacin (4.2%), and 7-amino-1-cyclopropyl-6-fluoro-4-oxo-1,4-dihydroquinoline-3-carboxylic acid (2.3%); Norfloxacin metabolites: N-acetylnorfloxacin (55.4%), desethylene-N-acetylnorfloxacin (8.8%), N-formylnorfloxacin (3.6%), and 7-amino-1-ethyl-6-fluoro-4-oxo-1,4-dihydroquinoline-3-carboxylic acid (2.1%)) were produced, then purified via high-performance liquid chromatography (HPLC) and characterized via mass spectrometry (MS) and nuclear magnetic resonance spectroscopy (NMR). In conclusion, among the all

metabolites N-Formylciprofloxacin and the four transformation products from norfloxacin are identified as mammalian metabolites.⁷²

Table 1.3 Oxidative reactions catalyzed by whole cells in the preparation of biologically active compounds at industrial scale.⁶⁴

Entry	Product	Biocatalyst	Production parameters	Drug	Company
1	16	<i>Gluconobacter oxidans</i>	Tons	α -Glucosidase inhibitors	Bayer AG
			90% yield		
			N.R.		
2	(S)- 17	<i>Trigonopsis variabilis</i> ATCC 10679, EC	N.R.	Vasopeptidase and antihypertensive metalloendopeptidase inhibitor	Bristol–Myers squibb
			50% yield		
			$ee_p = >99\%$		
3	18 (HOPS)	<i>Beauveria bassiana</i> LU 700	Tons	Herbicides	BASF AG
			99% yield		
			–		
4	19	<i>Streptomyces</i> sp. Y-110	N.R.	Pravastatin anticholesterolemic	Sankyo Company/ Bristol–Myers Squibb
			70% yield		
5	21	<i>Arthrobacter</i> sp.	70 g L ⁻¹ d ⁻¹	Pharmaceuticals and agrochemicals compounds	Mitsubishi chemical corporation
			99% yield		
			N.R.		
6	(S)- 22	<i>Escherichia coli</i> JM 101	4.5 g L ⁻¹ h ⁻¹	Starting materials	DSM
			93% yield		
			$ee_p > 99\%$		
7	(S)- 23	<i>Pseudomonas oleovorans</i> ATCC 29347EC	>7 g L ⁻¹	Starting materials	DSM
			90% yield		
			$ee_p = 99.9\%$		
8	(3R,6S)- 24 + (3S,6R)- 25	<i>Acinetobacter calcoaceticus</i>	kg	Alternative for Baeyer–Villiger oxidations	Sigma–Aldrich
			92% yield		
9	(R)- 28	<i>Saccharomyces cerevisiae</i>	100 g	Antitumoral taxane derivatives	Johanson y cols.
			97% yield		
			$ee_p > 99\%$		

In summary, the practical benefits of the employment of microbial systems as potential models for drug metabolism can be listed as below:⁶⁹

1. Compared to cell/tissue cultures and laboratory animals, cultures of microorganisms can be handled easily. Additionally, necessary culture media can be easily prepared with low costs.
2. Require mild incubation conditions.
3. Useful for cases that regio- and stereo-specificity is involved.
4. Employed in the synthetic reactions where tedious steps are involved.
5. Easy to adapt high scale production of metabolites which are intended to be used in pharmacology and toxicology studies.
6. The most preferred metabolic reactions could be predicted.
7. Novel molecules can be isolated with new or distinct activities.
8. Since it only requires a simple repetitive process which is a periodical sampling of incubation media, it is an easy process even the metabolization of the drug requires large number of strains.
9. It is possible to decrease concentration of used natural drugs which makes detection, isolation and structure elucidation easier and allows fast comparison with mammalian metabolites, thanks to high metabolic capabilities of microorganisms.

1.5. Microbial transformation of saponins

The properties of biocatalysts such as performing reaction with extremely regio and stereo selective manner make them a fascinating candidate in usage for complex steroid molecules. Moreover, since the bioconversion of these molecules with chemical synthesis processes which need mild conditions is highly destructive for environment, biotransformation approaches emerge and gain ground in industry by creating solutions to these problems.

First microbial example which is the α -7 hydroxylation of cholesterol by *Proactinomyces roseus* was described by Kramli and Horvath in 1949. In the early 1950s, the Upjohn Company reported that *Rhizopus arrhizus* transformed progesterone to 11 α -progesterone, while the Squibb Institute reported the same reaction by *Aspergillus niger*. Microbial transformation of the progesterone decreased the number of steps in the production of cortisone acetate from deoxycholic acid drastically (removed 10-12 steps

from 31 steps), increased the yield and cost effectivity (the production cost of 1 gram cortisone decreased from \$200 to \$6 and eventually \$1).^{73, 74}

Biotransformation of organic compounds via microorganisms led to generate a vast amount of different variety and complex structures, such as triterpenoids. Thanks to their chemo, regio and stereospecific character of microbial biotransformation, it can be possible to produce a variety of semi-synthetic analogues and/or novel structures which is hard or almost imposible to produce through chemical synthesis. These phenomena leads scientist to perform lots of studies of microbial transformation of triterpenoids to obtain different structures and increase druggability and bioactivity.⁷⁵

Cycloastragenol, (20R,24S)-3 β ,6 α ,16 β ,25-tetrahydroxy-20,24-epoxycycloartane, is the genuine sapogenin of astragaloside IV which is a valuable molecule with pharmacological properties like anti-inflammatory, anti-viral, anti-aging and anti-oxidant properties, a major bioactive constituent of *Astragalus* plants. Moreover, it can increase telomerase activity and helps to retard the cellular aging, can induce IL-2 to trigger immune system and helps to increase antiviral function of human lymphocytes. These properties make it a good antiaging agent which can be used for different purposes.⁷⁵ Kuban et al investigated the biotransformation of cycloastragenol with two fungal strains, *Cunninghamella blakesleeana* NRRL 1369 and *Glomerella fusarioides* ATCC 9552, and the bacterium *Mycobacterium* sp. NRRL 380. Their studies revealed that biotransformation with fungi mainly resulted in hydroxylated metabolites together with products formed by cyclization, dehydrogenation and Baeyer–Villiger oxidation resulting in a ring cleavage while only 3-oxo-cycloastragenol which is a single oxidation product obtained with bacteria.⁷⁶

In another study performed by Bedir et al. the microbial transformation of *Astragalus* sp. derived sapogenins, namely cycloastragenol, astragenol and cyclocanthogenol, by *Cunninghamella blakesleeana* NRRL 1369 and *Glomerella fusarioides* ATCC 9552 were investigated. The unique enzyme system of both fungi resulted hydroxylation, cyclization, dehydrogenation and oxidation reactions. On the other hand, *G. fusarioides* offered oxidative biotransformations, especially Baeyer–Villiger type oxidations and hydroxylations.⁷⁷

Apart from the studies of our group, there are only two reports about the biotransformation of commercially important cycloastragenol CA. One of these studies was carried out by Yang et al. In this study, Biotransformation of cycloastragenol, a natural tetracyclic triterpenoid which has anti-aging activity, performed whole cell

fermentation process with three filament fungus strain, namely *Cunninghamella elegans* AS 3.1207, *Syncephalastrum racemosum* AS 3.264 and *Doratomyces stemonitis* AS 3.1411. As a result, 15 metabolites, thirteen of them are new, were obtained. The three fungal strains showed important biocatalytic preferences: *C. elegans* catalyzed hydroxylation reactions, mainly on the 28- and 29-CH₃ groups; *S. racemosum* can catalyzed both a unusual ranunculane skeleton and rare 9(10)a-homo19-nor-cycloartane skeleton via complicated rearrangement reactions.⁷⁸ Feng et al., investigated of biotransformation of CA by two strains of filamentous fungi, which are *Syncephalastrum racemosum* AS 3.264 and *Alternaria alternata* AS 3.4578, and isolated 27 different metabolites in which 18 of them are novel compounds. The two fungal strains exhibited distinct biocatalytic features result in unique structures which are difficult to obtain via chemical reactions. To exemplify *S. racemosum* could catalyze ring expansion and epoxidation reactions to form 3b,10b-epoxy- or 6a,19a-epoxy-9,10- seco-cycloartane structures, whereas *A. alternata* preferred to catalyze acetylation reactions, especially at 3-OH, 6-OH and 19-OH.⁷⁹

CHAPTER 2

MATERIALS AND METHODS

2.1 Materials

Biological and chemical materials used in this study and the instruments used are given below.

2.1.1 Endophytic Fungi

Endophytic fungi which were used in the biotransformation studies were isolated from *Astragalus condensatus* and *Astragalus angustiflorus* in the TUBITAK project # 114Z958.

Table 2.1 Phylogenetic analysis results of isolates based on ITS rDNA sequences

Strain code	Host Plant / plant tissue in which it is isolated	Fungal sequence	Accession no.	Similarity (%)
1E2L1	<i>Astragalus angustiflorus</i> / Leaf	<i>Alternaria alternata</i>	KU866390.1	99
1E4CR-1	<i>Astragalus condensatus</i> / Root	<i>Podospora</i> sp.	LC109288.1	99
1E2L-1	<i>Astragalus angustiflorus</i> / Leaf	<i>Fusarium torulosum</i>	JX534258.1	100
1E2R1	<i>Astragalus angustiflorus</i> / Root	<i>Leptosphaeria</i> sp.	KT269871.1	100
1E4AS-1	<i>Astragalus condensatus</i> / Stem	<i>Fusarium</i> sp.	KT269061.1	100
1E3AS1-1	<i>Astragalus angustiflorus</i> / Stem	<i>Fusarium acuminatum</i>	JX534294.1	100
*1E1BL-1	<i>Astragalus angustiflorus</i> / Leaf	<i>Alternaria eureka</i>	FR799468.1	100
1E4AL	<i>Astragalus condensatus</i> / Leaf	<i>Allophaeosphaeria cytisi</i>	KT306947.1	95
*1E2AR1-1	<i>Astragalus angustiflorus</i> / Root	<i>Neosartorya hiratsukae</i>	FR733873.1	100
1E1BR2	<i>Astragalus angustiflorus</i> / Root	<i>Fusarium solani</i>	KT583204.1	100
1E4CS	<i>Astragalus condensatus</i> / Stem	<i>Fusarium</i> sp.	KT323109.1	100
1E4BS1	<i>Astragalus angustiflorus</i> / Stem	<i>Penicillium roseopurpureum</i>	KJ775658.1	100
1E4CS-1	<i>Astragalus condensatus</i> / Stem	<i>Phaeosphaeria</i> sp.	KJ188706.1	89
1E4BR2-2	<i>Astragalus angustiflorus</i> / Root	<i>Penicillium</i> sp.	JQ781815.1	100
*1E4BL1	<i>Astragalus angustiflorus</i> / Leaf	<i>Camarosporium laburnicola</i>	KY497784	99

*Endophytic fungi species selected for biotransformation and isolation studies

2.1.3 Media

In this study, four different growth media were used. PDA was used for activation of the organisms, PDB and B.O. were used in biotransformation studies and the last one was used for the growth of HEKN cells.

2.1.3.1 Medium 1: Potato Dextrose Agar (PDA)

39 g of the medium (Merck Millipore-110130) was boiled in 1000 ml distilled water until it became fully dissolved. After that it was sterilized by autoclave at 121 °C (15 psi pressure) for 15 minutes.⁸⁰

2.1.3.2 Medium 2: Biotransformation Medium (B.O.)

The mentioned media contents given in Table 2.2, were mixed until they were completely dissolved in 1000 ml distilled water. After that pH was adjusted to 6 and medium was sterilized by autoclaving for 15 minutes at 121 °C (15 psi pressure).⁸⁰

Table 2.2 Contents of the biotransformation medium

Component	Amount(g)
D-(+)-Glucose	20
Yeast extract	5
NaCl	5
K ₂ HPO ₄	5
Peptone	5

2.1.3.3 Medium 3: Potato Dextrose Broth

24 g of the medium (Merck Millipore-110130) was mixed in 1000 ml distilled water until it was fully dissolved and sterilized by autoclaving at 121 °C (15 psi pressure) for 15 minutes.⁸⁰

2.1.3.4 Medium 4: Media components for growing of HEKN cells

Before culturing Hekn cells (Human Primary Epidermal Keratinocyte, ATCC; PCS-200-010), the cell medium containing the components given below was prepared. Hekn Cells were replicated in Dermal Cell Basal media (PCS-200-030) containing the components given below at 37 °C (%5 CO₂).

Table 2.3 Media components for Hekn Cells

Components	Volume	Final Concentration
Bovine Pituitary Extract (BPE)	2 ml	0.4%
Rh-TGF- α	0.5 ml	0.5 ng/ml
l-Glutamine	15 ml	6 mM
Hyrocortisone Hemisuccinate	0.5 ml	100 ng/ml
Epinephrine	0.5 ml	1 mM
Rh Insulin	0.5 ml	5 mg/ml
Apo-Transferrin	0.5 ml	1 mM

2.1.4 Used Chemicals

The chemicals used in molecular and isolation-purification studies are listed below.

2.1.4.1 Chemical reagents used in molecular studies

1 kb Ladder: New England Biolabs GmbH

Agarose: BD (Becton Dickinson)

Acetic acid: Carl Roth & Co. KG

Bromphenol blue: Roche Diagnostics GmbH

EDTA: Sigma-Aldrich, Ksilen siyanol: Ohly GmbH & Co. KG

FICOLL 400: Sigma-Aldrich

JumpStartTMTaq: Sigma-Aldrich

ReadyMixTM: Sigma-Aldrich

Midori Green Direct: DNA Nippon Genetics Europe GmbH

Tris Base: Carl Roth & Co. KG

2.1.4.2 Chemicals and Adsorbents used in extraction and isolation studies

Acetonitrile: VWR Chemicals

Ethyl acetate: Sigma-Aldrich

Chloroform: Sigma-Aldrich

Methanol: Sigma-Aldrich

n-hexane: Sigma-Aldrich

Dichloromethane: VWR Chemicals Sulfuric Acid: Merck

Dimethyl Sulfoxide (DMSO): Sigma-Aldrich

Acetone: Sigma-Aldrich

Hydrochloric acid: Merck, Darmstadt

Potassium hydroxide:

Kieselgel 60 F254 Teen Layer Chromatography (TLC): Merck

RP-18 F254s Teen Layer Chromatography (TLC): Merck

RP-18 (Chromabond C18): Macherey-Nagel

Kieselgel 60, 70-230 mesh: Merck

Sephadex LH-20: GE Healthcare Life Sciences

Pyridine-d₅: Merck

2.1.5. Instruments

Nuclear Magnetic Resonance Spectrometry: Varian AS 400; Bruker 500

Mass Spectrometry: Agilent 1200/6530 Instrument – HRTOFMS

UV Imaging system: Vilber Lourmat, Autoclave: Nüve 90L

Electronic Balance: PRECISA XB 220A SCS

SpeedVac Concentrator: Thermo Scientific Savant SPD 121P

Freeze Dryer: Labconco FreeZone Freeze Dry System

Shaking Incubator: SR-JSSI-300C, Electrophoresis power supply: Thermo

Rotary Evaporator: Heidolph Laborota 4001; ISOLAB

Homogeniser (Precelly 24, Bertin Corp.)

PCR Machine: Mastercycler nexus Gradient, Eppendorf

Gel imaging system: FastGene[®] gelPic LED Box, NIPPON Genetics Europe Gmb

2.2 Methods

Preliminary experiments for biotransformation of the substrate were investigated. It was followed by the scale-up studies. Then extraction, isolation and purification studies were carried out on the extracts obtained from biotransformation studies. After that, structural determination studies were done. Finally, telomerase activation of the obtained derivatives were screened.

2.2.1 Biotransformation studies

The microbial transformation process took place at two scales; analytical and preparative.

2.2.1.1 Analytical Scale

Stock cultures of endophytic fungi stored at +4 °C were revived on PDA (potatodextrose-agar) containing petri dishes at 25 °C. 2% inoculum obtained from the 9-day-old suspension cultures with Tween 80 (0.1%) was used in the biotransformation studies. A one-stage fermentation was performed where 20(27)-octanor cycloastragenol was fed to the media 72 h after the inoculation. Biotransformation studies were carried out using 250 mL flasks including 50 mL of media and 10 mg of 20(27)-octanor cycloastragenol. Submerged (25 °C, 180 rpm) culture condition was tested in the analytical scale, taking 2 mL samples on days 1,3,5,8,11,14 and 21. The supernatants were extracted with ethyl acetate. After that, the extracts were compared with the reference (substrate) on a TLC plate and checked whether the new metabolites were formed or not (Figure 2.3). Organisms with different metabolite profiles were determined and preparative scale studies were started.

2.2.1.2 Preparative Scale

All microorganisms were screened for their biotransformation effectiveness based on the chemical diversity of the products in the extracts using the analytical scale method explained above. Best preliminary results were observed with *Alternaria eureka*,

Camarosporium laburnicola and *Neosartorya hiratsukae* and further studies were carried out by using these fungi for the microbial transformation.

As a result, the preparative-scale studies continued with 2000 ml flasks at 25 °C and 180 rpm. When the preparative scale biotransformation studies were completed, post-biotransformation processes were started.

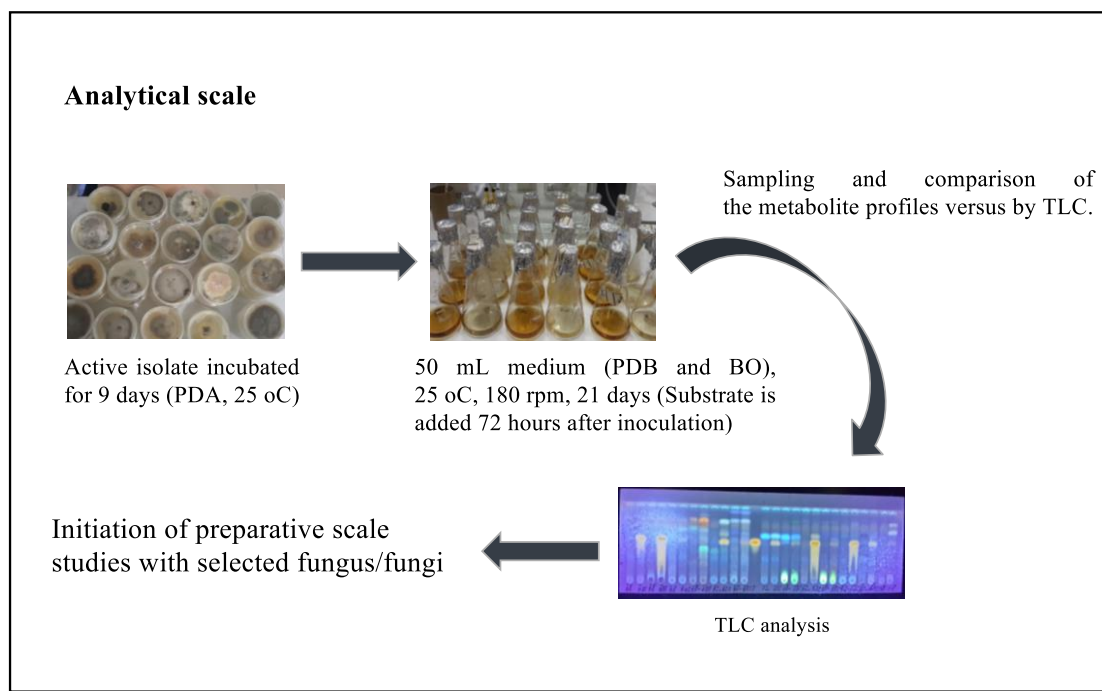


Figure 2.3 Analytical scale biotransformation studies

2.2.2 Post- Biotransformation Procedures

After the preparative scale studies, fungal cells were removed from the medium using a vacuum Buchner funnel and liquid-liquid extraction was performed for 4 times using a volume of EtOAc equal to the liquid medium. The ethyl acetate phases were evaporated in the rotary evaporator at 40 °C under low pressure. The TLC analysis of the extracts were performed using Silica gel 60 F₂₅₄ and/or reversed-phase Silica gel 60 RP-18 F₂₅₄ coated aluminum plates. Compounds were visualized by spraying 20% aq.H₂SO₄ onto the TLC plates followed by heating up to 110°C until the spots became visible.

During the TLC analysis the following solvent systems were used:

In the normal phase silica gel TLC analysis; Hexane: Ethyl acetate: Methanol (10: 10: 3; 10: 10: 4), Chloroform: Methanol (90:10; 80:20), Chloroform: Methanol: Water (90: 10: 0.5; 85: 15: 0.5; 80: 20: 1; 70: 30: 3)

In the reversed-phase silica gel (RP-C₁₈) TLC analysis; Methanol: Water (80:20), Acetonitrile: Water (60:40)

In accordance with these analyzes, chromatographic methods were determined, and then isolation studies were started. During prefractionation and isolation stages; Open Column Chromatography and Vacuum Liquid Chromatography were used. In this study silica gel 60, RP C-18 and Sephadex LH-20 were used as adsorbents. The structures of purified metabolites were elucidated by spectral methods (1D-, 2D-NMR and MS). Post-biotransformation processes are schematized in Figure 2.4.

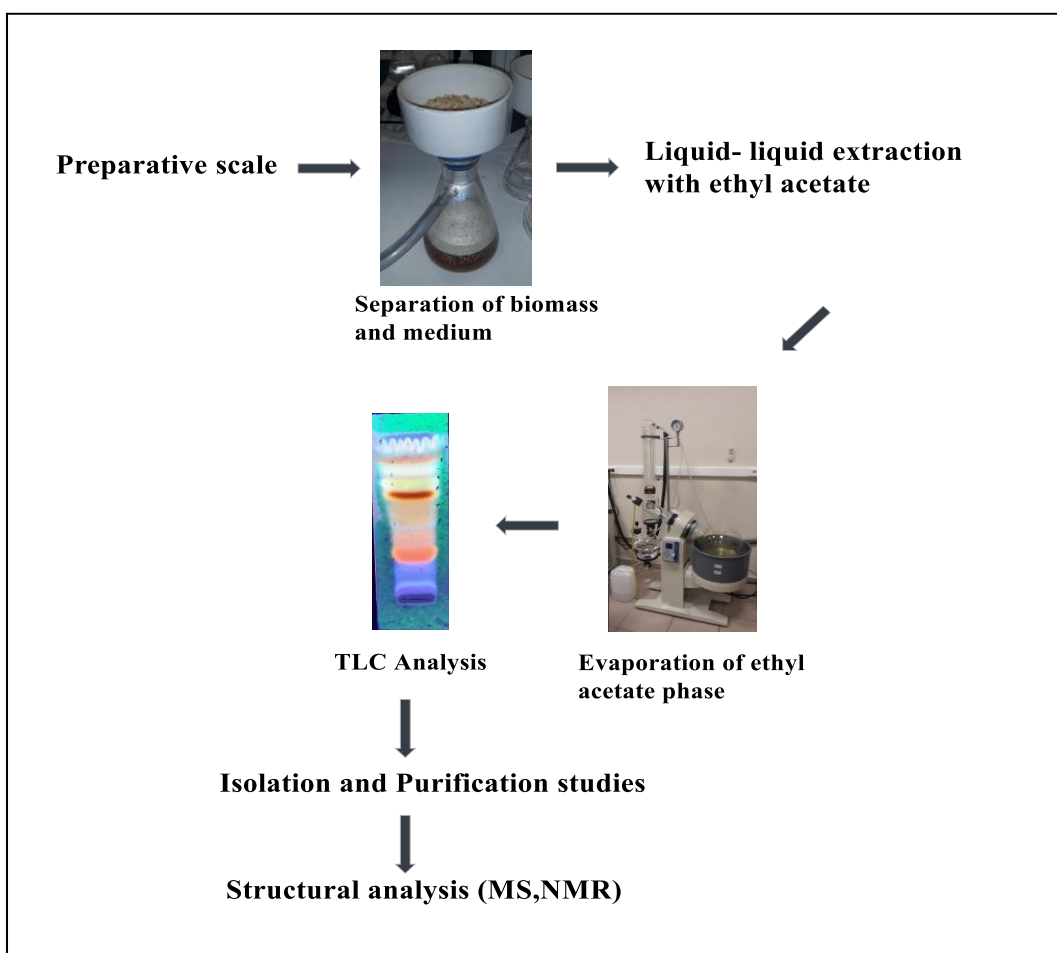


Figure 2.4 Post-biotransformation processes

2.2.2.1 Extraction, Isolation and Purification Studies

After preparative scale biotransformation, extraction, isolation and purification studies were carried out.

2.2.2.1.1 Biotransformation Studies of 20(27)-octanor cycloastragenol by *Alternaria eureka*

Preparative scale biotransformation studies of 20(27)- octanor cycloastrageol by *Alternaria eureka* were carried out for 14 days at 25 °C /180 rpm and two different media called Biotransformation Medium and Potato Dextrose Broth were used. After incubation, the Buchner funnel was used to remove the cells from the media under vacuum and the medium were extracted with an equal volume of EtOAc. The results obtained from TLC profiles of EtOAc extracts of BM (2.4g) and PDB (4.46 g) are shown in Figure 2.5. The scheme of the isolation studies on the extracts are presented in Figure 2.6 and Figure 2.7.

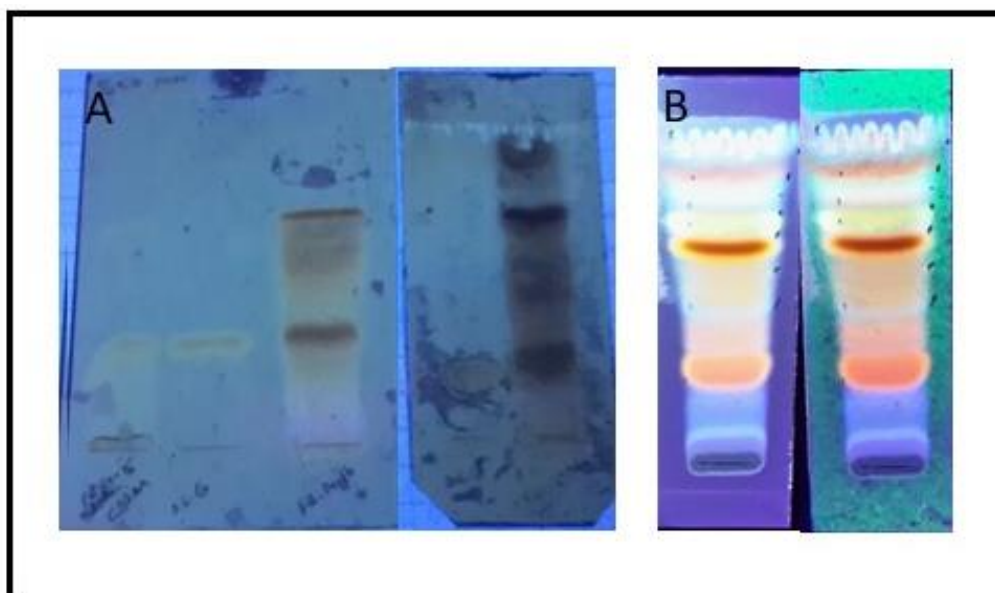


Figure 2.5 TLC chromatograms of the EtOAc extract obtained from preparative scale biotransformation study of *Alternaria eureka* biotransformation extracts (A. Biotransformation in BM, B. Biotransformation in PDB (Silica gel, 10:10:3; n-Hex:EtOAc:MeOH).

Isolation studies of EtOAc extract (2.4 g) obtained from Biotransformation Medium were started with Sephadex LH-20 (75 g) column chromatography that was employed with 100% MeOH to give one main fraction (Fr.14-16). Then, the fraction was chromatographed vacuum liquid chromatography (VLC) with a gradient solvent system containing ACN: H₂O (15:85→ 100:0). The fractions with similar profiles were pooled together, and 3 main fractions were obtained. The subfraction Fr.18-22 were subjected to silica gel (10g) column using CHCl₃: MeOH (95:5) as the solvent system to give **A-SCG-01**. Fr.72-112 was subjected to Silica gel column chromatography and the column was employed with solvent system containing CHCl₃: MeOH (98:2, 97:3, 96:4) mixtures to obtain **A-SCG-07**. The subfractions Fr.41-46 and Fr.6-16 were subjected to VLC and the columns employed with the solvent systems respectively MeOH-H₂O (75:25) and MeOH-H₂O (45:55) respectively. **A-SCG-06** and **A-SCG-03** molecules were obtained from isolation studies of fractions Fr.41-46 and Fr.6-16 respectively. The isolation steps were illustrated in detail in Figure 2.6.

Isolation studies of EtOAc extract (4.46 g) obtained from Potato Dextrose Broth media were started with Sephadex LH-20 (75 g) column chromatography using the solvent system MeOH: CHCl₃ (1:1) mixture to give one main fraction (Fr.21-27). Silica gel column chromatography was performed on Fr. 21-27 using C₆H₁₂: EtOAc: MeOH (10:10:1, 10:10:1.5, 10:10:2) as the eluting solvent system. The fractions with similar profiles were pooled together, and 7 subfractions were obtained. After that, the isolation steps presented in Figure 2.7 were performed on four of those subfractions and 5 metabolites were obtained as pure. The isolation steps were illustrated in detail in Figure 2.7.

2.2.2.1.2 Biotransformation Study of 20(27)-octanor cycloastragenol by *Camarosporium laburnicola*

Preparative scale biotransformation studies of 20(27)-octanor cycloastrageol (500 mg) by *Camarosporium laburnicola* were continued for 6 days at 25 °C /180 rpm in PDB. After incubation, the Buchner funnel was used to remove the cells from the media under vacuum and the media extracted with an equal volume of EtOAc.

The TLC profile of EtOAc extract obtained after preparative scale biotransformation is illustrated in Figure 2.8. Isolation studies on the extract are presented in Figure 2.9.

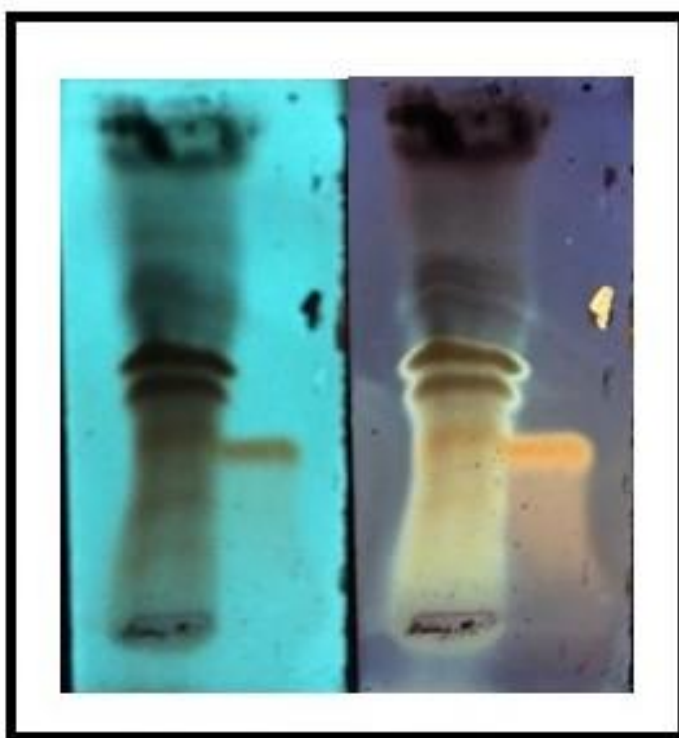


Figure 2.6 The TLC profile of EtOAc extract obtained after preparative scale biotransformation study of *Camarosporium laburnicola* (RP-C₁₈, Mobile phase; 50% ACN).

Isolation studies on the EtOAc extract (652 mg) obtained from Potato Dextrose Broth media were started with vacuum liquid chromatography (RP-C₁₈) that was employed with solvent system ACN:H₂O (30:70) mixture to give Fr. 4-12 and **E-SCG-02**. After the acetonitrile phase was evaporated, the water phase was poured into a separating funnel and the pH of water phase was adjusted to bring into 12 adding ammonia. An equal volume of chloroform was added, and shaken. After the phase separation, the aqueous phase was collected, and the pH was adjusted to 4 by adding formic acid. The partition step was repeated with chloroform. Lastly, after phase separation, chloroform phase containing the **E-SCG-1** was collected.

2.2.2.1.3 Biotransformation Study of 20(27)- octanor cycloastragenol by *Neosartorya hiratsukae*

Preparative scale biotransformation studies of 20(27)- octanor cycloastragenol with *Neosartorya hiratsukae* were continue for 18 days at 25 °C /180 rpm in Potato Dextrose Broth. After incubation, the Buchner funnel was used to remove the cells from the media under vacuum and extracted with an equal volume of EtOAc. The TLC profile of EtOAc extracts obtained from PDB (6.982 g) obtained result is shown in Figure 2.10. Isolation studies on the extracts are presented in Figure 2.11 and Figure 2.12.

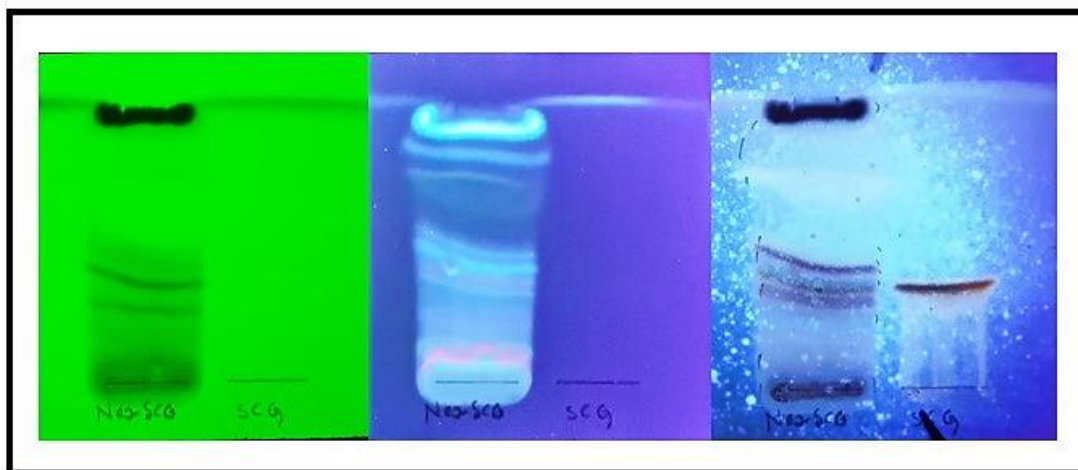


Figure 2.7 The TLC profile of EtOAc extract obtained after preparative scale biotransformation study of *Neosartorya hiratsukae* (Silica gel, 90:10; CH₂Cl₂:MeOH).

Firstly, 6.982 g of EtOAc extracts was subjected to a Sephadex LH-20 (90 g) column chromatography and eluted with EtOAc: MeOH (1:1, 0:100). The fractions with similar profiles were pooled together, and 1 main fraction was obtained. Fr. 20-46 was chromatographed Silica gel (165 g) column chromatography with solvent system CH₂Cl₂:MeOH (100:0→0:100) mixtures. Isolation process was continued 4 of the sub-fractions to obtained and as a result of 6 molecules was isolated. Details of the isolation procedures are shown in Figure 2.11 and Figure 2.12.

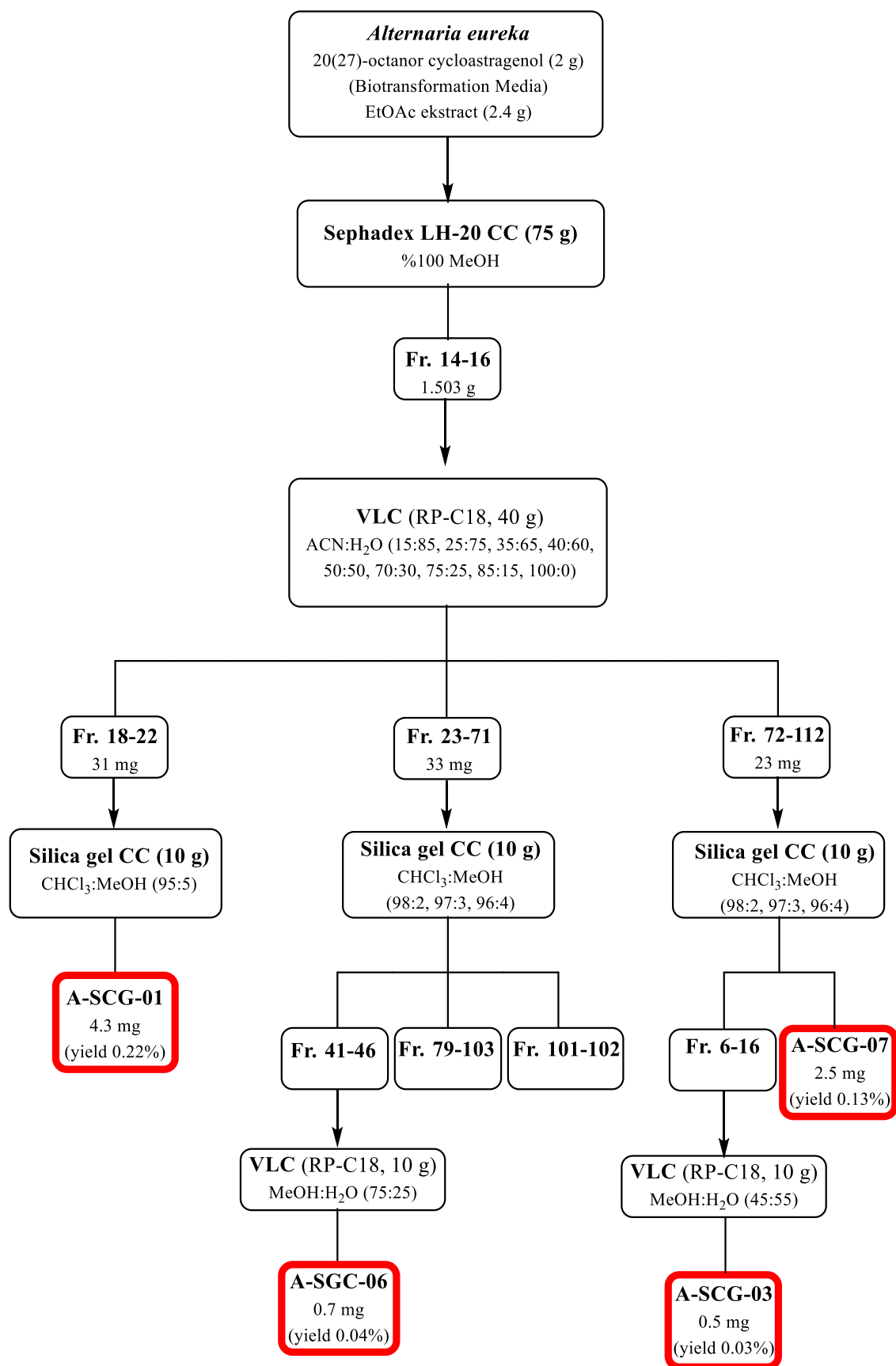


Figure 2.8 Isolation scheme of *Alternaria eureka* EtOAc extract (BM)

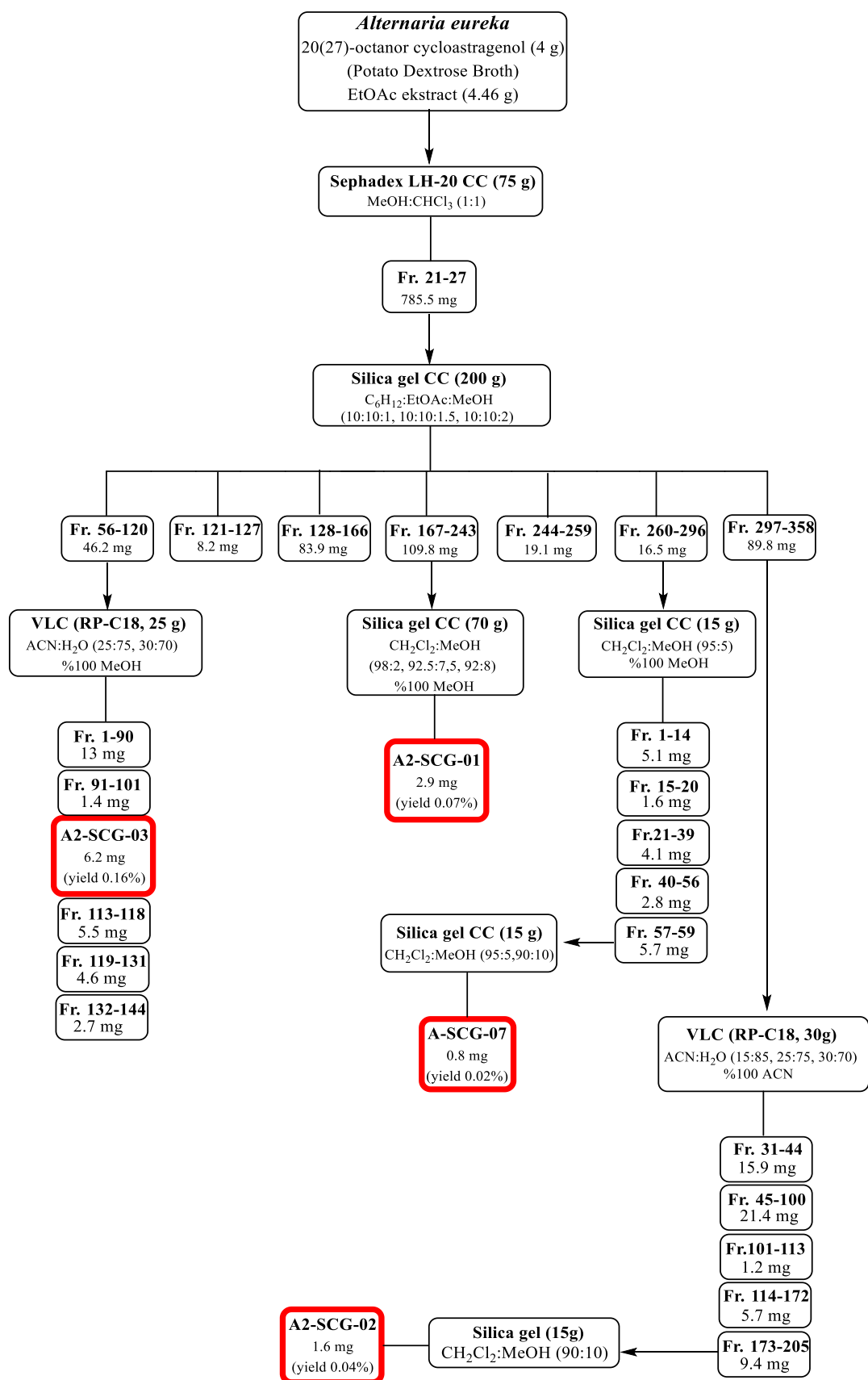


Figure 2.9 Isolation scheme of *Alternaria eureka* EtOAc extract (PDB)

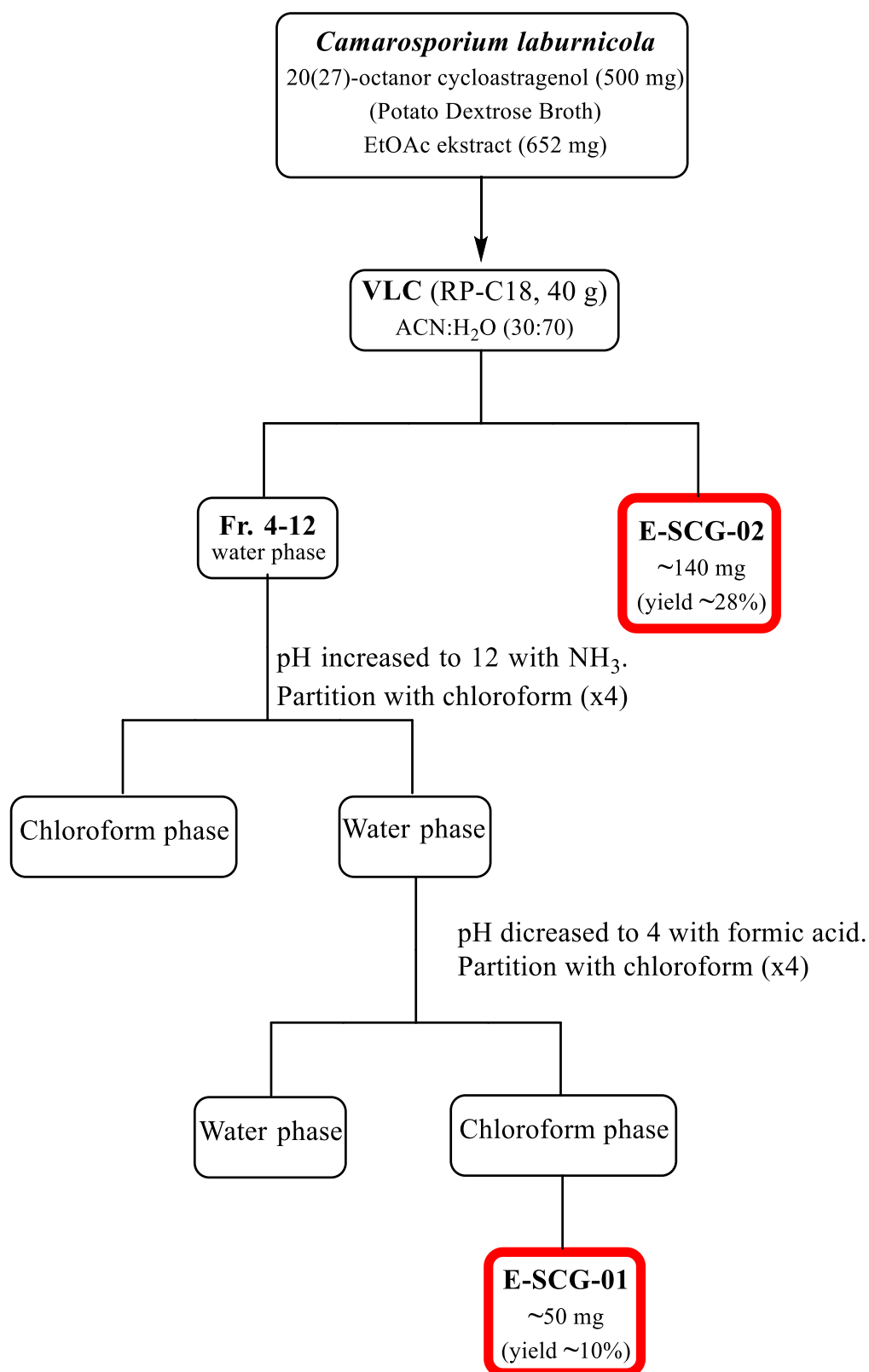


Figure 2.10 Isolation scheme of *Camarosporium laburnicola* EtOAc extract

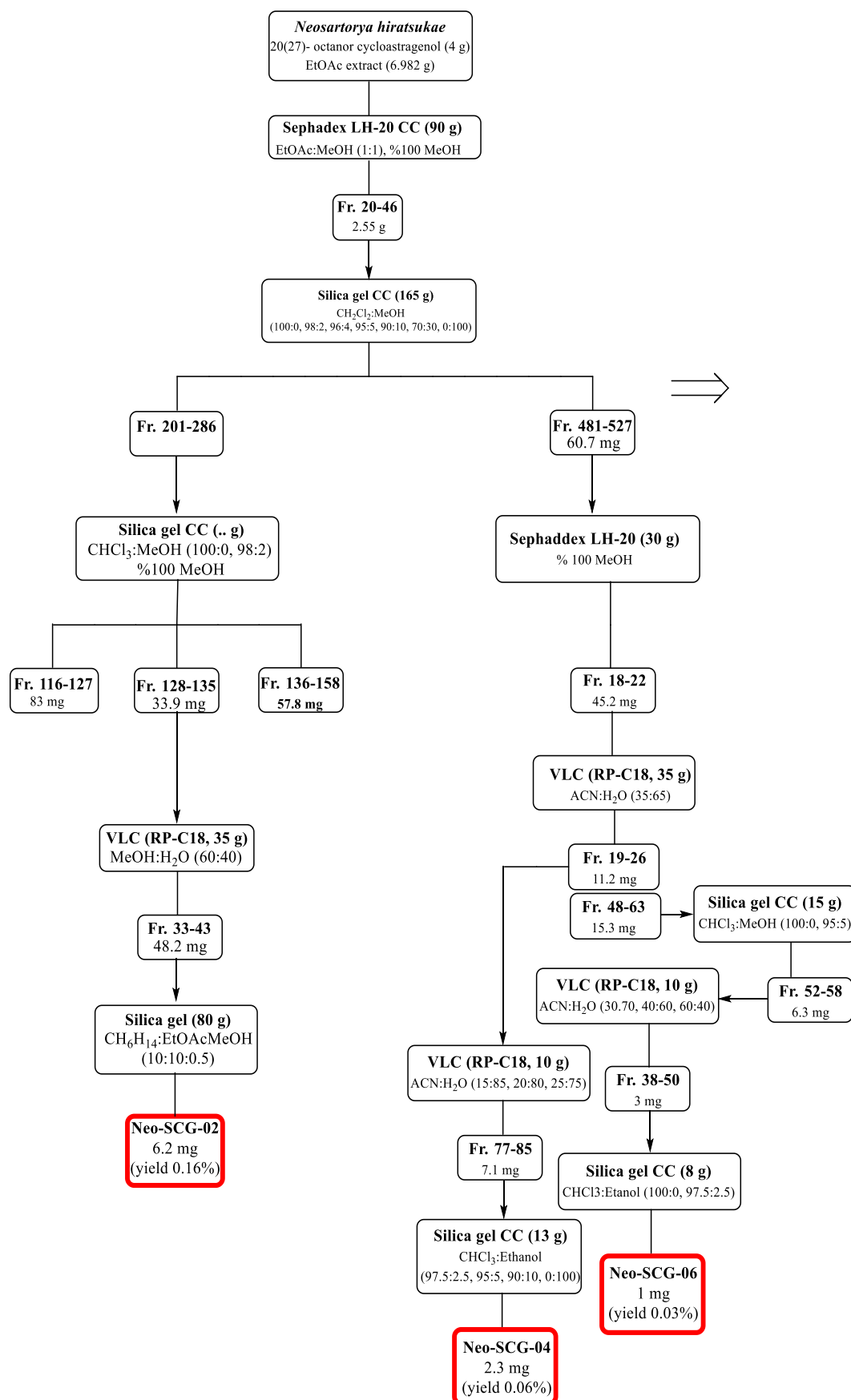


Figure 2.11 Isolation scheme of *Neosartorya hiratsukae* EtOAc extract (Part 1)

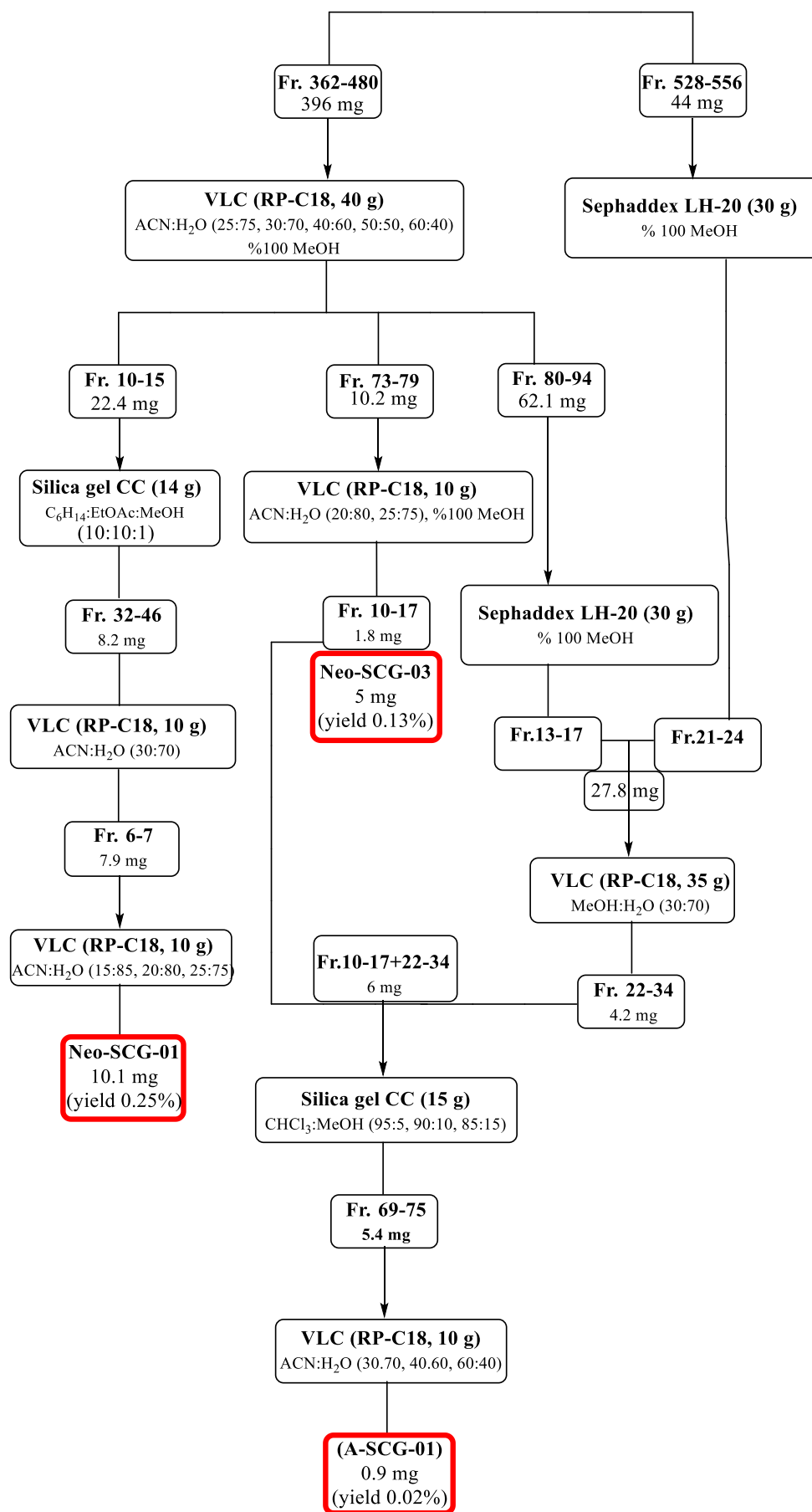


Figure 2.12 Isolation scheme of *Neosartorya hiratsukae* EtOAc extract (Part 2)

2.2.3 Bioactivity Screening Studies

In parallel to biotransformation studies, the metabolites with sufficient amount and high purity were tested towards activation of telomerase versus DMSO control group on HEKN cell line.

2.2.3.1 Determination of Telomerase Activation

TELOTAGGG PCR ELISA^{PLUS}kit (Roche; 12013789001, 16X version) which have a highly sensitive and quantitative method in telomerase negative cells such as human fibroblast and keratinocyte cells, was used in the discovery of telomerase activators. The TELOTAGGG Telomerase PCR ELISA^{PLUS}kit steps are schematized in Figure 2.13.

Studies were carried out according to the optimized TELOTAGGG PCR ELISA^{PLUS}kit protocol:

I. Preparation of the cellular extract:

The purified molecules were applied to Hekn cell lines at previously determined dose range. Upon completion of the 24-hour incubation, the cells were collected and counted by hemocytometer.

- 2×10^5 cells were transferred to clean ependorf and centrifugated at 3000 g for 5 min (+ 2- + 8 degrees).
- The supernatant was carefully removed without damaging the cell pellet.
- The pelleted cells were suspended in 200 μ l lysing buffer (Solution 1) and incubated on ice for 30 min.
- Optional: If the lysis process is not performed immediately, the pellets can be stored at -80 ° C until use. If frozen cell pellets are to be used; The pellets should be thawed on ice before the lysing buffer was added.
- After completion of incubation period: The lysates were centrifugated at 16000 g for 20 min (+2- +8 degrees).
- The supernatant was cooled and transferred to clean ependorfs carefully.

II. Elongation / Amplification:

Optional: If PCR reaction won't be performed immediately; the obtained lysates should be stored at -80°C.

The PCR reaction is designed for the group of samples and the control group. For both positive-negative samples and the sample to be investigated, 25 µl of the reaction mixture (Solution 2) and 5 µl of the internal standard solution (Solution 3) were transferred into the PCR tubes

For samples:

- 2 µl of cell lysate was added for each PCR sample.

For control group:

- From a low or high concentration TS8 control sample (Solution 4 or 5), 1 µl was transferred to another PCR tube.
- From the lysis buffer (Solution 1), 1 µl was transferred to another PCR tube.

(The lysis buffer acts as a negative control group.)

Table 2.4 PCR program

	Time	Temperature	Cycle
Primary Elongation	10-30 dk	25°C	1
Telomerase inactivation	5 dk	94°C	1
Amplification:			
Denaturation	30 s	94°C	30
Connecting (Annealing)	30 s	50°C	
Polymerization	90 s	72 °C	
	10 dk	72 °C	1
Finale temperature		4 °C	

III. Hybridization and photometric detection

- For each sample 10 µl of denaturing agent (Solution 7) was added to 96-well plates without nuclease.
- 2.5 µl of the amplification product was transferred to well plate and incubated for 10 min at +15 and +25 ° C
- According to the determined flow chart; 100 µl Hybridization Buffer T (Solution 8) was added to some of the samples and 100 µl Hybridization Buffer IS (Solution 9) was added to the other samples.
- After homogenization, 100 µl of the reaction mixture were taken and transferred to the MP module coated with streptavidin.

- After the transfer process; the MP module was incubated at 300 rpm for 2 hours at 37°C.
- When the incubation was complete, the hybridization solutions were carefully removed.
- Each well was washed 3 times with 1X Wash buffer (Solution 10) (250 µl was added per well in each wash and Wash buffer was carefully removed.).
- The prepared Anti-DIG-HRP solution (Solution 11) was added to each well.
- The MP module was carefully covered with special coating paper and incubated at 300 rpm for 30 min at 15-25 ° C.
- Once the incubation is complete, the solution was carefully removed from the well.
- Each well was washed 5 times with 1X Wash buffer (Solution 10). (250 µl was added per well each wash and the wash buffer was carefully removed.)
- 100 µl of TMB substrate solution (Solution 13) heated at room temperature was added to each well.
- The MP module was carefully covered with special coating paper and incubated at 300 rpm for 10-20 minutes at 15-25 ° C.
- When the incubation is complete, the color change was terminated by adding the Finishing agent (Solution 14) without any removal.
- Within 30 minutes, the samples were measured at 450 nm and 690 nm (reference wavelength) using Microplate reader.

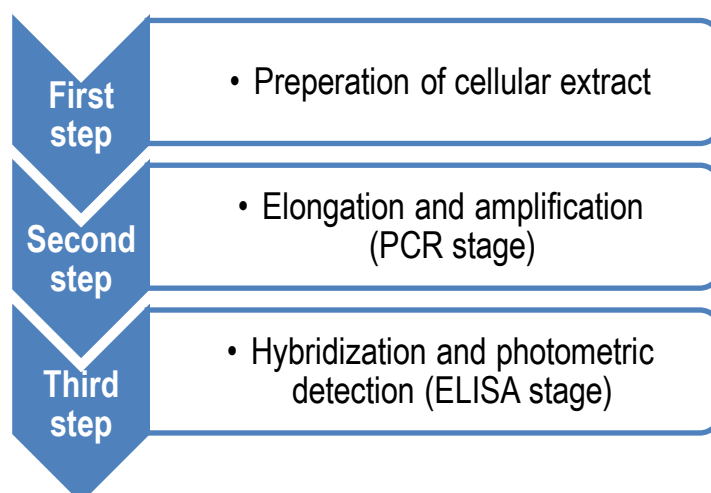


Figure 2.13 TELOTAGGG Telomerase PCR ELISA^{PLUS} kit steps

CHAPTER 3

RESULTS AND DISCUSSION

3.1 Results of Biotransformation Studies

Biotransformation studies were performed on two scales as indicated in chapter 2. As a result of screening studies, organisms with a higher metabolite content were selected and preparative scale studies were started. The metabolite profiles obtained as a result of the screening studies are shown in Figure 3.1.

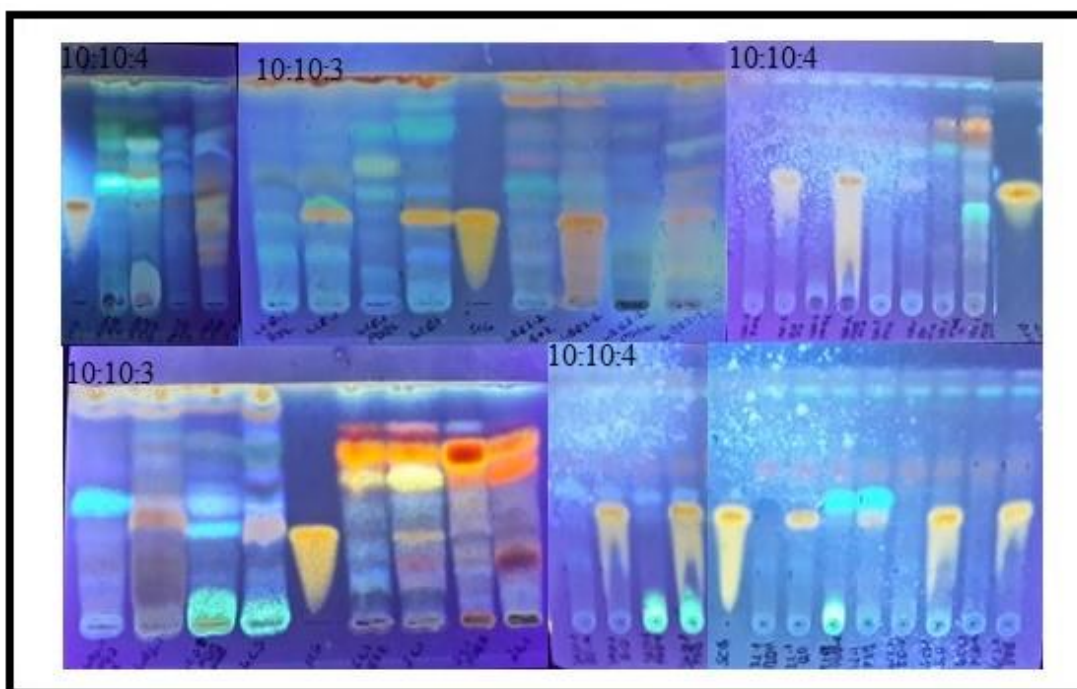


Figure 3.1 The metabolite profiles of screening biotransformation studies n-Hex:EtOAc:MeOH (Silica gel, 10:10:3, 10:10:4)

3.2 Structure Elucidation of The Pure Compounds

As a results of biotransformation studies performed with *Alternaria eureka*, *Camarosporium laburnicola* and *Neosartorya hiratsukae*, 15 metabolites, 14 of which

were new, were isolated. Structure determination of the metabolites was performed based on spectroscopic methods (1D-, 2D NMR and MS).

3.2.1 Pure Compounds Isolated from Biotransformation by *Alternaria eureka*

A-SCG-01, A-SCG-03, A-SCG-06, A-SCG-07, A2-SCG-01, A2-SCG-02 and A2-SCG-03 were isolated from biotransformation study of 20(27)-octanor cycloastragenol by *Alternaria eureka*.

3.2.1.1 Structure Elucidation of A-SCG-01

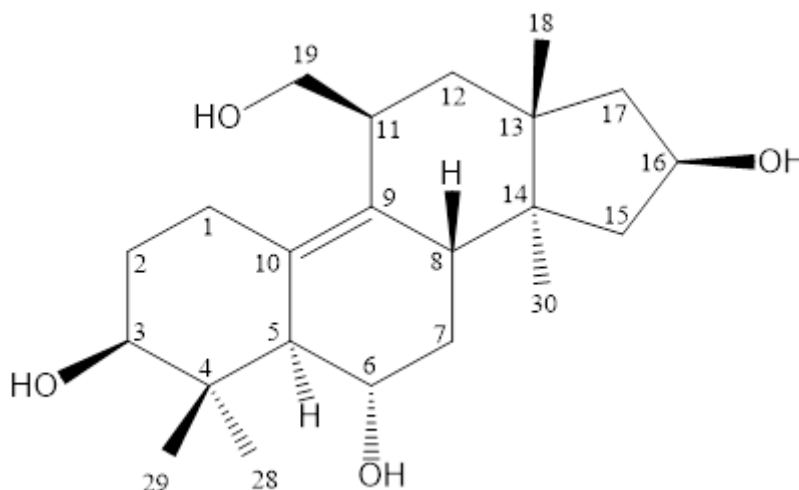


Figure 3.2 Chemical structure of A-SCG-01

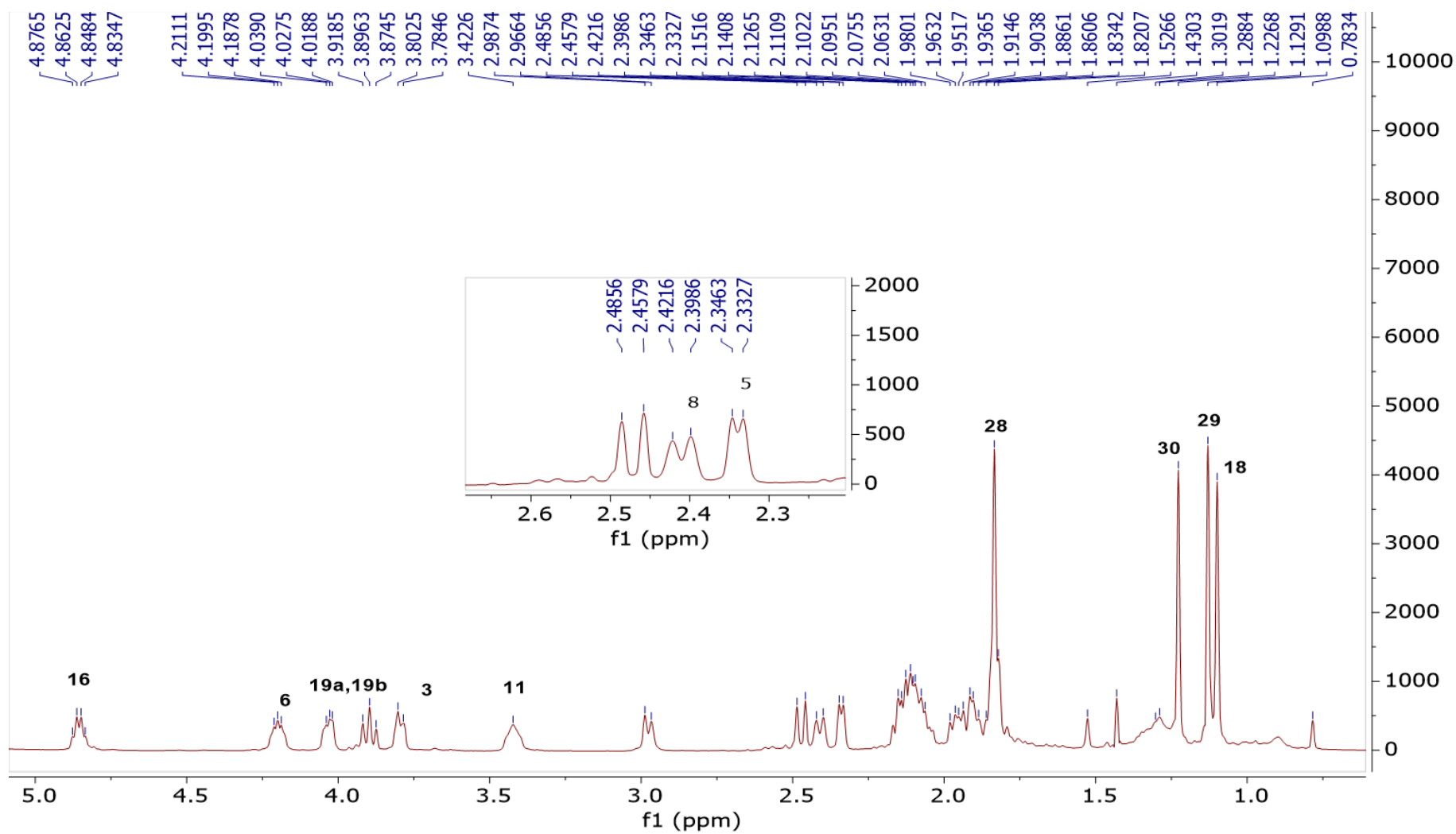
The absence of the characteristic AX system signals in the up-field region belonging to the 9,19- cyclopropane ring in the ^1H -NMR spectrum implied a ring cleavage. Four tertiary methyl groups in the up-field region, and the characteristic signals belonging to the H-3, H-6 and H-16 oxymethyne protons were observed readily. In the DEPT-135 and ^{13}C -NMR spectrum, the presence of a new oxymethylene resonance at δ 68.9 in the low field suggested a monooxygenation, whereas two double bond signals (δ 135.8, 133.7) were also appearant in the carbon spectrum. Based on no correlation of the double bond carbons with any proton in the HSQC spectrum, the presence of a tetrasubstituted olefinic system was verified. Based on our previous studies with those of

Astragalus sapogenols metabolized by *C. blakesleeana*,^{78, 81} **A-SCG-01** was proposed to go through a ring-cleavage followed by a methyl migration affording a C-9(10) double bond with a primary alcohol substitution at C-11. This assumption was also confirmed with the $^2J_{C-H}$ and $^3J_{C-H}$ long-distance correlations in the HMBC spectrum from C-10 to H-5; C-9/C-10 to H-1, and C-19 to H₂-12.

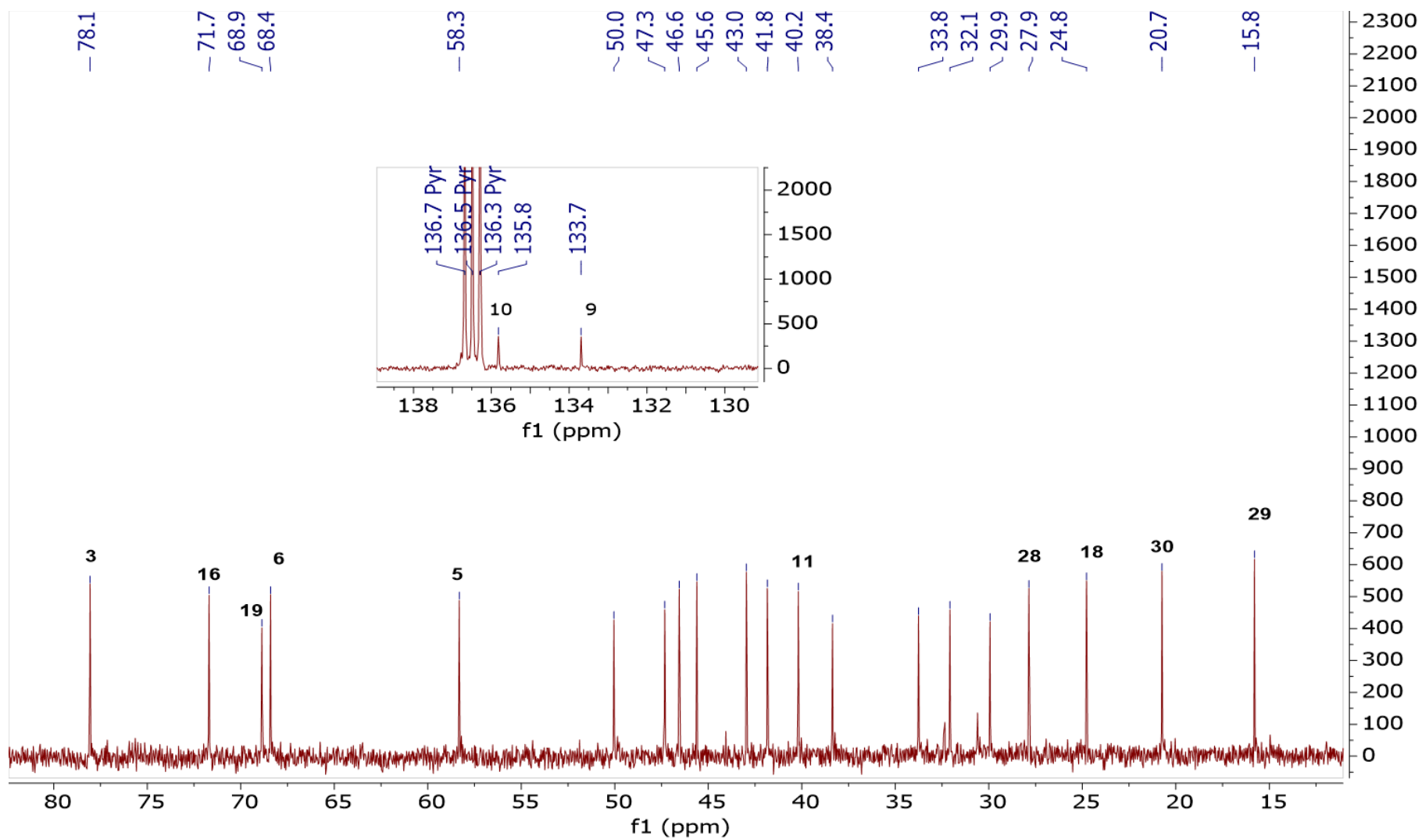
The methyl migration to position C-11 created a new stereocenter on the structure. Relative stereochemistry of this center was determined by evaluating the ROESY correlations. The δ 4.03 resonance (one of the H₂-19 protons) in the low field showed strong correlation with the δ 2.98 signal (one of the H-1 protons). This H-1 proton was not interacting with H-5 indicating that it was on the upper face (β) of the molecule. On the other hand, the weak interaction of the other H-19 proton (δ 3.90), with both H₃-18 and the δ 2.47 signal of H-12, correlating with each other, substantiated that the C-19 had β configuration. Thus, the structure of **A-SCG-01** was established as shown in Figure 3.2.

Table 3.1 1H and ^{13}C NMR data of A-SCG-01 (125/500 MHz, C₅D₅N)

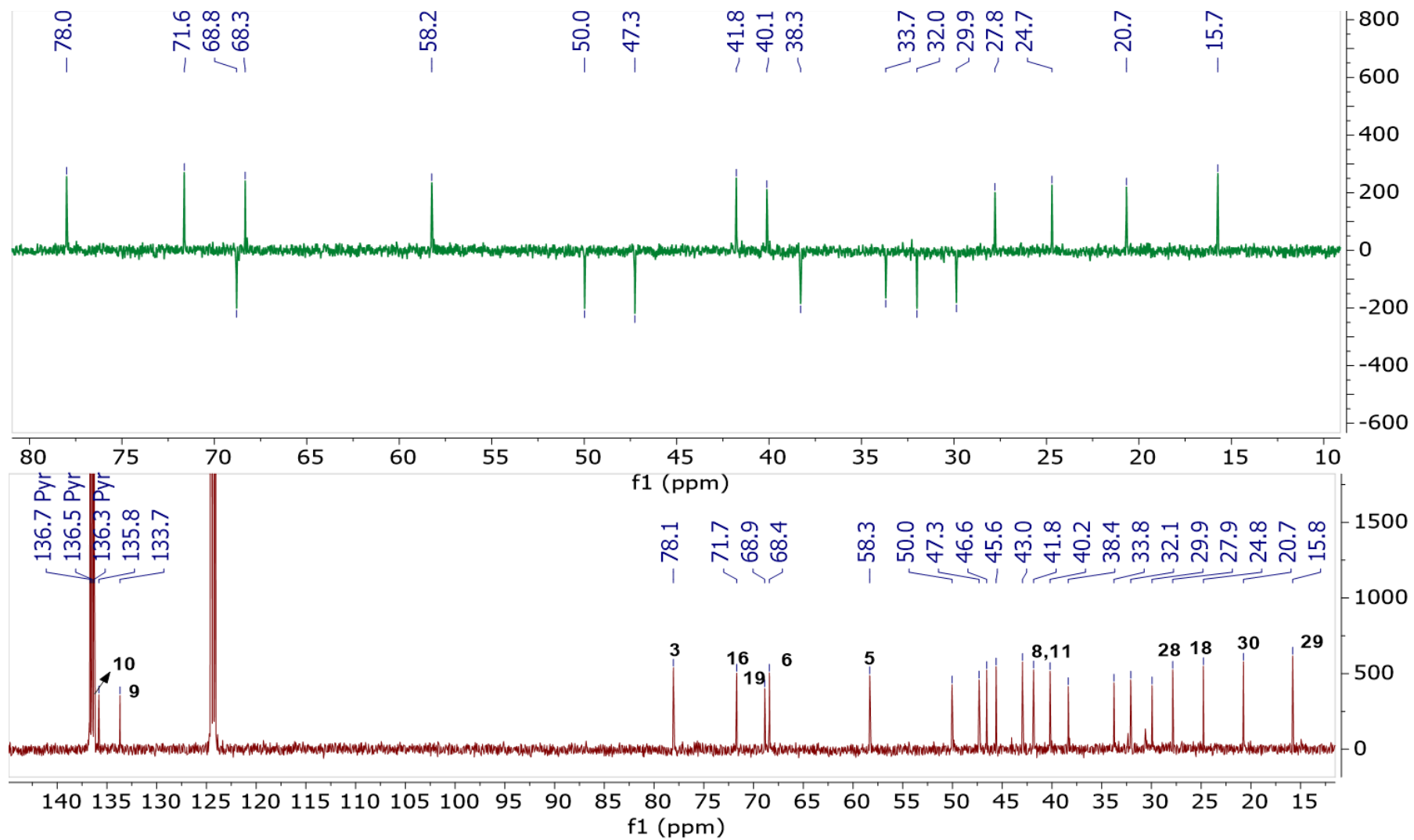
C/H	δ_C (ppm)	δ_H (ppm), J (Hz)
1	29.9	2.98 d (10.5), 1.91 m
2	33.8	1.91 m, 2.10 m
3	78.1	3.79 m
4	43.0	
5	58.3	2.34 d (6.8)
6	68.4	4.20 m
7	38.4	1.83 m, 2.09 m
8	41.8	2.41 d (11.5)
9	133.7	
10	135.8	
11	40.2	3.42 m
12	32.1	1.96 dd (8.0, 13.8), 2.47 d (13.8)
13	46.6	
14	45.6	
15	47.3	1.83 m, 2.14 m
16	71.7	4.86 m
17	50.0	2.05 m, 2.13 m
18	24.8	1.10 s
19	68.9	3.90 t (11.0), 4.03 m
28	27.9	1.83 s
29	15.8	1.13 s
30	20.7	1.23 s



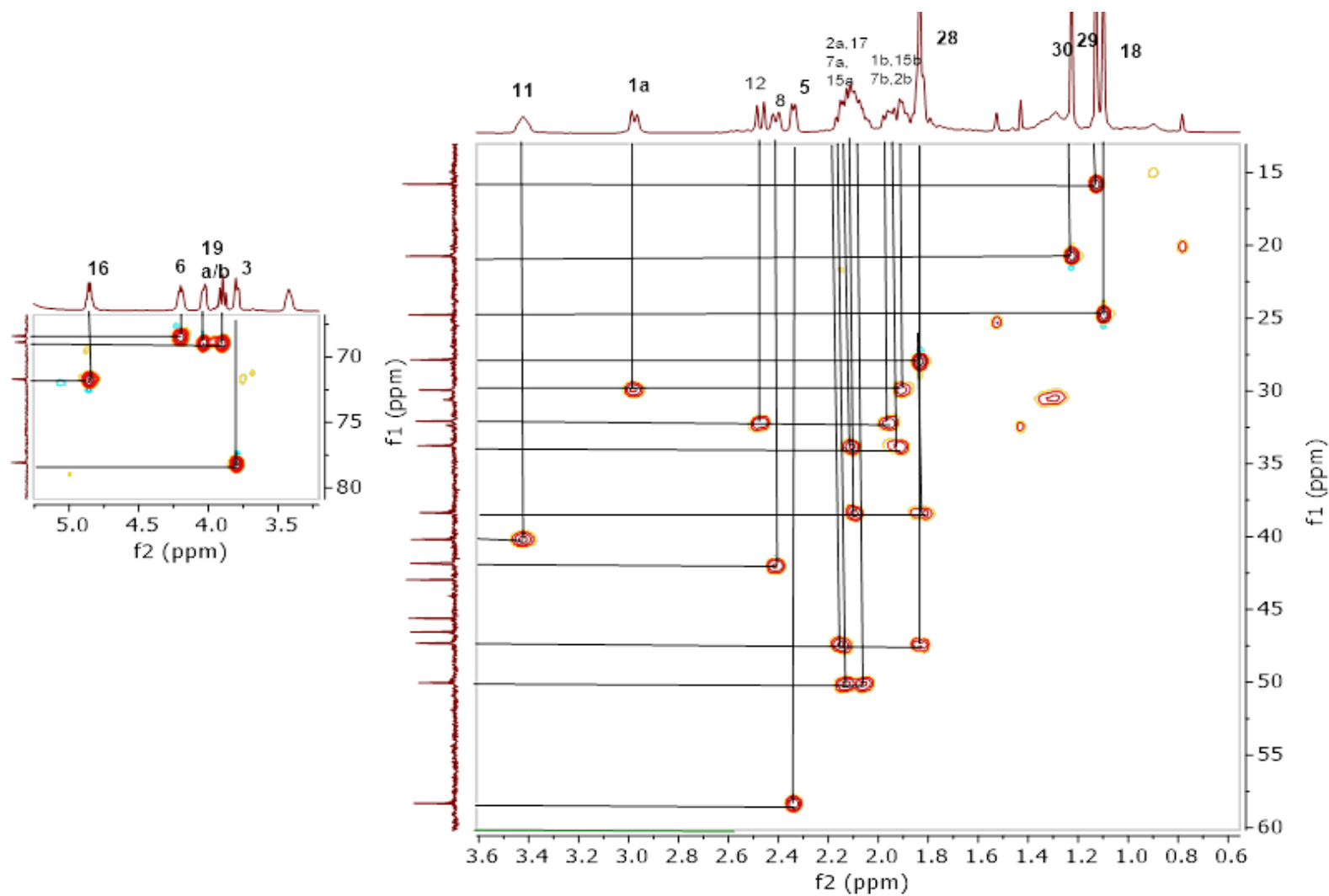
Spectrum 3.1 ^1H -NMR Spectrum of A-SCG-01



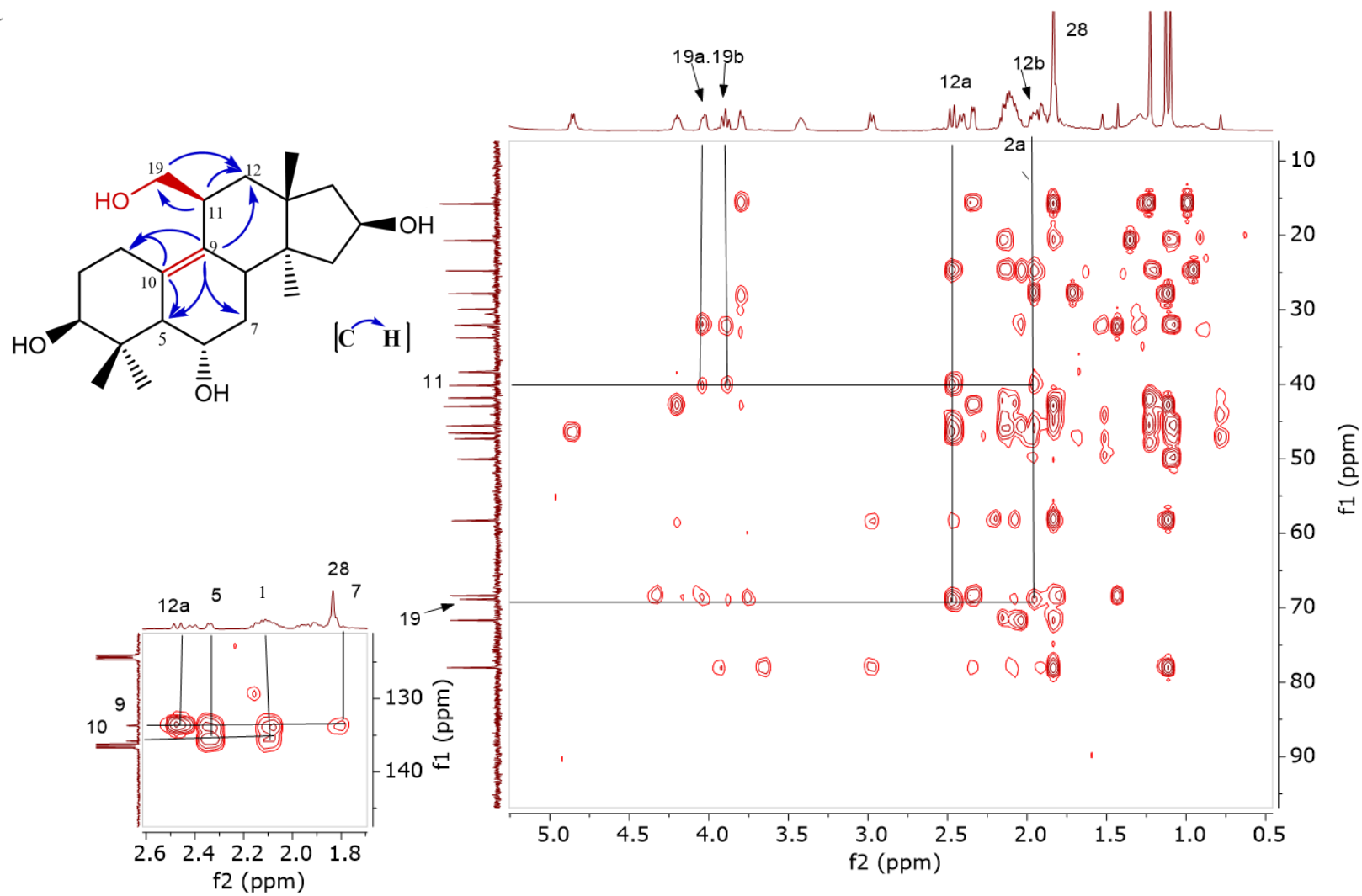
Spectrum 3.2 ^{13}C -NMR Spectrum of A-SCG-01



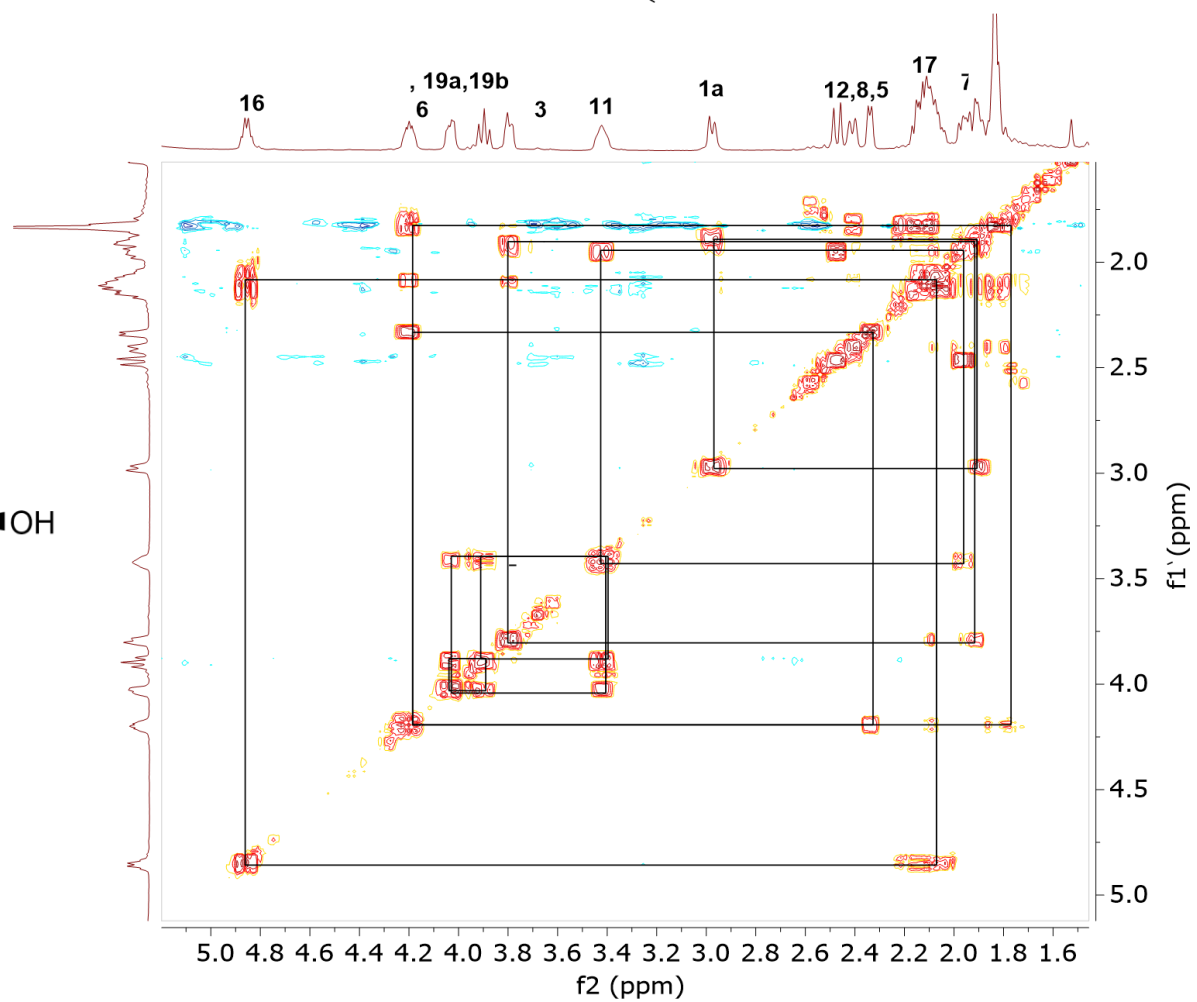
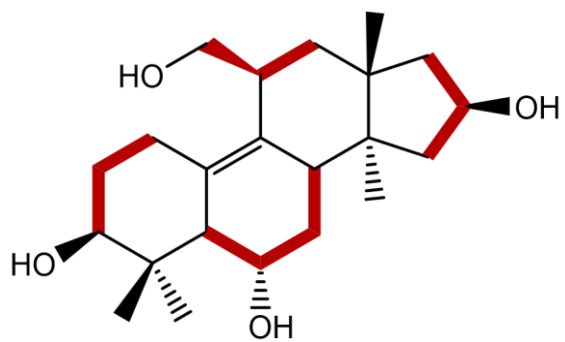
Spectrum 3.3 DEPT spectrum of A-SCG-01



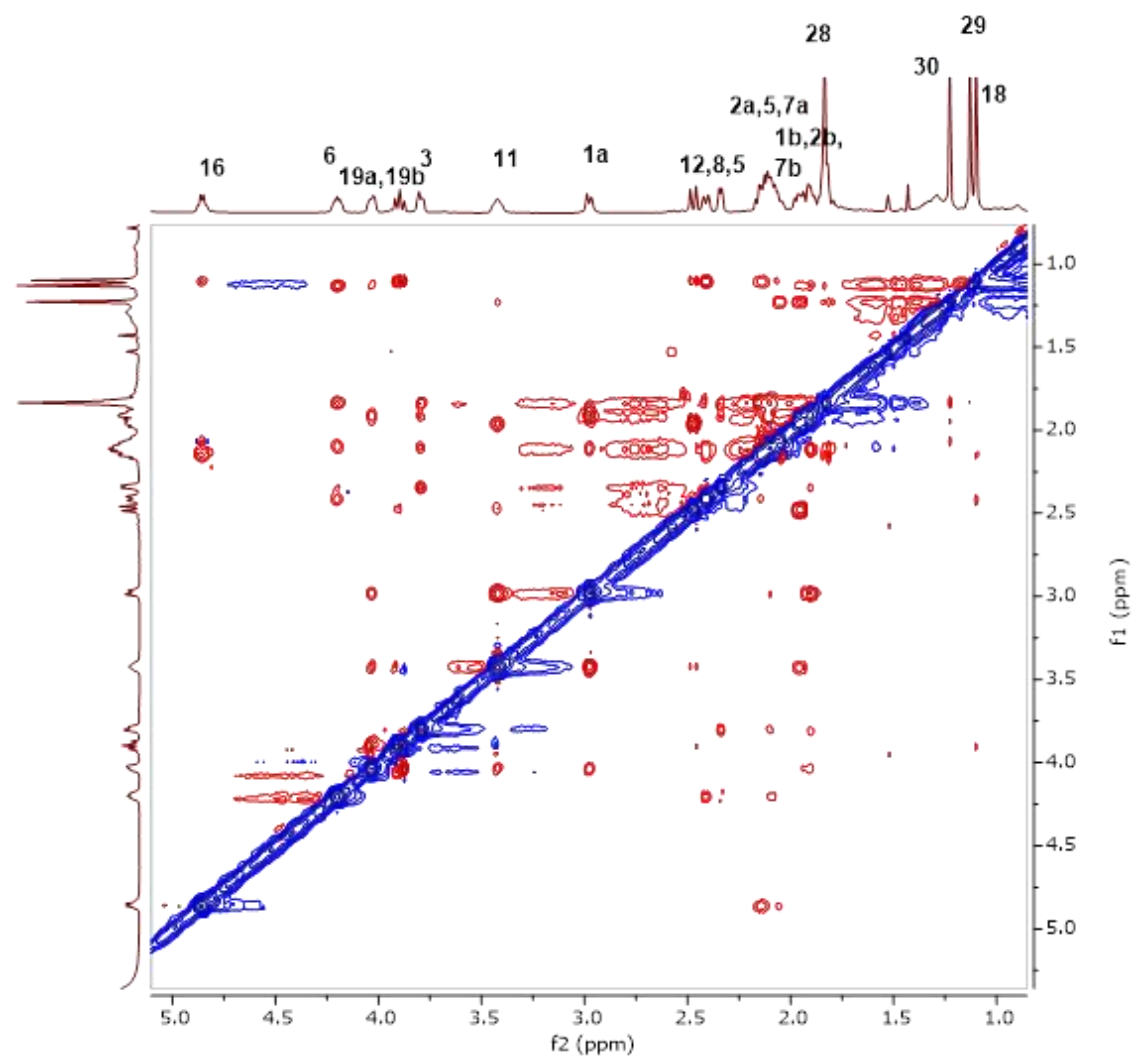
Spectrum 3.4 HSQC spectrum of A-SCG-01



Spectrum 3.5 HMBC spectrum of A-SCG-01



Spectrum 3.6 COSY spectrum of A-SCG-01



Spectrum 3.7 ROESY spectrum of A-SCG-01

3.2.1.2 Structure Elucidation of A-SCG-03

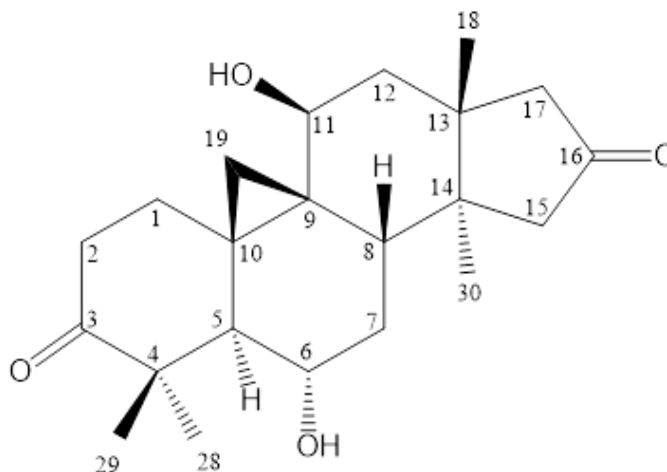


Figure 3.3 Chemical structure of **A-SCG-03**

In the HR-ESI-MS spectrum of **A-SCG-03**, a major ion peak was observed at m/z 395.1992 $[M+Cl]^-$ suggesting the molecular formula $C_{22}H_{32}O_4$.

In the 1H -NMR spectrum, four tertiary methyl group signals were observed in the up-field region, while one of the distinctive 9,19-cyclopropane ring AX system signals was missing (δ 0.61, H-19b). A detailed inspection of the COSY and HSQC spectra revealed that H-19a (δ 1.70) undergone a significant down field shift (ca. 1.0 ppm). The observed down-field shift is a common feature of C-11 hydroxylated cycloartanes.⁷⁶ Additionally, the distinctive hydroxymethine protons H-3 and H-16 were not present in the 1H -NMR spectrum, indicating their oxidation. The additional oxymethyne proton at δ 4.31, which corresponded to a carbon at δ 64.5 in the HSQC spectrum, was readily assigned to H-11 verifying monooxygenation. The ^{13}C NMR spectrum of **A-SCG-03** was low-quality due to its scarce amount; therefore, the carbon data was unambiguously determined by the HSQC and HMBC spectra. The HMBC spectrum of the **A-SCG-03** showed that two resonances lower than 0 ppm in the F1 plane interacted with the signals in the up-field. The reason was an operational error due to setting the sweep width narrow for carbon scale. So, the carbonyl carbons resonating over 210 ppm were folded in the spectrum and were observed below 0 ppm. This important observation verified aforementioned oxidations in the structure. Accordingly, the $^3J_{C-H}$ long-distance interactions of one of these carbonyl signals with H₃-28 (δ 1.50) and H₃-29 (δ 1.80) protons in the HMBC spectrum, and low-field shift of the H-2 proton signals (δ 2.61 and

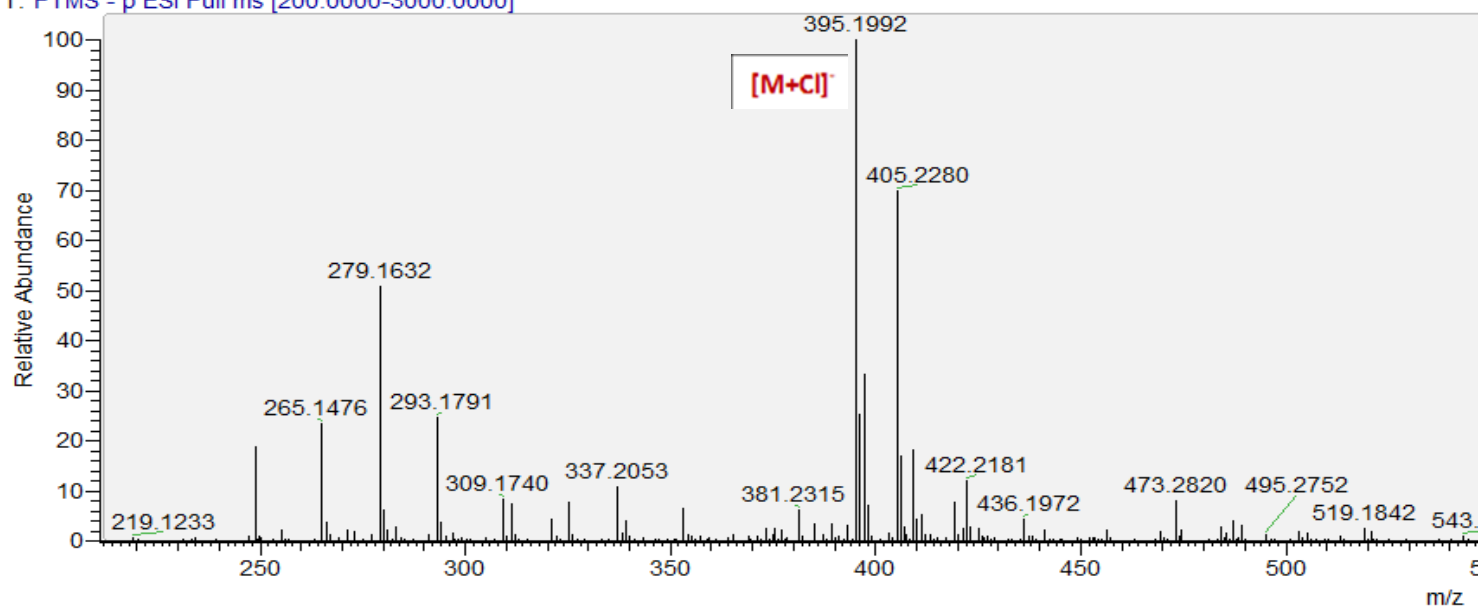
2.74) substantiated the oxidation at C-3 position. The proton signals originating from the methylene groups detected in the HSQC (H₂-15: δ 2.12, 2.37; H₂-17: δ 2.07, 2.47) resonated in the lower field slightly, whereas these protons showed cross peaks with the other carbonyl carbon in the HMBC spectrum. Based on this data, the second carbonyl group was undoubtedly located at C-16.

In addition, low-field shift of C-12 resonance together with the $^3J_{C-H}$ long-distance correlation of δ 64.5 signal with one of H₂-12 protons (δ 2.55) were evident to prove abovementioned hydroxylation at C-11. The orientation of C-11(OH) was determined by evaluating the ROESY spectrum. The interaction between H-11 (δ 4.31) and H₃-30 (δ 1.04) was evident to conclude that C-11 (OH) was β -oriented. As a result, the structure of **A-SCG-03** was identified as 11 β -hydroxy,3,16-dioxo-20(27)-octanor cycloastragenol.

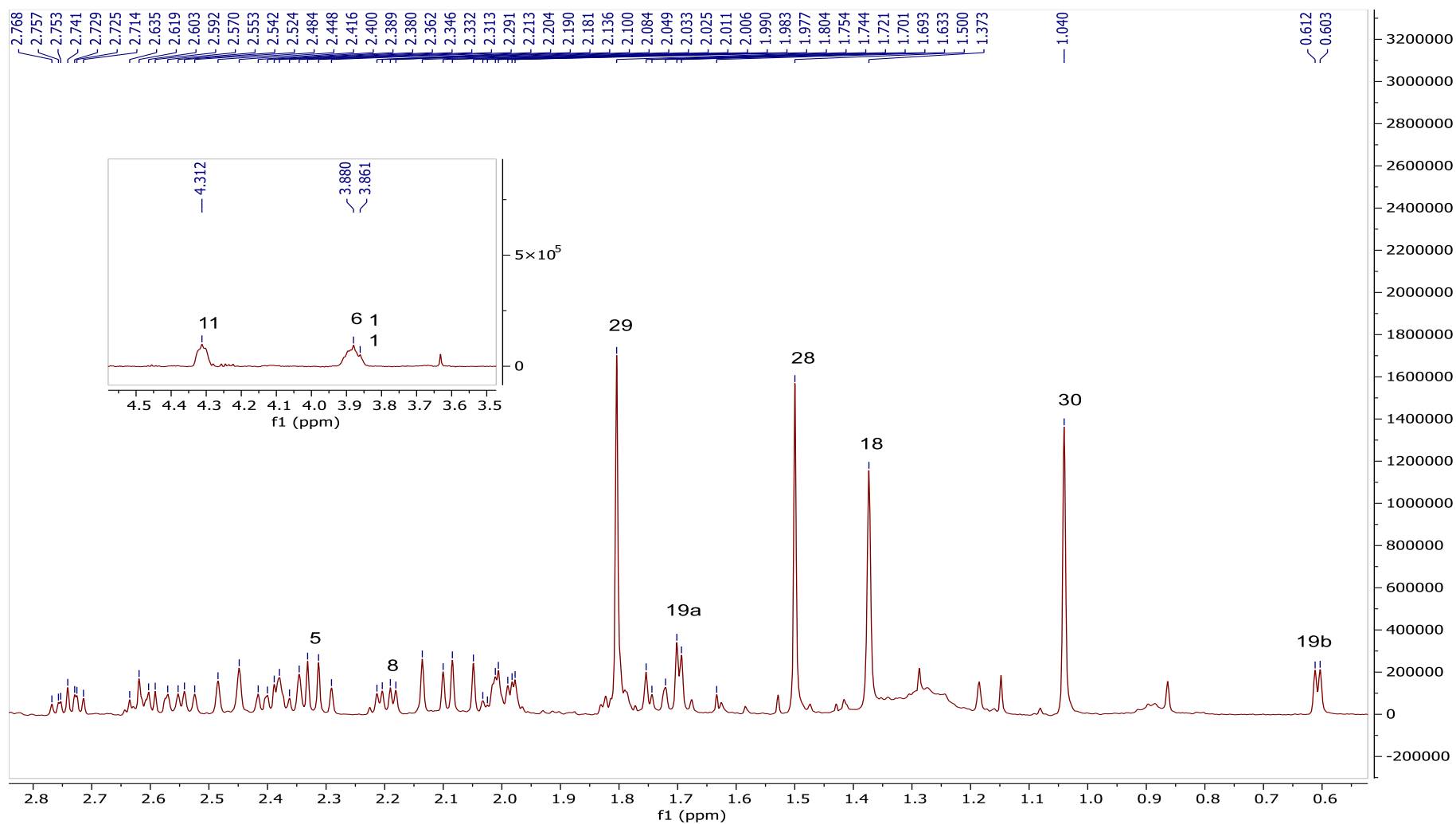
Table 3.2 ^1H and ^{13}C NMR data of **A-SCG-03** (125/500 MHz, C₅D₅N)

C/H	δ_{C} (ppm)	δ_{H} (ppm), J (Hz)
1	30.6	1.98 m, 2.38 m
2	37.1	2.61 m, 2.74 ddd (13.4, 7.6, 5.6)
3	+210.0	
4	51.3	
5	54.7	2.32 d (9.3)
6	68.4	3.87 m
7	39.0	1.70 m, 1.81 m
8	46.5	2.20 dd (11.5, 4.6)
9	29.3	
10	29.9	
11	64.5	4.31 m
12	44.8	1.98 m, 2.55 dd (14.2, 8.8)
13	42.3	
14	44.7	
15	51.1	2.12 d (17.7), 2.37 m
16	+210.0	
17	52.3	2.07 d (17.9), 2.47 d (18.1)
18	25.8	1.38 s
19	22.1	0.61 d (4.3), 1.70 d (3.9)
28	21.3	1.50 s
29	28.7	1.80 s
30	21.2	1.04 s

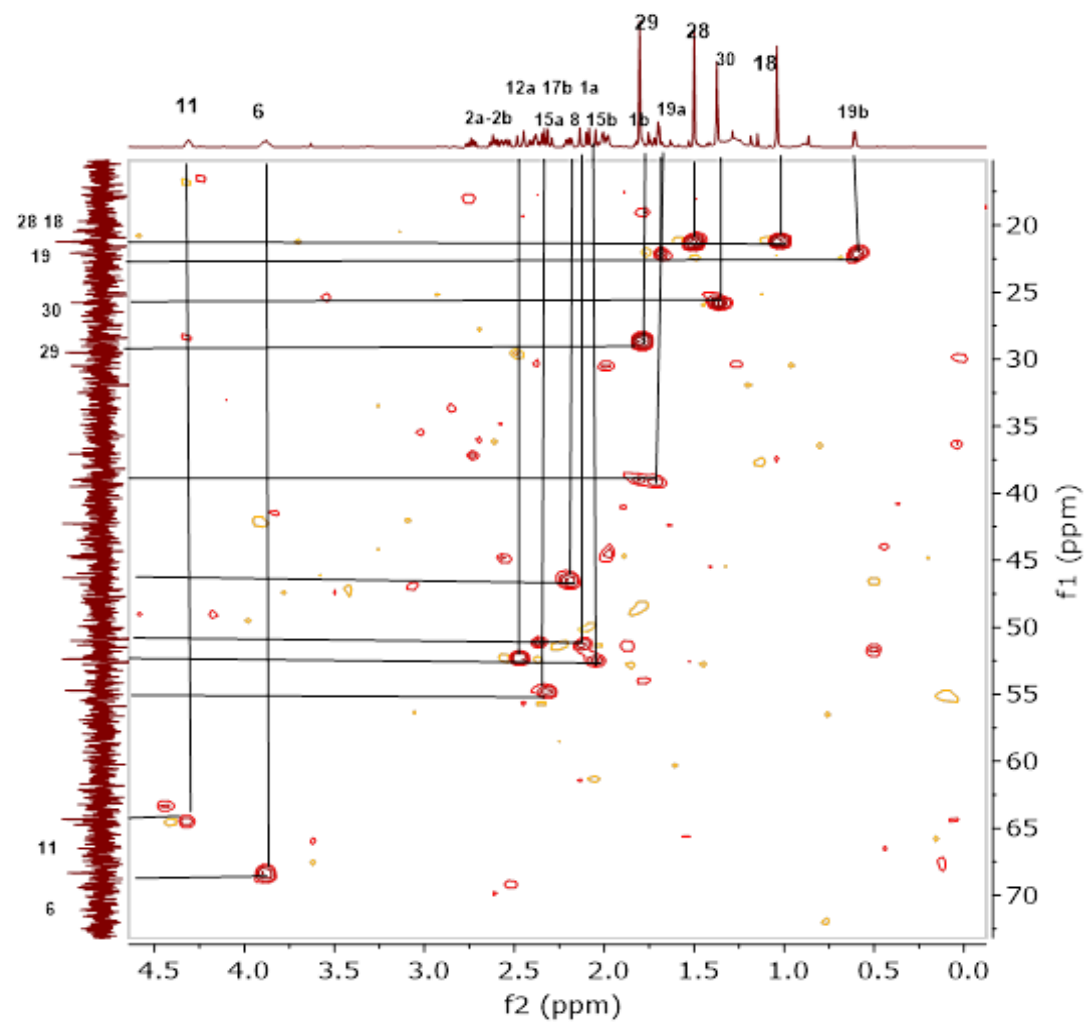
Erdal Sample A-SCG-03 Negative - 23-05-2019 #41 RT: 0.18 AV: 1 NL: 2.96E8
T: FTMS - p ESI Full ms [200.0000-3000.0000]



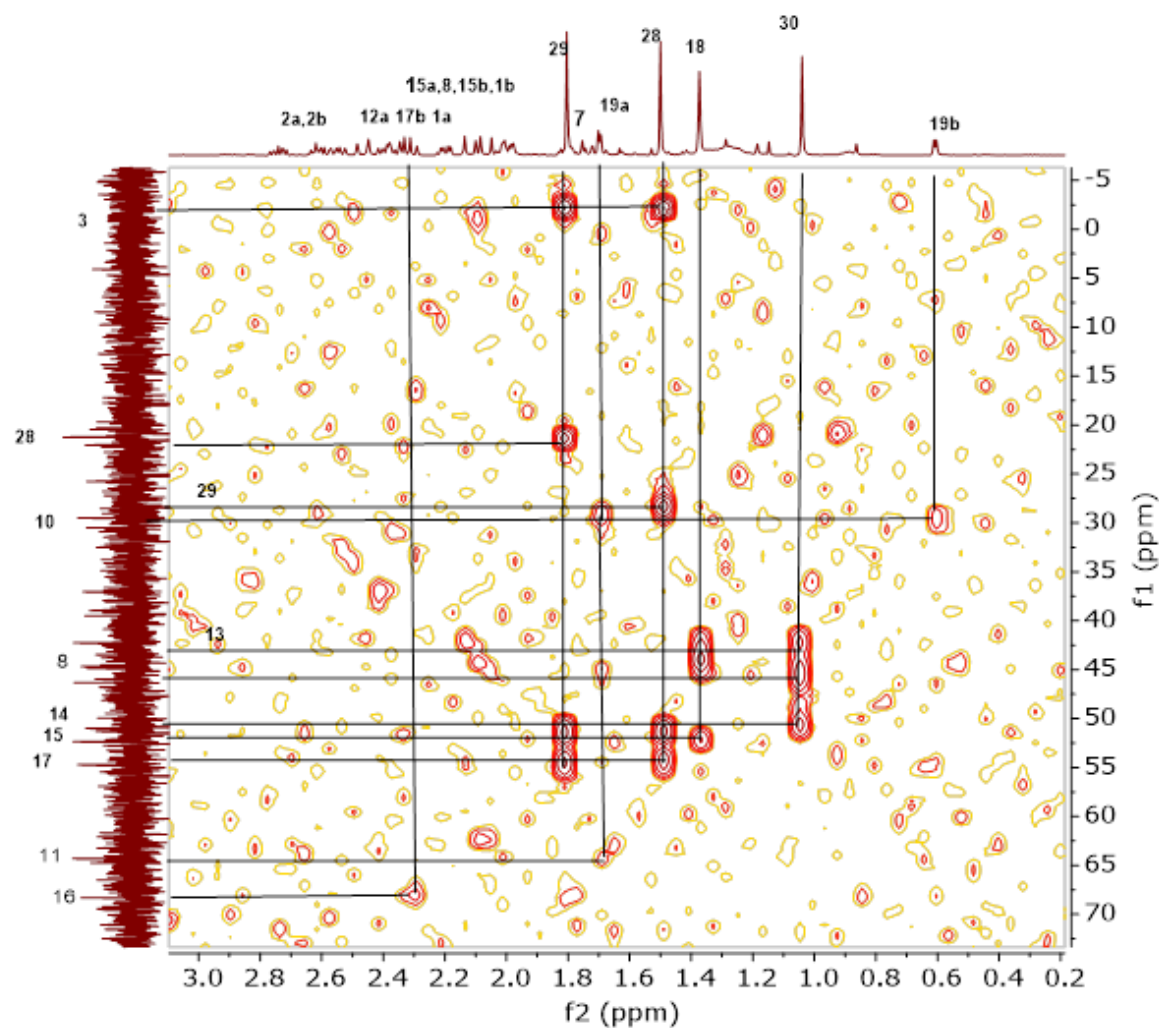
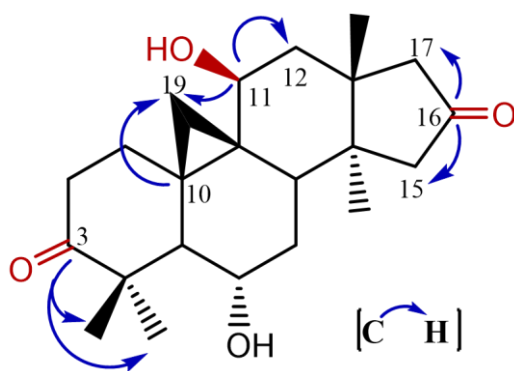
Spectrum 3.8 HR-ESI-MS spectrum of **A-SCG-03** (negative mode)



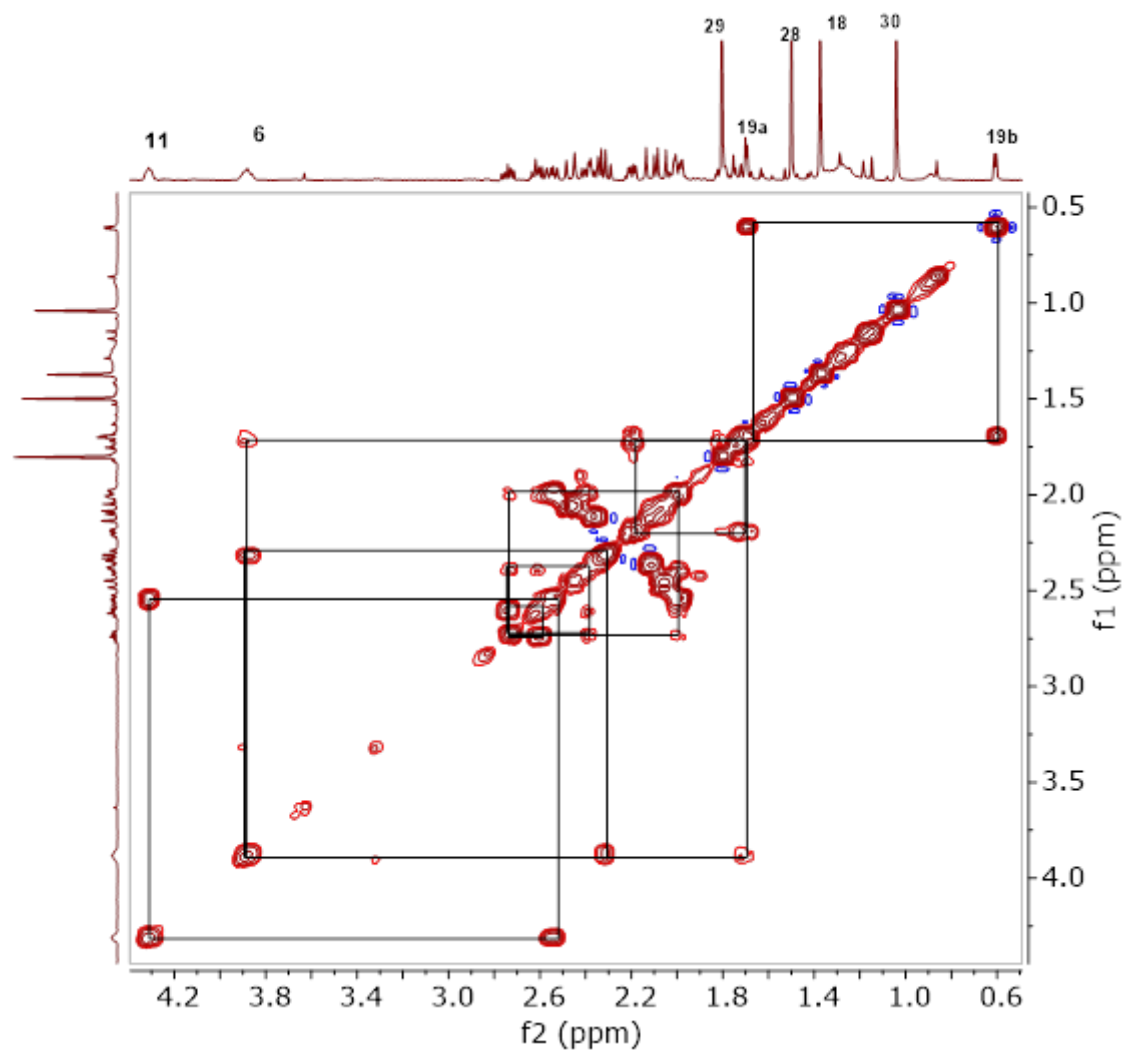
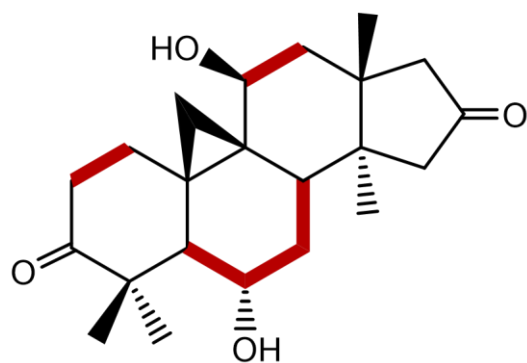
Spectrum 3. 9 ^1H -NMR Spectrum of A-SCG-03



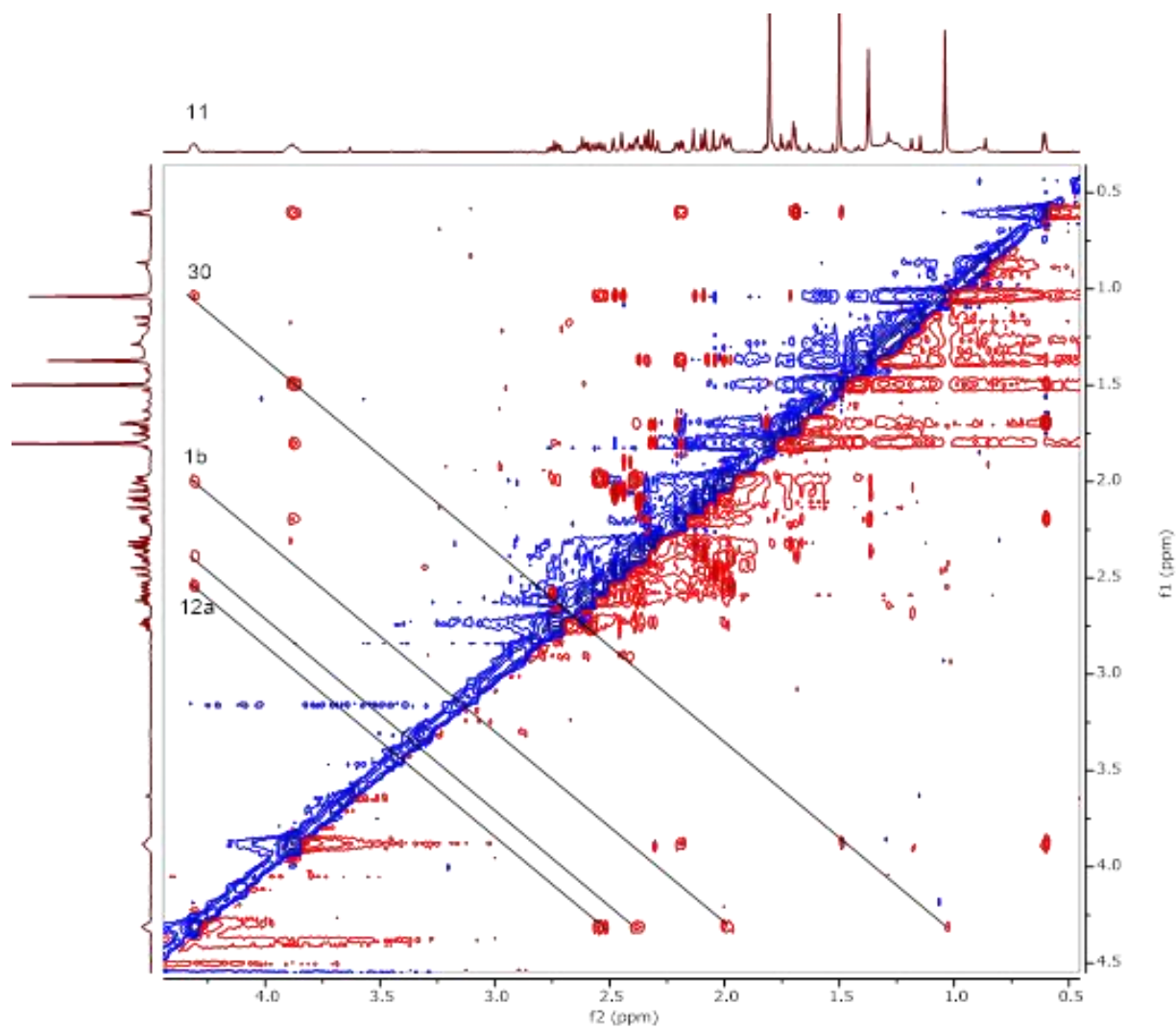
Spectrum 3.10 HSQC spectrum of A-SCG-03



Spectrum 3.11 HMBC spectrum of A-SCG-03



Spectrum 3.12 COSY spectrum of A-SCG-03



Spectrum 3.13 ROESY spectrum of A-SCG-03

3.2.1.3 Structure Elucidation of A-SCG-06

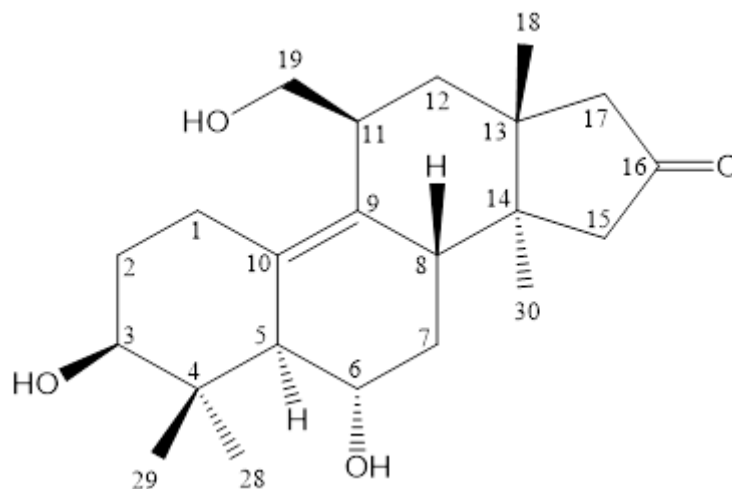


Figure 3.4 Chemical structure of **A-SCG-06**

In the HR-ESI-MS (negative mode) of **A-SCG-06**, a major ion peak was observed at m/z 397.2149 $[M+Cl]^-$ indicating a molecular formula of $C_{22}H_{34}O_4$.

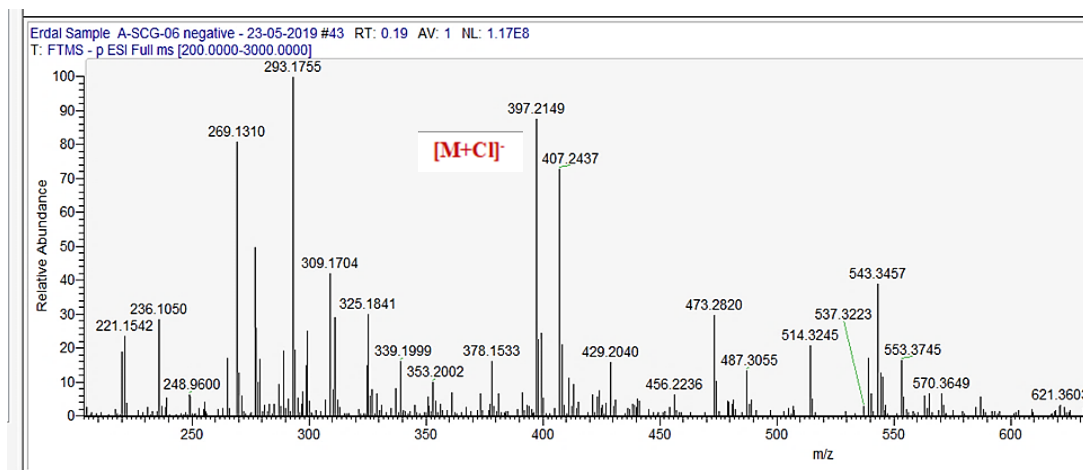
The minute amount of **A-SCG-06** resulted in unreadable carbon spectrum; therefore, full assignment of the carbon signals was based on interpretation of the HSQC and HMBC spectra.

In the 1H -NMR spectrum, the signals deriving from 9,19-cyclopropane ring were lacking, which implied a ring cleavage as in **A-SCG-01**. In addition, the hydroxymethine proton H-16 was absent. In the HSQC spectrum, the carbon signal at δ 68.2 correlated with two proton resonances at δ 3.88 and 4.02 (AB system), signifying an oxymethylene group. On the other hand, a carbonyl signal at δ +210.0 together with two olefinic carbon signals (δ 136.0 and 138.1) were evident from the HMBC spectrum. In the HSQC spectrum, no correlations of any protons with the double bond carbons indicated a tetrasubstituted olefinic system. The double bond was located between C-9 and C-10 based on the HMBC $^3J_{C-H}$ cross peaks from δ 136.0 (C-9) resonance to H-1 and H-5, as well as from δ 138.1 (C-10) to H-1. Furthermore, the HMBC correlation between H₂-12 and C-19 suggested that the cyclopropane methylene carbon (C-19) migrated over to C-11. The similarity between the spectral data of **A-SCG-01** and previously reported biotransformation products of cycloastragenol not only supported our assumption but also helped us to deduce the relative stereochemistry of C-19 to be β .^{76, 78} Additionally, the $^3J_{C-H}$ long-distance correlations of H₂-15 (δ 2.05 and 2.38) and H₂-17 (δ 2.43 and 2.03)

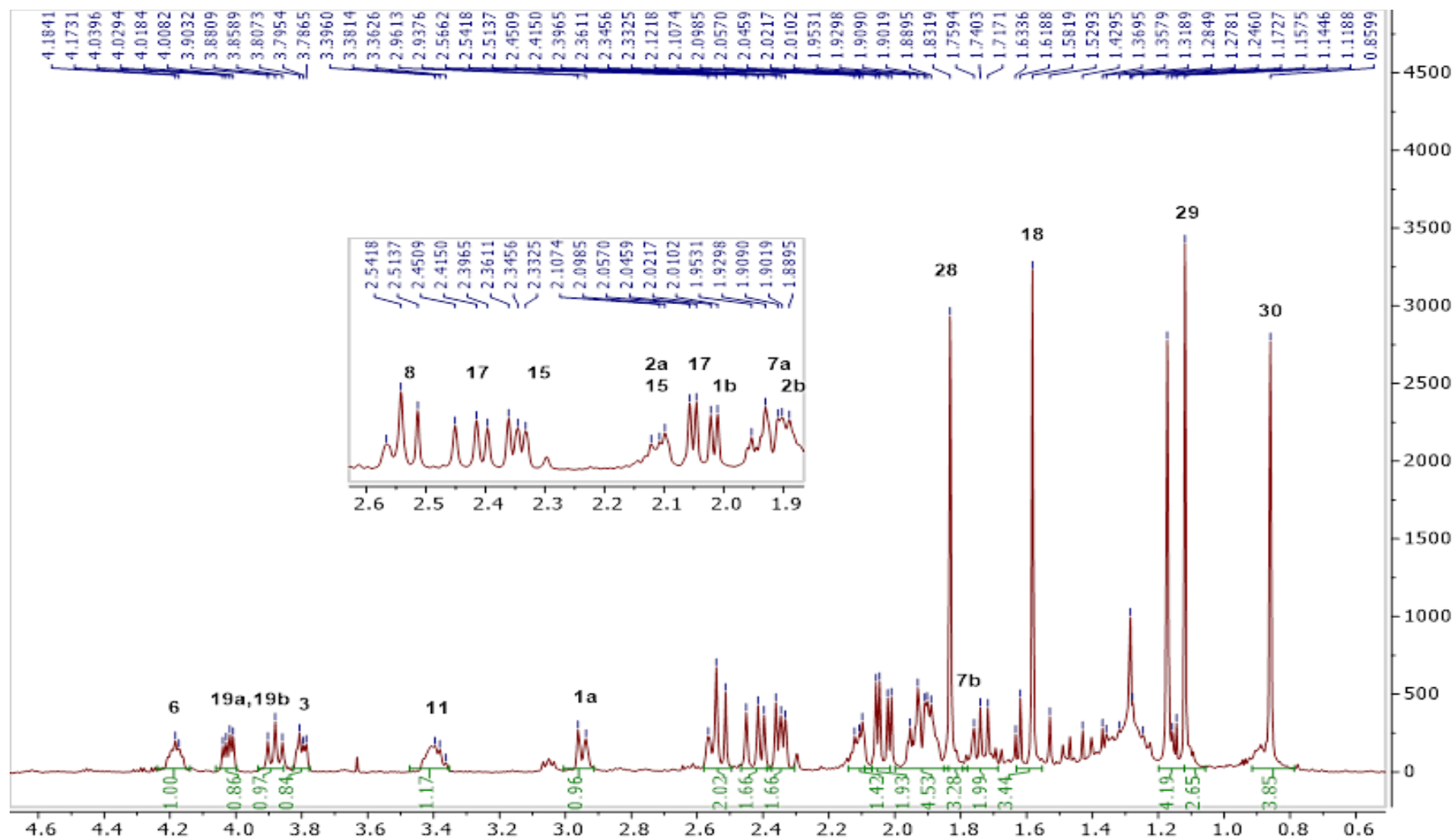
with the carbonyl carbon at δ +210.0 confirmed the oxidation to afford a C-16-oxo metabolite. It needs to be stressed that as the sweep width for carbon in the HMBC spectrum was not well adjusted, the carbonyl carbon was folded onto the spectrum as in **A-SCG-03**. As a result, the structure of **A-SCG-06** was identified as shown in Figure 3.4.

Table 3.3 ^1H and ^{13}C NMR data of **A-SCG-06** (125/500 MHz, $\text{C}_5\text{D}_5\text{N}$)

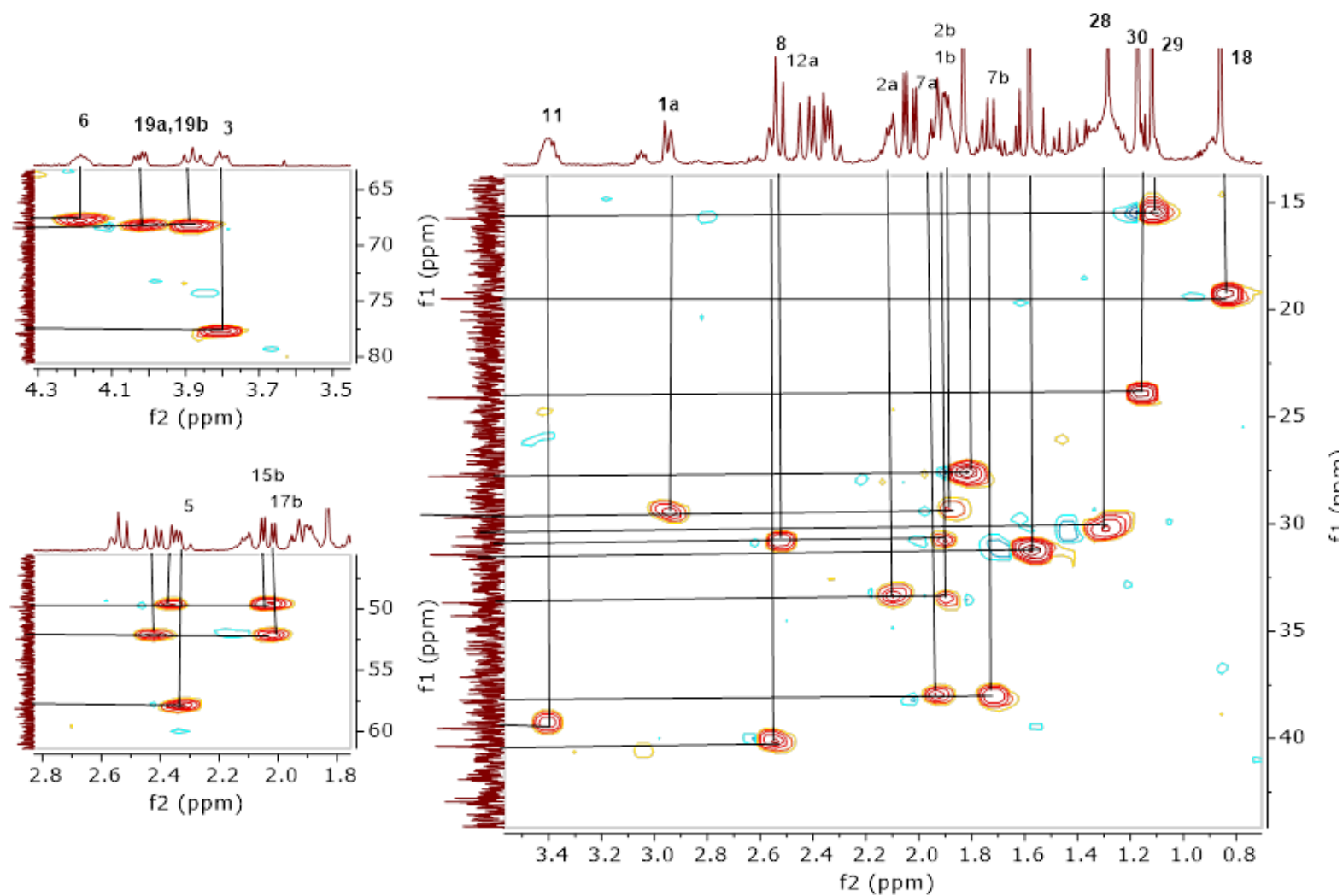
C/H	δ_{C} (ppm)	δ_{H} (ppm), J (Hz)
1	29.4	2.95 d (11.9), 1.88 m
2	33.4	2.10 m, 1.90 m
3	77.7	3.80 dd (10.5, 4.5)
4	42.9	
5	57.9	2.34 d (6.6)
6	67.8	4.18 m
7	38.0	1.94 m, 1.74 m
8	40.1	2.54 m
9	136.0	
10	138.1	
11	39.3	3.39 m
12	30.9	2.53 d (14.1), 1.90 m
13	44.2	
14	41.4	
15	49.6	2.05 d (17.5), 2.38 d (17.5)
16	+210.0	
17	52.1	2.03 d (18), 2.43 d (18)
18	23.9	1.17 s
19	68.2	4.02 dd (10.6, 5.1), 3.88 t (11.1)
28	27.6	1.83 s
29	15.5	1.12 s
30	19.3	0.86 s



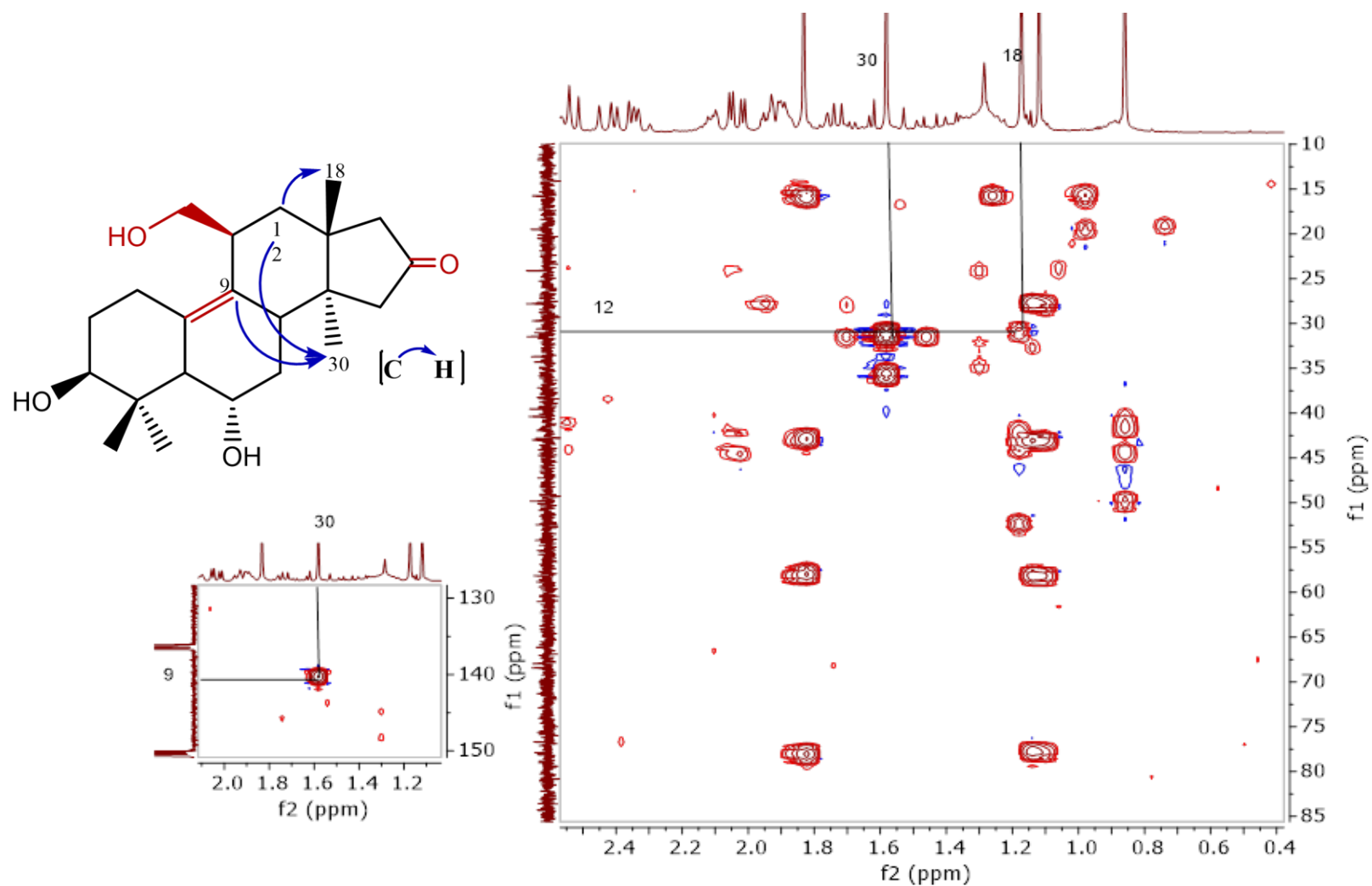
Spectrum 3.14 HR-ESI-MS spectrum of **A-SCG-06** (negative mode)



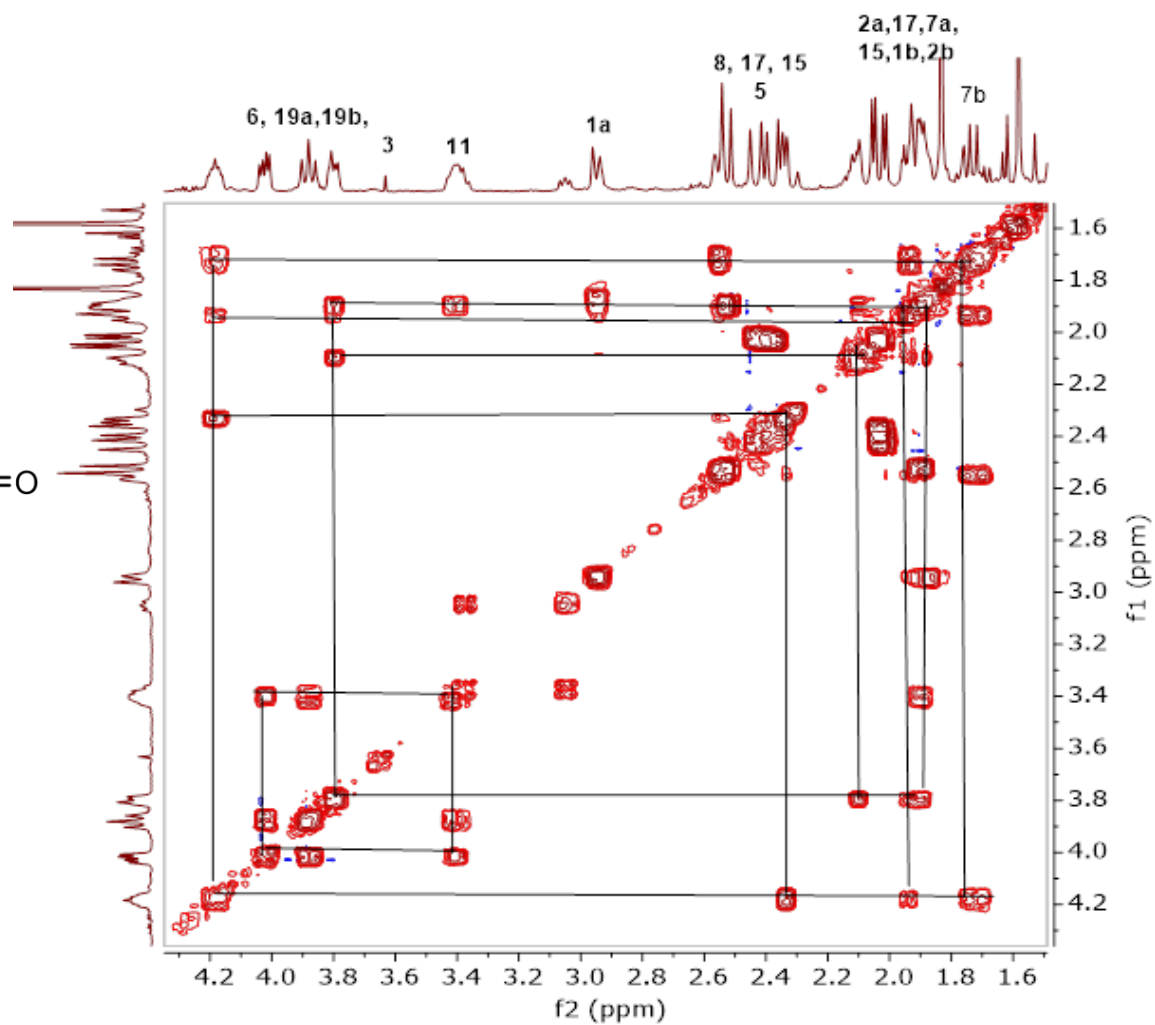
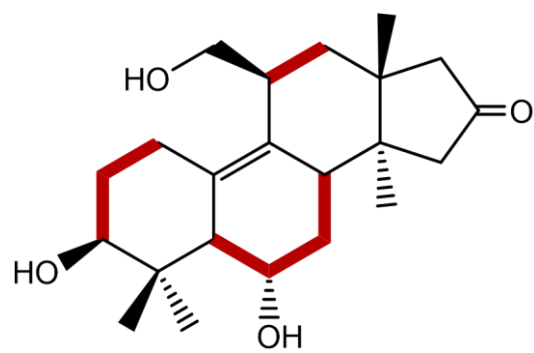
Spectrum 3.15 ^1H -NMR Spectrum of A-SCG-06



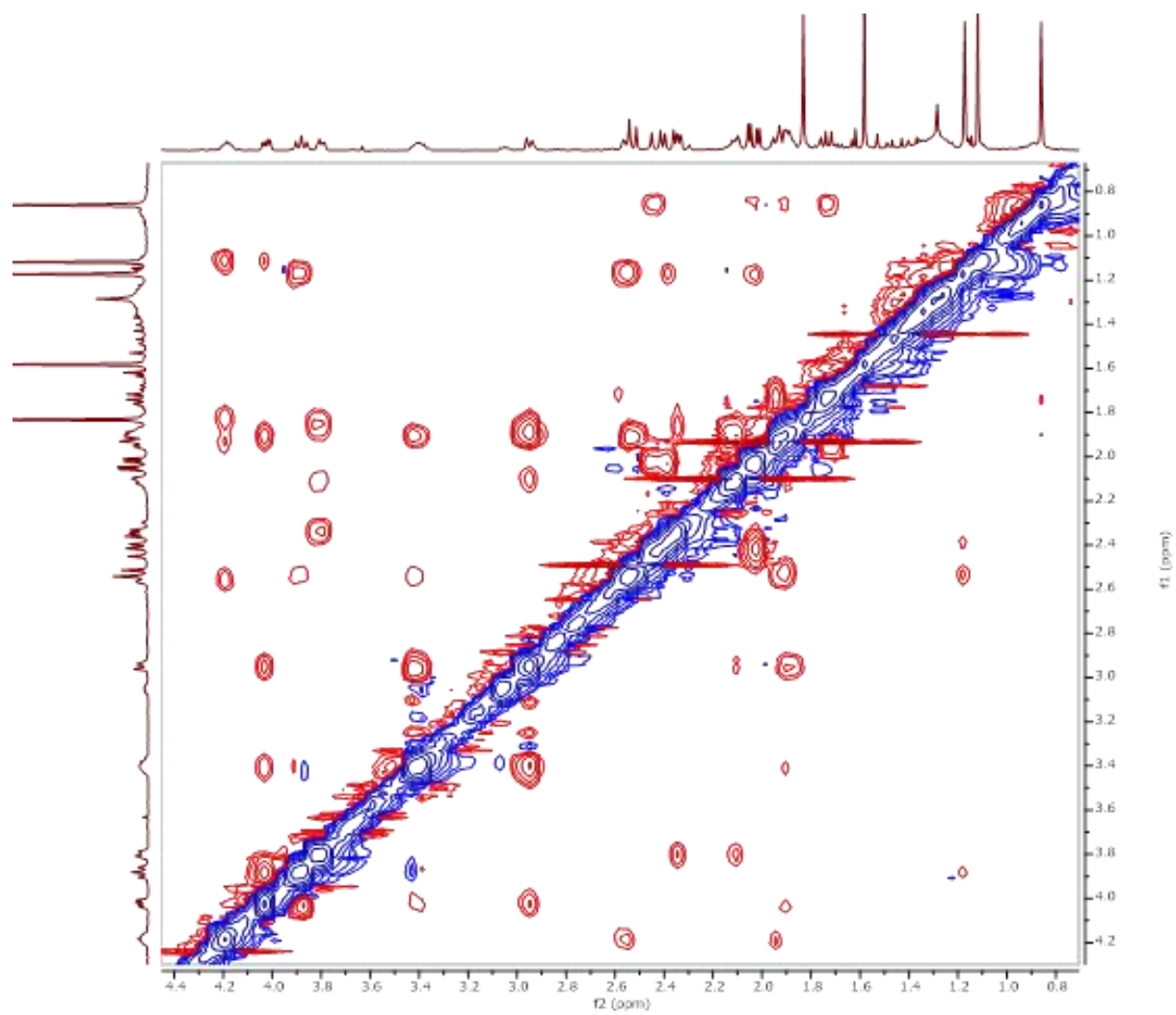
Spectrum 3.16 HSQC spectrum of **A-SCG-06**



Spectrum 3.17 HMBC spectrum of A-SCG-06



Spectrum 3.18 COSY spectrum of A-SCG-06



Spectrum 3.19 ROESY spectrum of **A-SCG-06**

3.2.1.4 Structure Elucidation of A-SCG-07

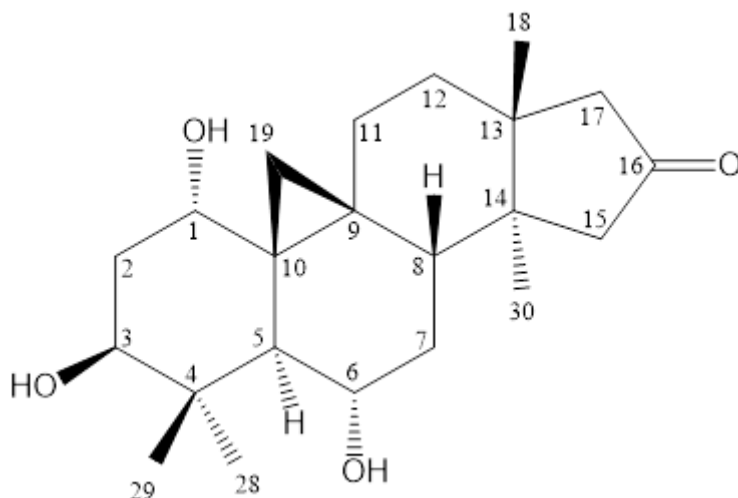


Figure 3.5 Chemical structure of **A-SCG-07**

In the HR-ESI-MS spectrum of **A-SCG-07**, a major ion peak was observed at m/z 399.22 $[M+Cl]^-$ indicating a molecular formula of $C_{22}H_{34}O_4$.

In the 1H -NMR spectrum, the characteristic AX system signals of 9,19-cyclopropane ring, four tertiary methyl groups in the up-field region, and the characteristic signals belonging to the H-3 and H-6 oxymethyne protons were detected readily. In the low field, there was no resonance corresponding to H-16; however, a broad singlet oxymethyne proton was observed at 3.83 ppm, suggesting to a transformation via monooxygenation.

In the ^{13}C -NMR spectrum; the characteristic C-16 signal resonating around at 71.81 ppm was absent, and the presence of a new resonance at δ 214.1 in the low field suggested oxidation of C-16(OH) to a carbonyl. The proton and carbon resonances assigned to the D ring for **A-SCG-07** were compatible with **A-SCG-06** indicating their similarity. Specifically, the cross peaks between H₂-15 (2.01, 1.98)/ H₂-17 (2.09, 2.06) and the carbonyl signal in the HMBC spectrum verified the oxidation position to be C-16.

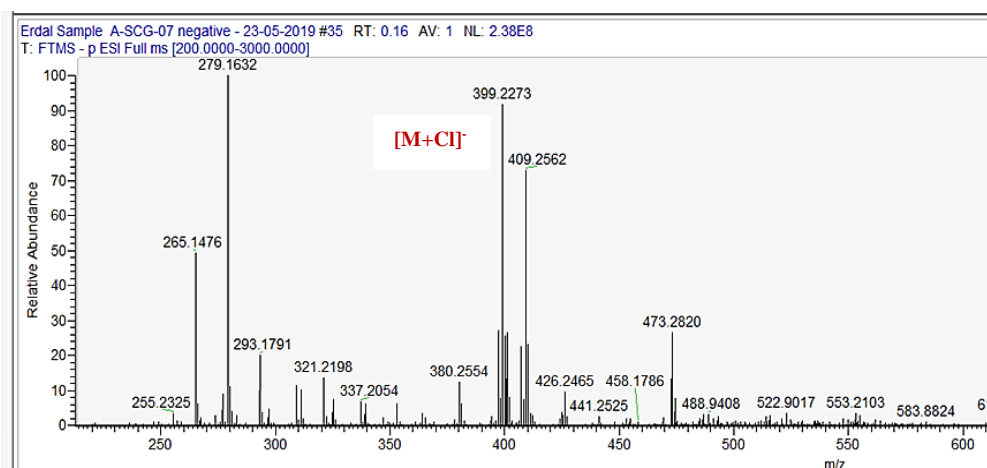
By using the HSQC spectrum, the corresponding carbon signal of the new proton at δ 3.83 was determined to be δ 73.0. In the COSY spectrum, the δ 3.83 proton coupled with a methylene group proton (H₂-2- δ 2.30, 2.53), which, in turn, showed correlations with the characteristic signal of H-3 (δ 4.54, dd, $J=11.8, 4.0$ Hz) helping us to locate the hydroxylation at C-1. As a matter of fact, in the HMBC spectrum, the $^3J_{C-H}$ long-distance

correlations between δ 73.0 and H₂-19 protons confirmed aforementioned deduction. The orientation of C-1(OH) was found to be α based on the ROESY cross peak between H-1 and β -oriented H-19a at δ 0.37. Thus, the structure of **A-SCG-07** was established as 1(α)-hydroxy,16-oxo derivative of 20,27-octanor cycloastragenol.

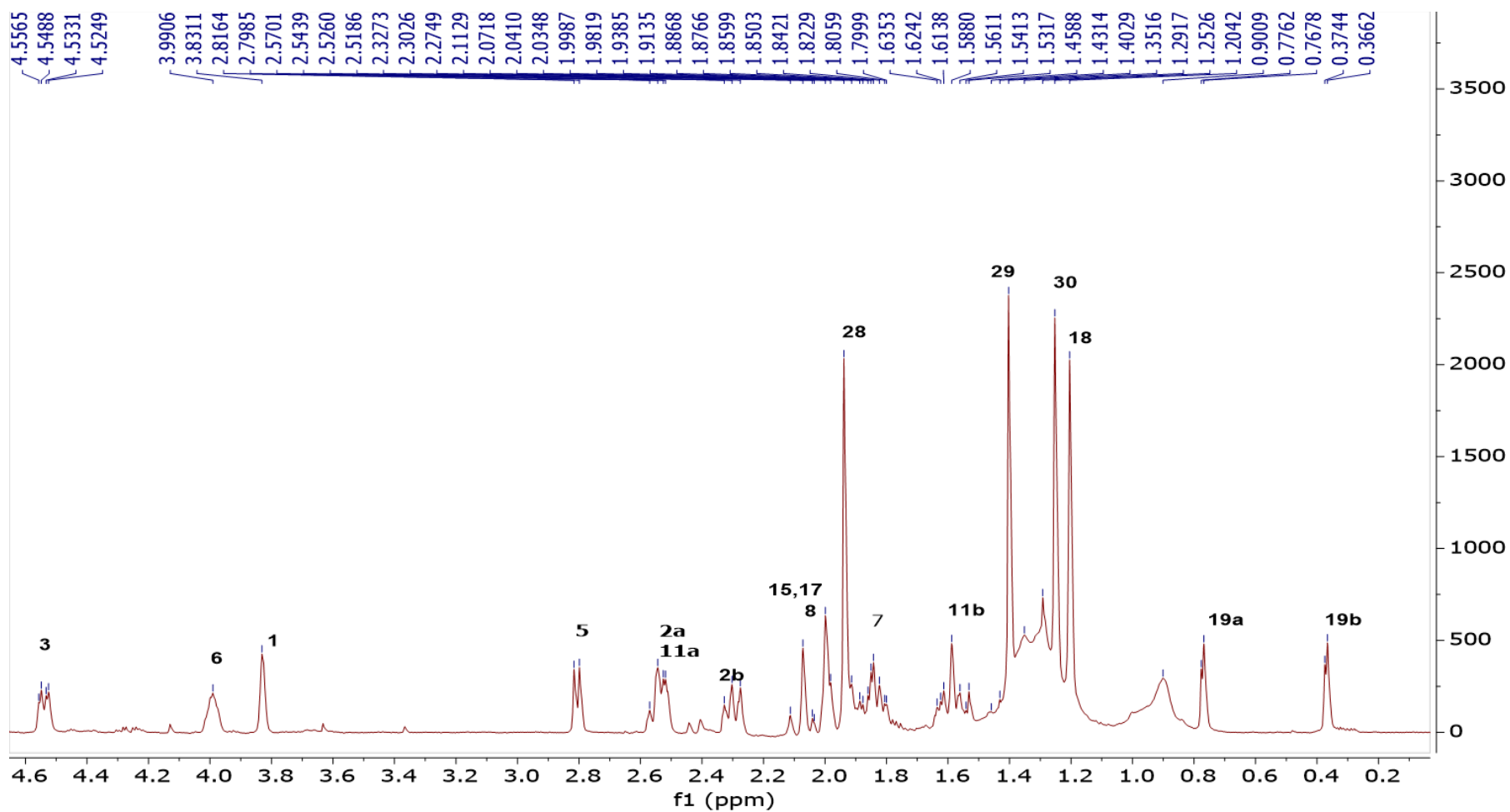
Table 3.4 ¹H and ¹³C NMR data of **A-SCG-07** (125/500 MHz, C₅D₅N).

C/H	δ_C (ppm)	δ_H (ppm), <i>J</i> (Hz)
1	73.0	3.83 brs
2	39.4	2.30 m, 2.53 m
3	74.1	4.54 dd (11.8, 4)
4	43.1	
5	47.1	2.81 d (8.9)
6	68.2	3.99 m
7	38.6	1.81 m, 1.85 m
8	45.4	1.99 m
9	22.2	
10	34.2	
11	26.1	2.54 m, 1.61 m
12	31.1	1.59 m, 1.91 m
13	42.0*	
14	44.9*	
15	52.2**	2.01 d (21), 1.98 m*
16	+214.1	
17	51.2**	2.09 d (20.6), 2.06 (18.5)*
18	25.3	1.20 s
19	29.5	0.37 d (4.1), 0.78 d (4.2)
28	29.6	1.94 s
29	16.0	1.40 s
30	19.9	1.25 s

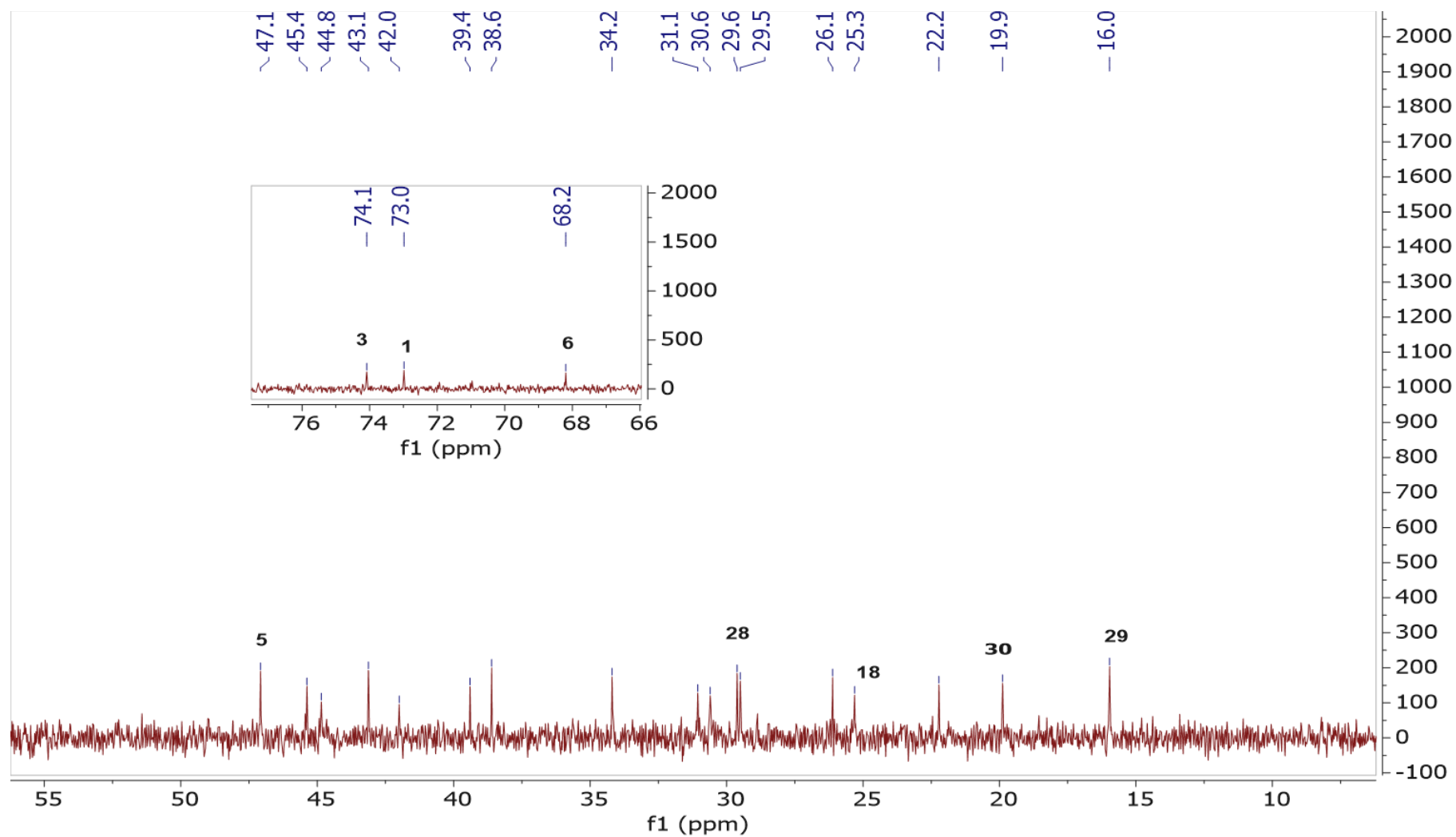
*, **: interchangeable.



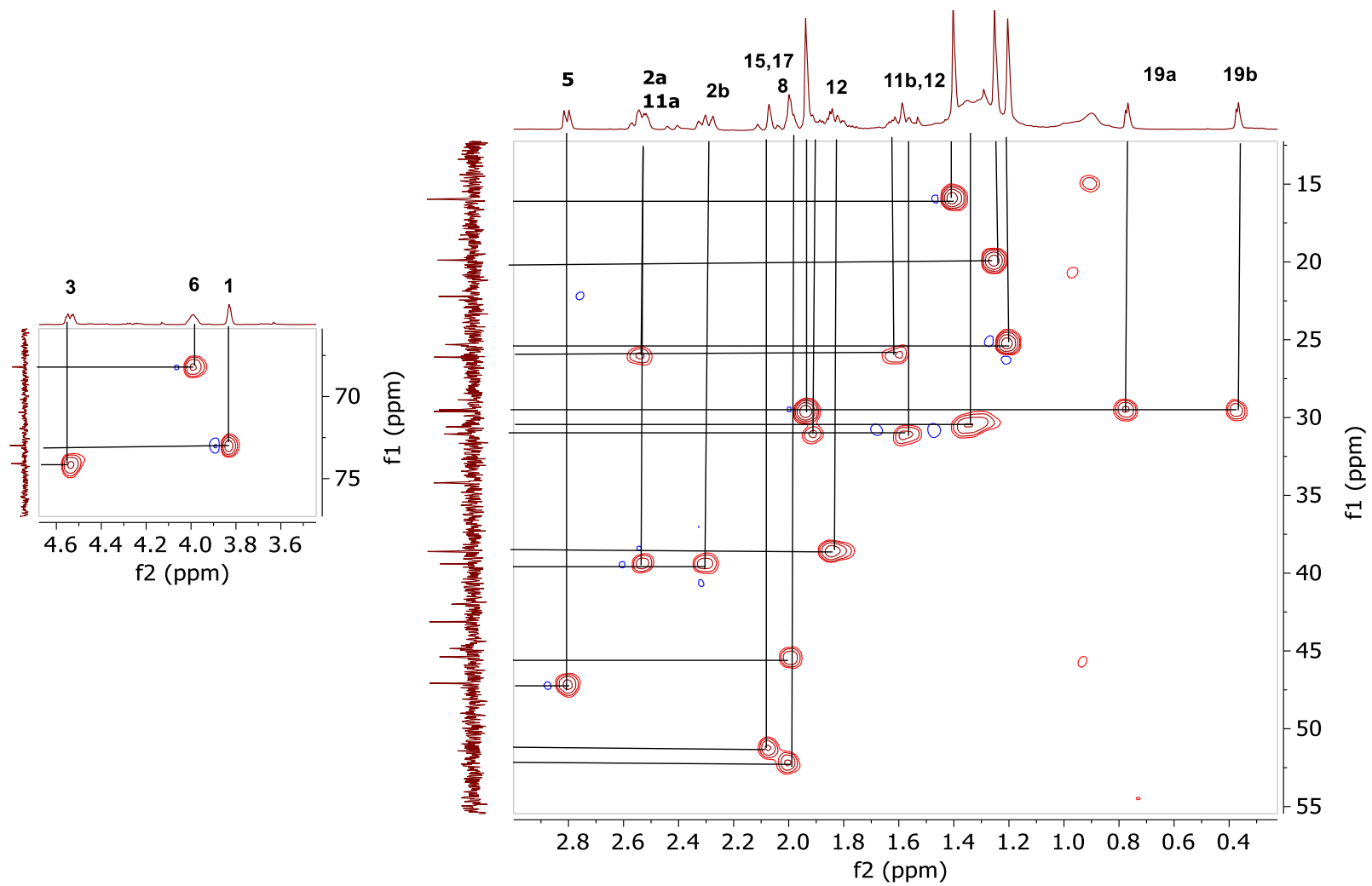
Spectrum 3.20 HR-ESI-MS spectrum of **A-SCG-07** (negative mode)



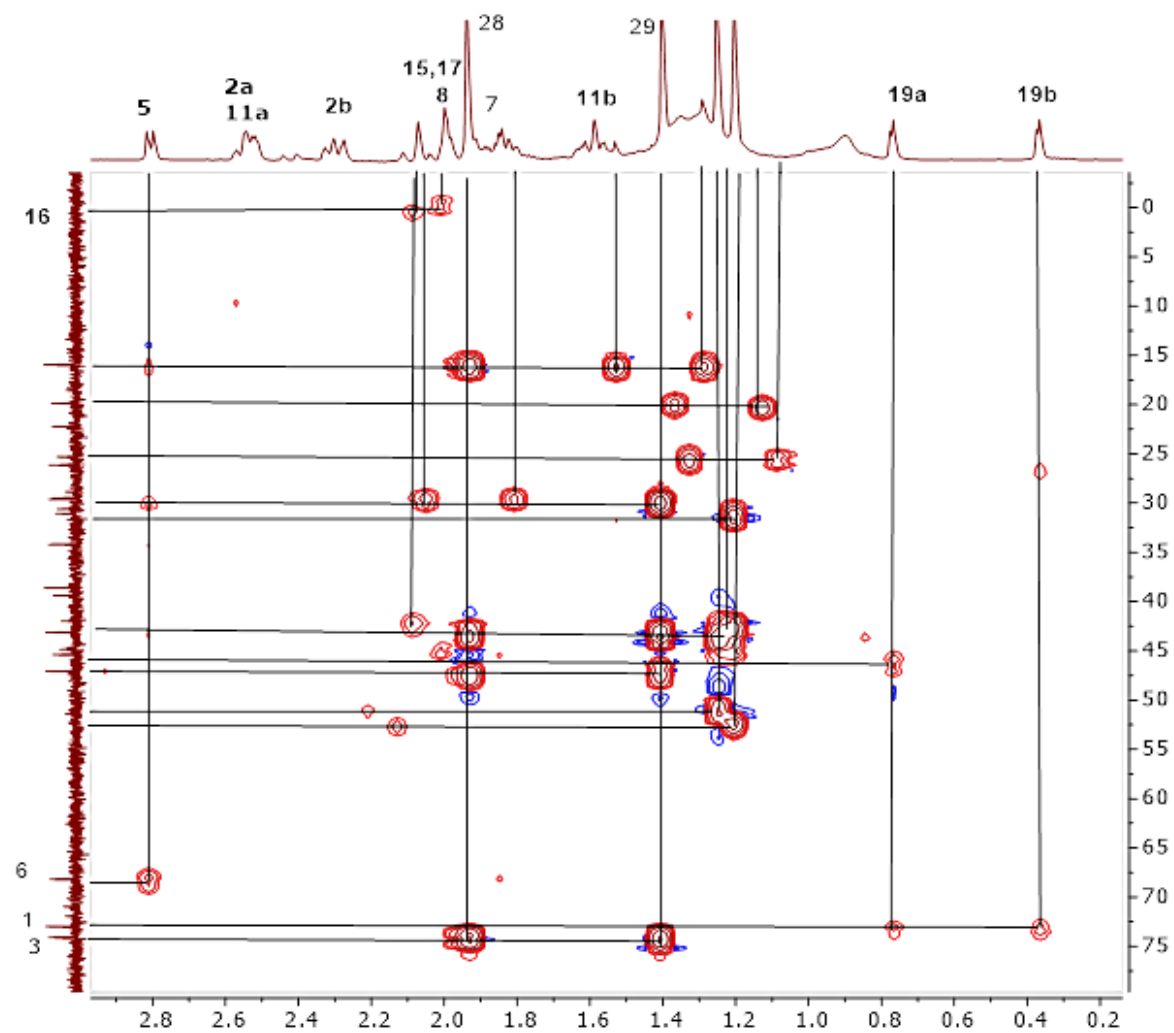
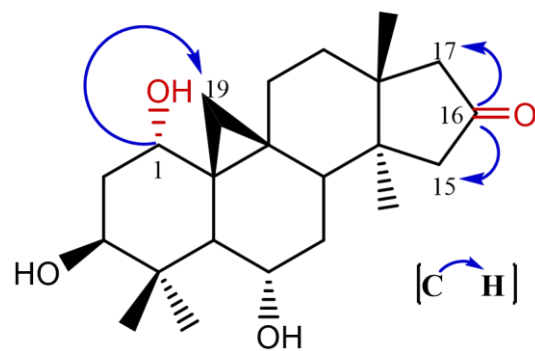
Spectrum 3.21 ^1H -NMR Spectrum of A-SCG-07



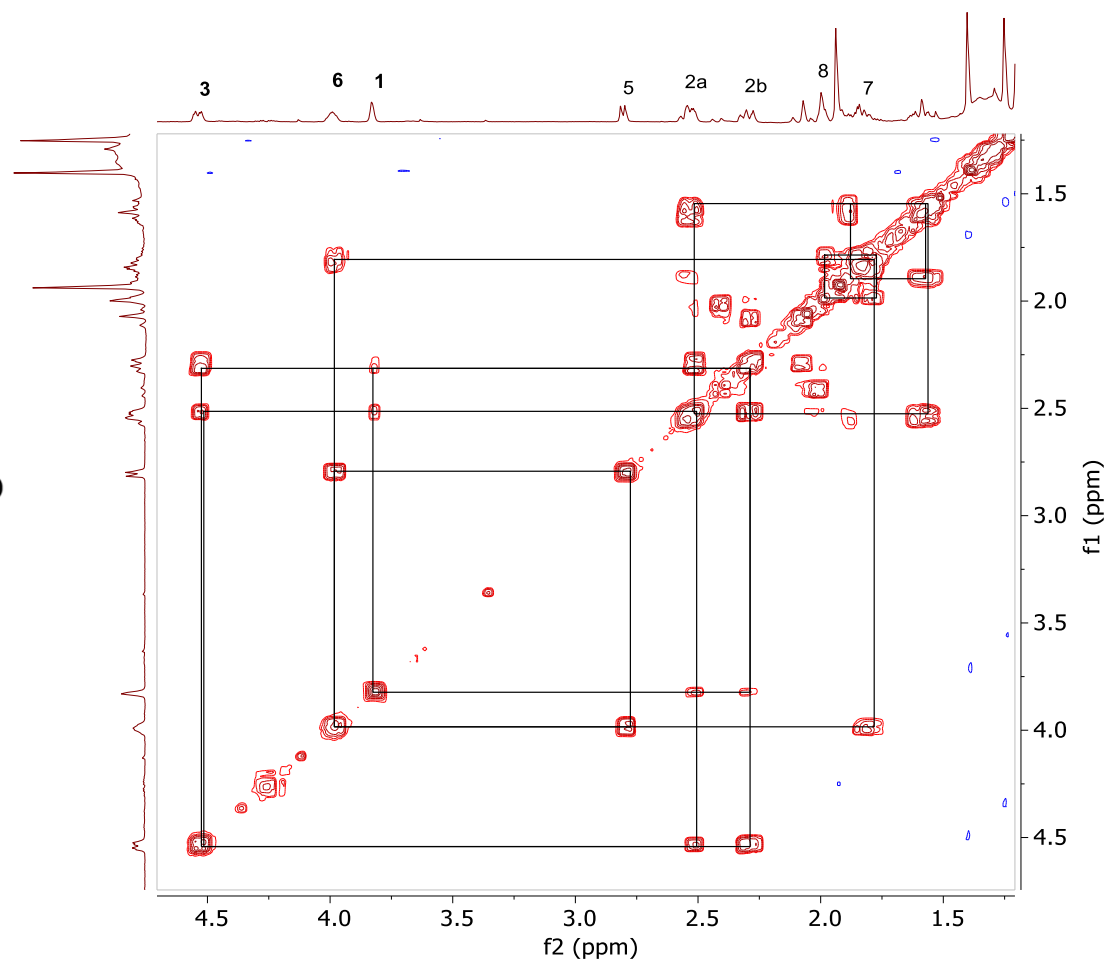
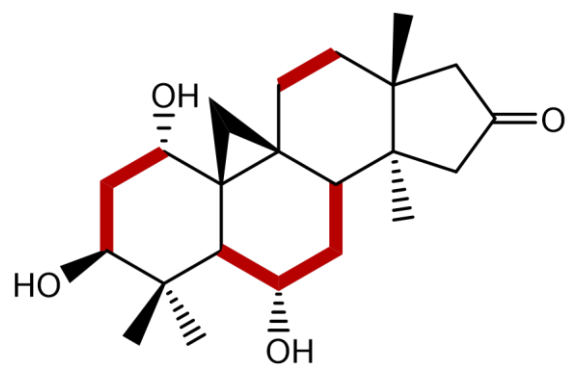
Spectrum 3.22 ^{13}C -NMR Spectrum of A-SCG-07



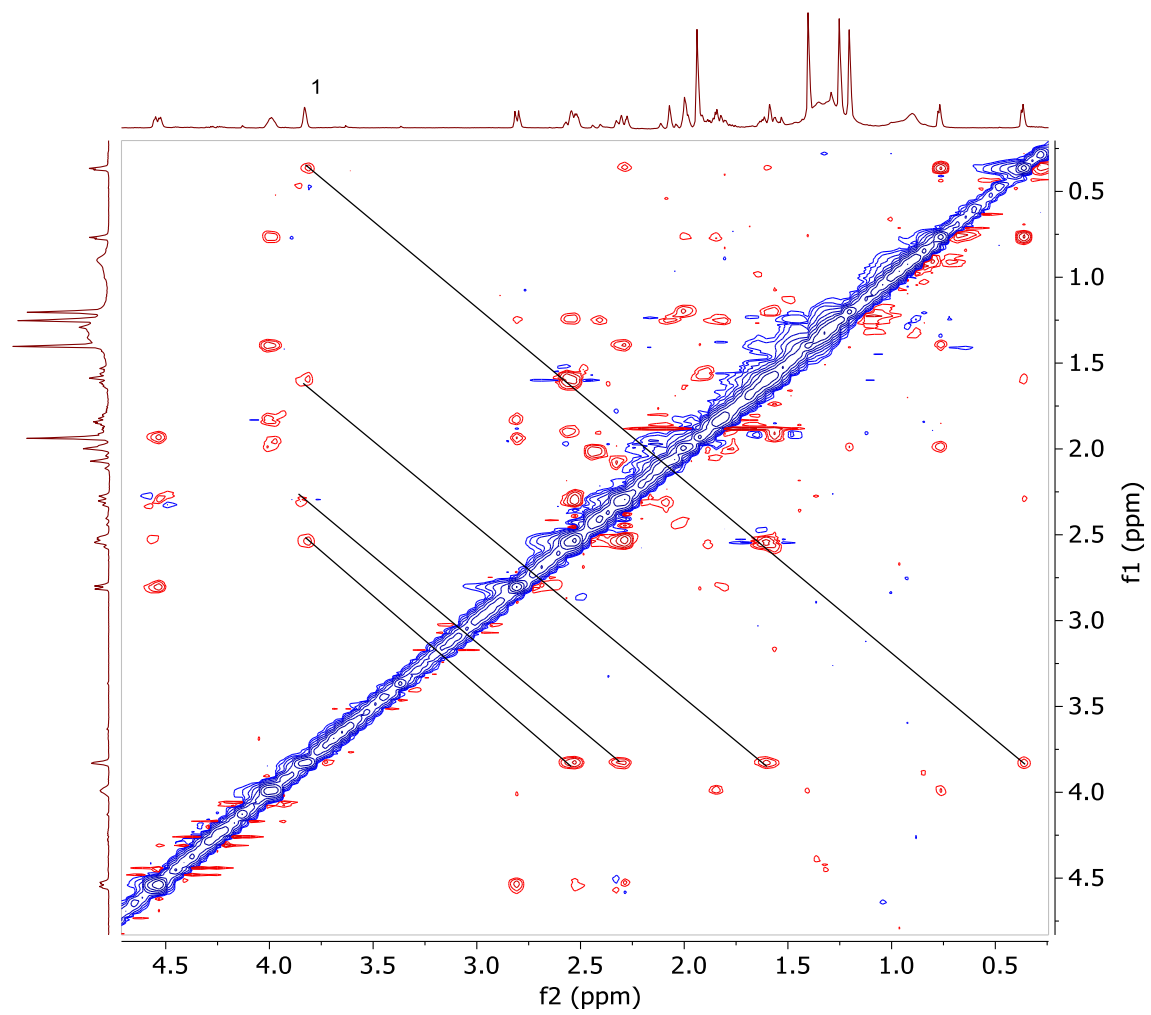
Spectrum 3.23 HSQC spectrum of **A-SCG-07**



Spectrum 3.24 HMBC spectrum of A-SCG-07



Spectrum 3.25 COSY spectrum of A-SCG-07



Spectrum 3.26 ROESY spectrum of A-SCG-07

3.2.1.5 Structure Elucidation of A2-SCG-01

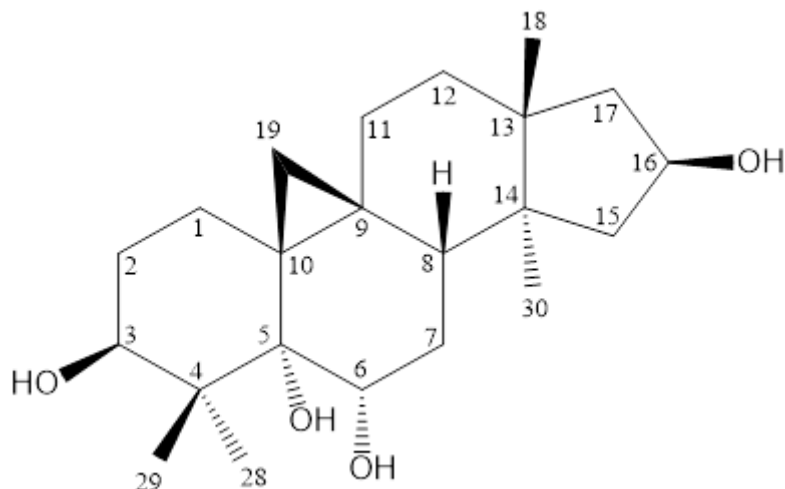


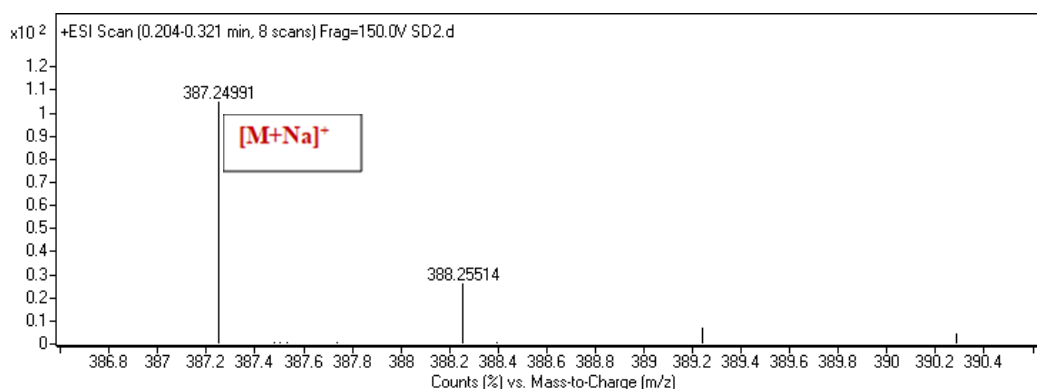
Figure 3.6 Chemical structure of **A2-SCG-01**

In the HR-ESI-MS spectrum of **A2-SCG-01**, a major ion peak was observed at m/z 387.25 $[M+Na]^+$ indicative of a molecular formula $C_{22}H_{36}O_4$.

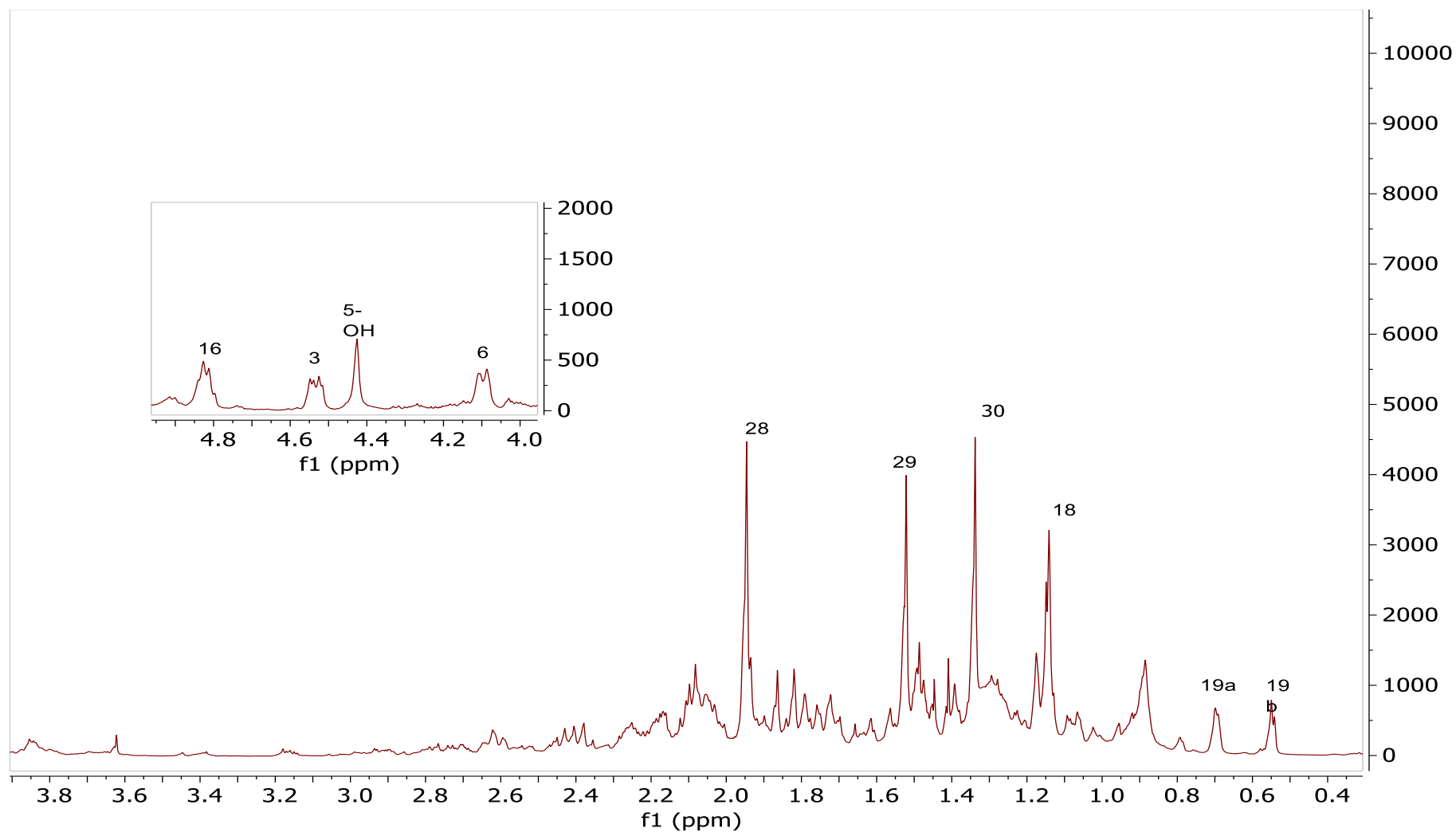
In the 1H NMR spectrum, the AX system signals of cyclopropane ring, four methyl groups in the up-field region, and the characteristic signals belonging to the H-3, H-6 and H-16 oxymethine protons in the low-field displayed no significant discrepancy compared to 20(27)-octanor cycloastragenol. In the ^{13}C NMR spectrum, apart from the C-3, C-6 and C-16, an oxygenated carbon at δ 76.5 was observed verifying the hydroxylation deduced based on the HR-MS data. In the HSQC spectrum, no correlation of this carbon with any proton indicated its quaternary nature. The δ 76.5 resonance was unambiguously assigned to C-5 based on the long-distance $^3J_{C-H}$ correlations in the HMBC spectrum from δ 76.5 to H₃-28 and H₃-29 protons. The COSY spectrum also helped us to locate the exchangeable protons of C-3(OH) and C-6(OH) due to the $^3J_{H-H}$ couplings with H-3 and H-6 protons. The other exchangeable proton resonating at α -4.25 (s) was assigned to C-5(OH), which in on the ROESY spectrum showed a cross peak with H₃-28 (α 1.62), suggesting their co-facial orientation. Thus, C-5(OH) was located on the alpha face of **A2-SCG-01**. Consequently, the structure of **A2-SCG-01** was established as 5(α)-hydroxy derivative of 20(27)-octanor cycloastragenol.

Table 3.5 ^1H and ^{13}C NMR data of **A2-SCG-01** (125/500 MHz, $\text{C}_5\text{D}_5\text{N}$)

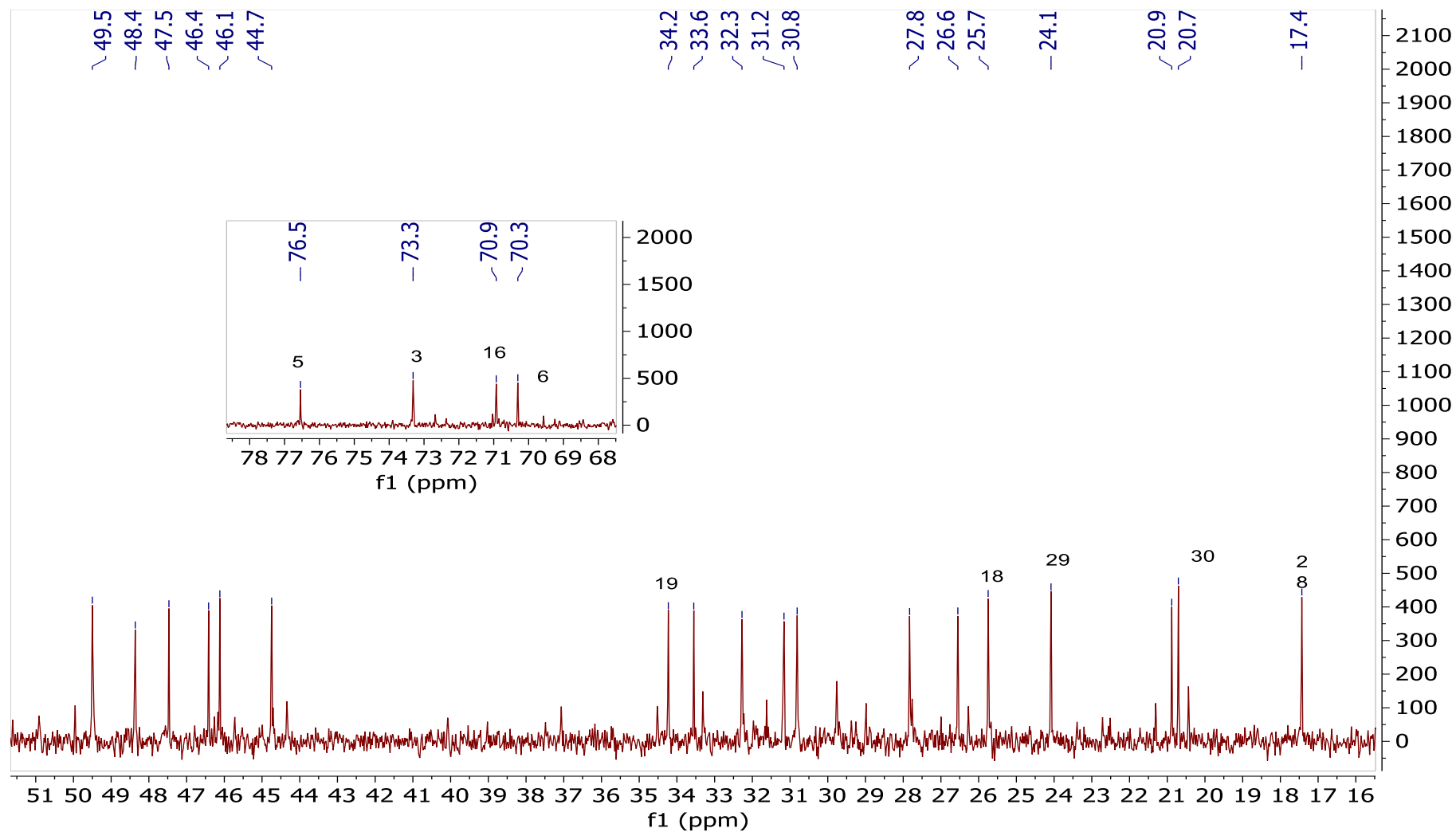
C/H	δ_{C} (ppm)	δ_{H} (ppm), J (Hz)
1	27.8	1.85 m, 1.88 m
2	31.2	2.16 m, 2.08 m
3	73.3	4.52 dd (11.4, 4.4)
4	44.7	
5	76.5	
6	70.3	4.08 t (8.6)
7	32.3	1.51 m, 2.77 m
8	47.5	1.77 m
9	33.6	
10	46.4	
11	26.6	1.20 m, 2.23 m
12	30.8	1.72 m, 1.55 m
13	46.1	
14	44.7	
15	48.4	1.82 m, 2.07 m
16	70.9	4.81 dd (14.1, 7.0)
17	49.5	2.06 m, 2.14 m
18	25.7	1.14 s
19	34.2	0.55 d (4.3), 0.70 d (4.4)
28	17.1	1.52 s
29	24.1	1.93 s
30	20.7	1.33 s



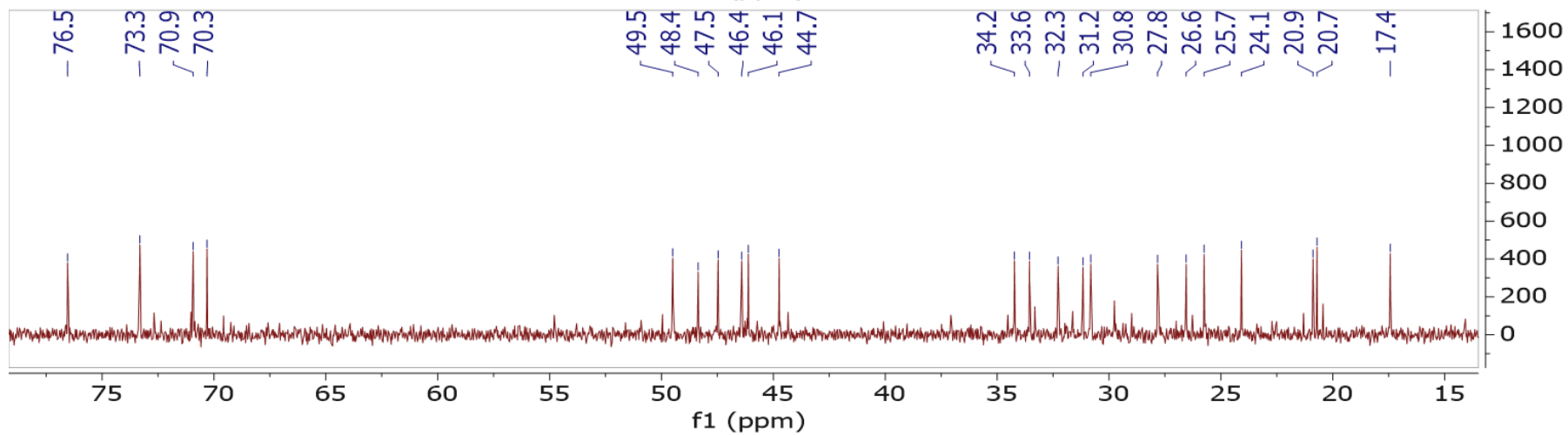
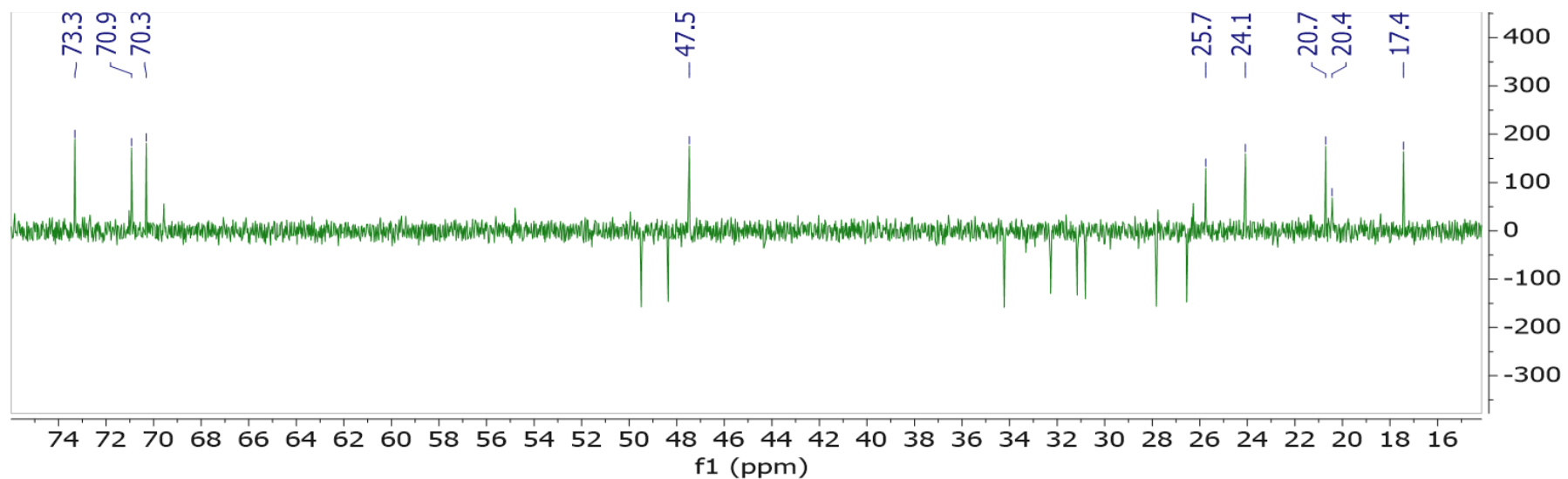
Spectrum 3.27 HR-ESI-MS spectrum of **A2-SCG-01** (positive mode)



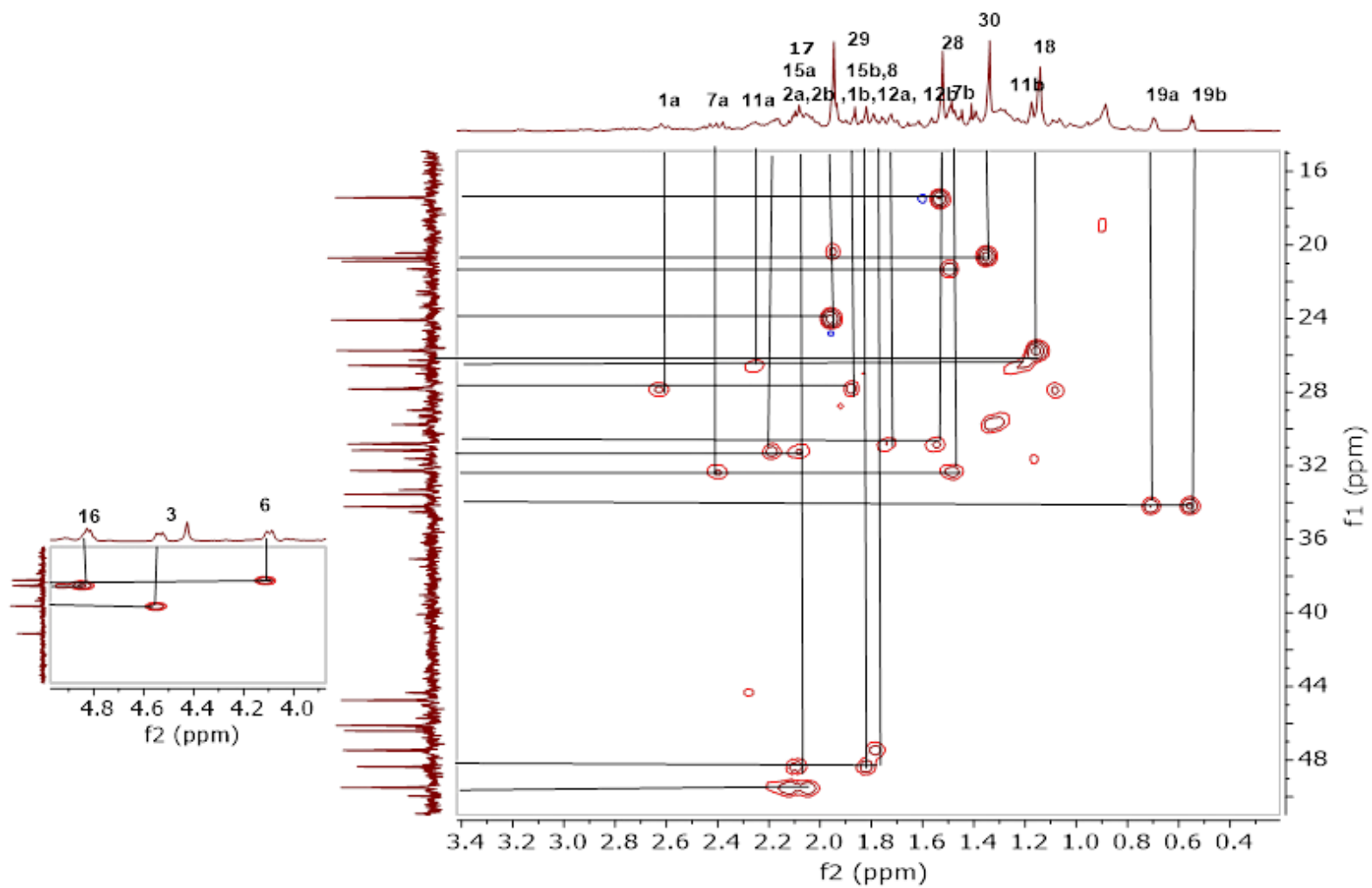
Spectrum 3.28 ^1H -NMR Spectrum of A2-SCG-01



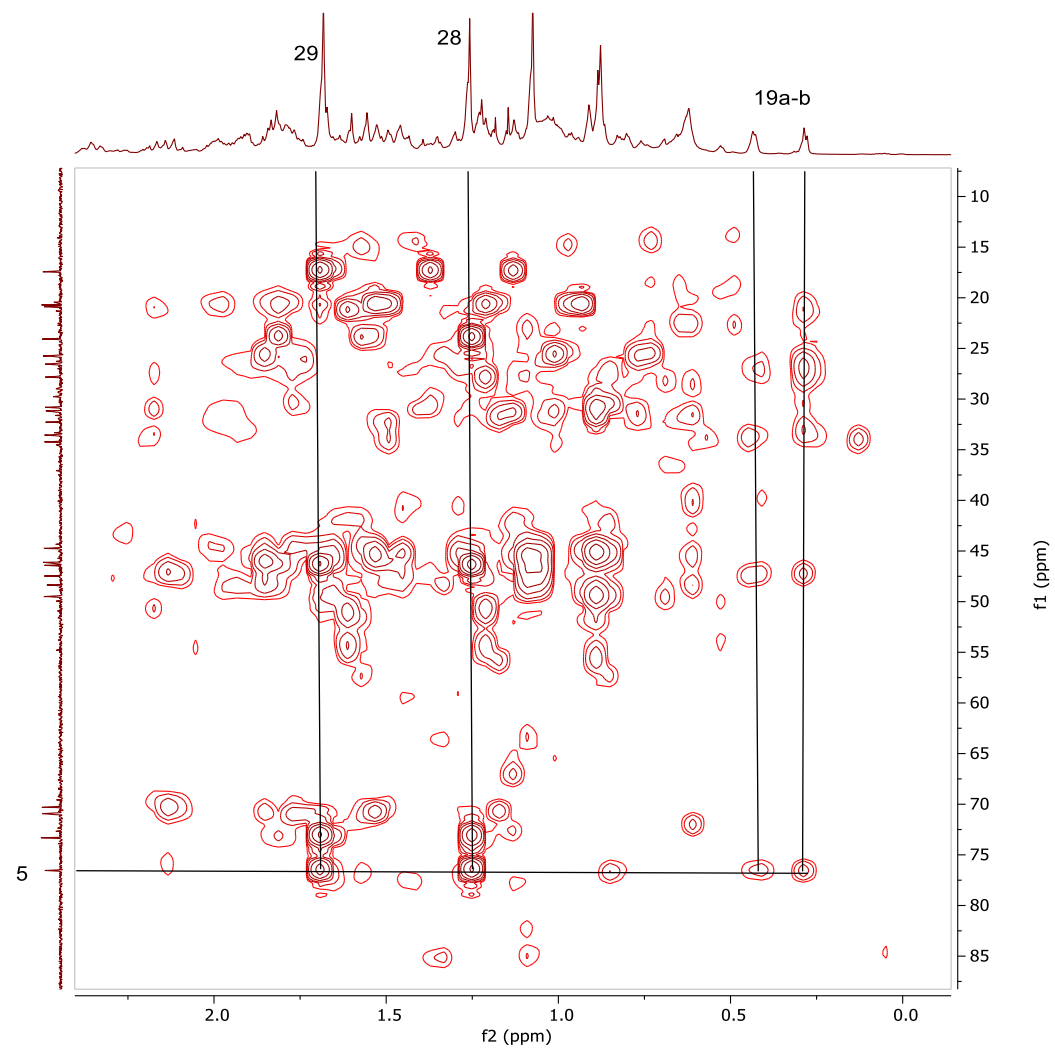
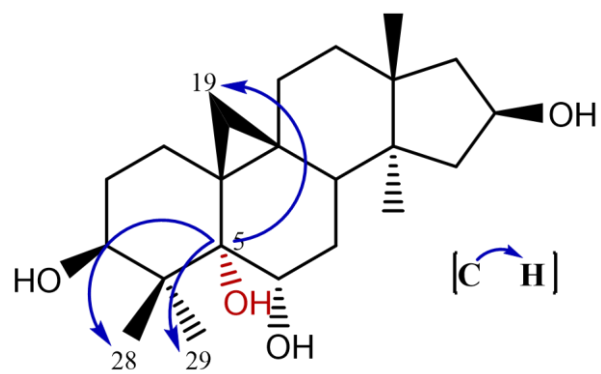
Spectrum 3.29 ^{13}C -NMR Spectrum of A2-SCG-01



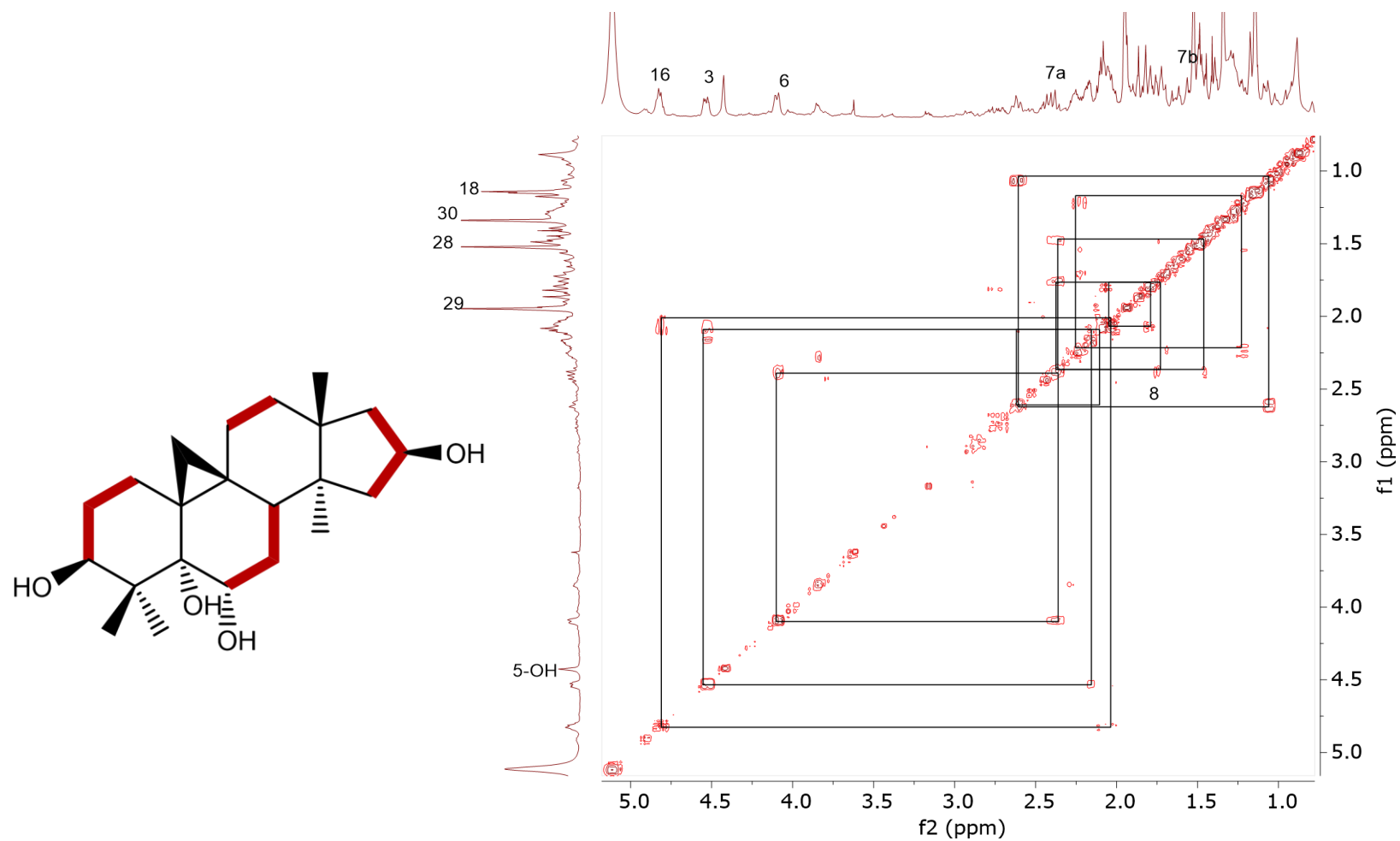
Spectrum 3.30 DEPT spectrum of A2-SCG-01



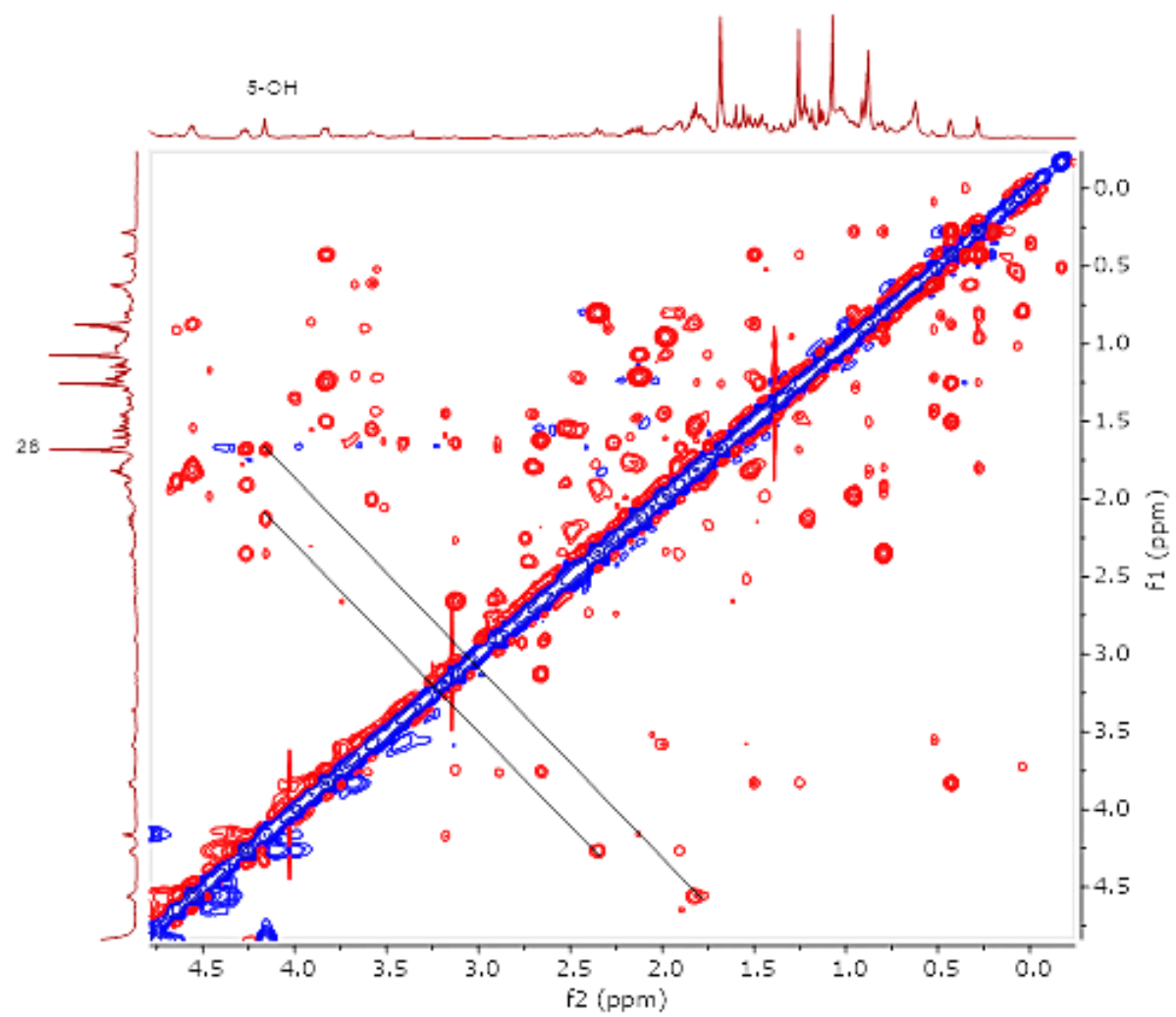
Spectrum 3.31 HSQC spectrum of A2-SCG-01



Spectrum 3.32 HMBC spectrum of A2-SCG-01



Spectrum 3.33 COSY spectrum of A2-SCG-01



Spectrum 3.34 ROESY spectrum of A2-SCG-01

3.2.1.6 Structure Elucidation of A2-SCG-02

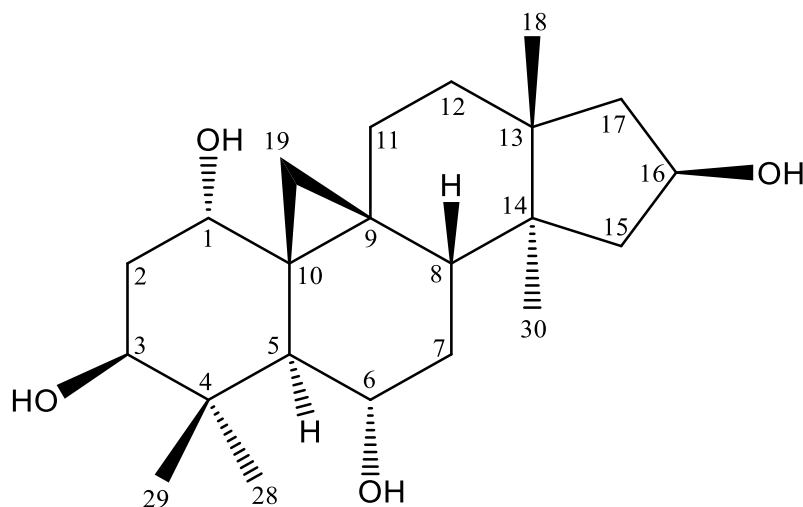


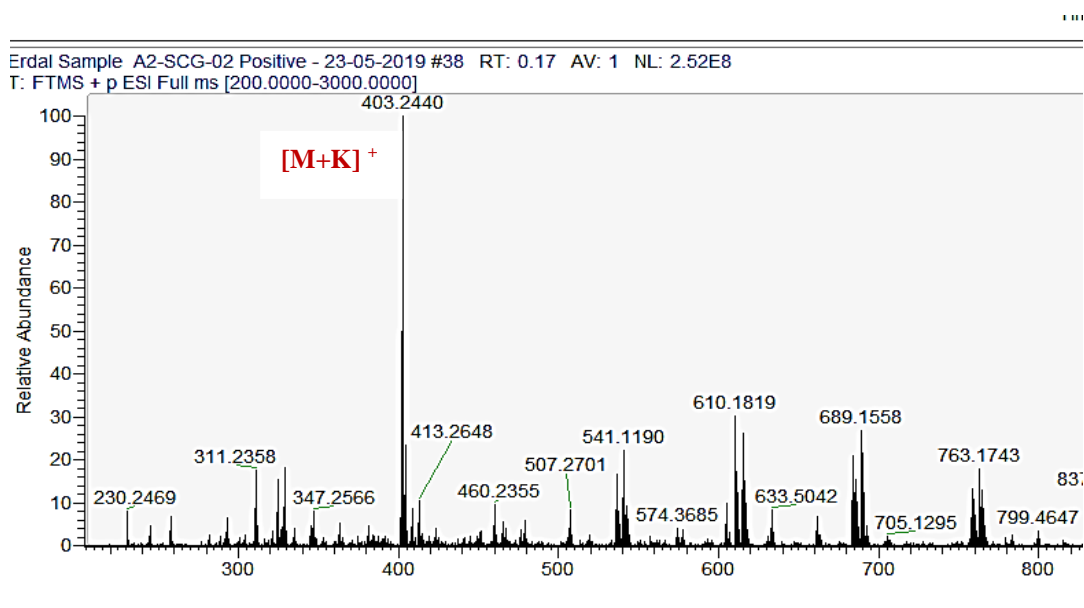
Figure 3.7 Chemical structure of **A2-SCG-02**

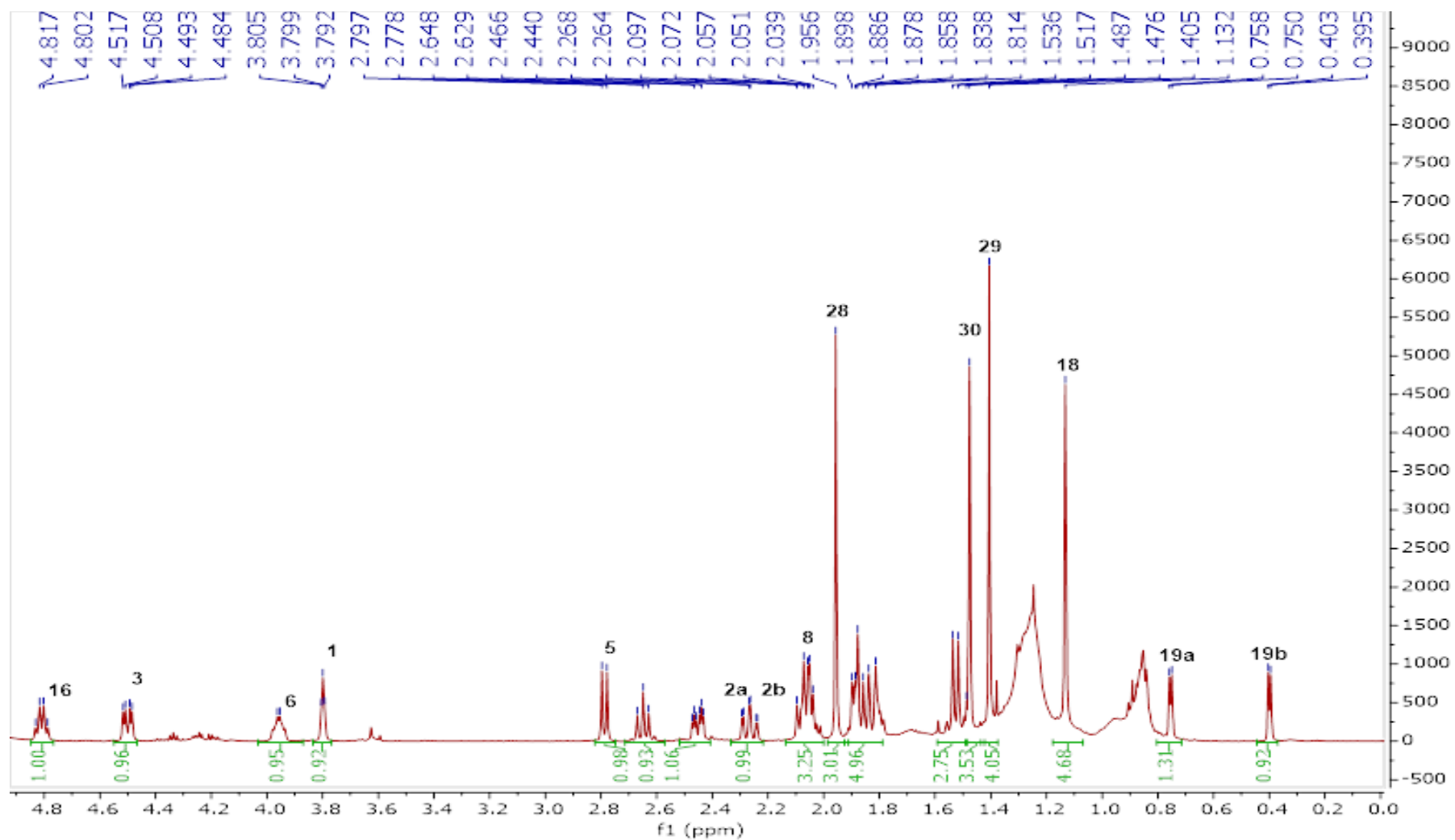
In the HR-ESI-MS spectrum of **A2-SCG-02**, a major ion peak was observed at m/z 403.2440 $[M+K]^+$ revealing not only the molecular formula of $C_{22}H_{36}O_4$, but also a monooxygenated metabolite due to 16 amu difference compared to the substrate (**SCG**).

The characteristic AX system signals of 9,19-cyclopropane ring, four tertiary methyl groups in the up-field region, and the characteristic signals belonging to the H-3, H-6 and H-16 oxymethyne protons were observed readily. For **A2-SCG-02**, a detailed inspection of the 1H NMR spectrum displayed a broad singlet signal at 3.80 ppm, which was consistent with hydroxyl group insertion as stated above. In the COSY spectrum, this proton coupled with a methylene (δ 2.45 and δ 2.27, H_2-2), which in turn coupled with an oxymethine proton at δ 4.50 (dd, 12.0, 4.4), ascribable to H-3. Finally, in the HMBC spectrum, a key long-range correlation between the 3.80 ppm signal and C-19 at δ 30.9 substantiated that the new hydroxyl group was at C-1. The relative stereochemistry at C-1 was determined by the ROESY spectrum. The orientation of C-1(OH) was deduced to be α on the basis of a cross peak between equatorially localized H-1 signal and H-19b at 0.40 ppm. Thus, the structure of **A2-SCG-02** was established as 1(α)-hydroxy derivative of 20(27)-octanor cycloastragenol.

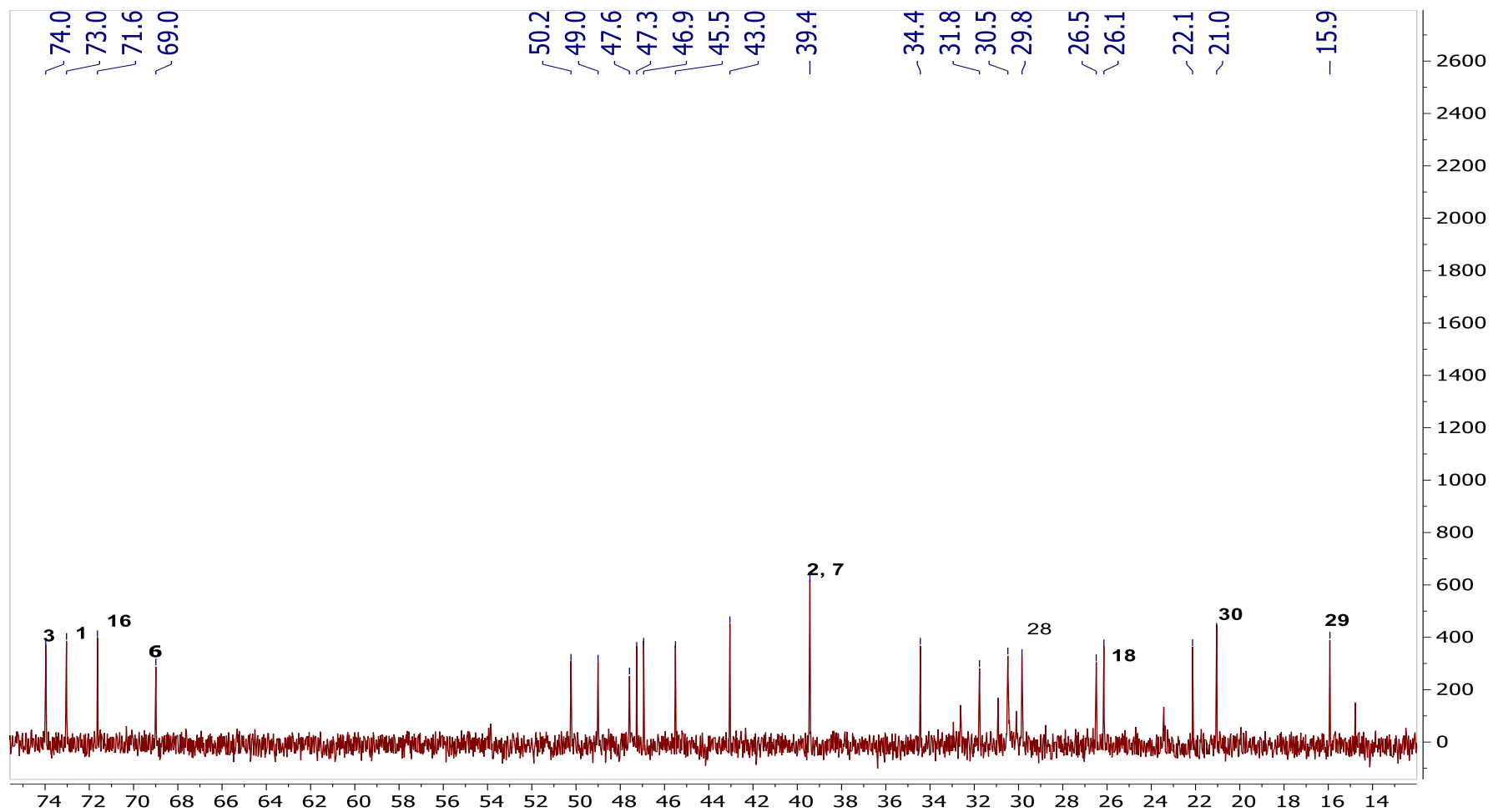
Table 3.6 ^1H and ^{13}C NMR data of **A2-SCG-02** (125/500 MHz, $\text{C}_5\text{D}_5\text{N}$)

C/H	δ_{C} (ppm)	δ_{H} (ppm), J (Hz)
1	73.0	3.80 brs
2	39.4	2.27 td (12.9, 2.8), 2.45 m
3	74.0	4.50 dd (12.0, 4.4)
4	43.0	
5	47.3	2.79 d (9.4)
6	69.0	3.96 m
7	39.4	1.86 m, 1.88 m
8	47.6	1.53 m
9	22.1	
10	34.4	
11	26.5	1.53 d (9.8), 2.65 t (10.3)
12	30.5	1.88-1.89 m,
13	45.5	
14	46.9	
15	49.0	1.82 m, 2.07 m
16	71.6	4.81 q (7.3)
17	50.2	2.02 m, 2.06 m
18	26.1	1.13
19	31.8	0.40 d (4.4), 0.75 d (4.3)
28	29.8	1.96 s
29	15.9	1.41 s
30	21.0	1.48 s

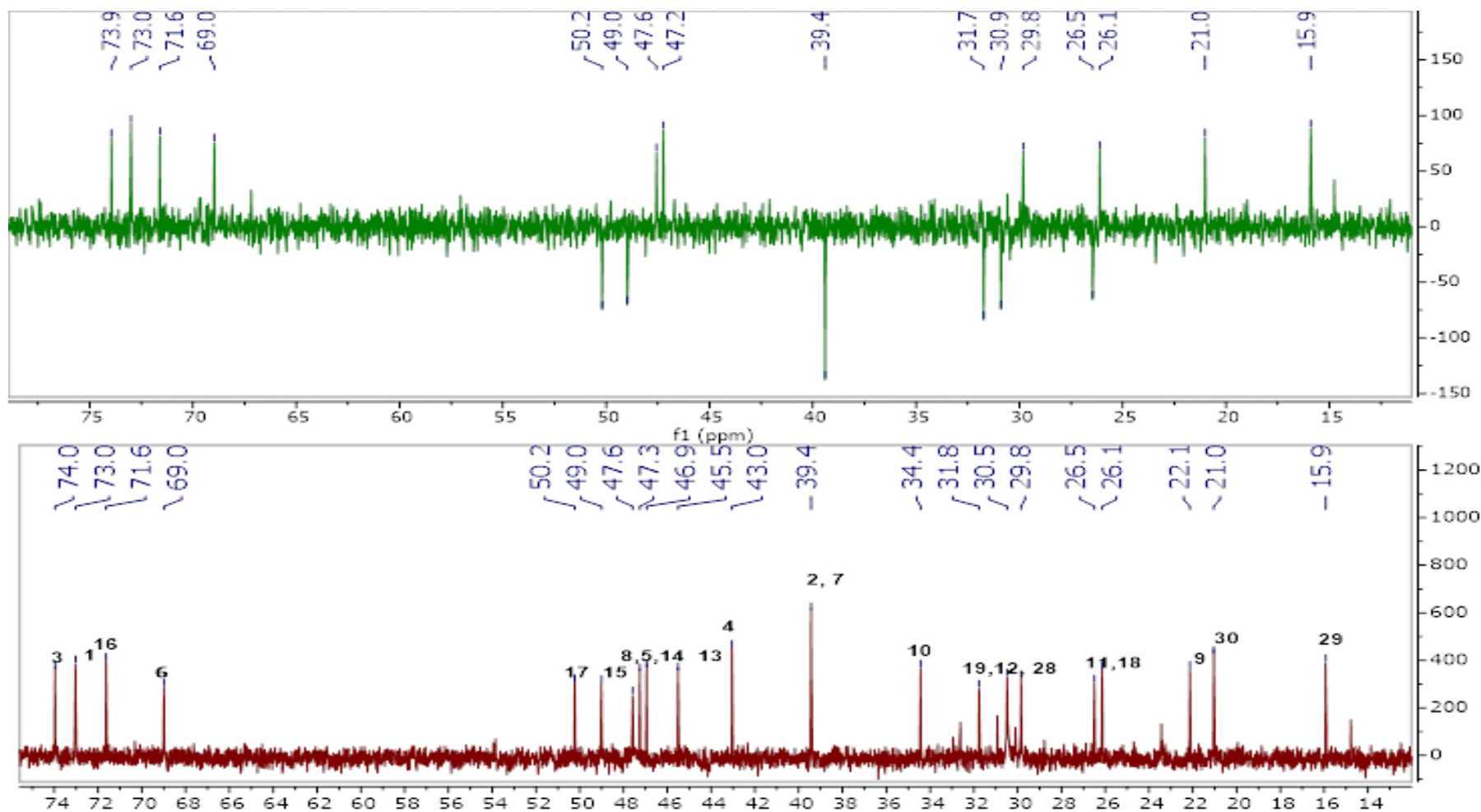
**Spectrum 3.35** HR-ESI-MS spectrum of **A2-SCG-02** (positive mode)



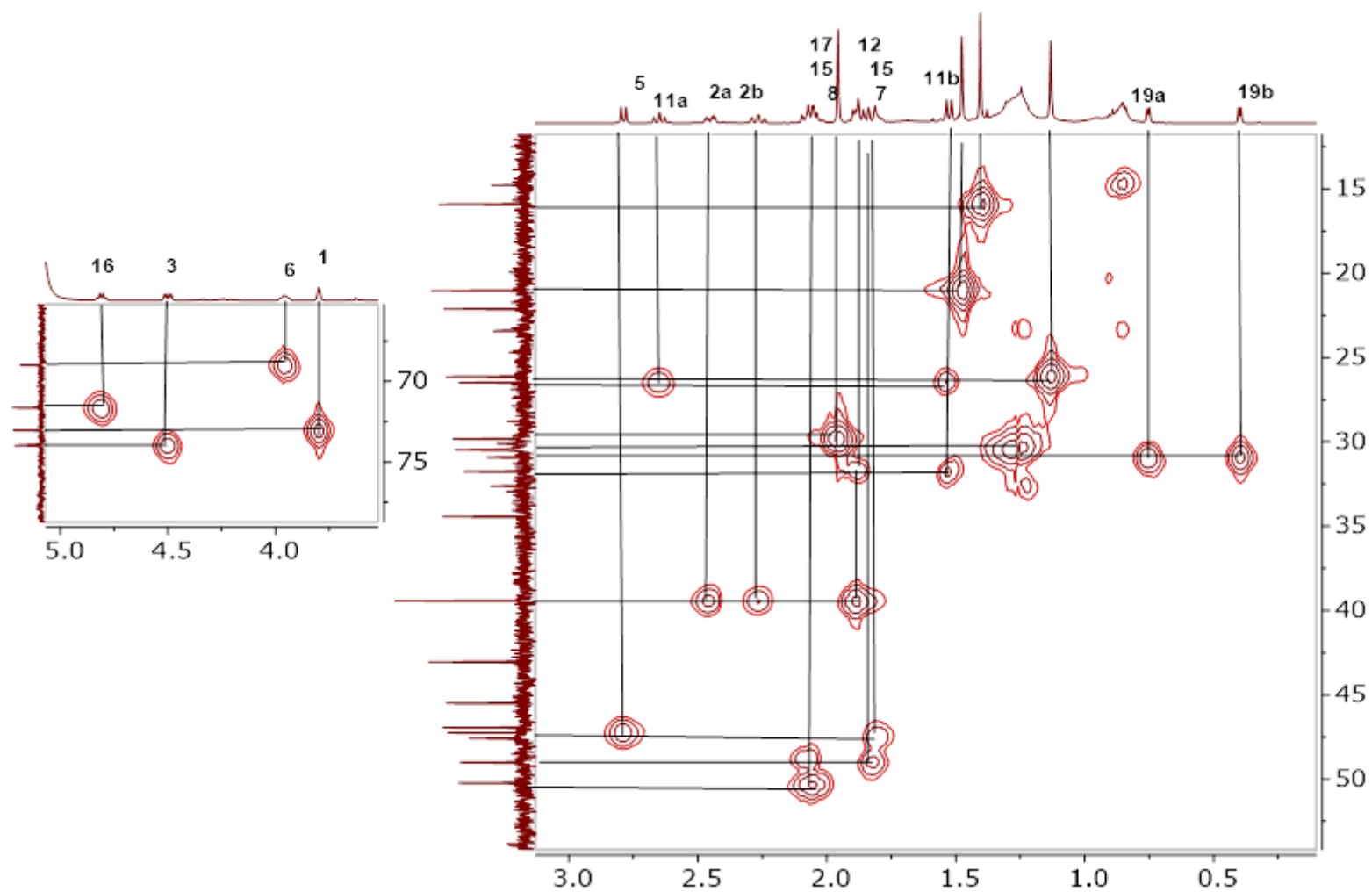
Spectrum 3.36 ^1H -NMR Spectrum of A2-SCG-02



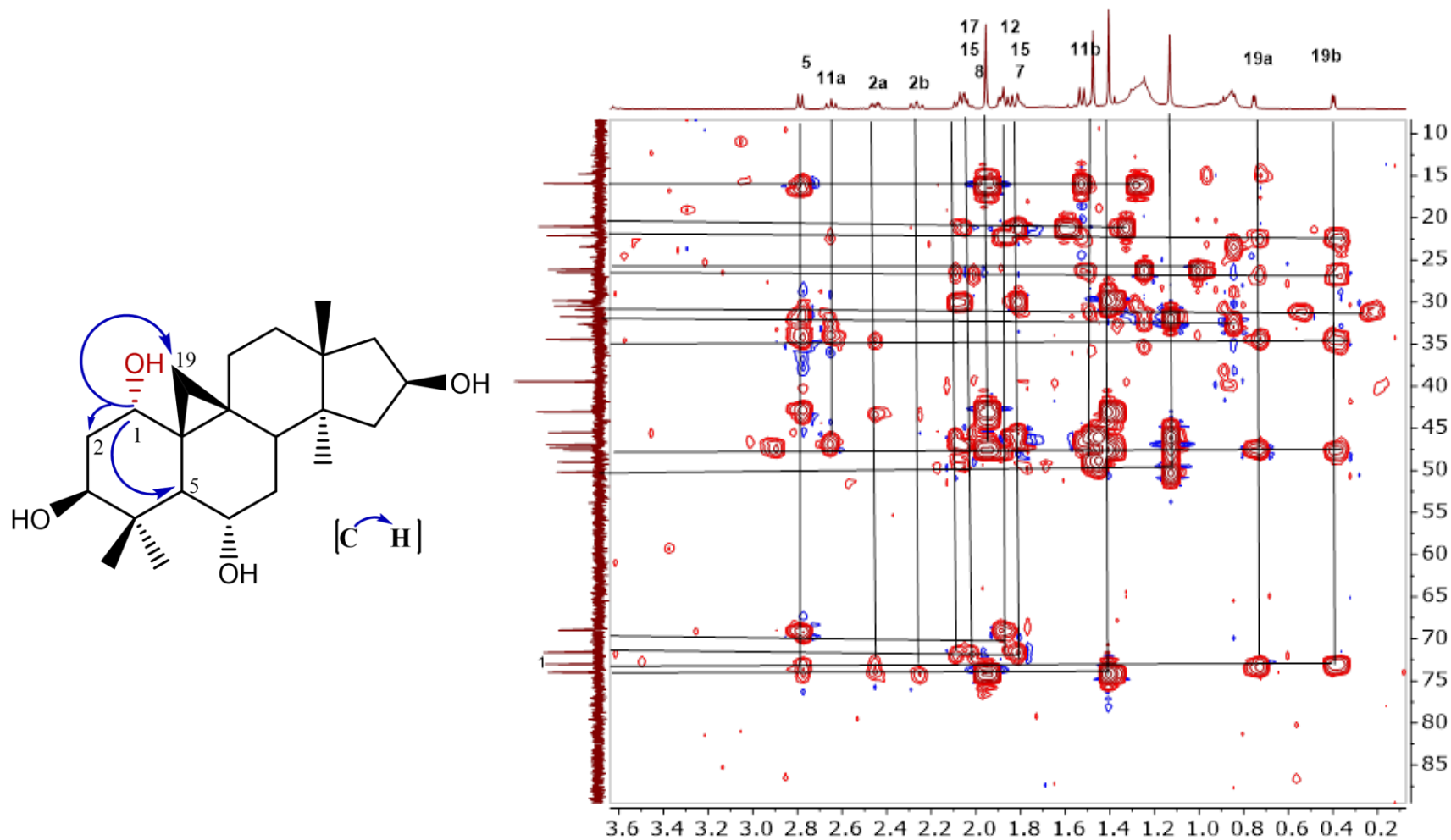
Spectrum 3.37 ^{13}C -NMR Spectrum of A2-SCG-02



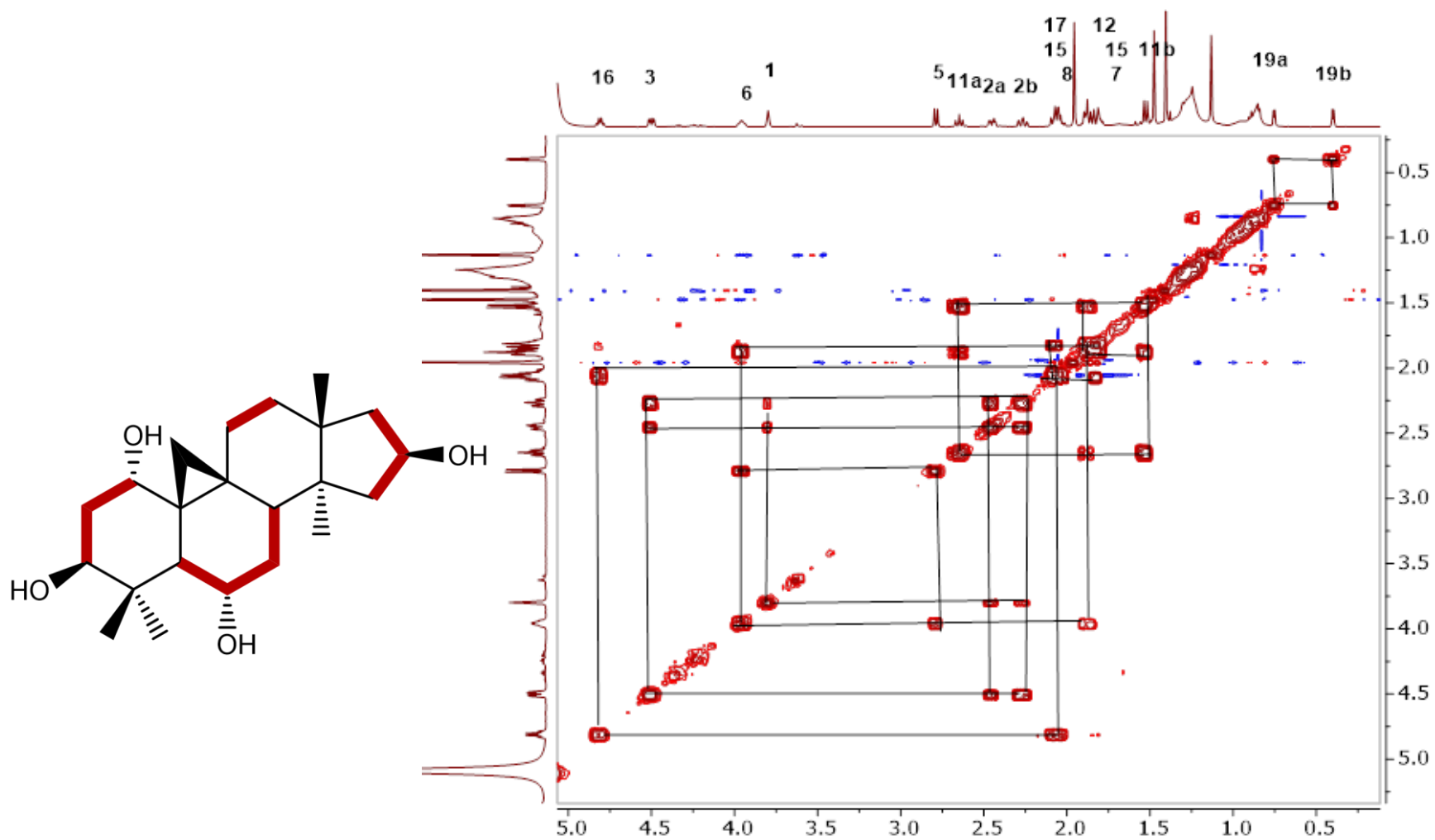
Spectrum 3.38 DEPT spectrum of A2-SCG-02



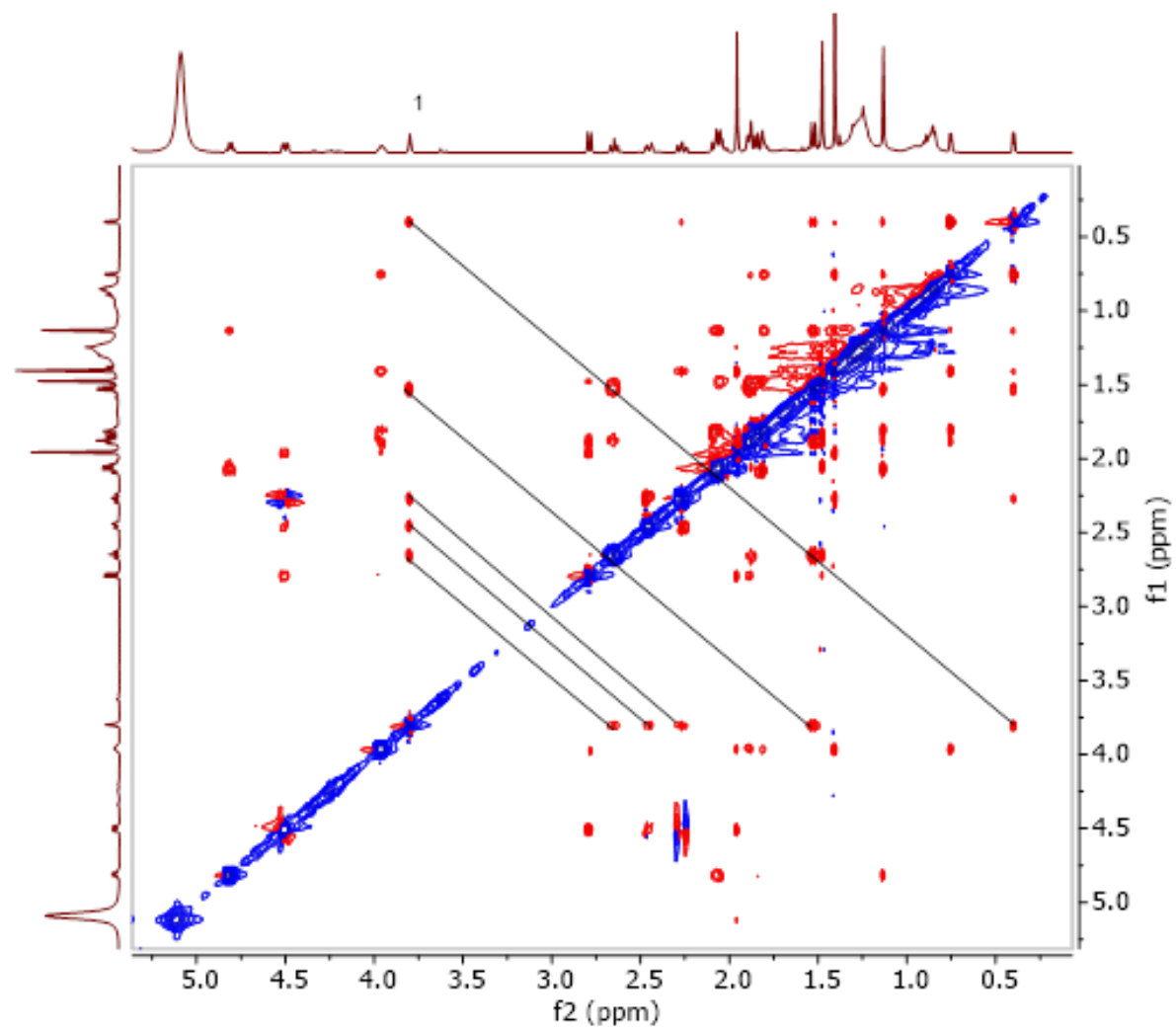
Spectrum 3.39 HSQC spectrum of A2-SCG-02



Spectrum 3.40 HMBC spectrum of A2-SCG-02



Spectrum 3.41 COSY spectrum of A2-SCG-02



Spectrum 3.42 ROESY spectrum of A2-SCG-02

3.2.1.7 Structure Elucidation of A2-SCG-03

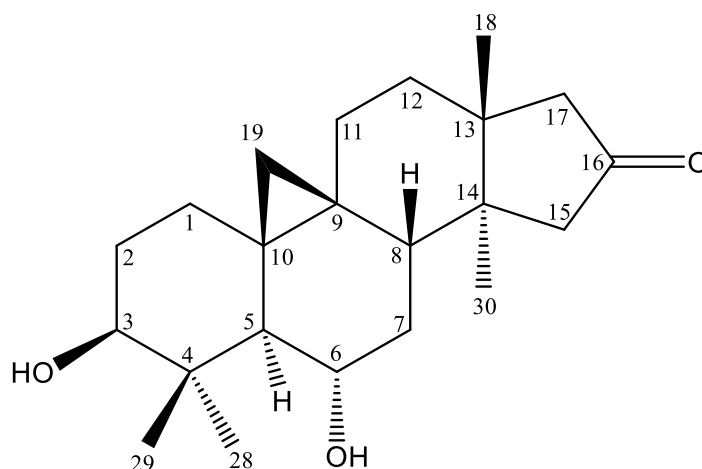
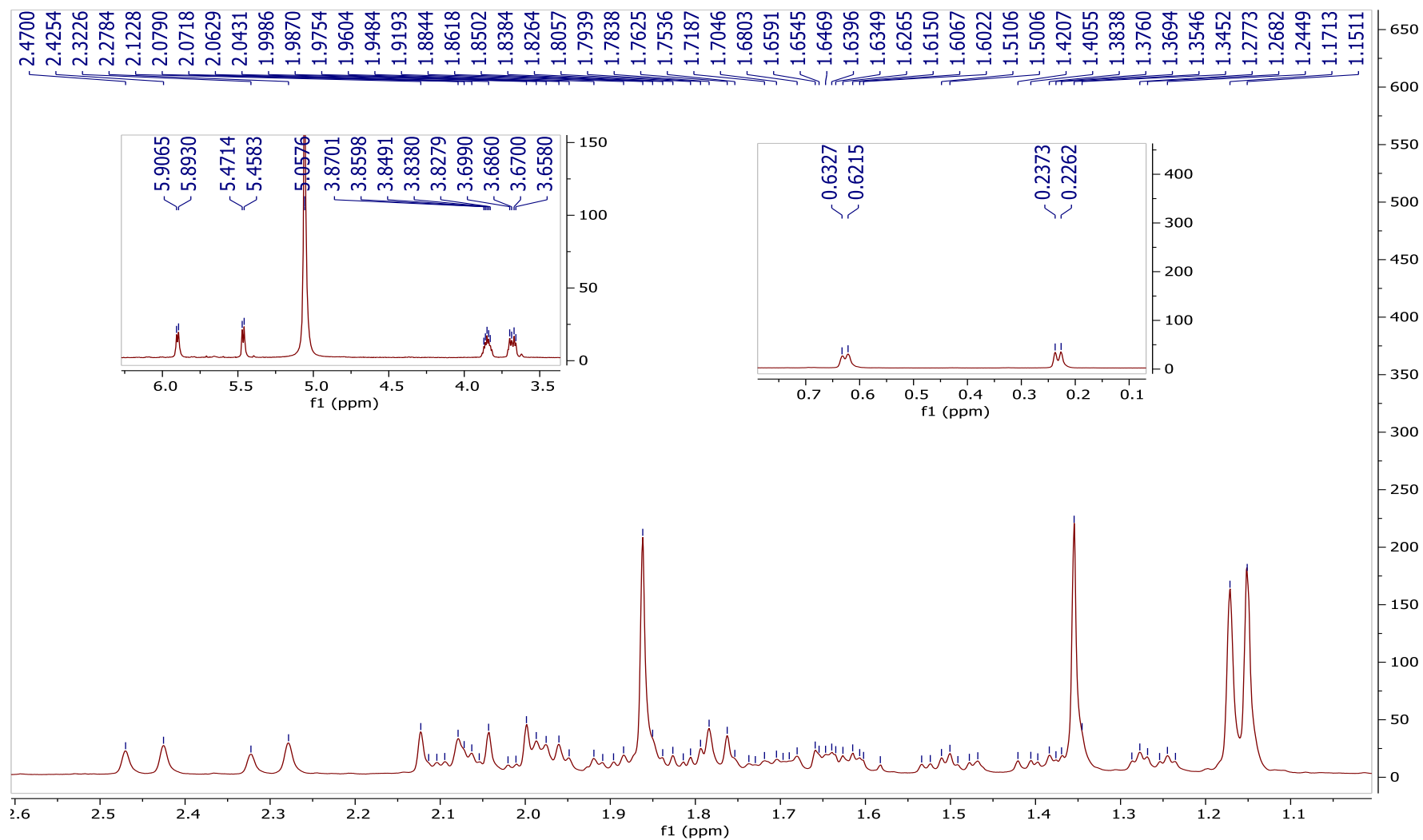


Figure 3.8 Chemical structure of **A2-SCG-03**

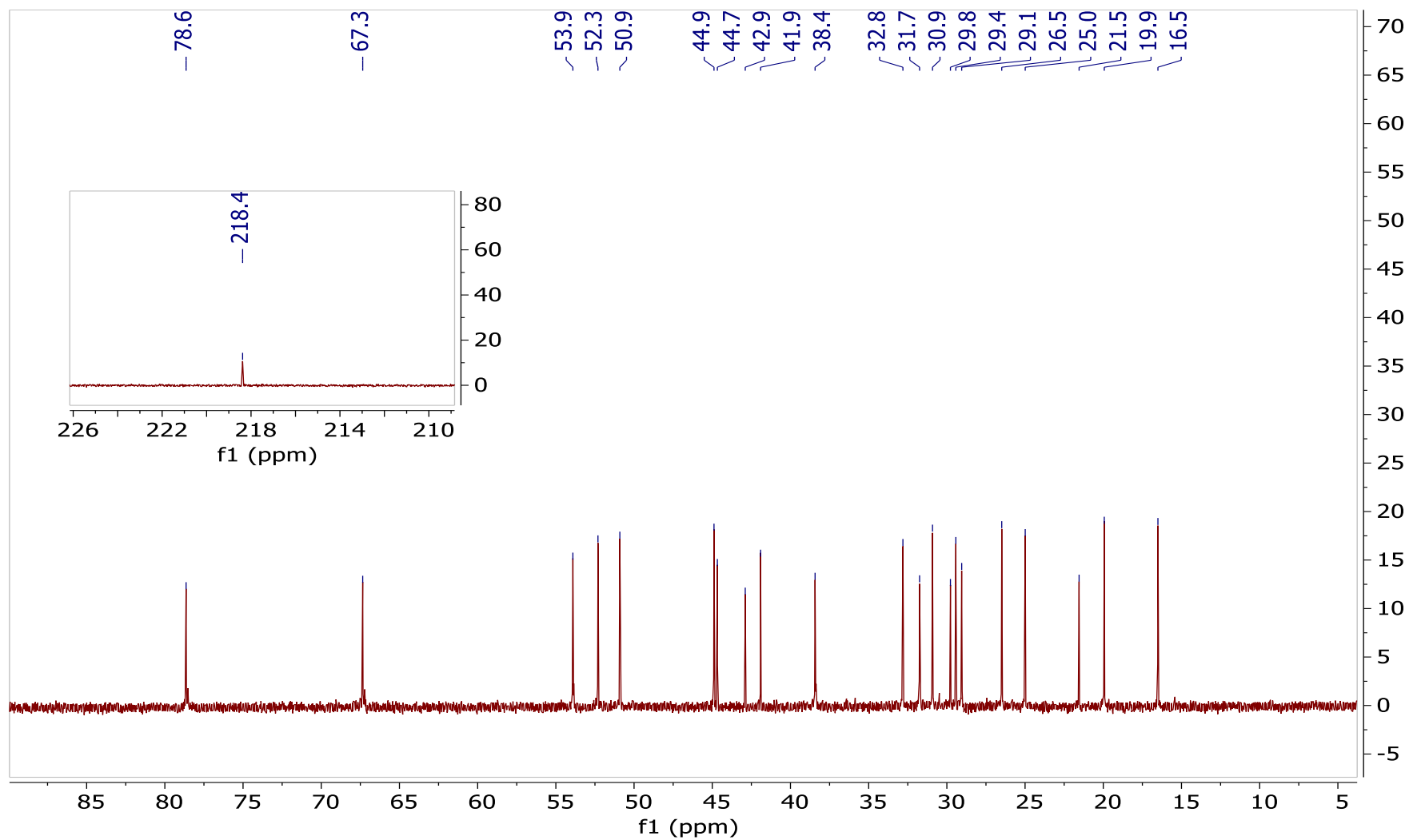
The structure of **A2-SCG-03** was determined as 16-oxo metabolite of 20(27)-octanor cycloastragenol by comparing its ^1H - and ^{13}C -NMR data with those of previously reported compound by our group.⁸⁰

Table 3.7 ^1H and ^{13}C NMR data of **A2-SCG-03** (125/500 MHz, $\text{C}_5\text{D}_5\text{N}$)

C/H	δ_{C} (ppm)	δ_{H} (ppm), J (Hz)
1	32.1	
2	31.1	
3	78.0	3.68 dd (11.3, 5.0)
4	42.2	
5	53.2	
6	66.7	3.85 tt (8.6, 4.6)
7	37.7	
8	44.2	
9	20.8	
10	28.7	
11	25.8	
12	30.2	
13	41.2	
14	44.0	
15	50.2	2.45 d (17.9), 2.30 d (17.7)
16	217.7	
17	51.6	
18	24.3	1.15 s
19	27.1	0.23 d (4.4), 0.63 d (4.5)
28	28.3	1.86 s
29	15.8	1.35 s
30	19.2	1.17 s



Spectrum 3.43 ^1H -NMR Spectrum of **A2-SCG-03**



Spectrum 3.44 ^{13}C -NMR Spectrum of A2-SCG-03

3.2.2. Pure Compounds Isolated from Biotransformation by *Camarosporium laburnicola*

E-SCG-01 and **E-SCG-02** were isolated from biotransformation study of 20(27)-octanor cycloastragenol by *Camarosporium laburnicola*.

3.2.2.1 Structure Elucidation of E-SCG-01

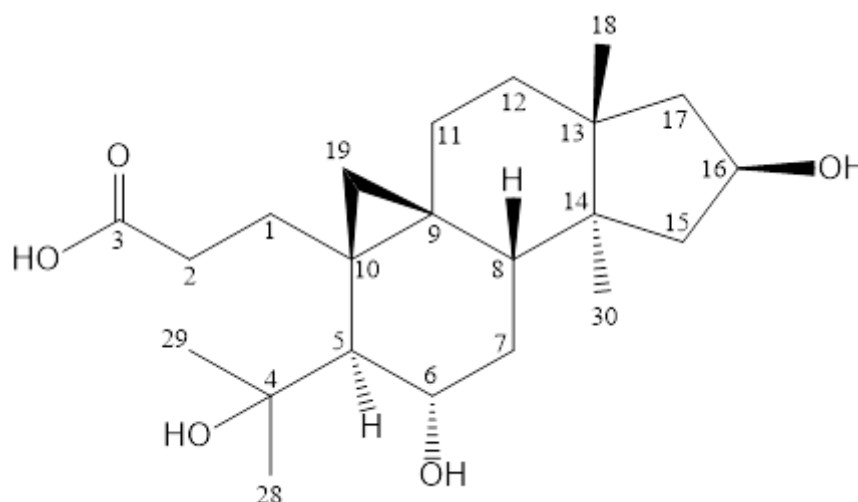


Figure 3.9 Chemical structure of **E-SCG-01**

In the HR-ESI-MS spectra of **E-SCG-01**, the molecular ion peaks were observed at m/z 403.2443 $[M+Na]^+$ suggesting a molecular formula of $C_{22}H_{36}O_5$.

The characteristic 9–19 cyclopropane signals of 20(27)-octanor cycloastragenol and the low-field characteristic signals belonging to the H-6 and H-16 were observed unchanged. In the ^{13}C NMR spectrum, the oxymethyne signal belonging to C-3 was lacking, and a carboxyl signal was deduced from δ 176.8 resonance. In addition, a quaternary carbon adjacent to oxygen (δ 76.4) was noticed. Since no other alterations were observed on the spectral data of B, C and D rings, a modification on the ring A was suggested.

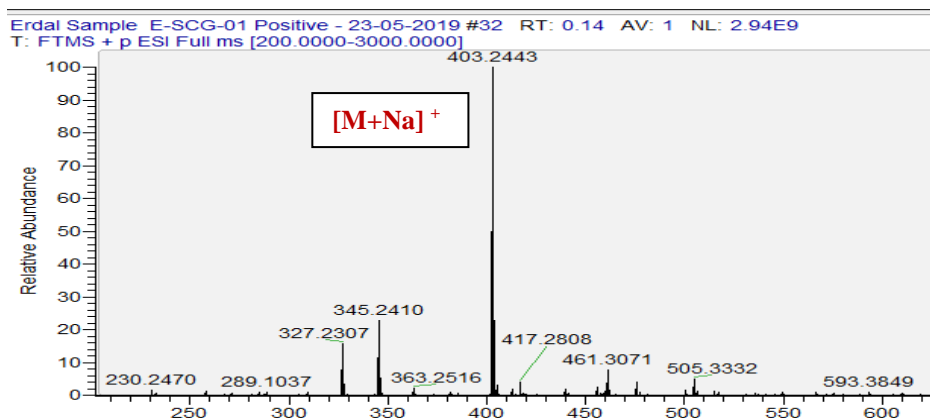
In the HMBC spectrum, the long-distance correlation of the carbon at δ 76.4 to H-5, H₃-28 and H₃-29 justified the hydroxylation at C-4. The fact that the carboxyl carbon at 176.8 ppm did not interact with CH₃-28/ CH₃-29 while interacting with two methylene groups proposed that **E-SCG-01** went through a cleavage reaction in the A-ring via

Baeyer–Villiger type oxidation. The observed data was consistent with those of 3,4-seco cycloartane metabolites, which were established during biotransformation studies with the fungus *Glomerella fusarioides* earlier.^{76,77 80}

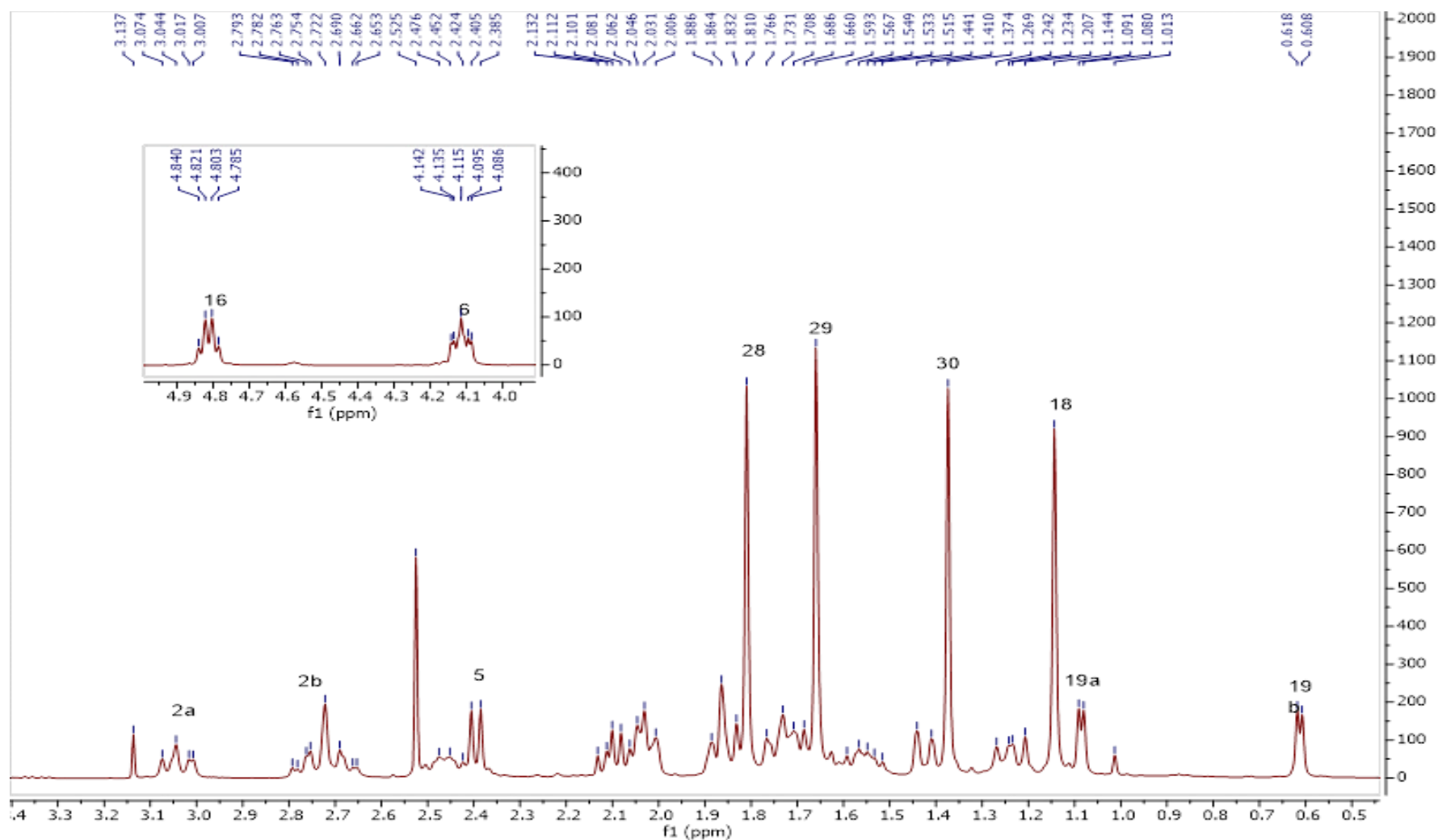
Since our spectral data were completely parallel with the previously determined biotransformation products, the structure of **E-SCG-1** was elucidated as shown in Figure 3.9.

Table 3.8 ¹³C- ve ¹H-NMR data of **E-SCG-01** (100/400 MHz, C₅D₅N).

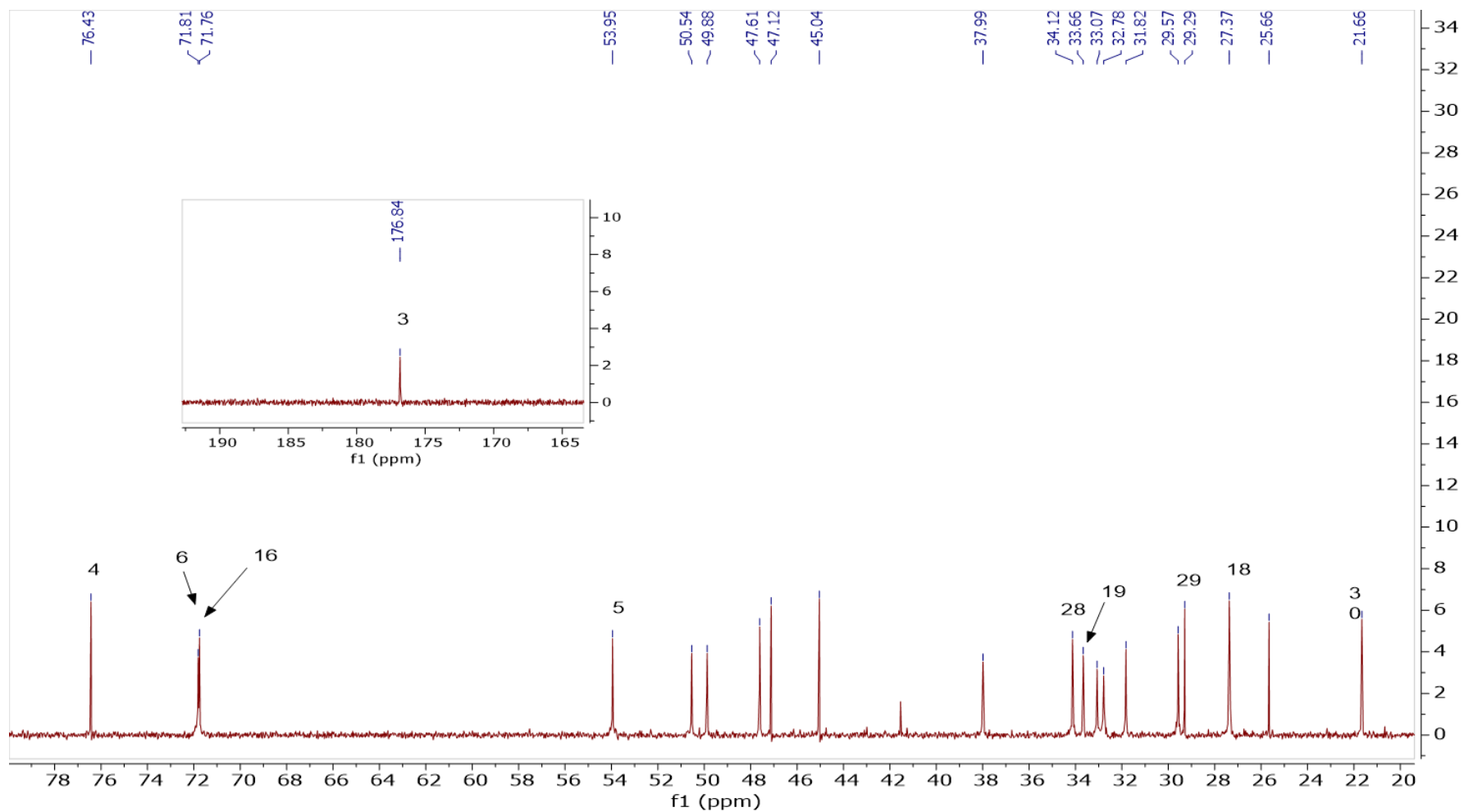
C/H	δ _C (ppm)	δ _H (ppm), <i>J</i> (Hz)
1	32.8	1.74 m, 2.73 m
2	33.1	3.04 m, 2.73 m
3	176.8	
4	76.4	
5	54.0	2.40 d (8.1)
6	71.8	4.11 m
7	38.0	1.86 m, 1.66 m
8	47.6	1.43 d (12.4)
9	25.7	
10	29.6	
11	27.4	2.45 m, 1.24 dd (14, 10.7)
12	31.8	1.55 m, 1.74 m
13	45.0	
14	47.1	
15	49.9	1.85 m, 2.03 m
16	71.8	4.81 dd (7.3, 7.4)
17	50.5	2.10 m, 2.03 m
18	27.4	1.14 s
19	33.7	1.09 d (4.2), 0.61 d (4.2)
28	34.1	1.81 s
29	29.3	1.66 s
30	21.7	1.37 s



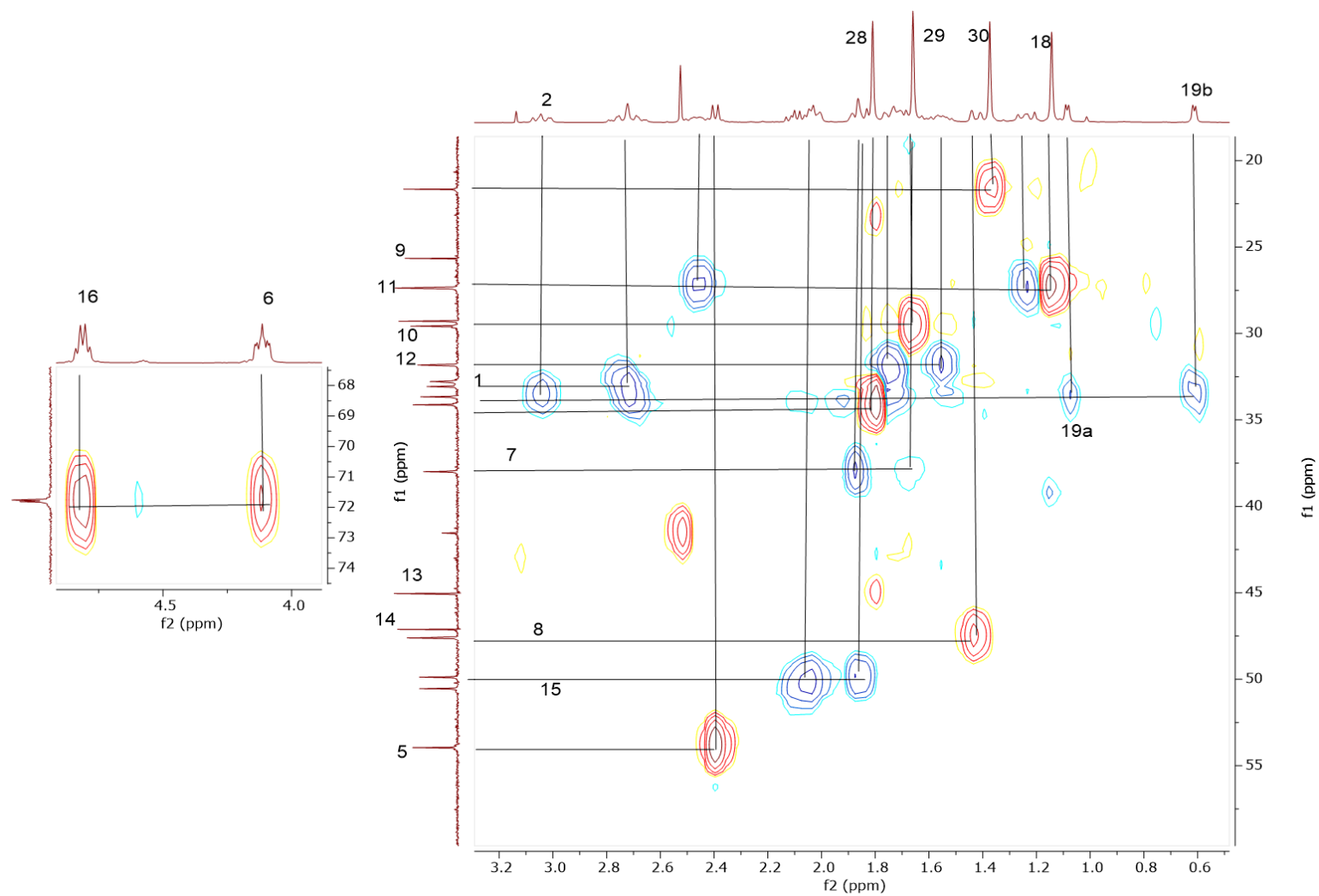
Spectrum 3.45 HR-ESI-MS spectrum of **E-SCG-01** (positive mode)



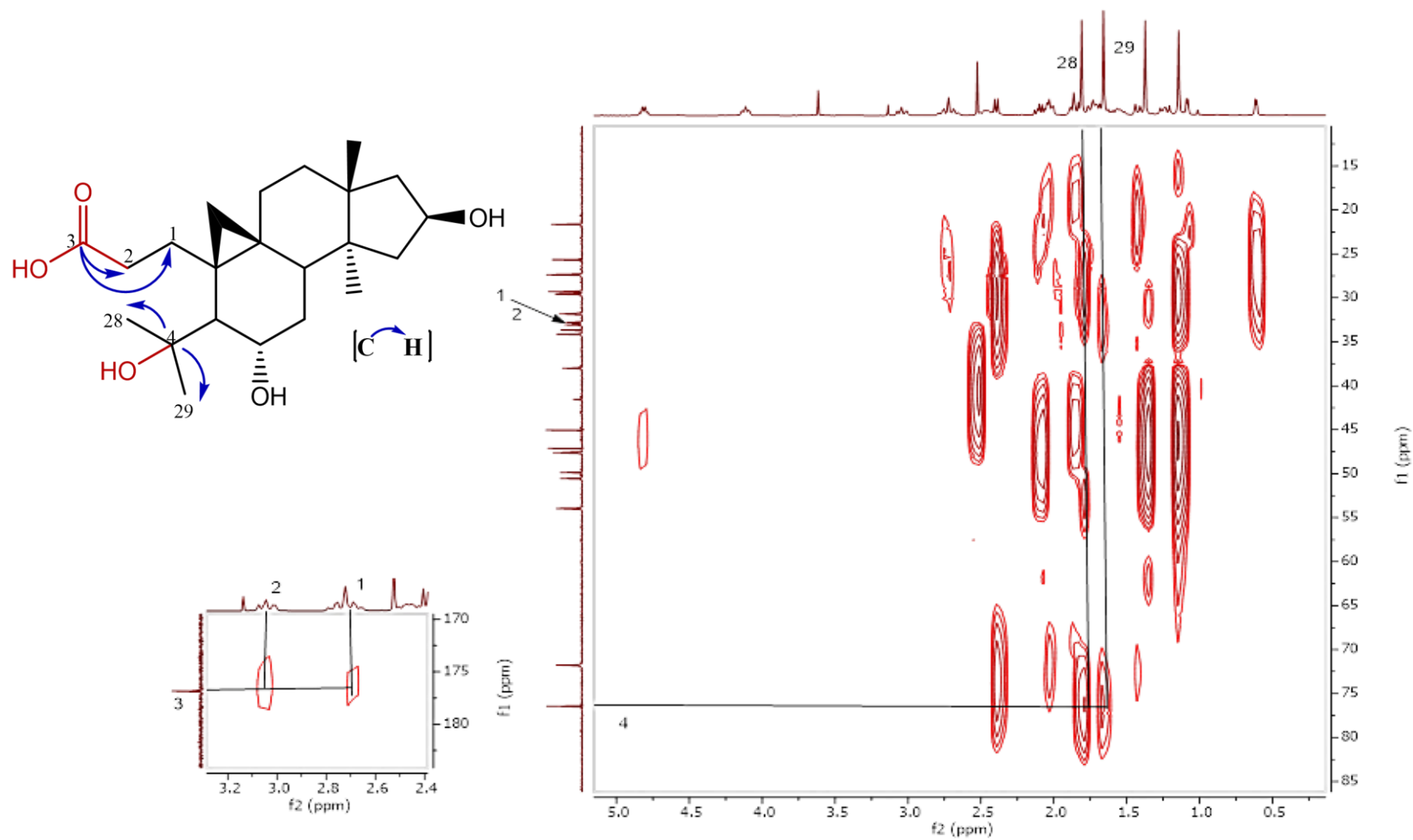
Spectrum 3.46 ^1H -NMR Spectrum of **E-SCG-01**



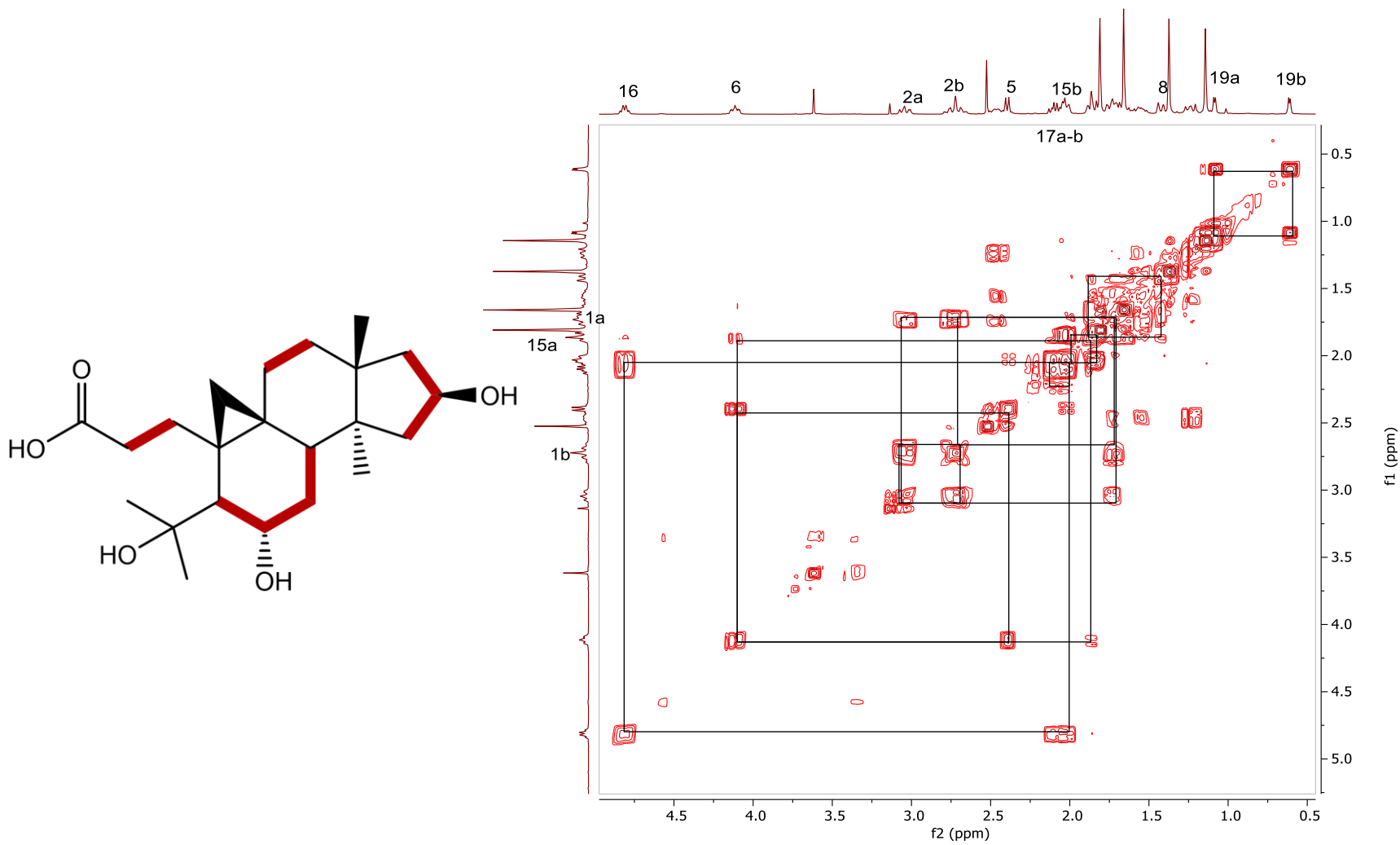
Spectrum 3. 47 ^{13}C -NMR Spectrum of **E-SCG-01**



Spectrum 3.48 HSQC spectrum of **E-SCG-01**



Spectrum 3. 49 HMBC spectrum of **E-SCG-01**



Spectrum 3. 50 COSY spectrum E-SCG-01

3.2.2.2. Structure Elucidation of E-SCG-02

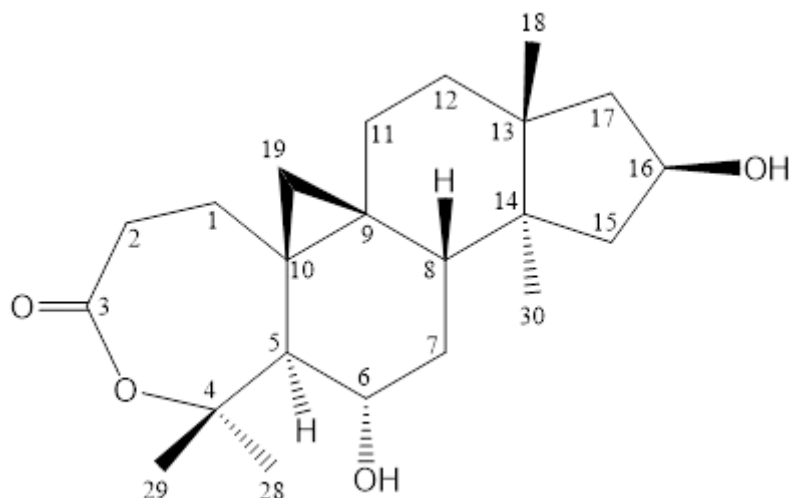


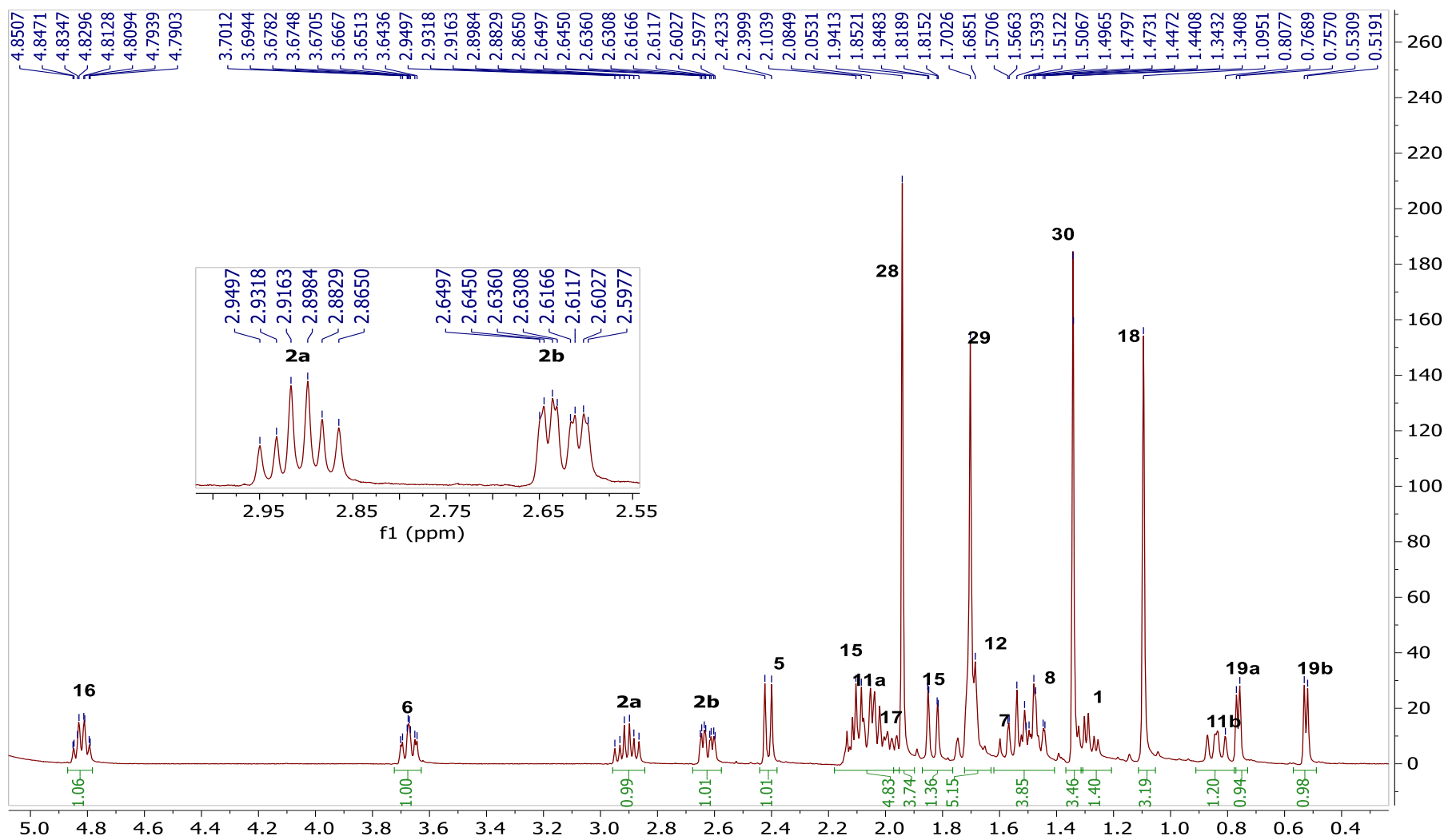
Figure 3.10 Chemical structure of E-SCG-02

From detailed inspection of 1D- and 2D NMR spectra, it was ascertained that the only modification for **E-SCG-02** was consistent with the ring A. The carboxyl signal at 174.4 ppm and its long-range correlations with two methylene groups (H-2 and H-1) suggested a ring opening for **E-SCG-02** at first glance as in **E-SCG-1**. However, an oxygenated quaternary carbon was observed at 86.1 ppm in the ^{13}C -NMR spectrum. In the HMBC spectrum, its long-range correlations with two methyl groups (δ 1.70 and 1.94; respectively CH₃-28 and CH₃-29) implied that it was C-4.

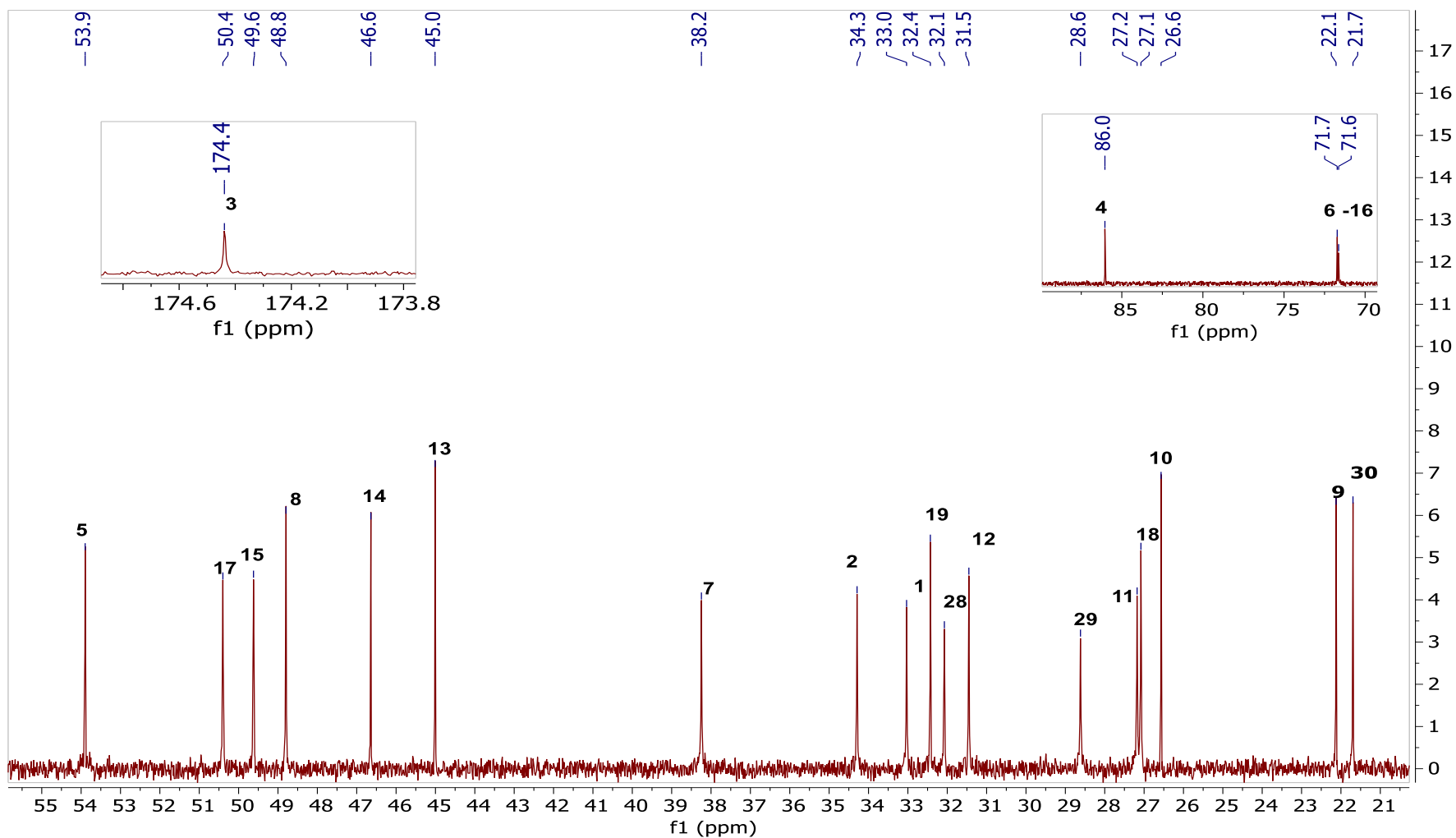
The downfield shift of C-4 resonance (about 10 ppm) compared to **E-SCG-01** and spectral data comparison with similar metabolites reported previously revealed that A ring was transformed into a 7-membered lactone ring as a result of the catalysis of Baeyer-Villiger-type P450 monooxygenase enzyme.^{76, 77} Thus, the structure of **E-SCG-02** was established as shown in Figure 3.10.

Table 3.9 ^{13}C - ve ^1H -NMR data of **E-SCG-02** (100/400 MHz, $\text{C}_5\text{D}_5\text{N}$).

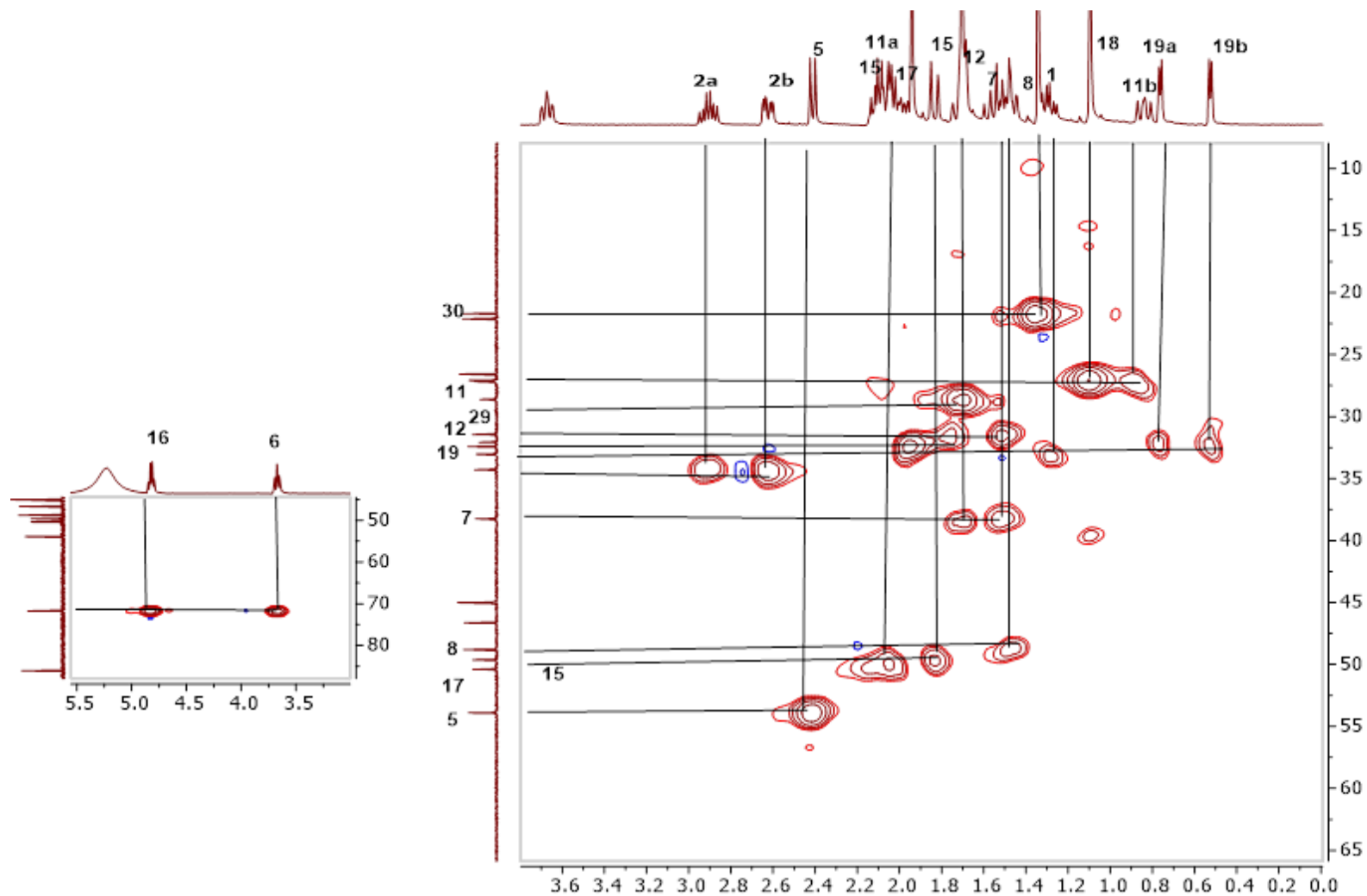
C/H	δ_{C} (ppm)	δ_{H} (ppm), J (Hz)
1	33.0	1.29 td (5.6, 13.6), 1.28 dd (5.9, 12.0)
2	34.3	2.91 td (13.3, 7.2), 2.62 dd (13.3, 4.5)
3	174.4	
4	86.1	
5	53.9	2.41 d (9.4)
6	71.7	3.67 td (10.4, 2.8)
7	38.3	1.55 m, 1.70 m
8	48.8	1.48
9	22.1	
10	26.6	
11	27.2	0.84 dd (14.4, 10.7), 2.10 m
12	31.5	1.51 m, 1.72 m
13	45.0	
14	46.7	
15	49.6	1.83 d (13.3), 2.04 m
16	71.6	4.82 dd (14.8, 7.4)
17	50.4	2.04 m, 2.09 m
18	27.1	1.10
19	32.4	0.52 d (4.7), 0.76 d (4.7)
28	32.1	1.94 s
29	28.6	1.70s
30	21.7	1.34



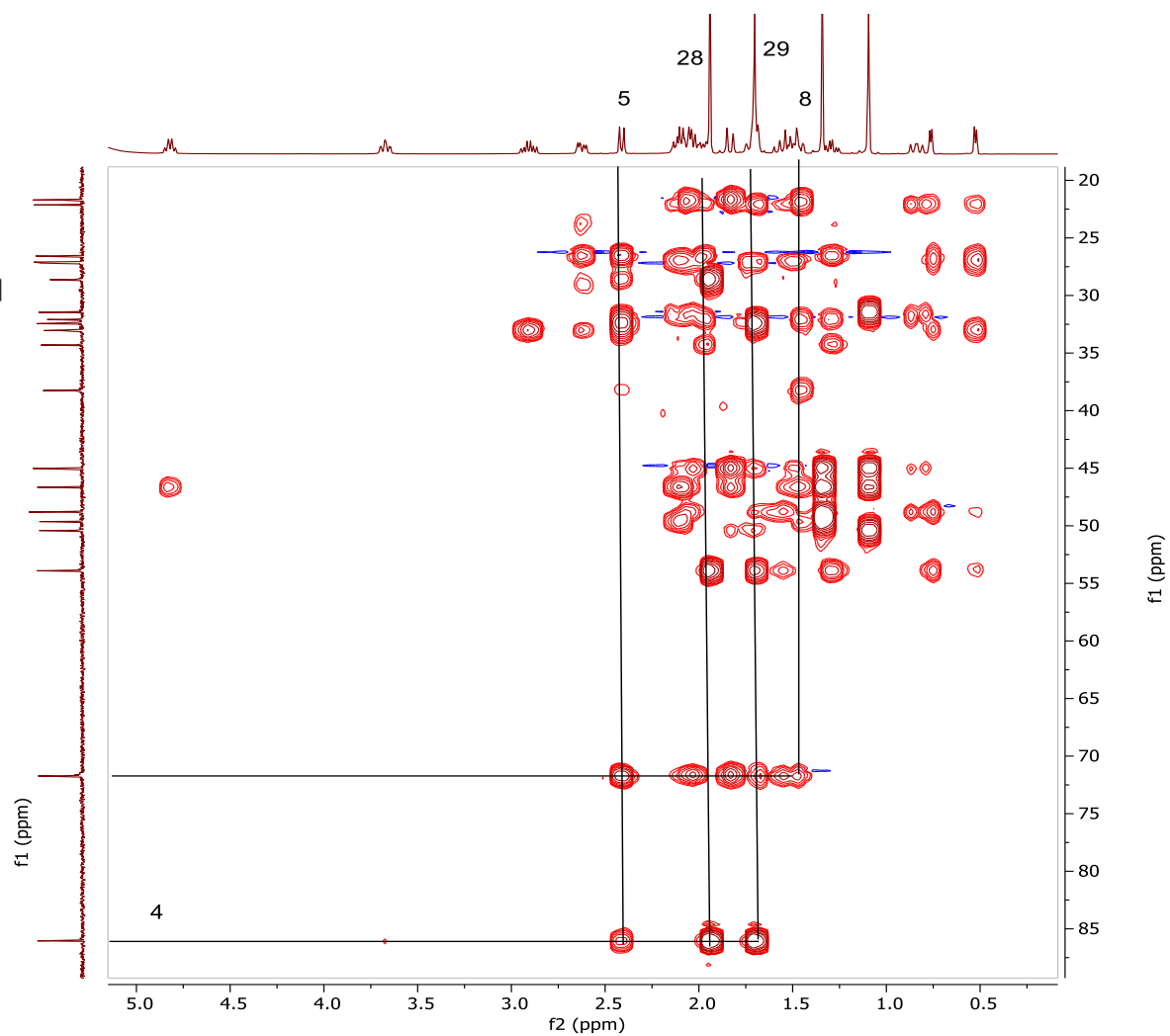
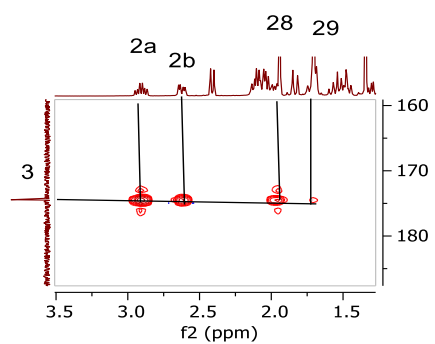
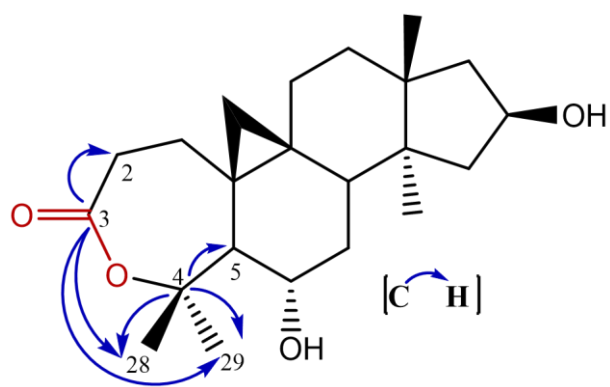
Spectrum 3.51 ^1H -NMR Spectrum of **E-SCG-02**



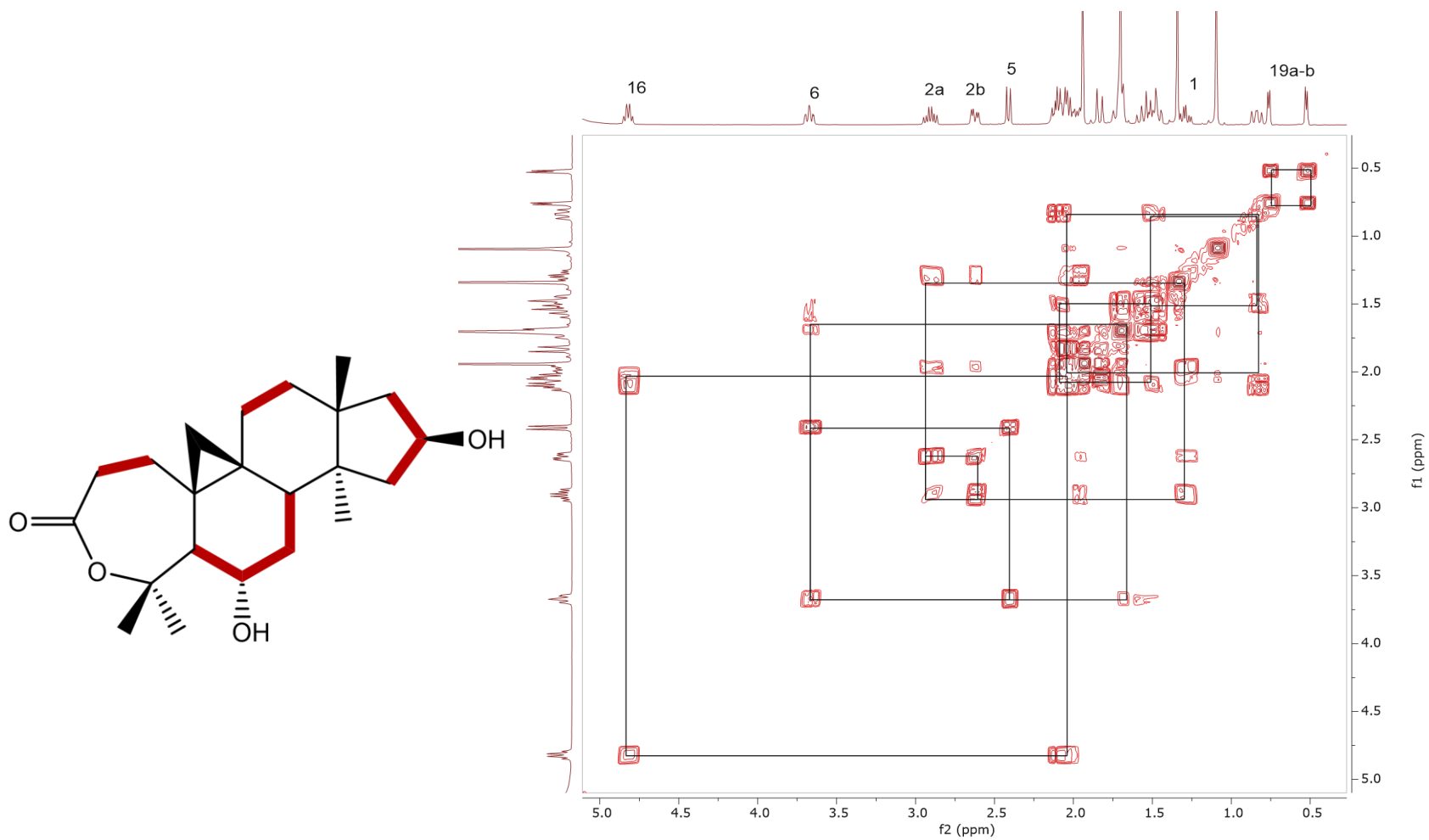
Spectrum 3.52 ^{13}C -NMR Spectrum of **E-SCG-02**



Spectrum 3.53 HSQC spectrum of **E-SCG-02**



Spectrum 3.54 HMBC spectrum of **E-SCG-02**



Spectrum 3.55 COSY spectrum of **E-SCG-02**

3.2.3 Pure Compounds Isolated from Biotransformation by *Neosartorya hiratsukae*

Neo-SCG-01, Neo-SCG-02, Neo-SCG-03, Neo-SCG-04 and Neo-SCG-06 were isolated from biotransformation study of 20(27)-octanor cycloastragenol by *Neosartorya hiratsukae*.

3.2.3.1 Structure Elucidation of Neo-SCG-01

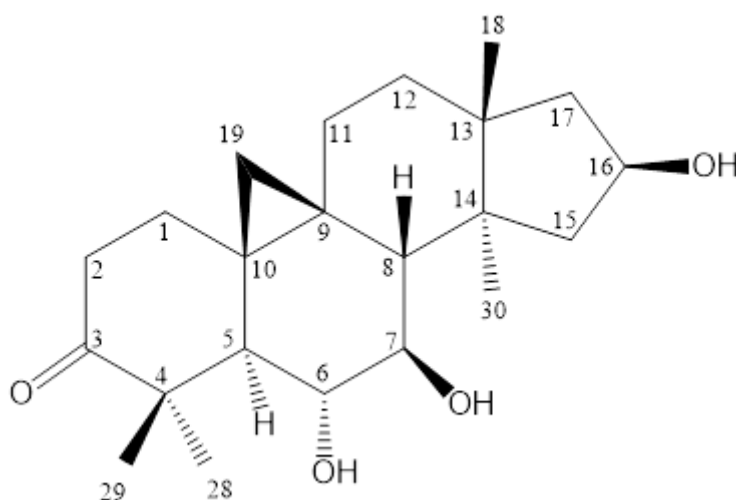


Figure 3.11 Chemical structure of Neo-SCG-01

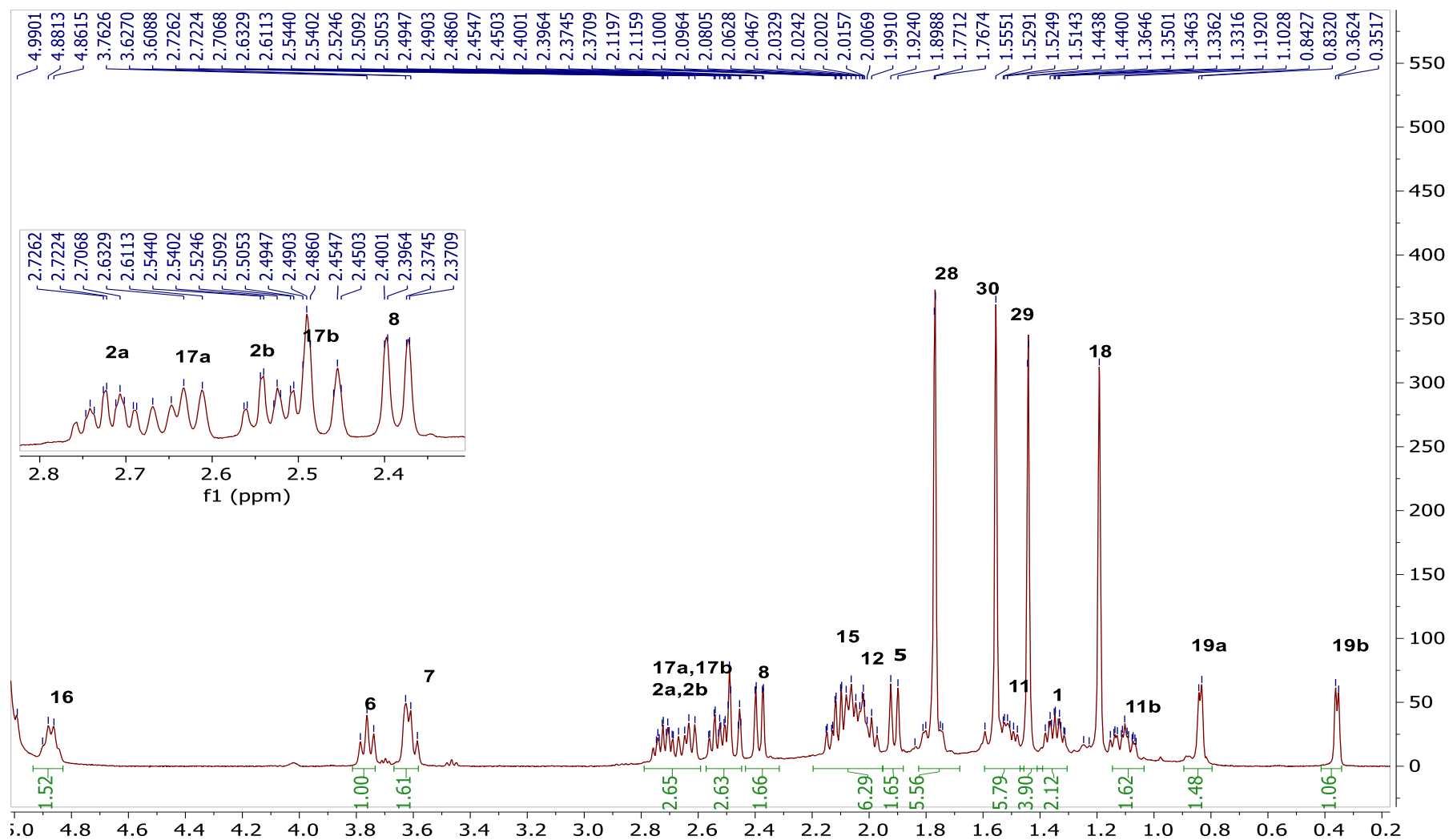
In the ^1H -NMR spectrum, the characteristic AX system signals of 9,19-cyclopropane ring, four tertiary methyl groups in the up-field region, and the characteristic signals belonging to the H-6 and H-16 oxymethyne protons were observed. In the low field, there was no resonance corresponding to H-3; however, an oxymethyne proton was observed at 3.63 ppm (t, $J=7.3$ Hz), implying to a transformation via monooxygenation.

In the ^{13}C -NMR spectrum; the characteristic C-3 signal resonating around 78.0 ppm was also absent, and the presence of a new resonance at δ 216.9 in the low field suggested oxidation of C-3(OH) to a carbonyl. By using the HSQC spectrum, the corresponding carbon signal of the new proton at δ 3.63 was determined to be δ 73.7. In the COSY spectrum, the δ 3.63 proton coupled with δ 3.76 (H-6, t, $J=9.4$ Hz) and δ 2.39 (H-8), helping us to locate the hydroxylation at C-7. The long-range HMBC cross peaks

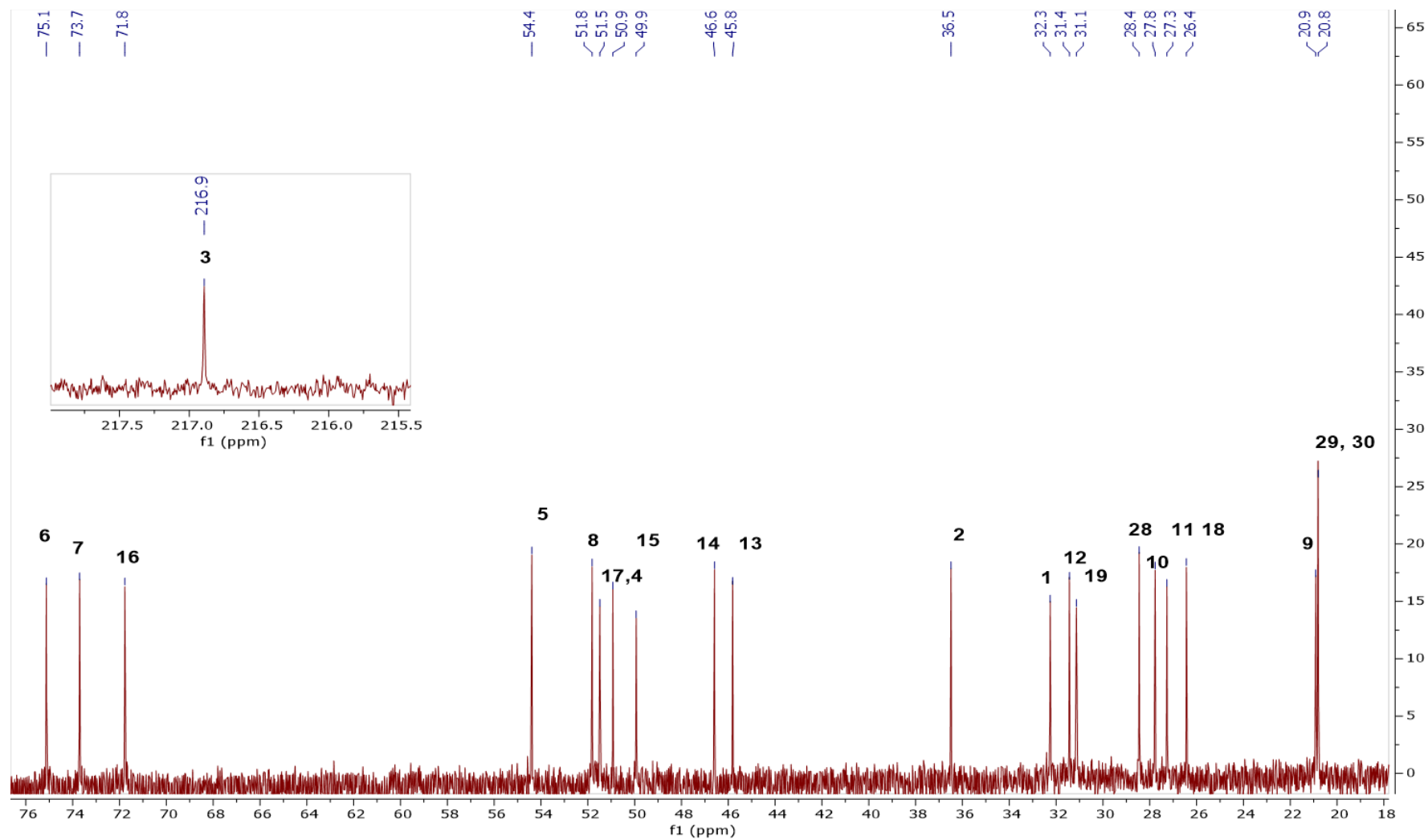
from H-5, H-6 and H-8 to C-7 also verified the position of monooxygenation. The orientation of C-7(OH) was found to be β based on the NOESY cross peak between H-1 and β -oriented H-19b at δ 0.37. Thus, the structure of **Neo-SCG-01** was established as 7(β)-hydroxy,3-oxo derivative of 20,27-octanor cycloastragenol.

Table 3.10 ^{13}C - ve ^1H -NMR data of **Neo-SCG-01** (125/500 MHz, $\text{C}_5\text{D}_5\text{N}$).

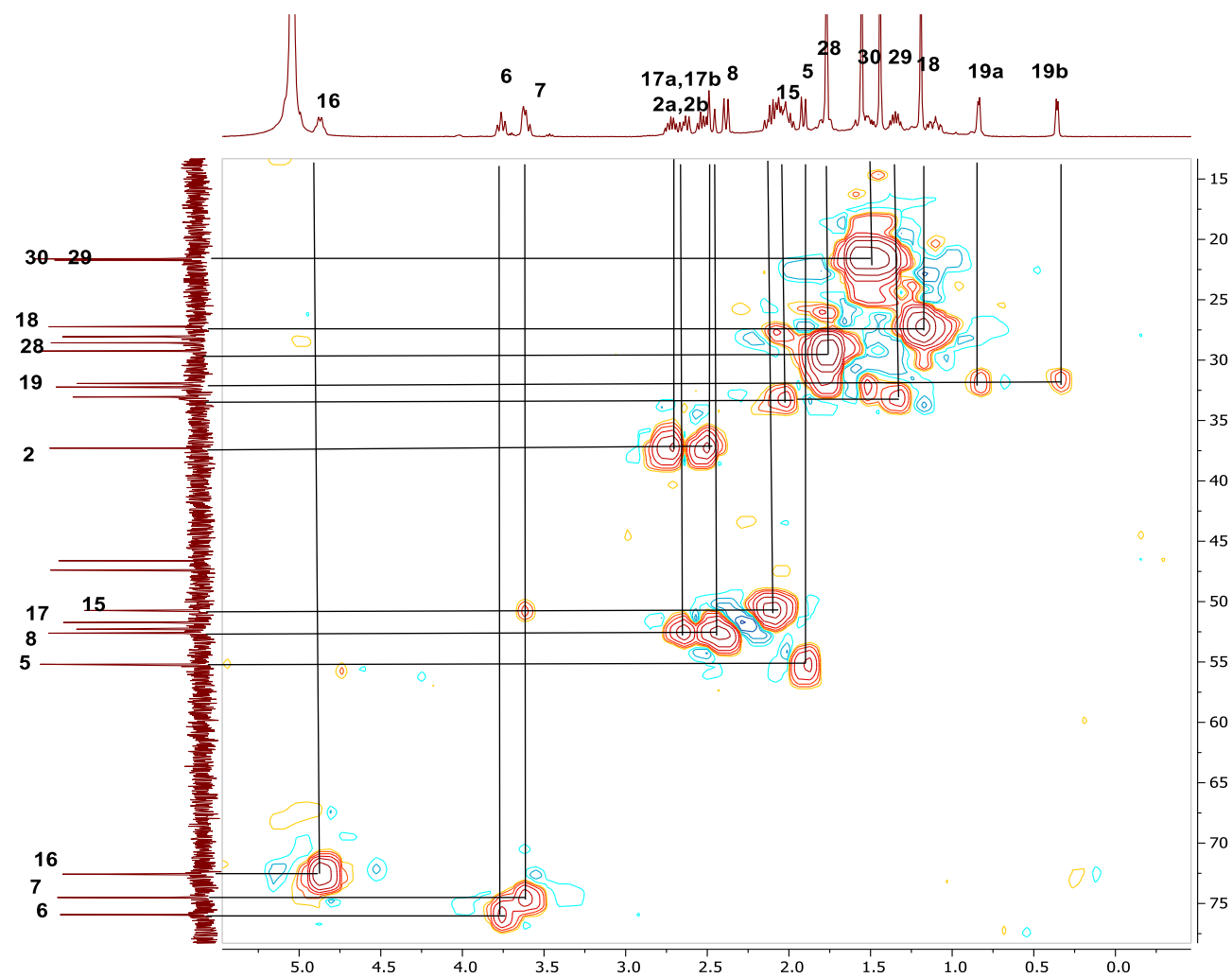
C/H	δ_{C} (ppm)	δ_{H} (ppm), J (Hz)
1	32.3	2.04 m, 1.35 m
2	36.5	2.53 ddd (13.9, 6.9, 1.5)
3	216.9	
4	50.9	
5	54.4	1.91 dd (10.0)
6	75.1	3.76 t (9.4)
7	73.7	3.63 t (7.3)
8	51.8	2.39
9	20.8	
10	27.8	
11	27.3	2.08
12	31.4	1.55 m, 1.77 m
13	45.8	
14	46.7	
15	49.9	2.14 m
16	71.8	4.87 dd (14.8, 7.9)
17	51.5	2.64 dd (14.4, 8.6), 2.72 tdd (7.7, 4.8, 1.89)
18	26.4	1.19 s
19	31.1	0.84 d (4.3), 0.36 d (4.3)
28	28.4	1.77 s
29	20.9	1.44 s
30	20.8	1.56



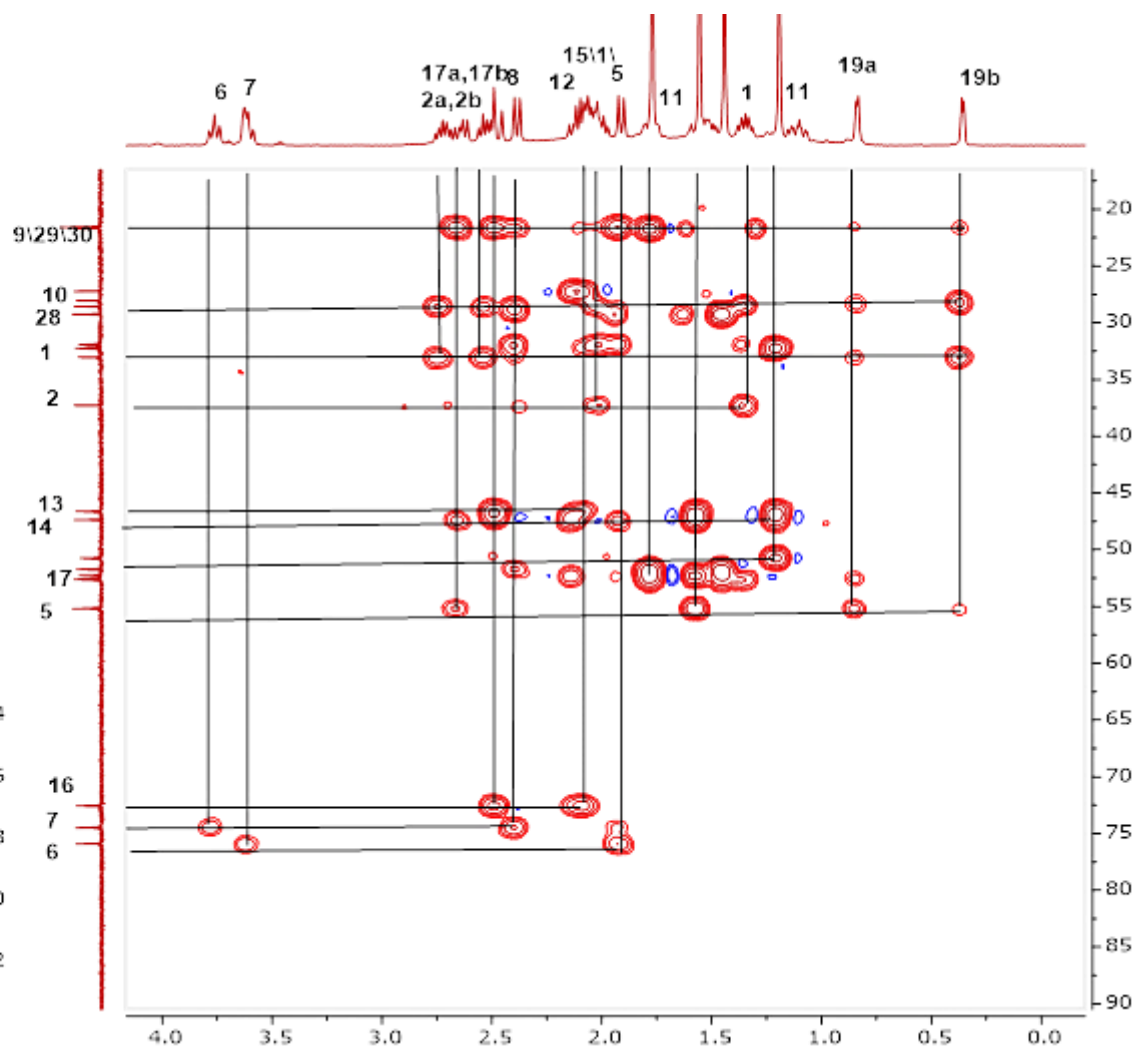
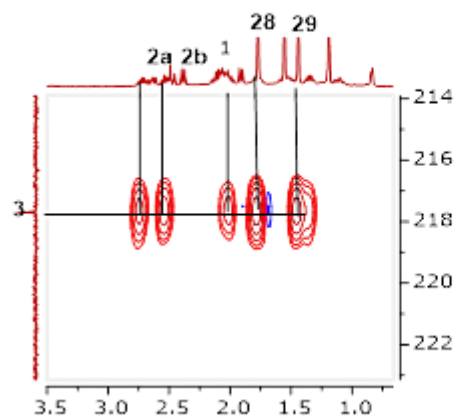
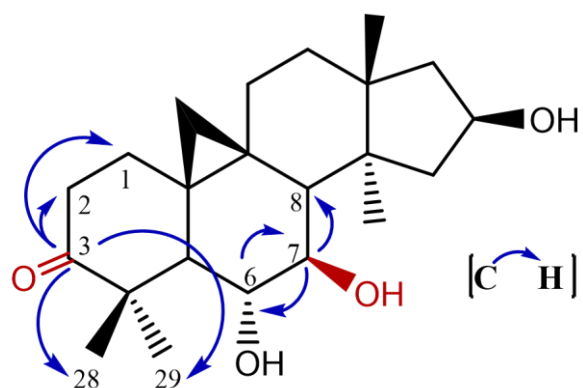
Spectrum 3.56 ^1H -NMR Spectrum of Neo-SCG-01



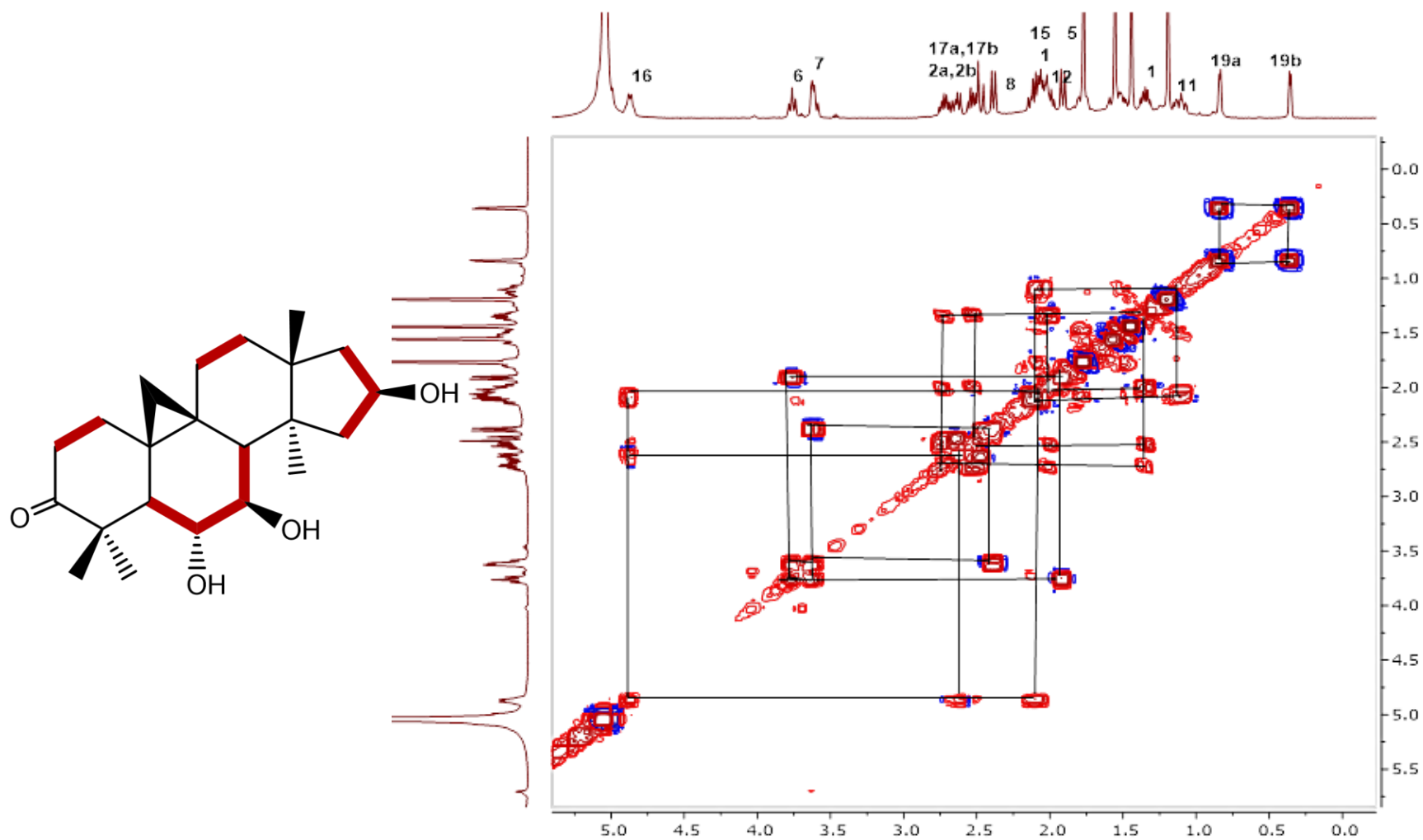
Spectrum 3.57 ^{13}C -NMR Spectrum of Neo-SCG-01



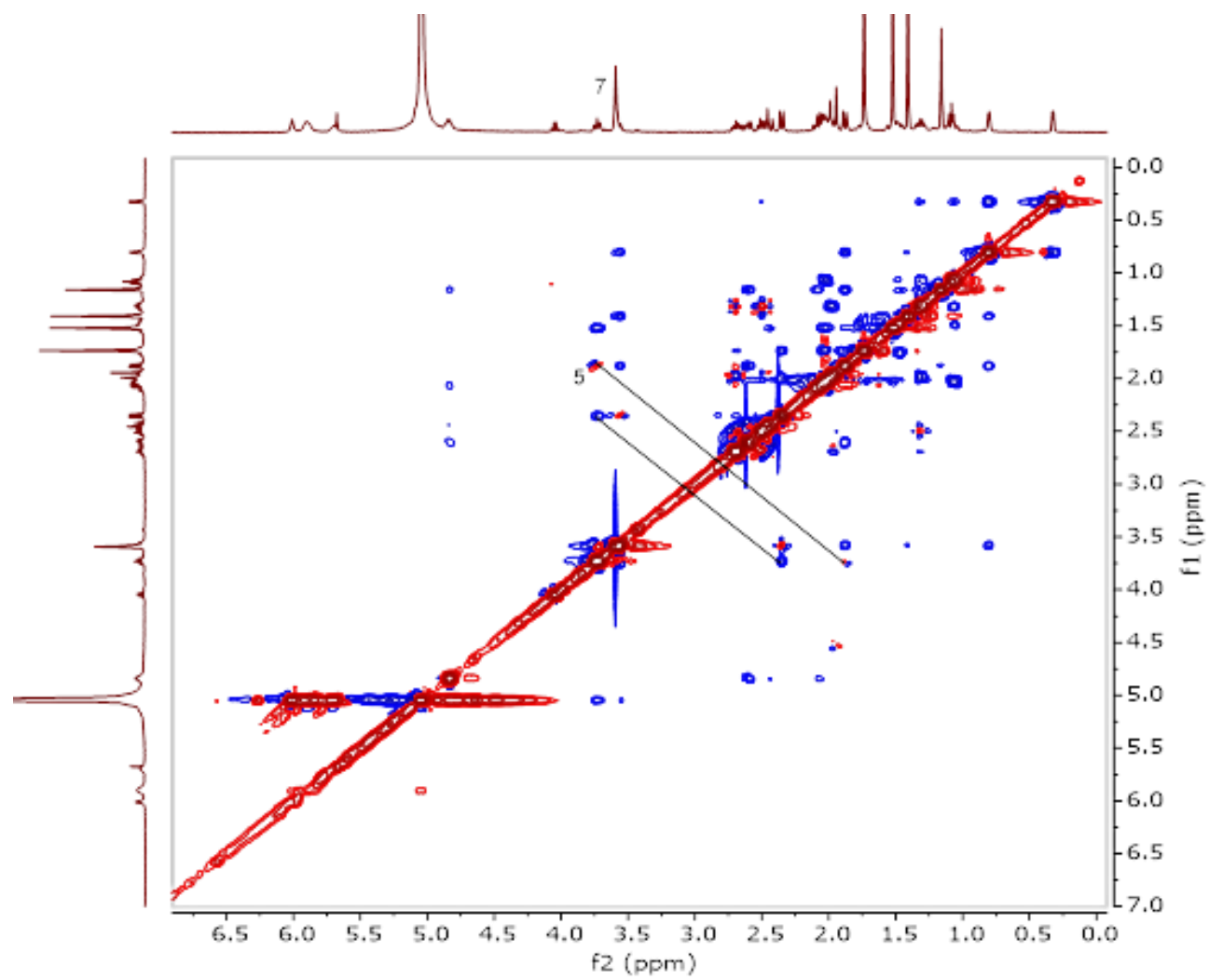
Spectrum 3.58 HSQC spectrum of Neo-SCG-01



Spectrum 3.59 HMBC spectrum of Neo-SCG-01



Spectrum 3.60 COSY spectrum of Neo-SCG-01



Spectrum 3.61 NOESY spectrum of Neo-SCG-01

3.2.3.2 Structure Elucidation of Neo-SCG-02

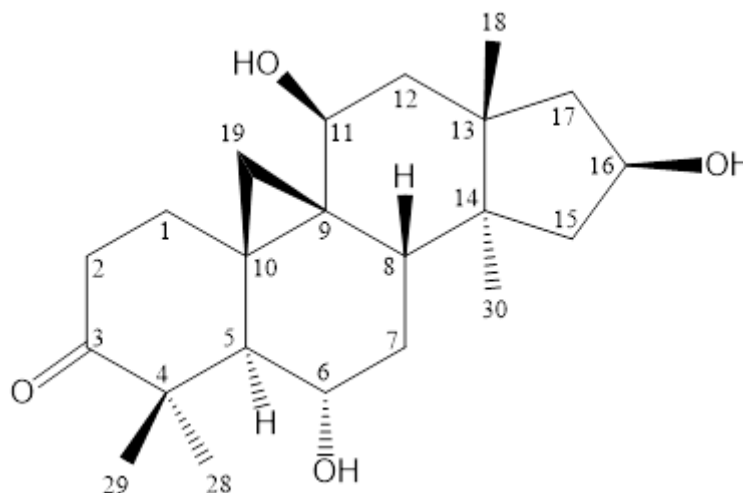


Figure 3.12 Chemical structure of **Neo-SCG-02**

In the HR-ESI-MS spectrum of **Neo-SCG-02**, a major ion peak was observed at m/z 385. 23476 $[M+Na]^+$ indicative of a molecular formula $C_{22}H_{34}O_4$.

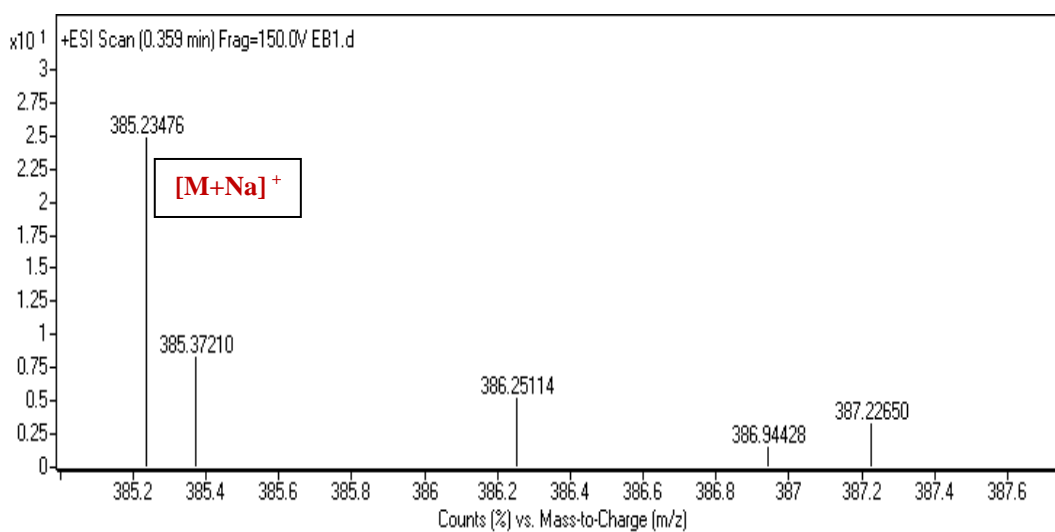
Initial inspection of the 1H -NMR spectrum of **Neo-SCG-02** displayed that one of the distinctive 9,19-cyclopropane ring AX system signals was missing as in **A-SCG-03**. A detailed inspection of the COSY and HSQC spectra revealed that H_{2-19} protons were resonating at δ 1.76 and 0.56, suggesting C-11 hydroxylation. The characteristic signals belonging to the H-6 and H-16 oxymethyne protons were present in the 1H -NMR spectrum, while there was no trace of H-3. The presence of a down-field resonance at δ 217.9 suggested oxidation of C-3(OH) to a carbonyl group. Additionally, an oxymethyne proton was observed at 4.37 ppm (t, $J=5.7$ Hz), which was readily assigned to H-11. By using the HSQC spectrum, the C-11 resonance was found to be δ 64.8.

In the HMBC spectrum, the key long-range correlations from C-3 (folded to upfield due to operational error) to H_3 -28 and H_3 -29, and from C-11 to H-19a and H-12b verified the abovementioned transformations.

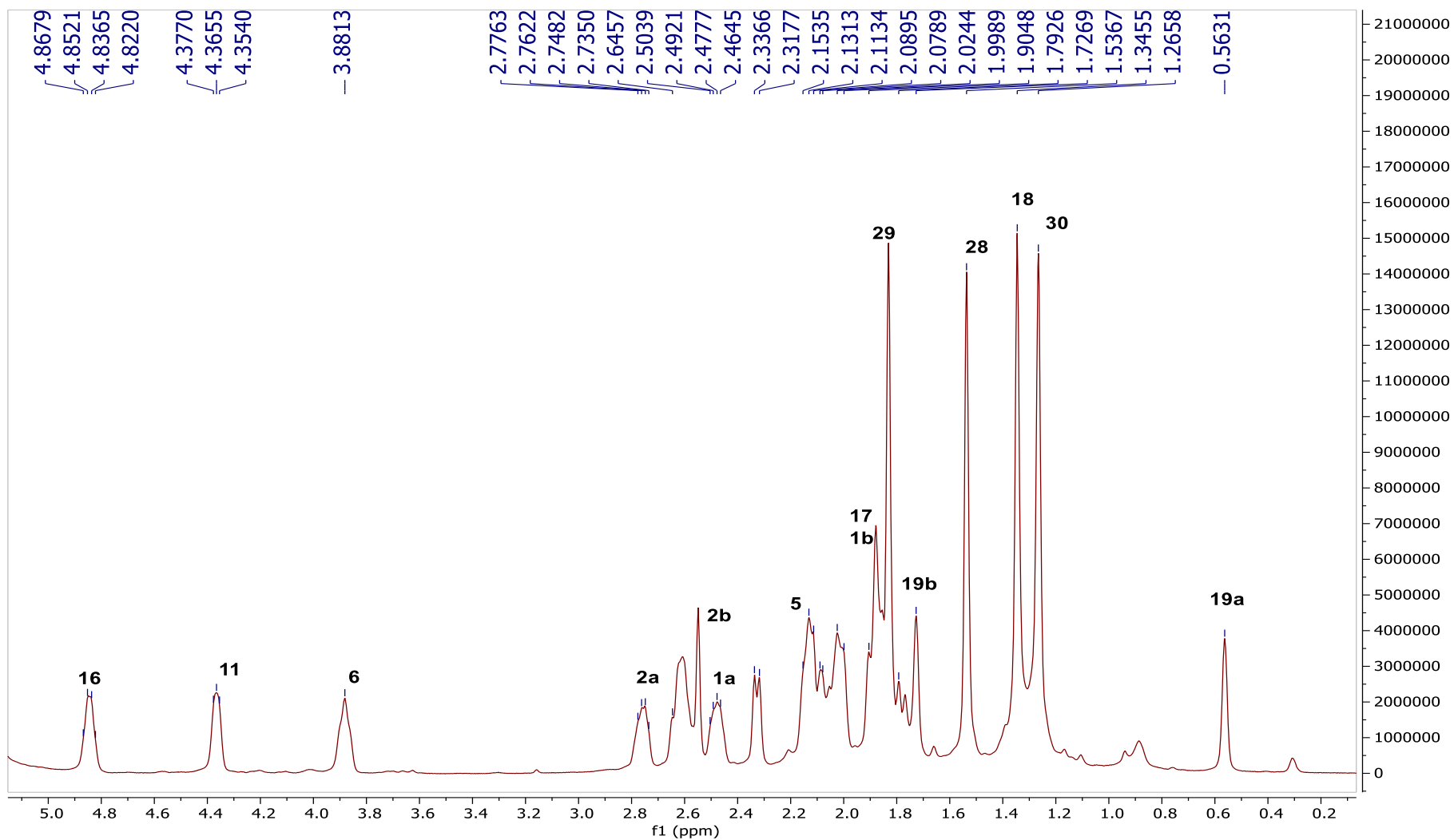
The orientation of C-11(OH) was proposed to be β based on the spectral data comparison with those of **A-SCG-03**. Thus, the structure of **Neo-SCG-02** was established as 11 β -hydroxy,3-oxo derivative of 20,27-octanor cycloastragenol.

Table 3.11 ^{13}C - ve ^1H -NMR data of **Neo-SCG-02** (125/500 MHz, $\text{C}_5\text{D}_5\text{N}$).

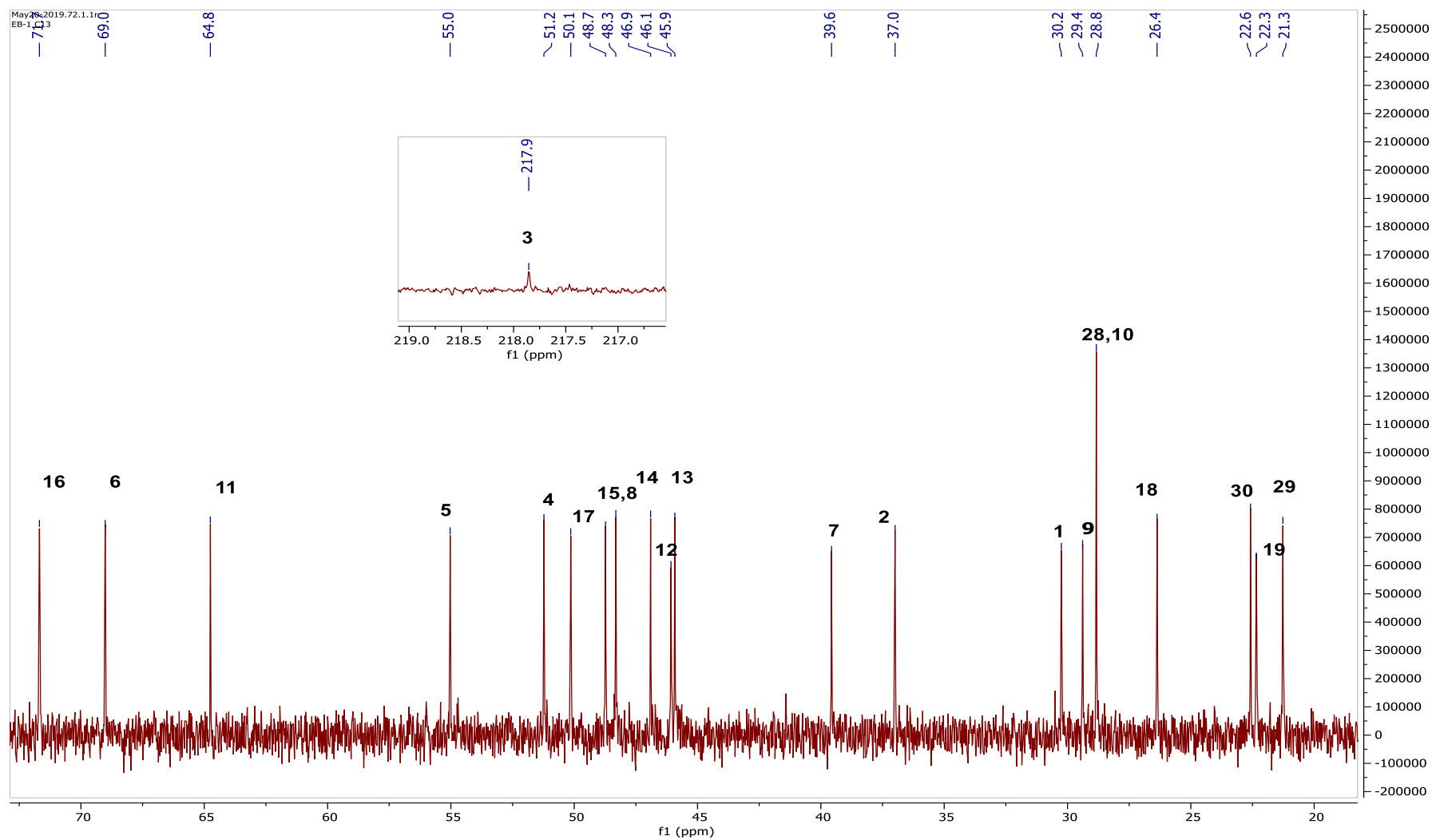
C/H	δ_{C} (ppm)	δ_{H} (ppm), J (Hz)
1	30.3	2.45 m, 2.04 m
2	37.0	2.74 m, 2.60 m
3	217.9	
4	51.2	
5	55.0	2.33 d (9.5)
6	69.0	3.88 bs
7	39.6	1.87 m, 1.87 m
8	48.3	2.03 m
9	29.4	
10	28.8	
11	64.8	4.37 t, (5.7)
12	46.1	2.60 m, 1.90 m
13	45.9	
14	46.1	
15	48.7	2.11 m, 1.86 m
16	71.7	4.84 q (7.6)
17	50.2	2.09 m, 2.07 m
18	26.3	1.25 s
19	22.4	0.56 d (4.4), 1.76 d (4.3)
28	28.8	1.82 s
29	21.3	1.52 s
30	22.6	1.34 s



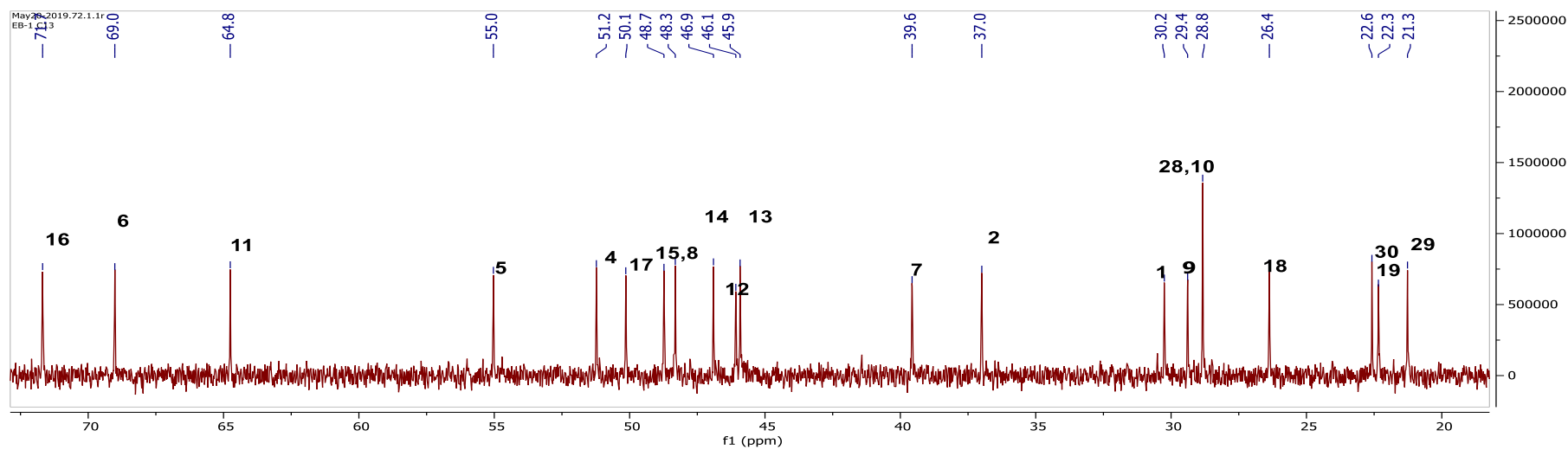
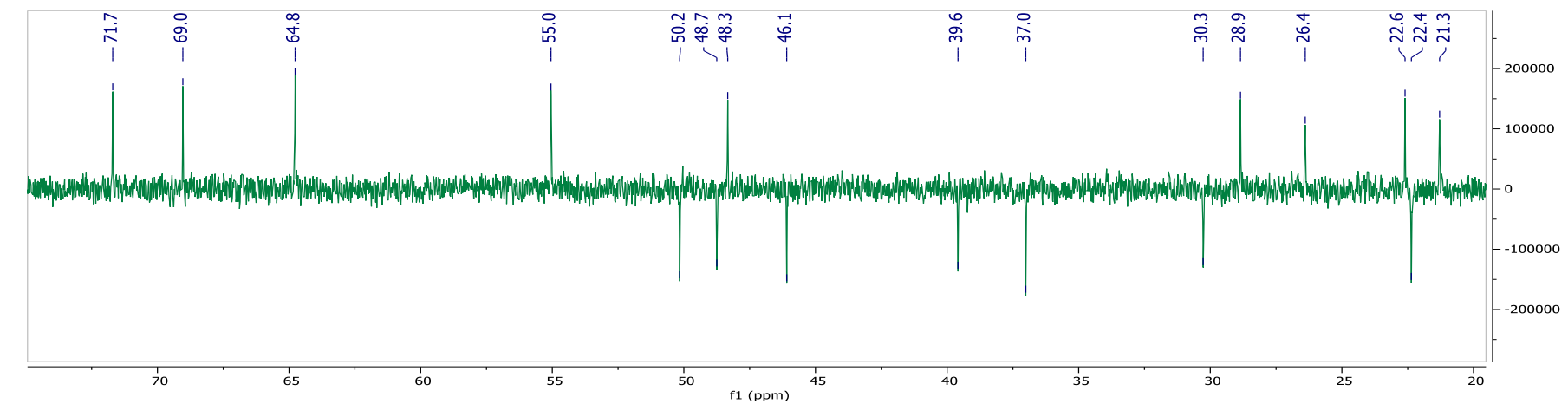
Spectrum 3.62 HR-ESI-MS spectrum of **Neo-SCG-02** (positive mode)



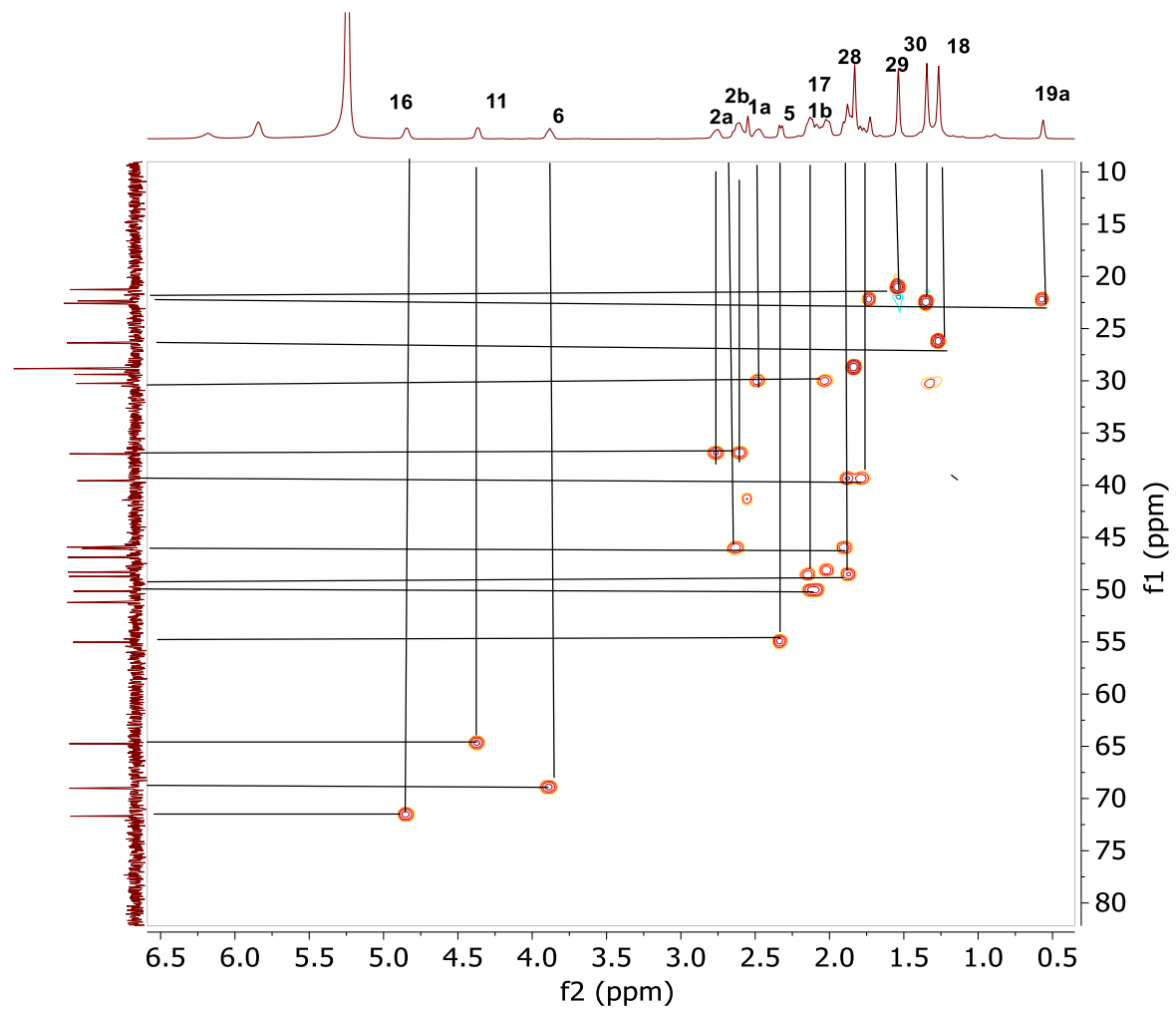
Spectrum 3.63 ^1H -NMR Spectrum of Neo-SCG-02



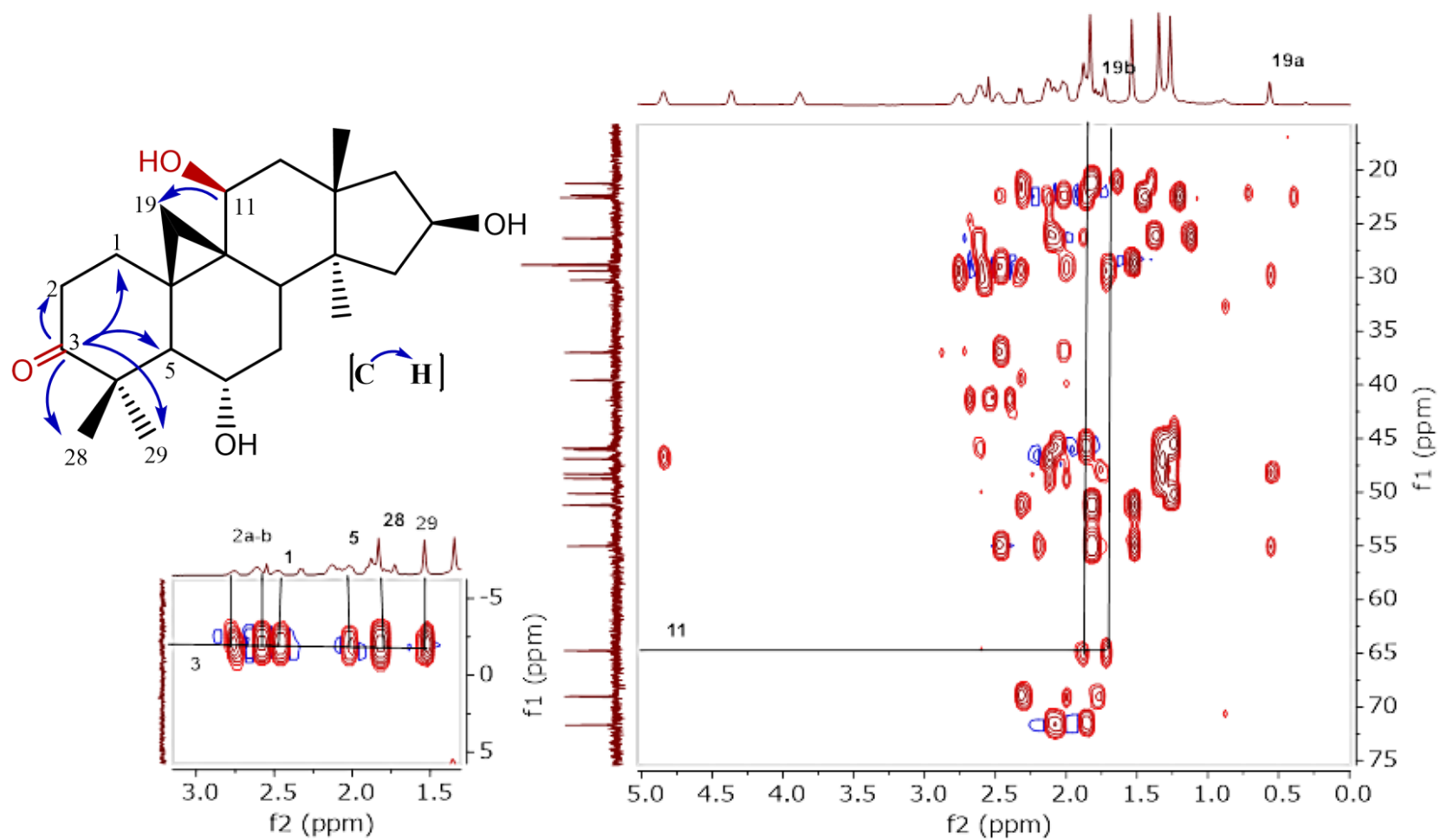
Spectrum 3.64 ^{13}C -NMR Spectrum of Neo-SCG-02



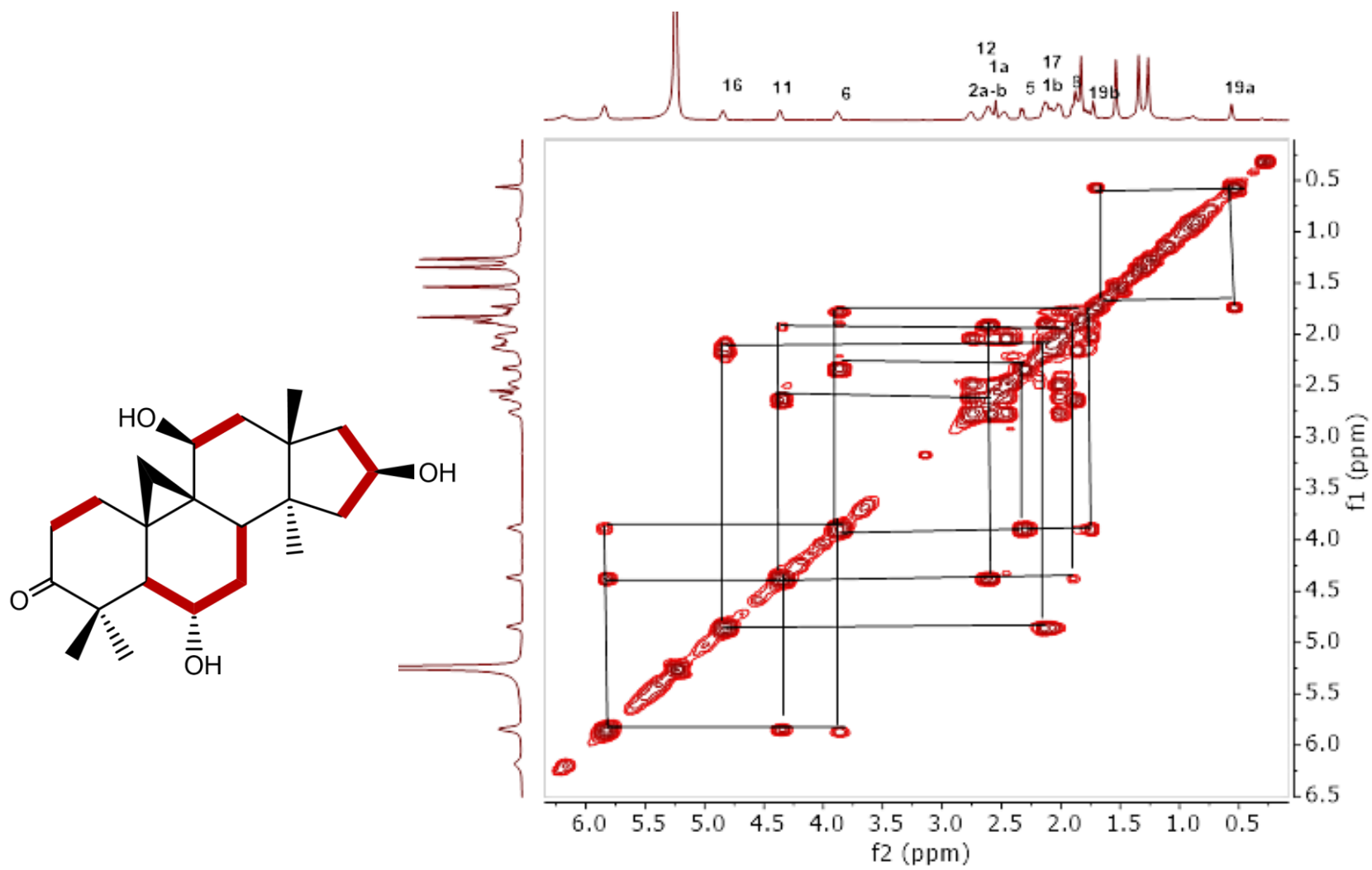
Spectrum 3.65 DEPT spectrum of Neo-SCG-02



Spectrum 3.66 HSQC spectrum of Neo-SCG-02



Spectrum 3.67 HMBC spectrum of Neo-SCG-02



Spectrum 3.68 COSY spectrum of Neo-SCG-02

3.2.3.3 Structure Elucidation of Neo-SCG-03

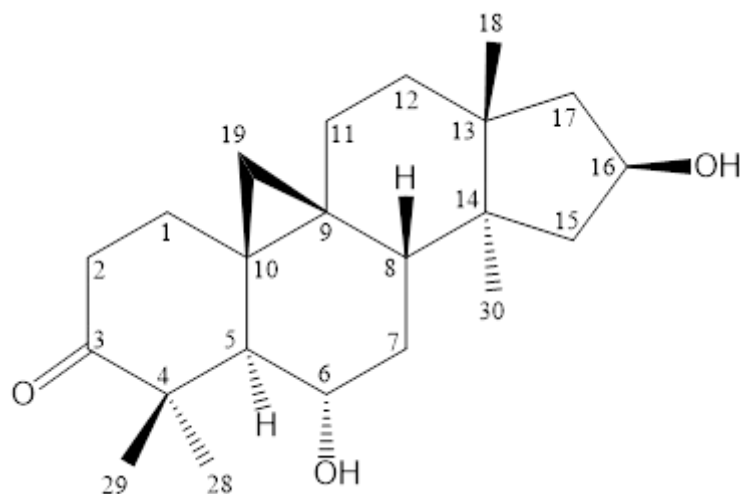


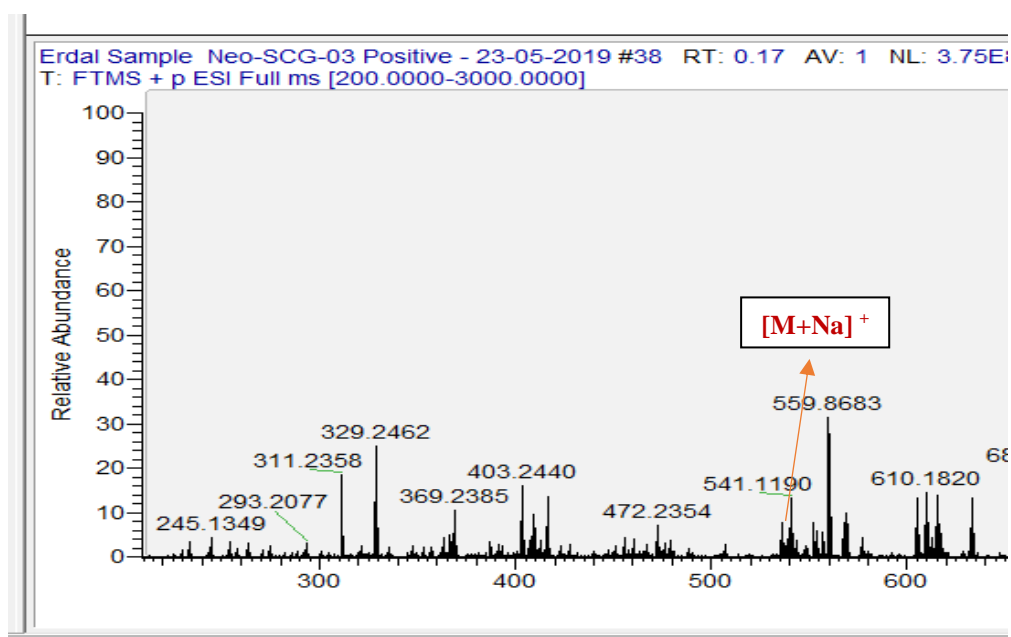
Figure 3.13 Chemical structure of **Neo-SCG-03**

In the HR-ESI-MS spectrum of **Neo-SCG-03**, a major ion peak was observed at m/z 369.2385 $[M+Na]^+$ suggesting a molecular formula of $C_{22}H_{34}O_3$.

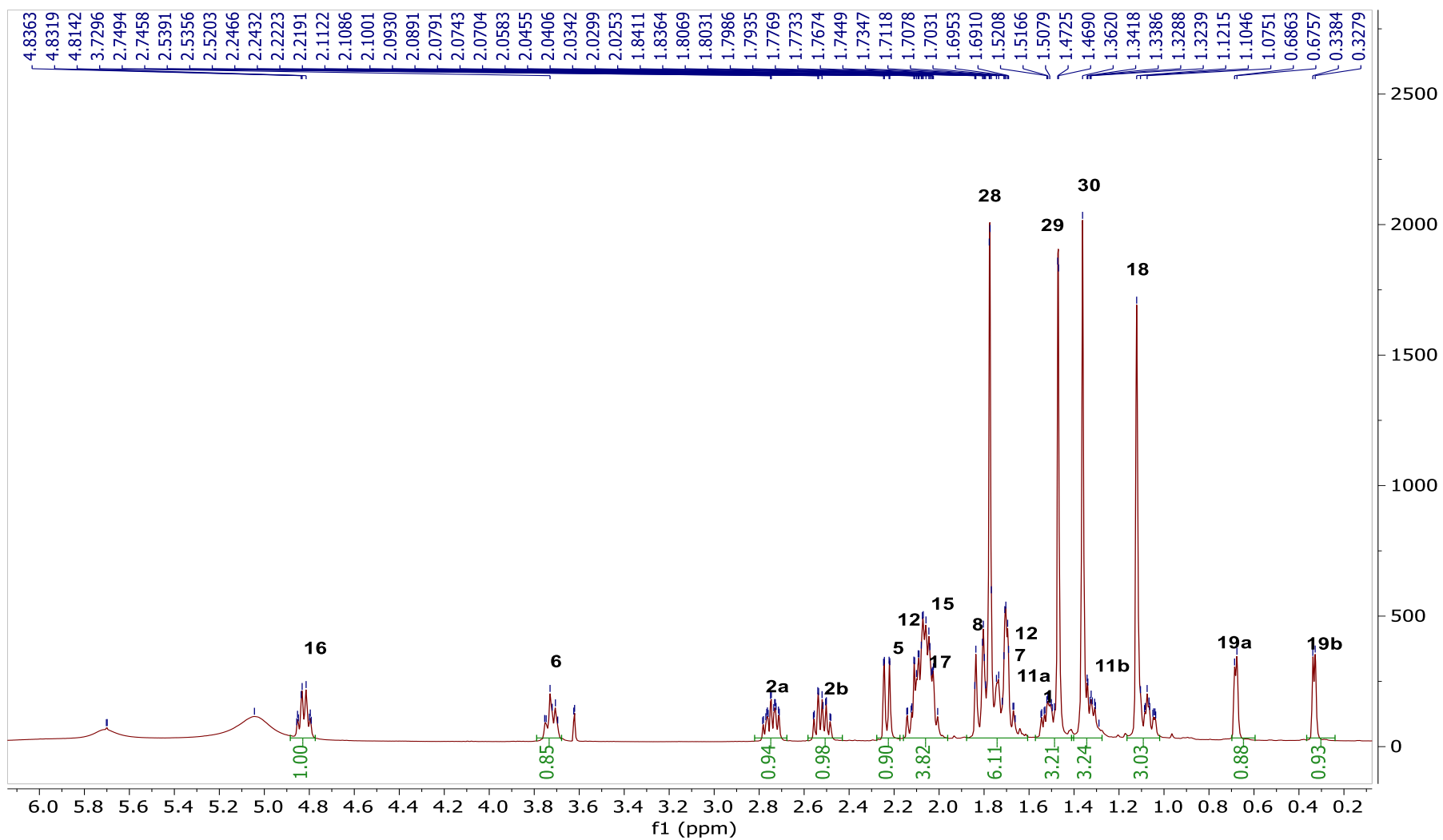
Apart from the hydroxymethyne signal of C-3, the characteristic signals of the starting molecule 20(27)-octanor cycloastragenol were present in the 1H -NMR spectrum of **Neo-SCG-03**. In the ^{13}C -NMR spectrum, the resonance at 217.2 ppm was obvious, implying a transformation of C-3 secondary alcohol to a carbonyl via an oxidation reaction. The long-distance correlations from the carbonyl carbon at δ 217.2 to H_3 -28 (δ 1.78)/ H_3 -29 (δ 1.47) and H-5 (δ 2.23, d, J = 9.6 Hz) confirmed the oxidation at C-3. Thus, the structure of **Neo-SCG-03** was established as 3-oxo derivative of 20,27-octanor cycloastragenol.

Table 3.12 ^1H and ^{13}C NMR data of **Neo-SCG-03** (125/500 MHz, $\text{C}_5\text{D}_5\text{N}$).

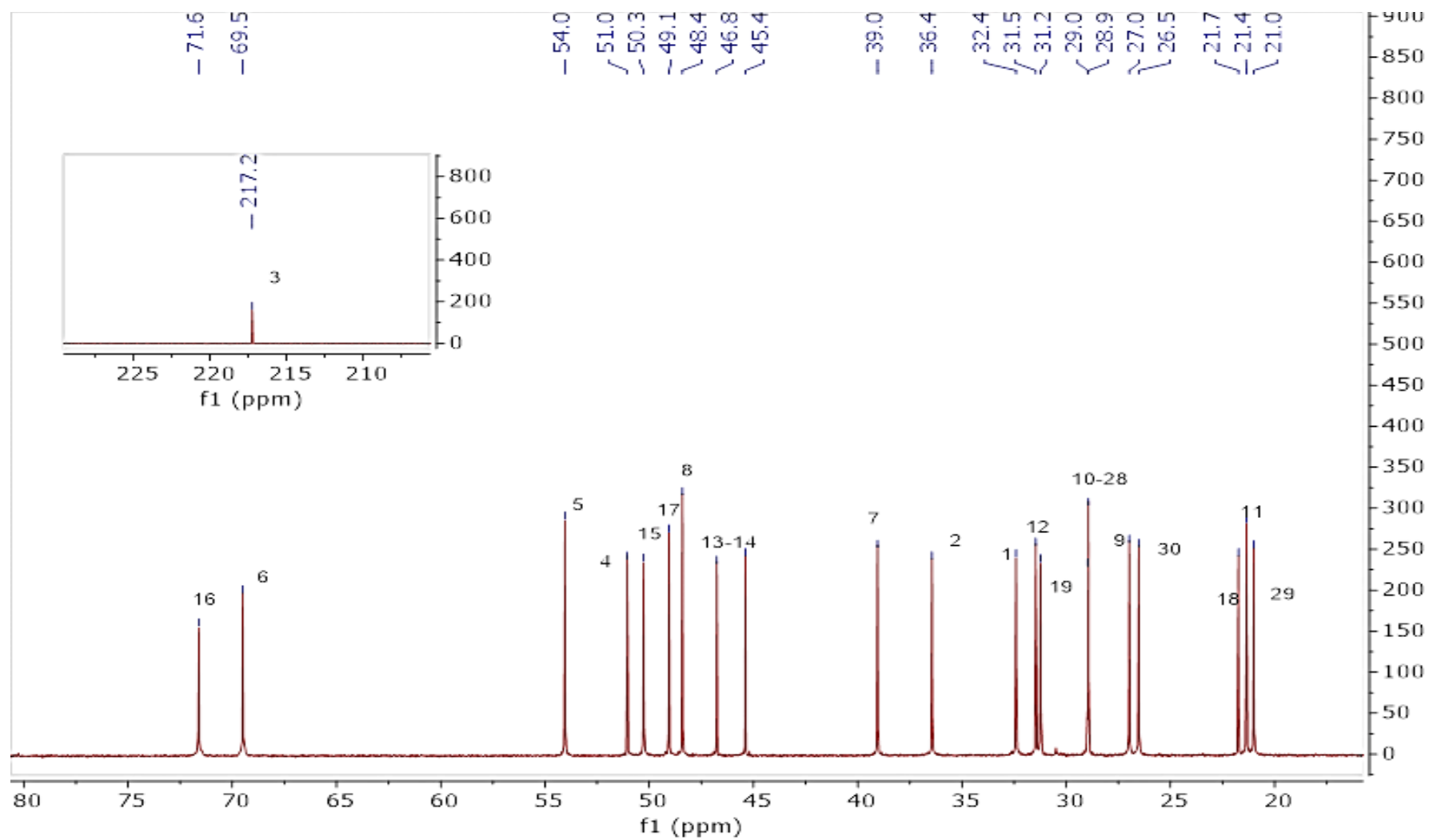
C/H	δ_{C} (ppm)	δ_{H} (ppm), J (Hz)
1	32.4	1.31 m, 2.03 m
2	36.4	2.75 m, 2.47 m
3	217.2	
4	51.0	
5	54.0	2.23 d (9.6)
6	69.5	3.73 t (9.0)
7	39.0	1.66 m, 1.81 m
8	48.4	1.70 m
9	27.0	
10	29.0	
11	21.4	1.07 m, 2.08 m
12	31.5	1.52 m, 1.74 m
13	46.8	
14	45.4	
15	50.3	2.10 m,
16	71.6	4.82 dd (7.7, 14.9)
17	49.1	1.83 m, 2.07 m
18	21.7	1.12 s
19	31.2	0.33 d (4.2), 0.68 d (4.2)
28	28.9	1.78 s
29	21.0	1.47 s
30	26.5	1.36 s



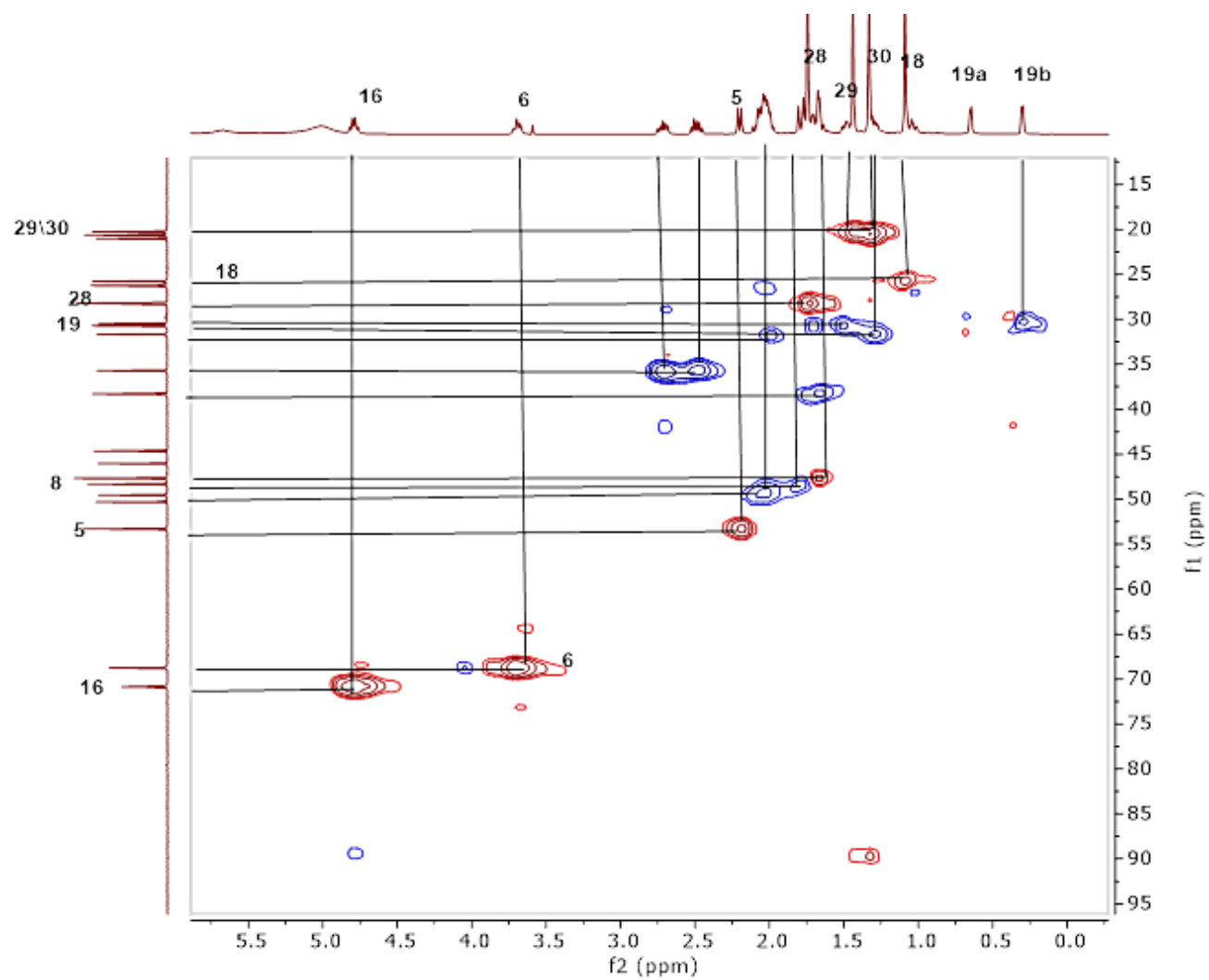
Spectrum 3.69 HR-ESI-MS spectrum of **Neo-SCG-03** (positive mode)



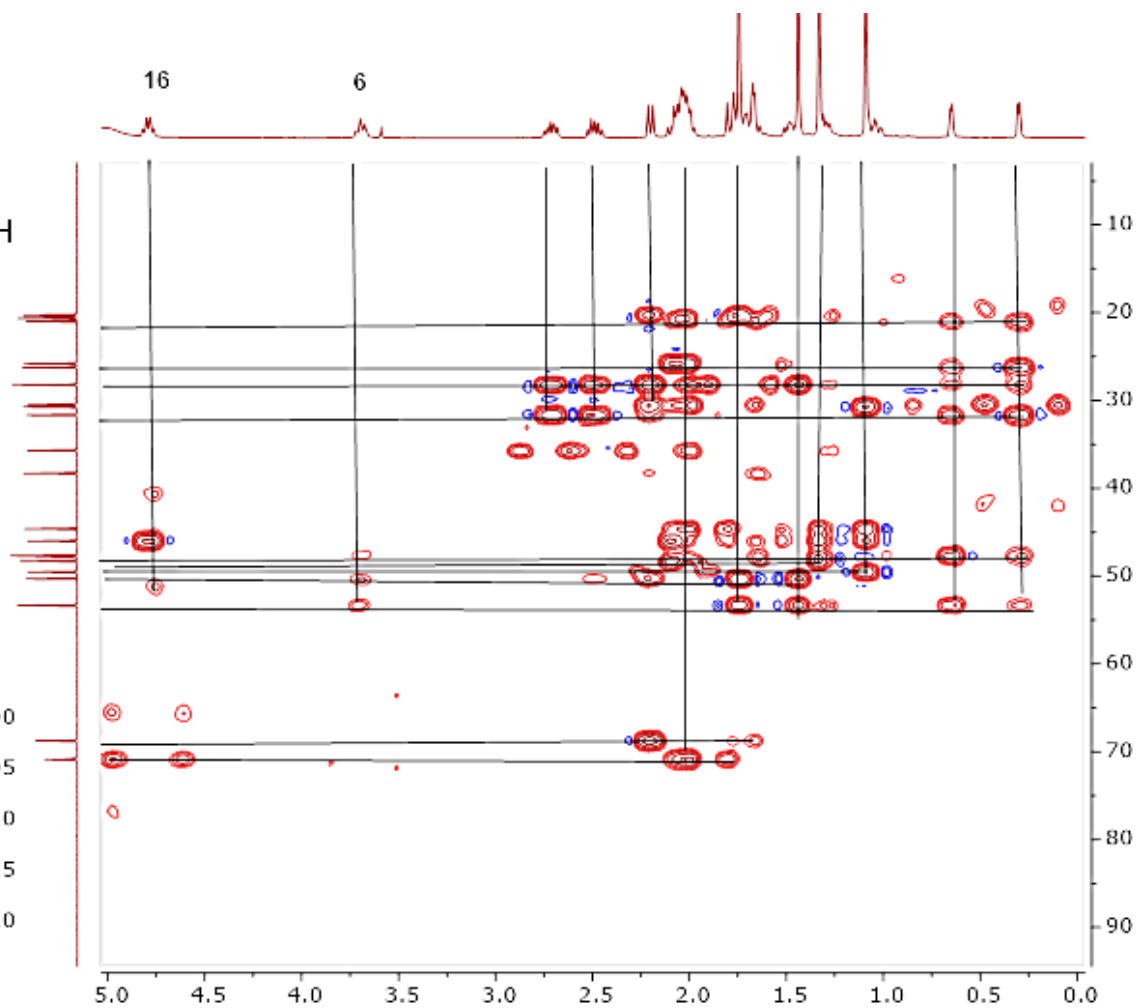
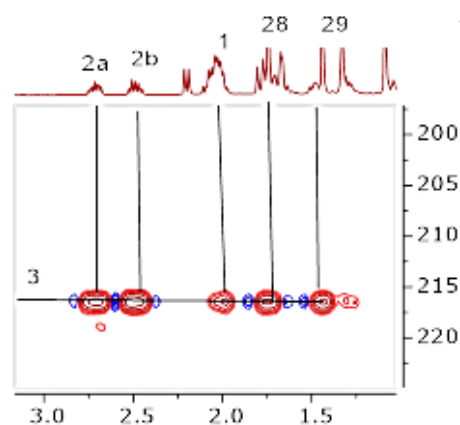
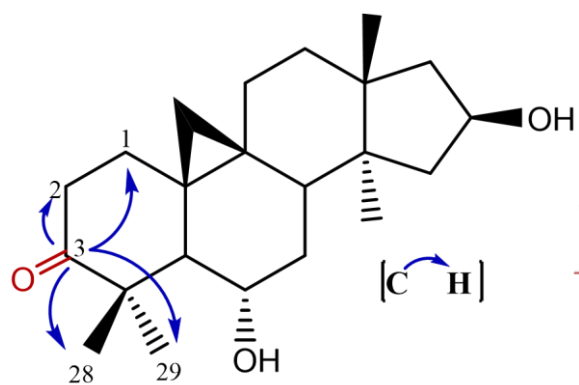
Spectrum 3.70 ^1H -NMR Spectrum of Neo-SCG-03



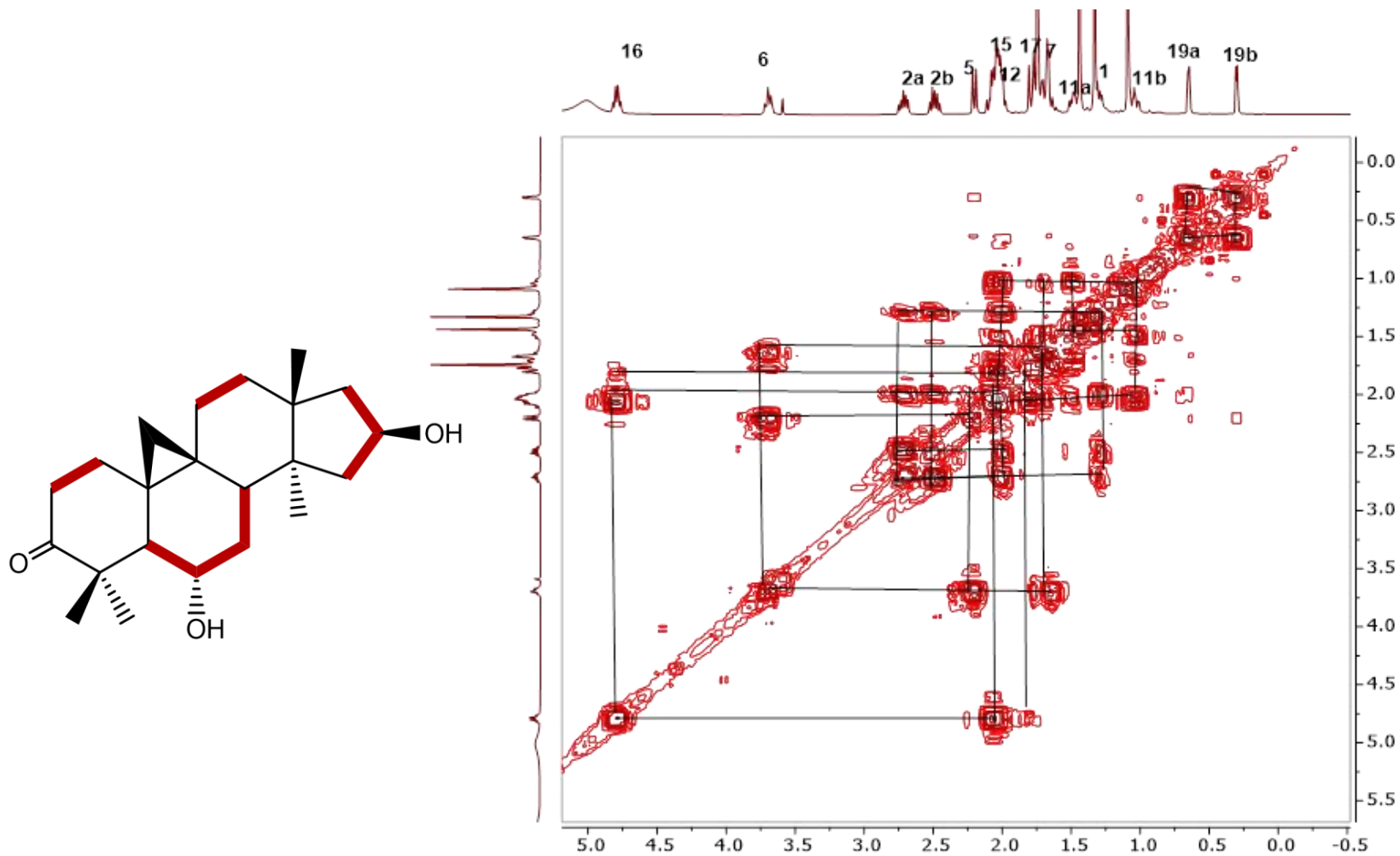
Spectrum 3.71 ^{13}C -NMR Spectrum of Neo-SCG-03



Spectrum 3.72 HSQC spectrum of Neo-SCG-03



Spectrum 3.73 HMBC spectrum of Neo-SCG-03



Spectrum 3.74 COSY spectrum of Neo-SCG-03

3.2.3.4 Structure Elucidation of Neo-SCG-04

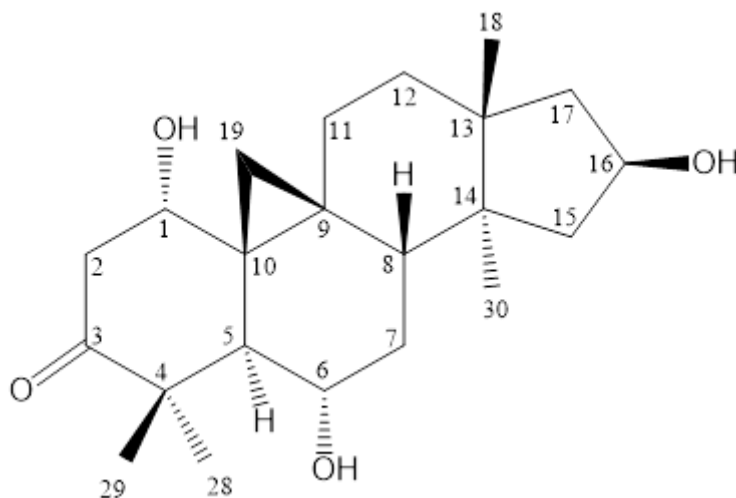


Figure 3.14 Chemical structure of **Neo-SCG-04**

In the HR-ESI-MS spectrum of **Neo-SCG-04**, a quasimolecular ion peak was observed at m/z 385.23451 $[M+Na]^+$ proposing a molecular formula of $C_{22}H_{34}O_4$.

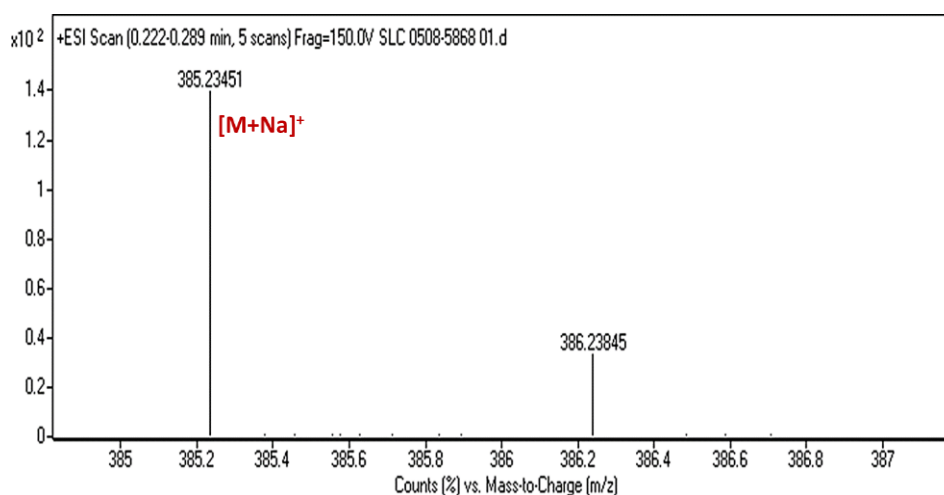
In the 1H -NMR spectrum, AX signals of 9,19-cyclopropane ring, four tertiary methyl groups in the upfield and characteristic signals belonging to the H-6 and H-16 oxymethyne protons in the lowfield showed no significant alteration compared to the substrate. In addition, the hydroxymethine proton at H-3 was not present in the 1H -NMR spectrum. A broad singlet signal observed at 4.02 ppm, corresponding with a carbon at δ 72.9 in the HSQC spectrum, indicating an additional oxymethine group in the structure. Additionally, the carbon signal at δ 215.8 indicated a carbonyl group in the structure. The long-distance correlations from the carbonyl carbon to H_3 -28 (δ_H 1.93)/ H_3 -29 (δ_H 1.46) and H-5 (δ_H 3.16, dd, $J=7.2, 2.5$ Hz) helped us to locate the oxidation at C-3. The new hydroxy group was located at C-1 on the basis of the COSY correlation of H-1 (δ 4.02) with H-2a (δ_H 3.13, d, $J=4.3$ Hz), and the long-distance correlation between the 72.9 ppm carbon signal and H_2 -19 (δ 0.56, d, $J=4.4$ Hz; δ 0.87, d, $J=4.4$ Hz)/ H-5 (δ 3.16, dd, $J=7.2, 2.5$ Hz).

The relative stereochemistry at C-1 was deduced based on the NOESY spectrum. H-1 (δ 4.02 brs) showed correlation with one of the H_2 -19 protons (δ_H 0.56, d, $J=4.4$ Hz), which provided evidence for the α -orientation of the hydroxy group at C-1. Thus, the new

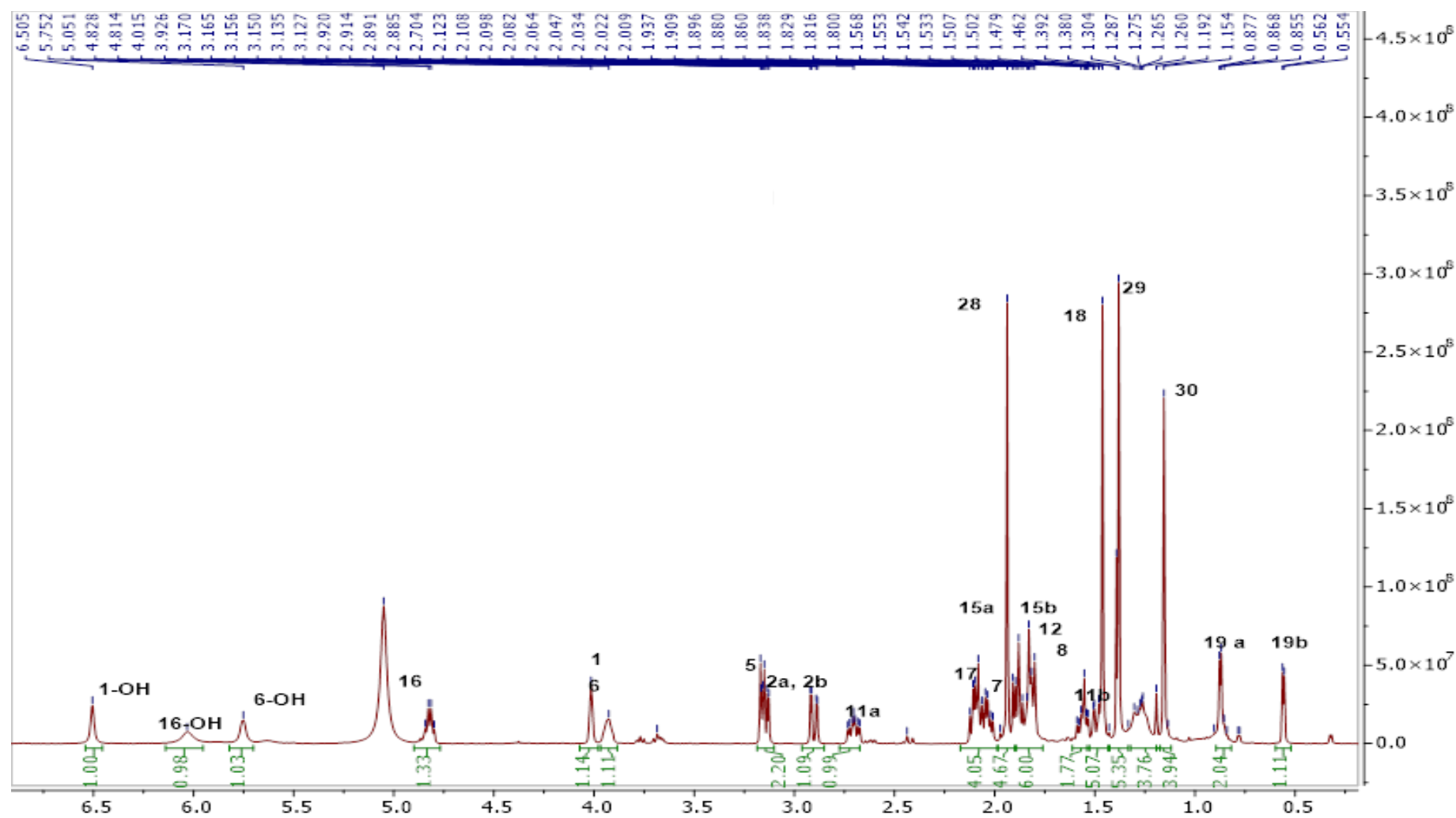
metabolite was characterized as 1 α -hydroxy,3-oxo derivative of 20(27)-octanor cycloastragenol.

Table 3.13 ^1H and ^{13}C NMR data of **Neo-SCG-04** (125/500 MHz, $\text{C}_5\text{D}_5\text{N}$).

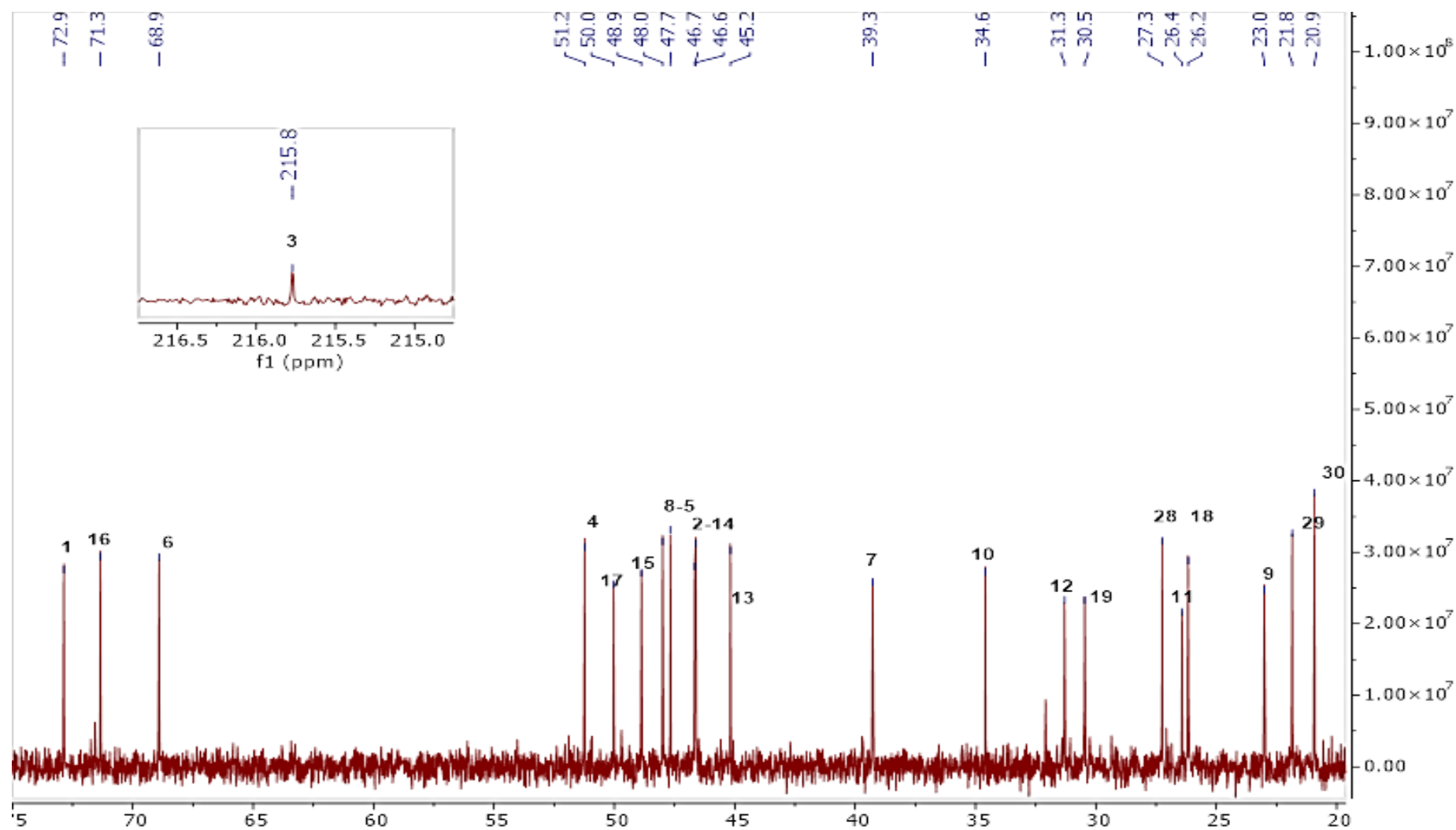
C/H	δ_{C} (ppm)	δ_{H} (ppm), J (Hz)
1	72.9	4.02 brs
2	46.7	2.90 dd (14.5, 3.2), 3.13 d (4.3)
3	215.8	
4	51.2	
5	47.7	3.16 dd (7.2, 2.5)
6	68.9	3.93n d (3.2)
7	39.3	1.86 m, 1.88 m
8	48.0	1.81 m
9	23.0	
10	34.6	
11	26.4	1.47 m, 2.70 m
12	31.3	1.55 m, 1.82 m
13	45.2	
14	46.6	
15	48.9	1.83 m, 2.09 m
16	71.3	4.82 dd (7.2, 14.6)
17	50.0	2.03 dd (12.7, 6.3), 2.10 dd (7.75, 12.6)
18	26.2	1.15 s
19	30.5	0.56 d (4.4), 0.87 d (4.4)
28	27.3	1.93 s
29	21.8	1.46 s
30	20.9	1.38 s



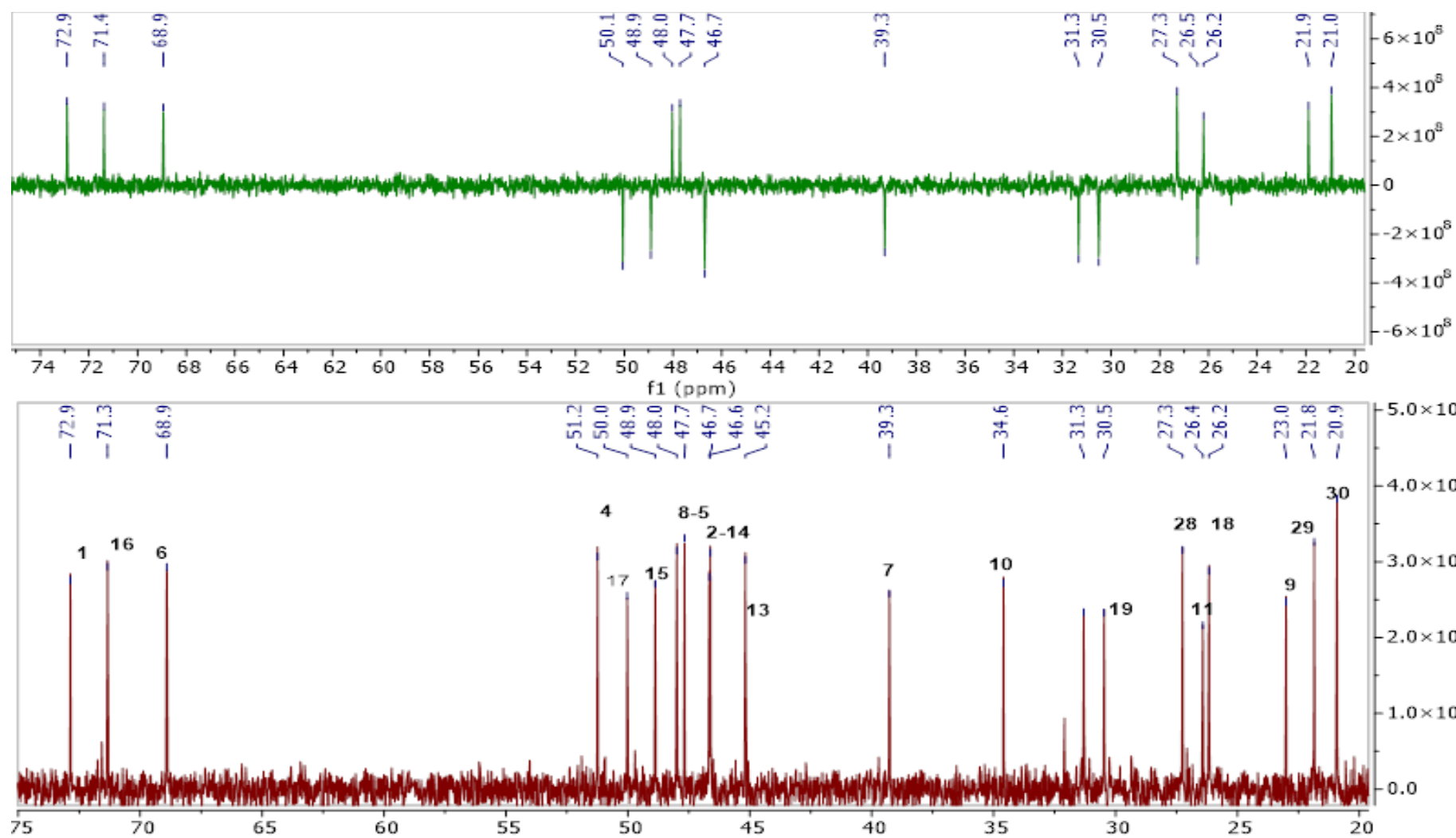
Spectrum 3.75 HR-ESI-MS spectrum of **Neo-SCG-04**(positive mode)



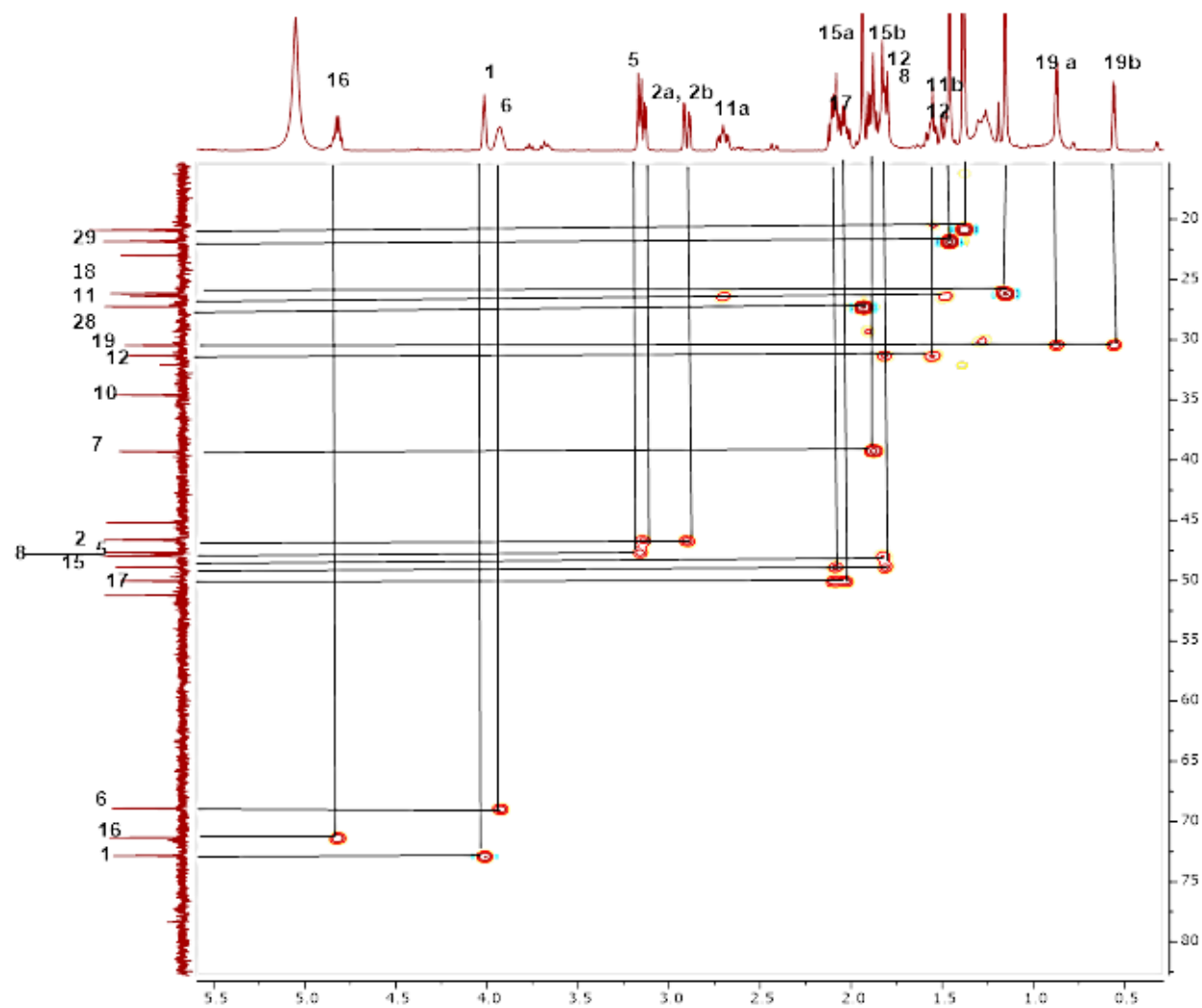
Spectrum 3.76 ^1H -NMR Spectrum of Neo-SCG-04



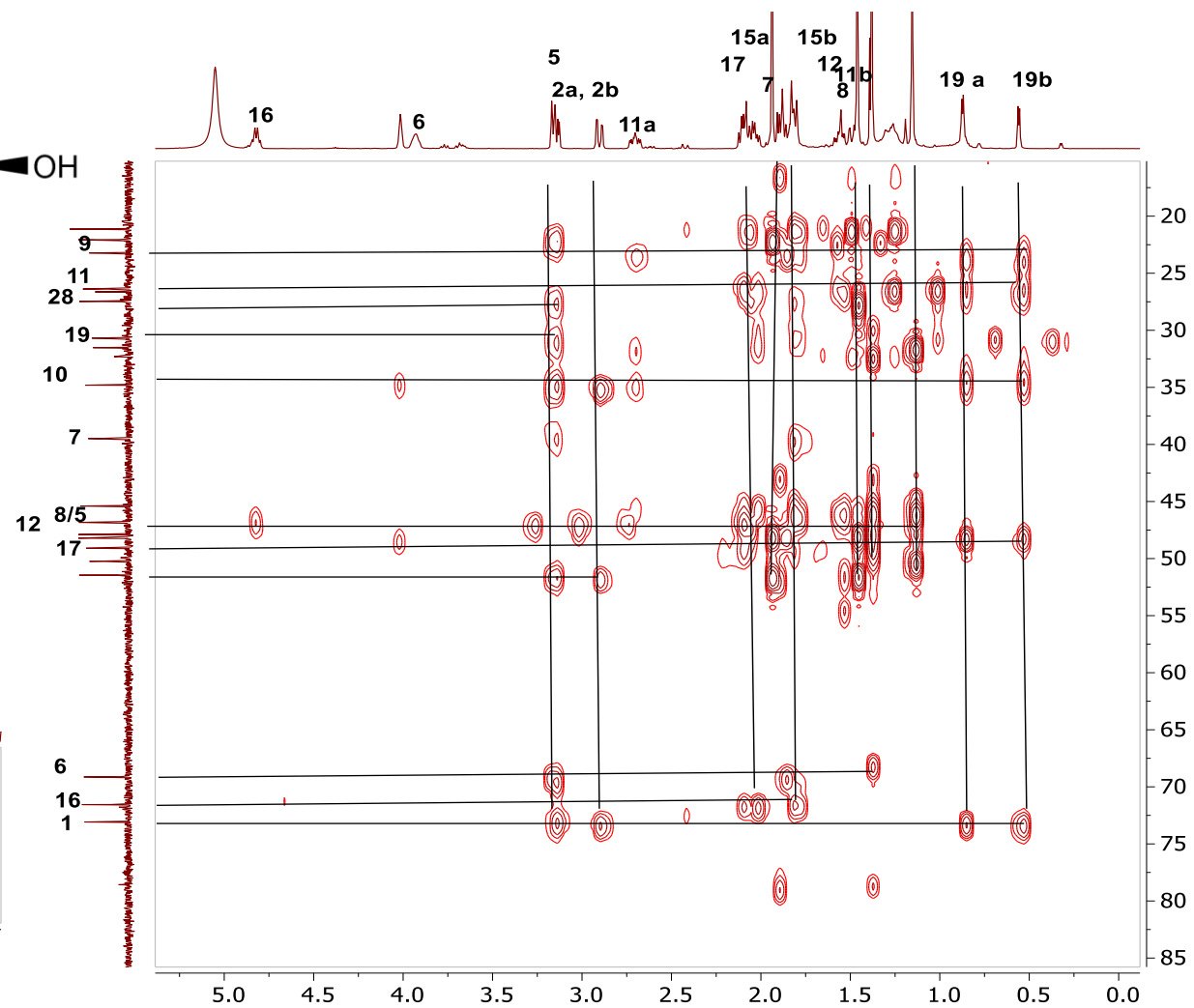
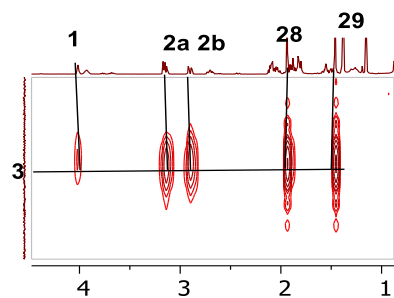
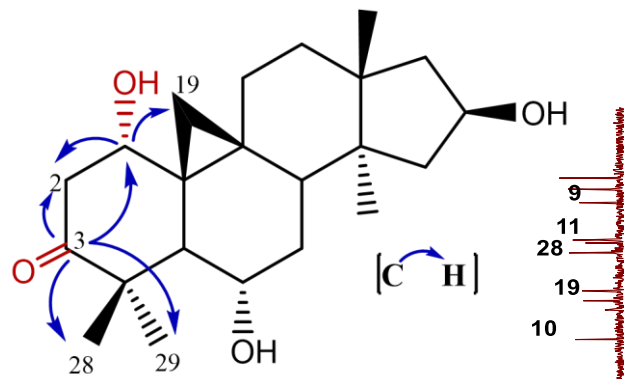
Spectrum 3.77 ^{13}C -NMR Spectrum of Neo-SCG-04



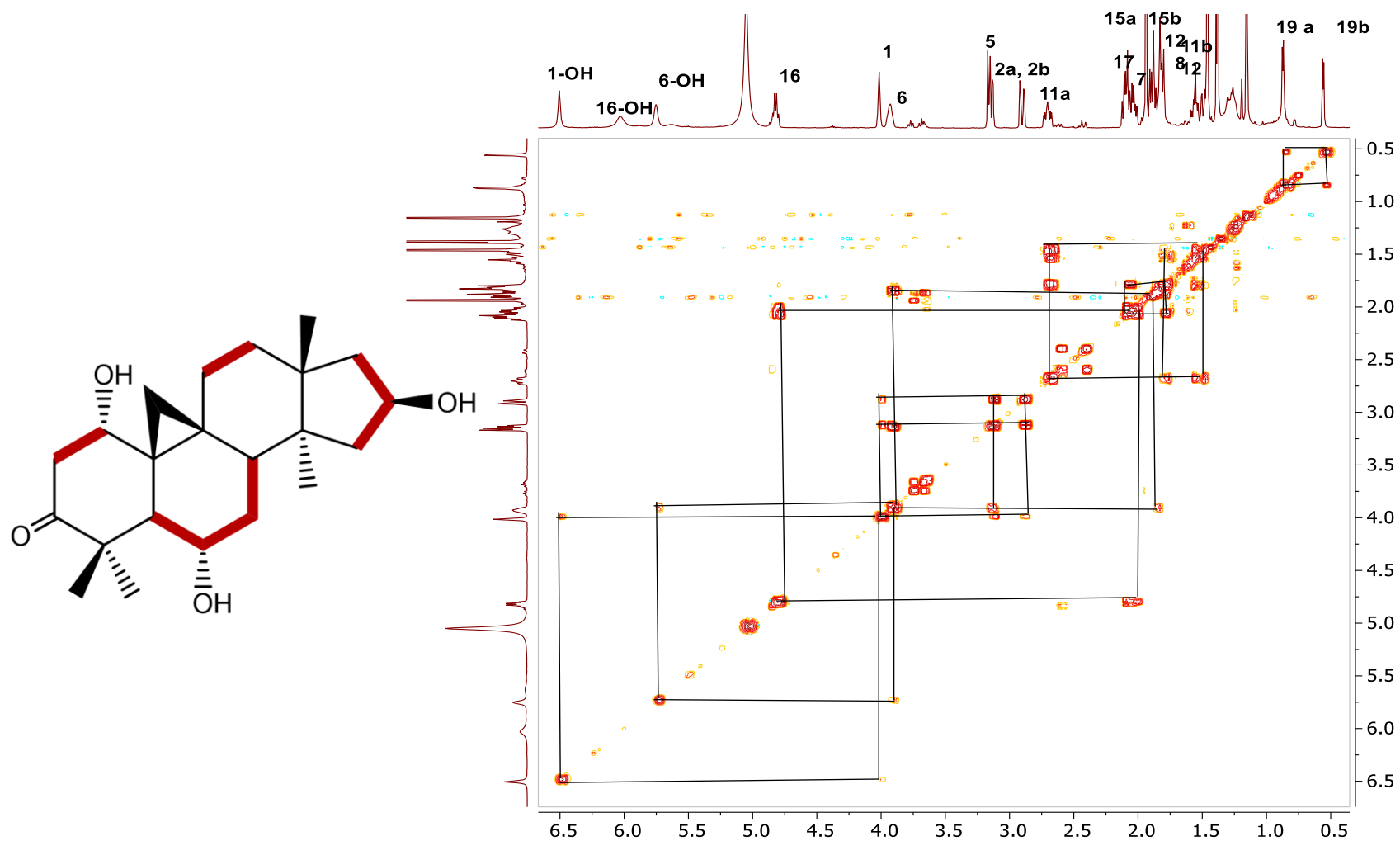
Spectrum 3.78 DEPT spectrum of Neo-SCG-04



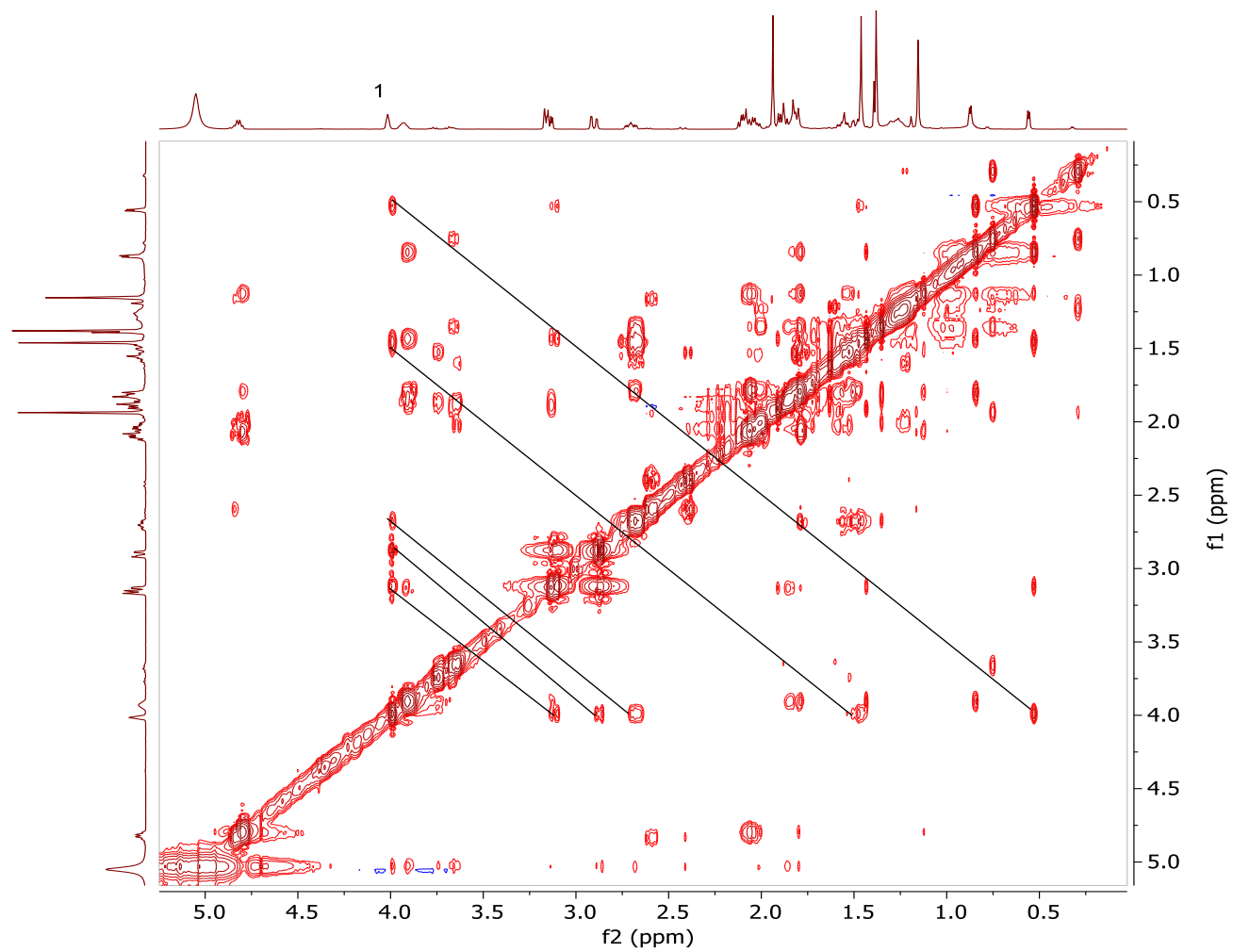
Spectrum 3.79 HSQC spectrum of Neo-SCG-04



Spectrum 3.80 HMBC spectrum of Neo-SCG-04



Spectrum 3.81 COSY spectrum of Neo-SCG-04



Spectrum 3.82 NOESY spectrum of Neo-SCG-04

3.2.3.5 Structure Elucidation of Neo-SCG-06

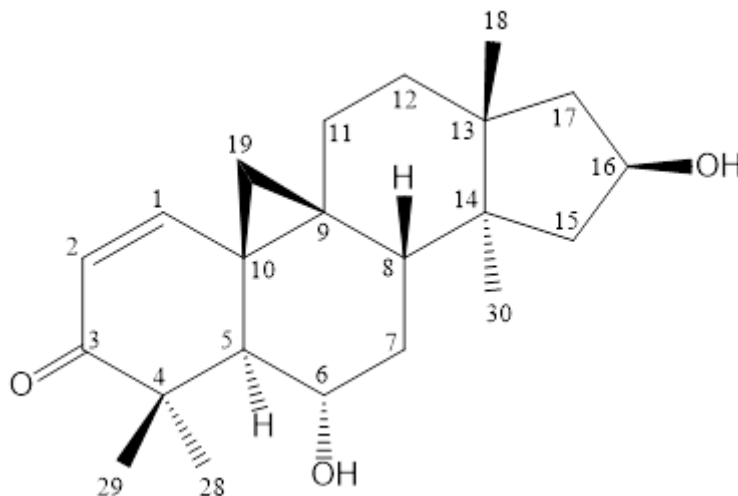


Figure 3.15 Chemical structure of **Neo-SCG-06**

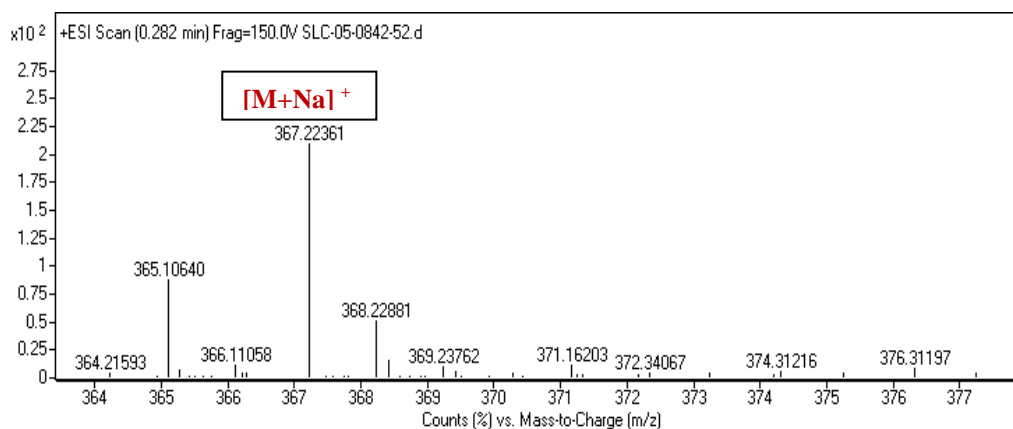
The molecular formula of **Neo-SCG-06** was established as $C_{22}H_{32}O_3$ by HR-ESI ($[M+Na]^+=367.22361$).

Neo-SCG-06 displayed the four tertiary methyl groups in the up-field, and the characteristic signals belonging to the H-6 and H-16 oxymethyne protons in the low-field region. In addition, in the 1H -NMR spectrum of **Neo-SCG-06** presented that one of the distinctive 9,19-cyclopropane ring AX system signals was missing. A detailed inspection of the COSY and HSQC spectra revealed that H_{2-19} protons were resonating at δ 1.22 (d, $J=4.4$ Hz) and 0.06 (d, $J=4.4$ Hz). Furthermore, the hydroxymethyne proton at H-3 was not observed and the signals derived from a disubstituted double bond δ 6.85 (d, $J=10.0$ Hz) and 6.23 (d, $J=10.0$ Hz) indicated that the extra unsaturation was the result of an olefinic system. Based on the coupling characteristics of the olefinic protons, it was inferred that the double bond was isolated as a single spin system. In the ^{13}C -NMR spectrum; the characteristic C-3 signal resonating around at 78.0 ppm was absent, and the presence of a new resonance at δ 205.3 in the low field suggested oxidation of C-3(OH) to a carbonyl. Specifically, the cross peaks between H_{3-28} (1.88, s)/ H_{3-29} (1.29, s)/H-5 (2.55, d, $J=9.4$ Hz)/H-1 (6.85, d, $J=10$ Hz) and the carbonyl signal in the HMBC spectrum verified the oxidation position to be C-3. On the other hand, two olefinic carbon signals at δ 154.3 and 127.4 were noticed from the ^{13}C -NMR spectrum. These olefinic signals were attributed to C-1 and C-2, respectively, according to HMBC correlations from H_2 -

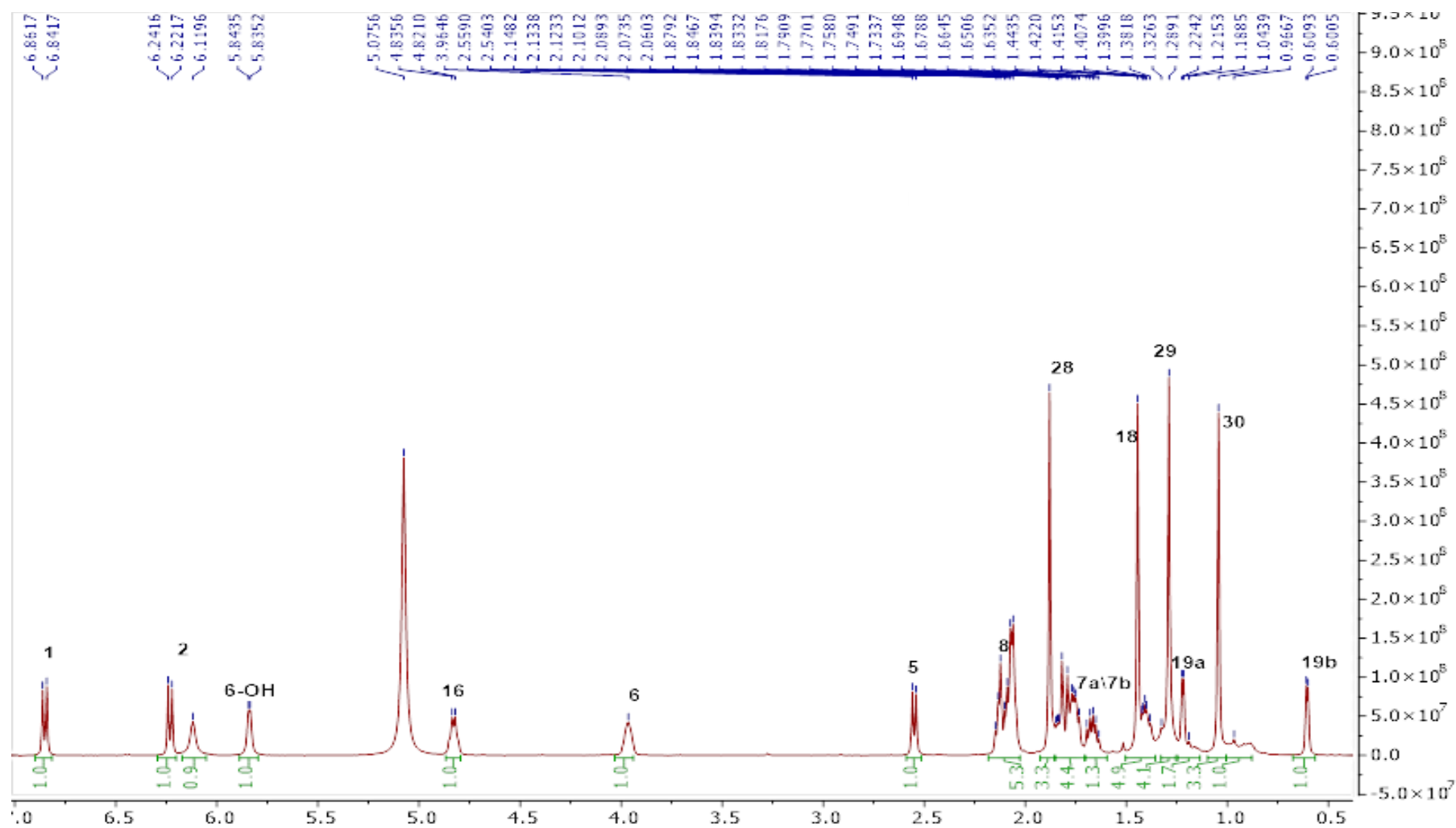
19 and H-5 to the signal at δ 154.3 resonance, and no correlation was observed between any protons with the carbon at δ 127.4 resonance. As a result, the structure of Neo-SCG-06 was established as 3-oxo,1(2)-en derivative of 20(27)-octanor cycloastragenol.

Table 3.14 ^1H and ^{13}C NMR data of **Neo-SCG-06** (125/500 MHz, $\text{C}_5\text{D}_5\text{N}$).

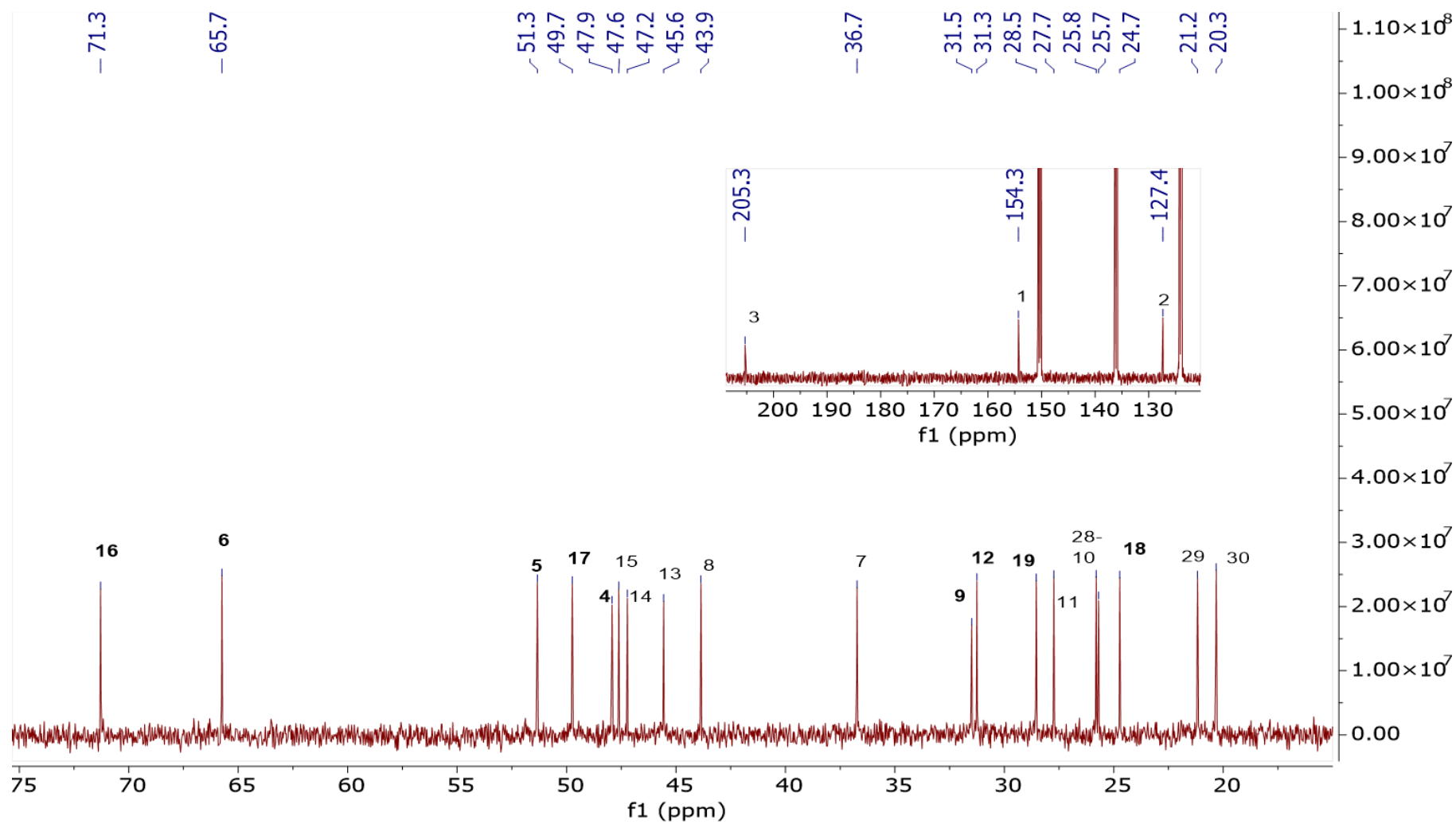
C/H	δ_{C} (ppm)	δ_{H} (ppm), J (Hz)
1	154.3	6.85 d (10)
2	127.4	6.23 d (10)
3	205.3	
4	47.9	
5	51.3	2.55 d (9.4)
6	65.7	3.96 dd (9.8, 5.3)
7	36.7	1.75 m, 2.09 m
8	43.9	2.12 m
9	31.5	
10	25.7	
11	27.7	1.76 m, 1.41 m
12	31.3	1.76 m, 2.14 m
13	45.6	
14	47.2	
15	47.6	1.76 m, 2.07 m
16	71.3	4.83 q (6.5)
17	49.7	2.07 m, 2.07 m
18	24.7	1.04 s
19	28.5	0.06 d (4.4), 1.22 d (4.4)
28	25.8	1.87 s
29	21.2	1.28 s
30	20.3	1.44 s



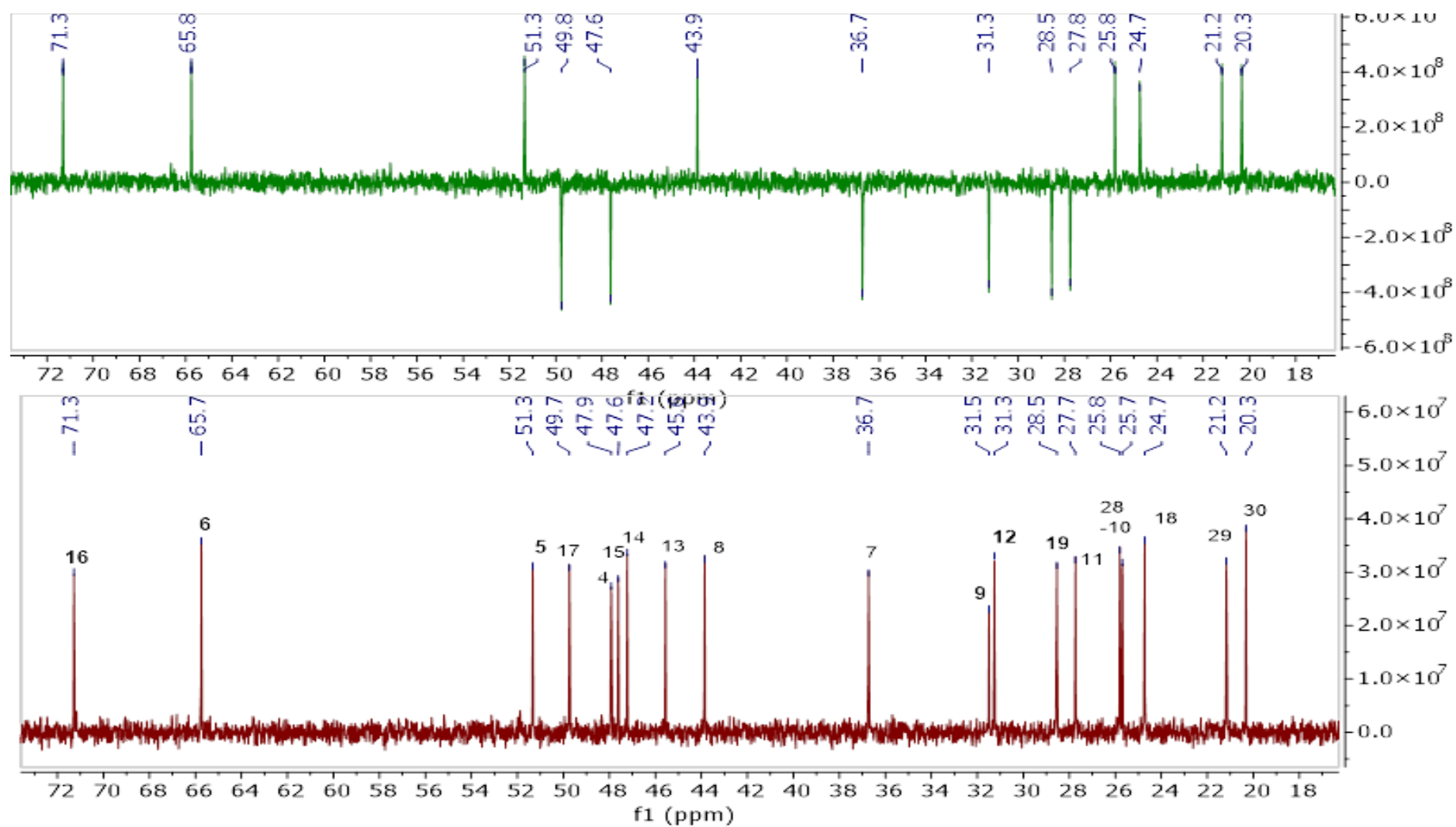
Spectrum 3.83 HR-ESI-MS spectrum of **Neo-SCG-06** (positive mode)



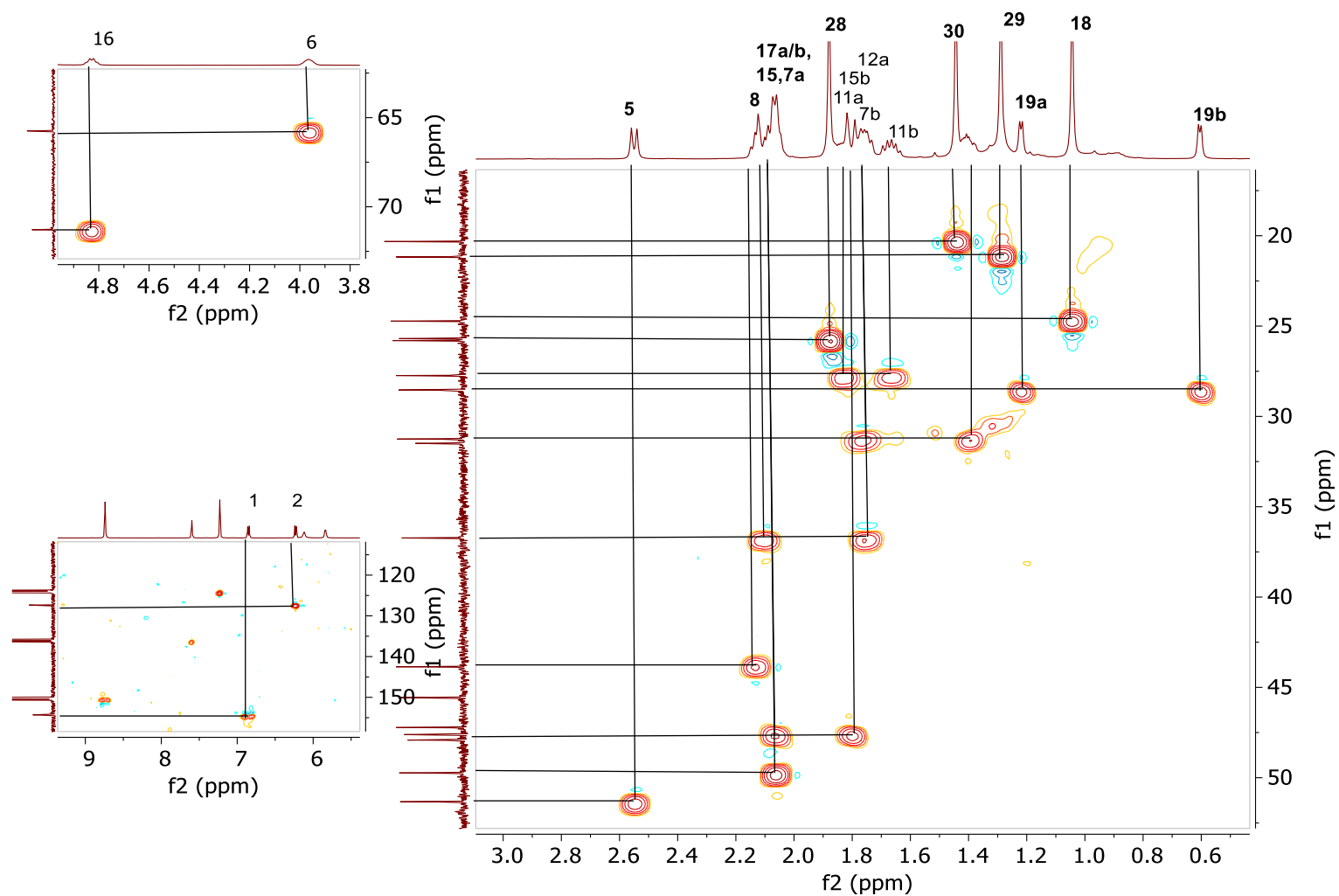
Spectrum 3.84 ^1H -NMR Spectrum of Neo-SCG-06



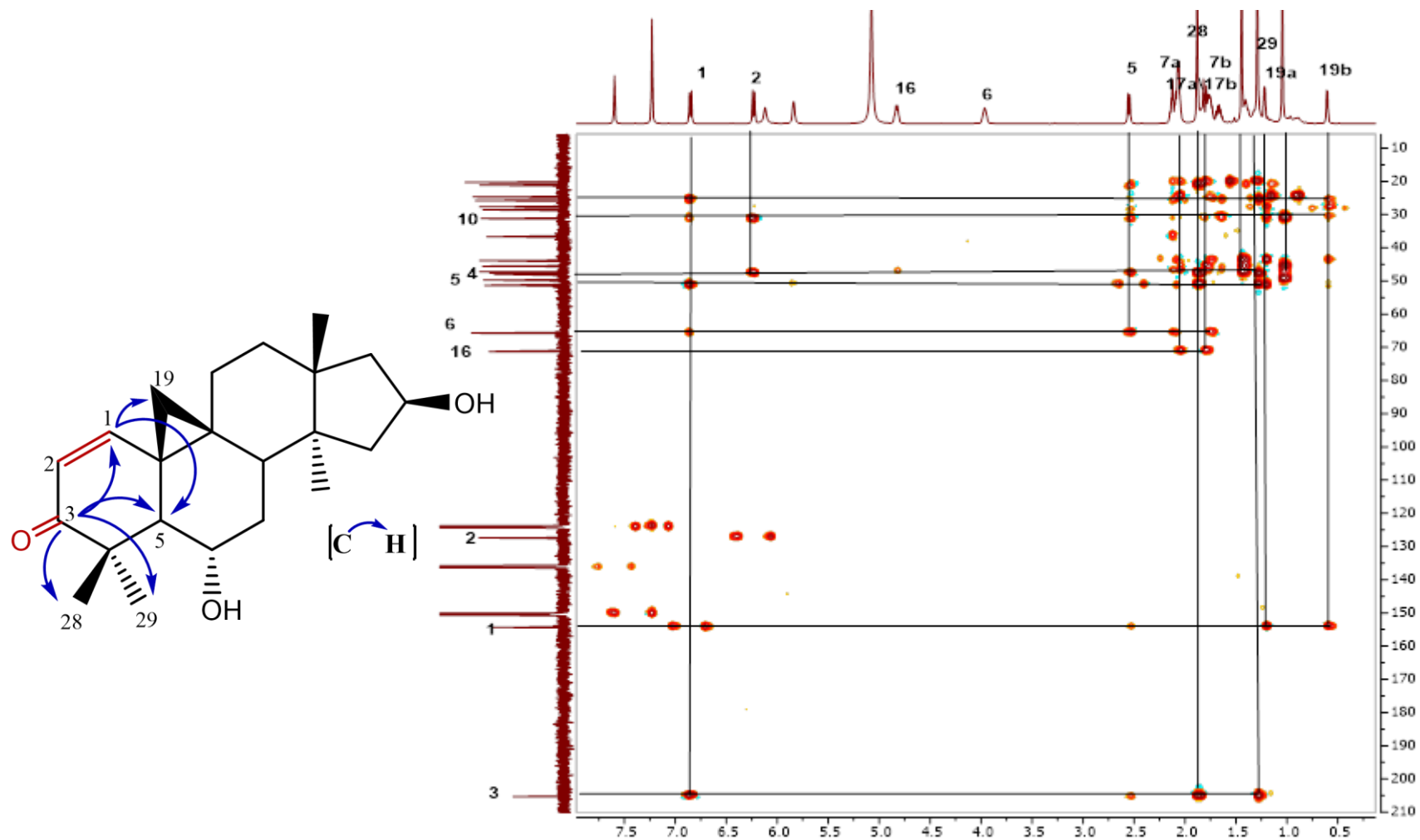
Spectrum 3.85 ^{13}C -NMR Spectrum of Neo-SCG-06



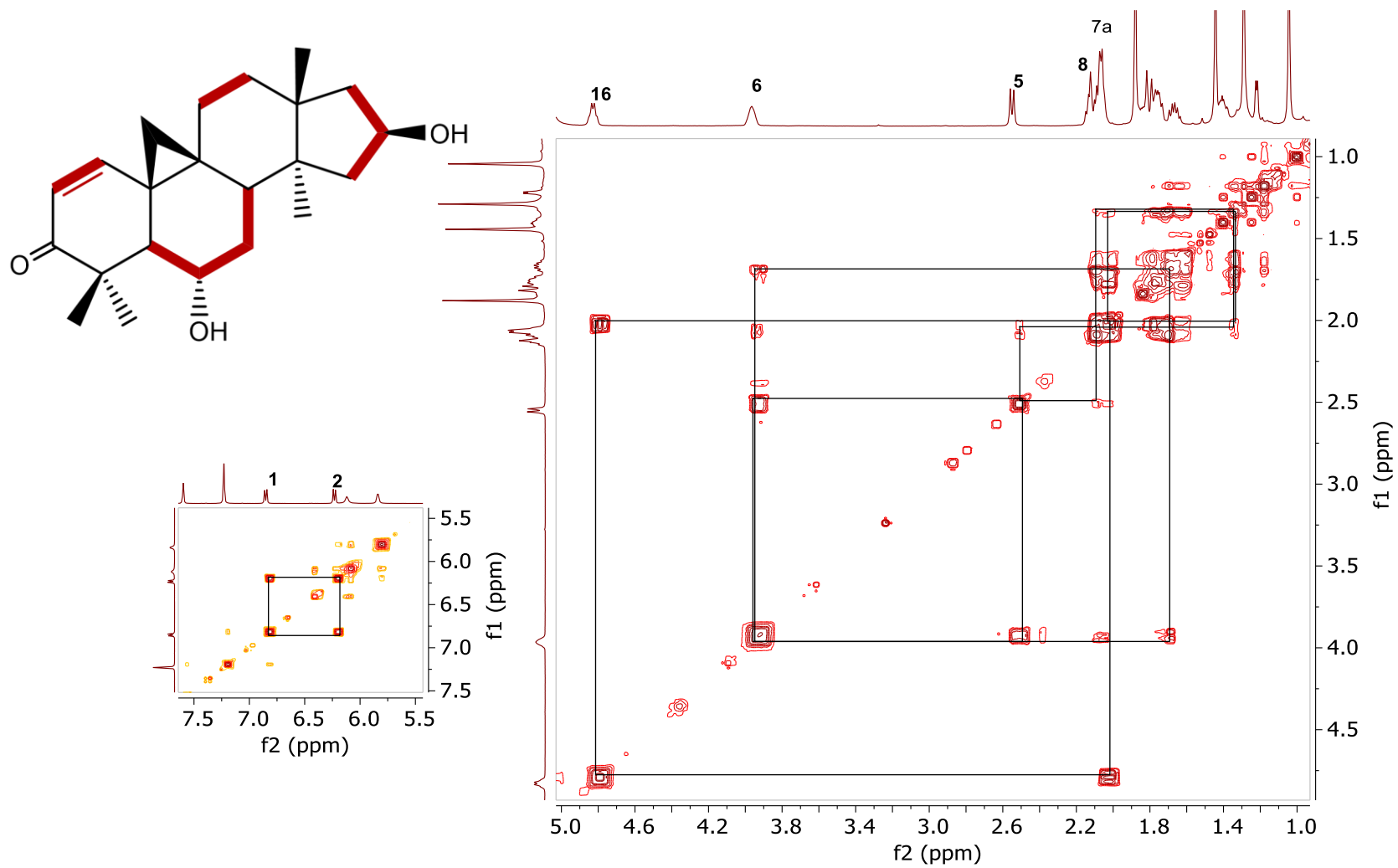
Spectrum 3.86 DEPT spectrum of Neo-SCG-06



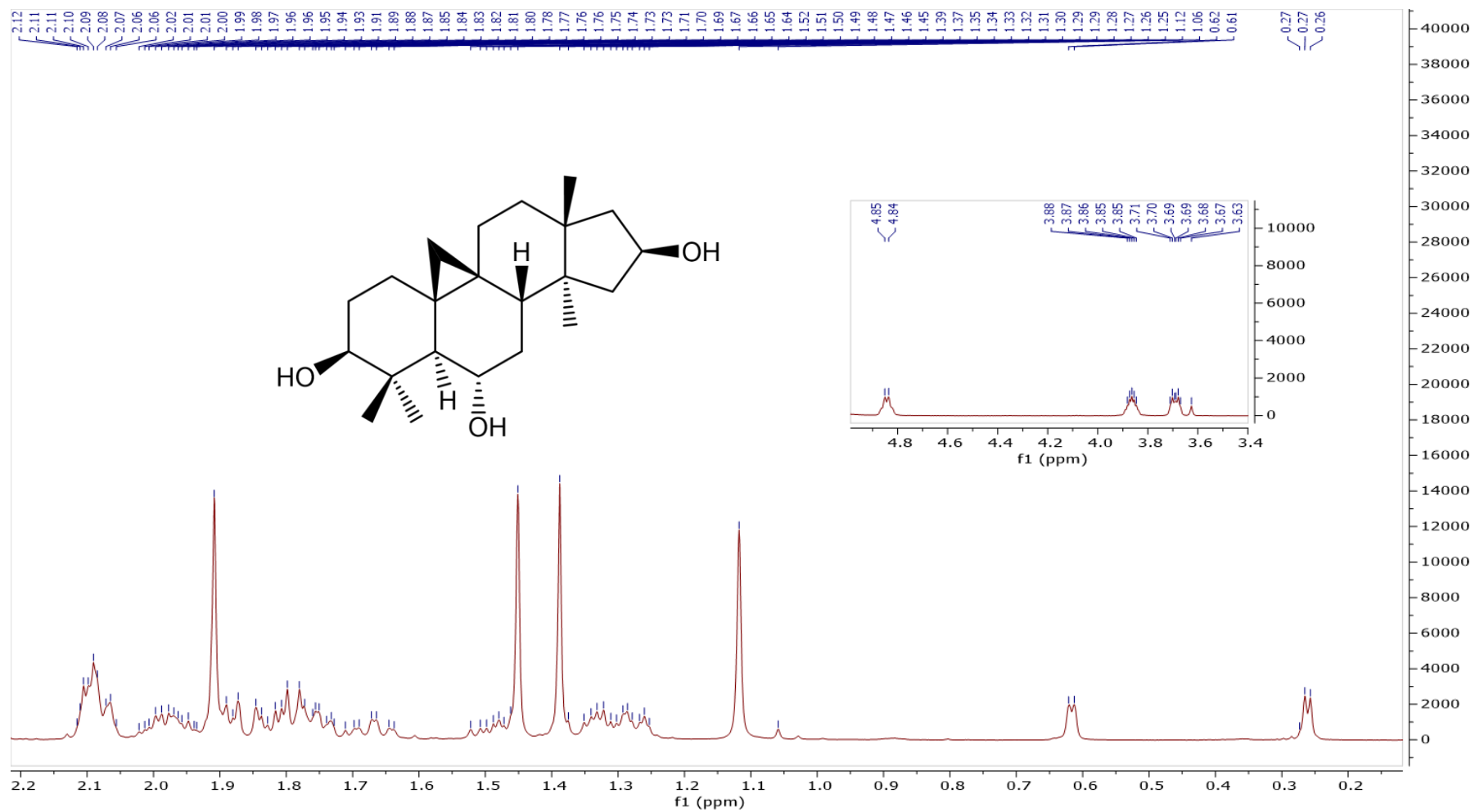
Spectrum 3.87 HSQC spectrum of Neo-SCG-06



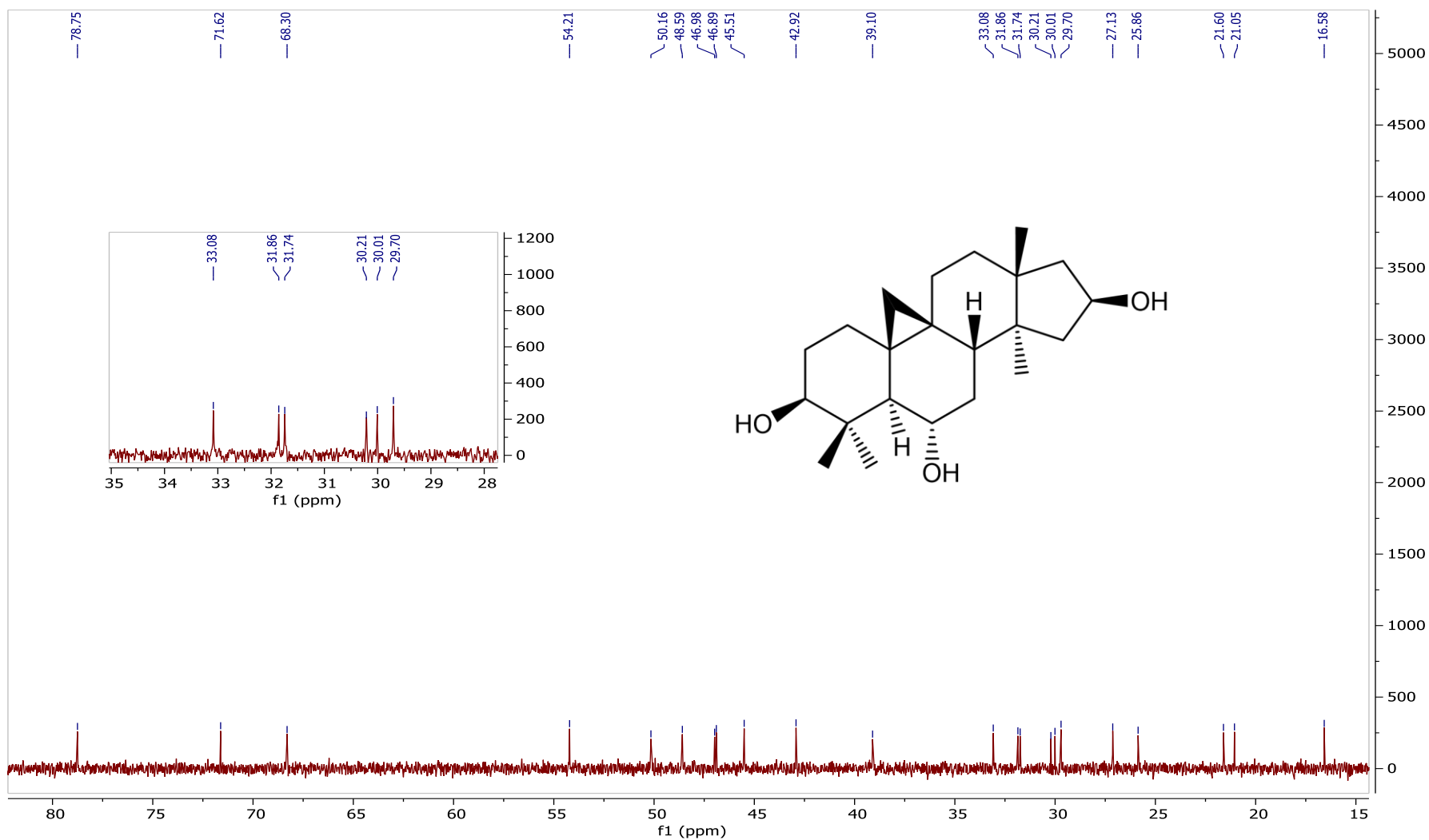
Spectrum 3.88 HMBC spectrum of Neo-SCG-06



Spectrum 3.89 COSY spectrum of Neo-SCG-06



Spectrum 3.90 ^1H -NMR spectrum of 20(27)-octanor cycloastragenol



Spectrum 3.91 ^{13}C -NMR spectrum of 20(27)-octanor cycloastragenol

3.3 Biological Activity Studies

Screening the effects of fungal metabolites by means of telomerase activation was one of the major aims of this work. Pure metabolites were tested towards activation of telomerase. The treatment dose range was set based on our previous studies.

3.3.1 Telomerase Activation Screening

Bioactivity studies were performed on HEKN cell line using TELOTAGGG PCR ELISA^{PLUS} kits as indicated in the methods section. Seven compounds selected based on their quantities and purity levels were screened for their effects on telomerase activation. Based on our preliminary telomerase activation tests (data not shown), the selected compounds were tested in the dose range of 0.1-30 nM [**E-SCG-01** and **E-SCG-02** (0.1-30 nM), **A-SCG-01**, **A2-SCG-02**, **Neo-SCG-01**, **Neo-SCG-02** and **Neo-SCG-03** (0.5-30 nM)]. The tests were performed at two different time points because of the parallel studies carried out during TUBITAK-114Z958 project. **E-SCG** series (**01** and **02**) and the remaining compounds were tested on different days. Moreover, Figure 3.17 and Figure 3.18 were given separately because the experiments were run on two different plates. As a result, some of the tested compounds compared to the control cells treated with DMSO exhibited noteworthy telomerase activation up to 12.39 fold (Figure 3.16). To be particular, in our first panel (Figure 3.16), CA and **E-SCG-01** were found to be quite potent with 11.04 and 12.39 fold activities (both at 0.1 nM), whereas **E-SCG-02** was also active at 2 nM exhibiting 7.81 fold activation. As seen in Figure 3.17, none of the compounds was notable in comparison to CA. **NEO-SCG-01** was another potent compound with 5.43 fold telomerase activation at 10 nM dose compared to 4.86 fold activity of CA (10 nM).

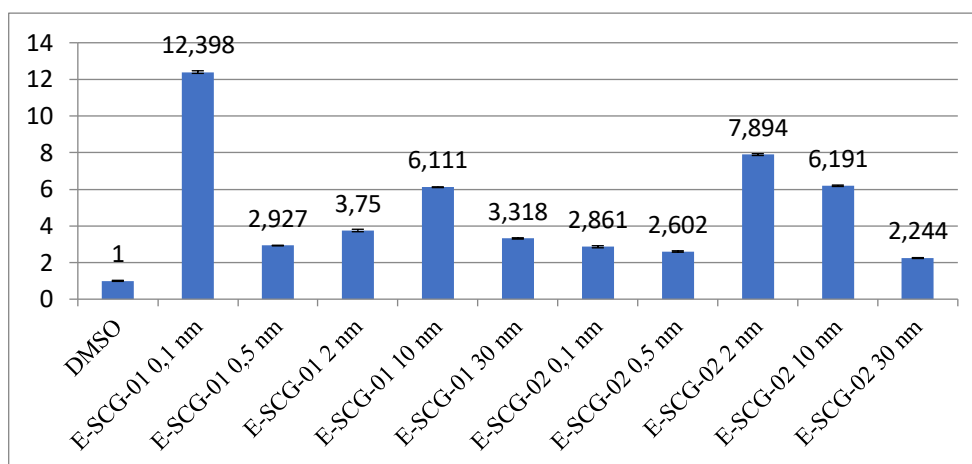


Figure 3.16 Effects of **E-SCG-01** and **E-SCG-02** molecules on telomerase enzyme activity in HEKN cells

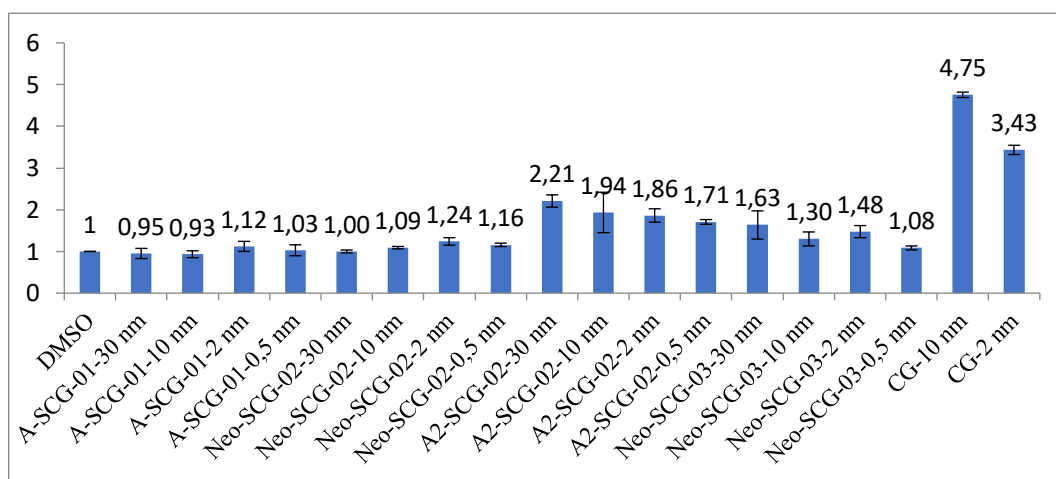


Figure 3.17 Effects of **A-SCG-01**, **Neo-SCG-02**, **A2-SCG-02**, **Neo-SCG-03** and **CA (CG)** molecules on telomerase enzyme activity in HEKN cells.

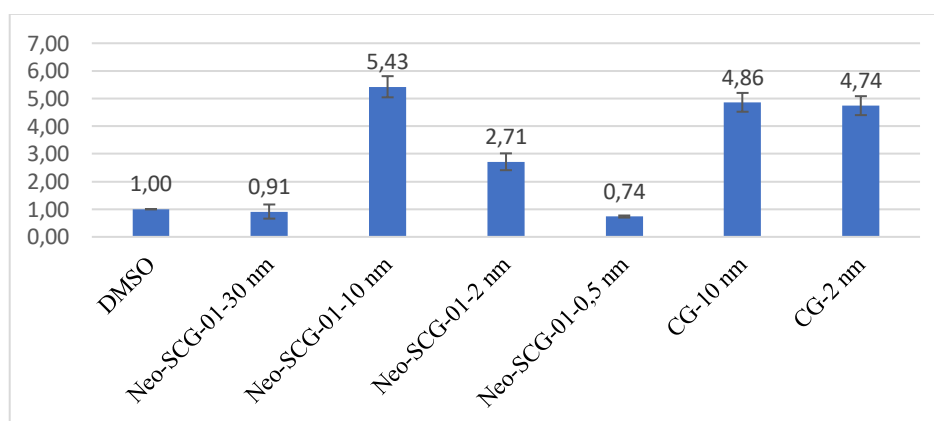
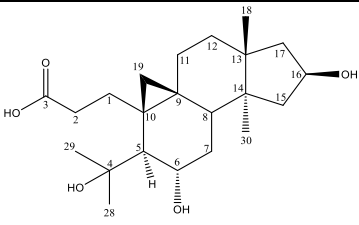
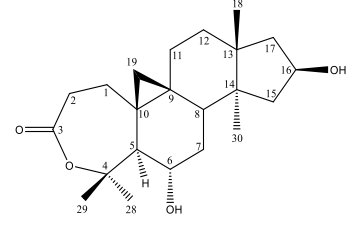
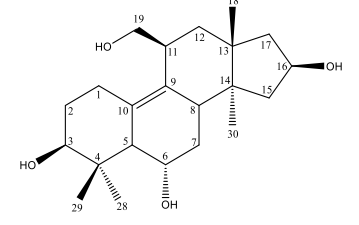
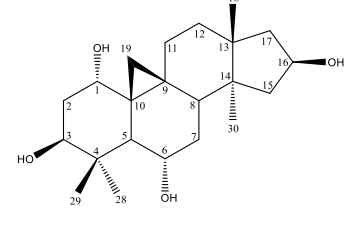
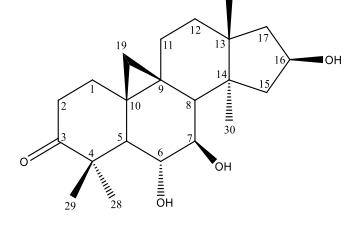
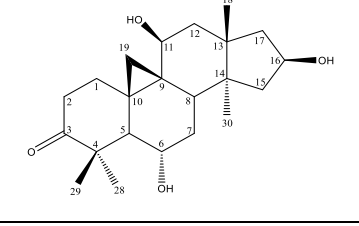
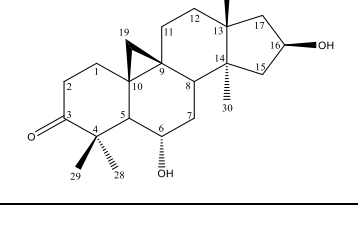


Figure 3.18 Effects of **Neo-SCG-01** and **CA (CG)** molecules on telomerase enzyme activity in HEKN cells

Table 3.15 Telomerase enzyme activation of selected compounds

Molecule structures	Molecule codes	Applied dosage(nM)	Increase against negative control (DMSO)
	E-SCG-01	0.1	12.398
		0.5	2.93
		2	3.75
		10	4.43
		30	3.32
	E-SCG-02	0.1	2.86
		0.5	2.60
		2	7.89
		10	6.19
		30	2.24
	A-SCG-01	0.5	1.03
		2	1.12
		10	0.93
		30	0.95
	A2-SCG-02	0.5	1.71
		2	1.86
		10	1.94
		30	2.21
	NEO-SCG-01	0.5	0.74
		2	2.71
		10	5.43
		30	0.91
	NEO-SCG-02	0.5	1.16
		2	1.24
		10	1.09
		30	1.00
	NEO-SCG-03	0.5	1.08
		2	1.48
		10	1.30
		30	1.63

CHAPTER 4

CONCLUSION

In this thesis, a biotransformation study on 20(27)-octanor cycloastragenol, a thermal degradation product of cycloastragenol (CA), was carried out. Endophytic fungi isolated from *Astragalus* species were utilized for our studies.

Biotransformations were started with analytical scale, including 15 endophytic fungi. The fermentation media were selected according to the previous reports and our preliminary studies. A single-step fermentation procedure was preferred, which was performed at 25 °C and 180 rpm. After the analytical scale; three fungi, viz. *Neosartorya hiratsukae*, *Alternaria eureka* and *Camarosporium laburnicola* were selected for larger scale preparative studies based on their metabolite diversities. After isolation and purification studies, 14 metabolites were isolated, and their structures were elucidated by spectral methods (1D-, 2D-NMR and HR-ESI-MS). Thirteen of the metabolites were found to be previously unreported compounds.

At preparative scale, seven metabolites were obtained from the biotransformation of 20(27)-octanor CA with *Alternaria eureka*, six of which were new compounds (Figure 4.1 and Figure 4.2). *Alternaria eureka* mainly catalyzed hydroxylation, oxidation and ring opening-methyl migration transformations. The monooxygenation reactions (hydroxylation) occurred at positions C-1, C-5 and C-11, whereas the oxidation reactions afforded C-3 and C-16 oxo products. The cleavage of 9,19-cyclopropane ring followed by migration of C-19 from C-10 to C-11 position as well as monooxygenation of C-19 to the primary alcohol (A-SCG-01) was notable. This unique reaction was first revealed by our group in the biotransformation study of CA and *C. blakesleeana* NRRL 1369, forming a new triterpene skeleton.⁸¹ The same enzymatic reaction was also observed for A-SCG-06 together with an additional modification at C-16 as oxidation.

Neosartorya hiratsukae was another fungus investigated for the biotransformation of 20(27)-octanor CA, affording hydroxylation, oxidation, ring cleavage-methyl migration metabolites as in *A. eureka*., *N. hiratsukae* catalyzed the oxidation reaction at C-3 and monooxygenations at C-1 and C-11 positions (Figure 4.3).

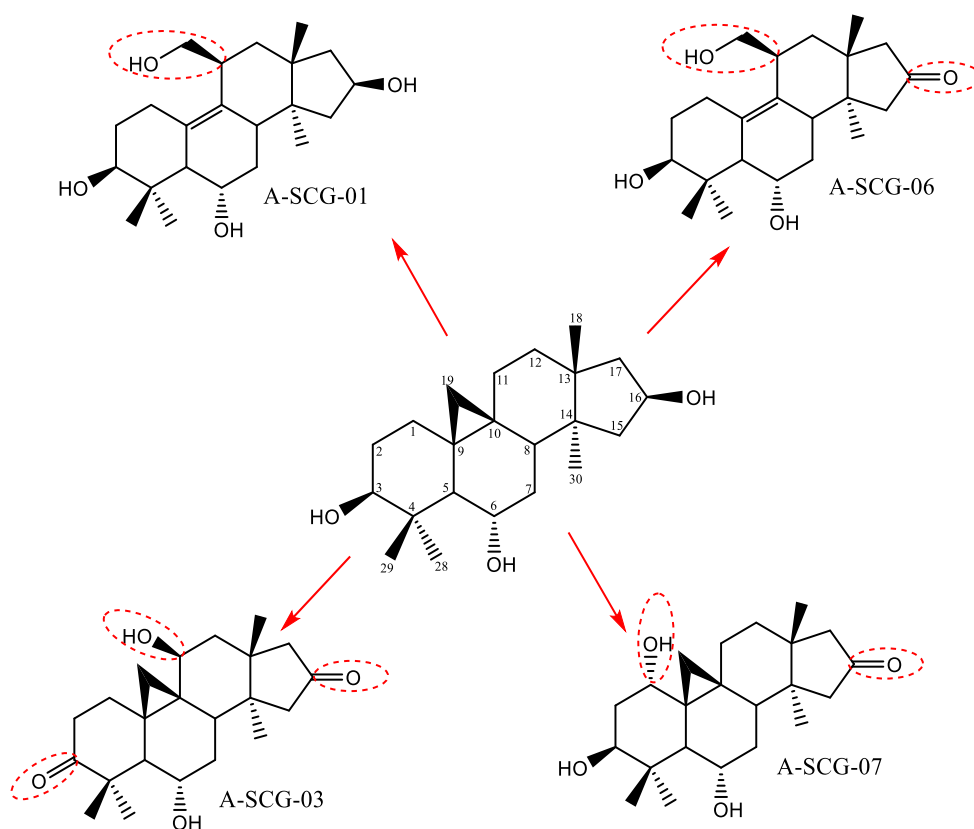


Figure 4.1 Metabolites derived from biotransformation of 20(27)-octanor cycloastragenol by *Alternaria eureka* (Biotransformation media)

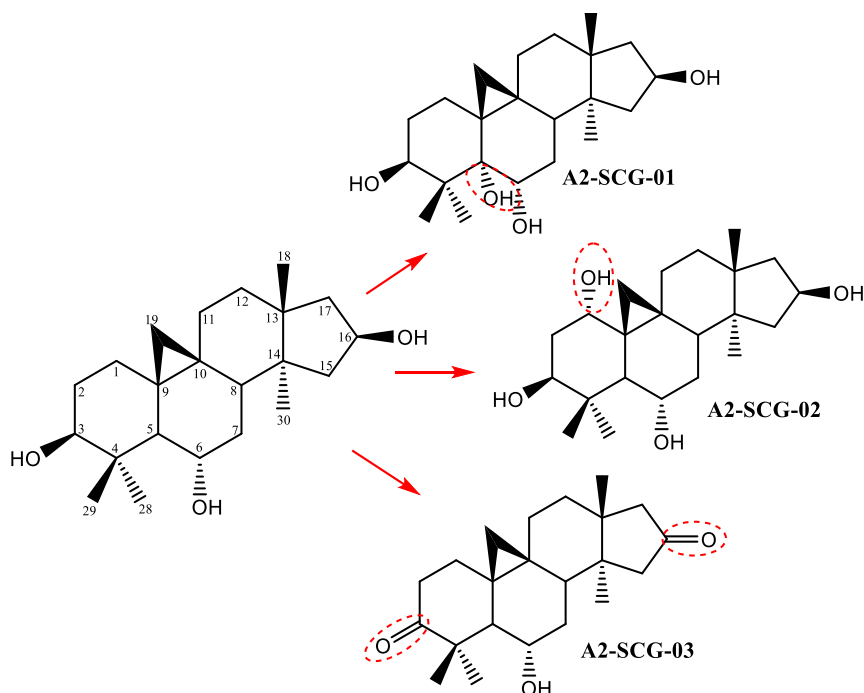


Figure 4.2 Metabolites derived from biotransformation of 20(27)-octanor cycloastragenol by *Alternaria eureka* (Potato Dextrose Broth)

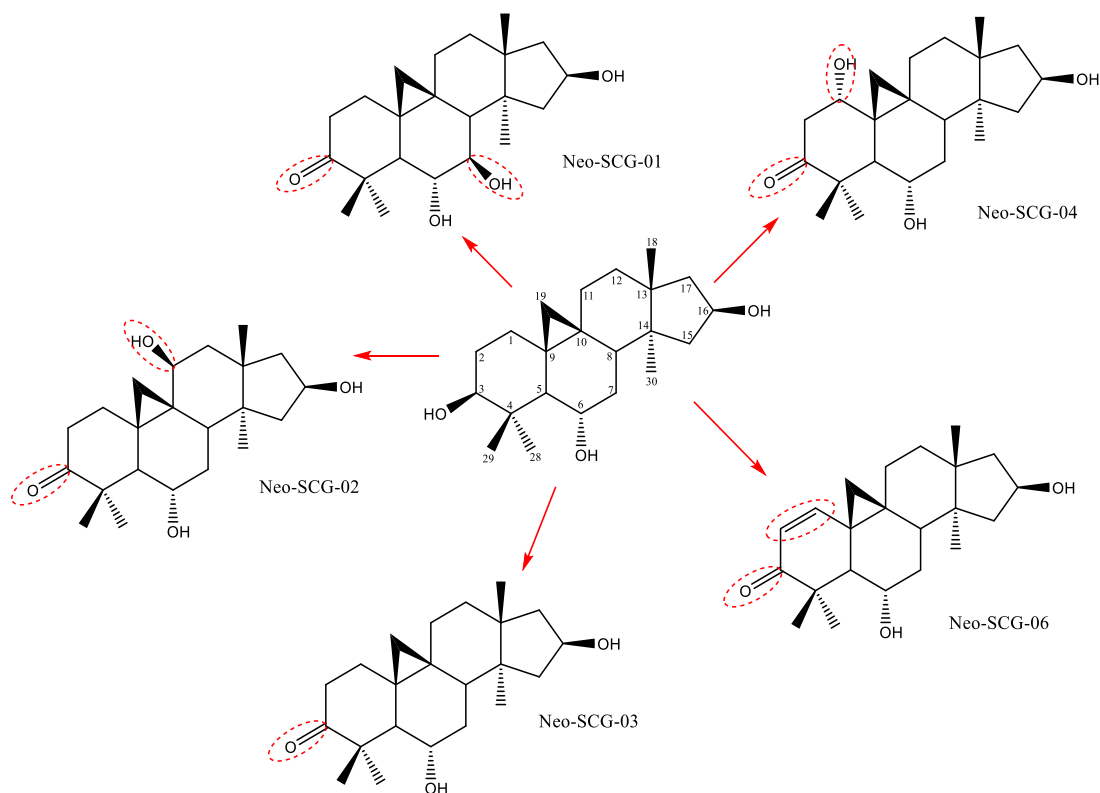


Figure 4.3 Metabolites derived from biotransformation of 20(27)-octanor cycloastragenol by *Neosartorya hiratsukae*

In the case of *Camarosporium laburnicola* studies, the Baeyer-Villiger oxidation reaction (**E-SCG-01**) was predominant to give A-ring modified metabolites. Specifically, lactone formation in **E-SCG-02** catalyzed by the Baeyer-Villiger monooxygenase (BVMO) was continued with a ring cleavage reaction via lactone hydrolase action to yield 3,4-seco cycloartane (**E-SCG-01**).

In our studies, oxidation of C-3 via dehydrogenase catalysis followed by BVMO and hydrolytic cleavage reactions provided the A-ring lacto and 3,4-seco metabolites (Figure 4.4 and Figure 4.5). This cascade reaction of *C. laburnicola* was also predominant in our previous studies implying the importance of newly discovered *C. laburnicola* as a whole cell catalysis system for especially BVMO.⁸⁰ We emphasize that the *C. laburnicola* has been discovered recently.⁸³ Until today, it has not been the subject of any work other than the taxonomic and phylogenetic studies carried out during its identification as a plant endophyte. For this reason, it is an untouched organism and the first studies for its potency as a biocatalyst are being carried out by our group.⁸⁰

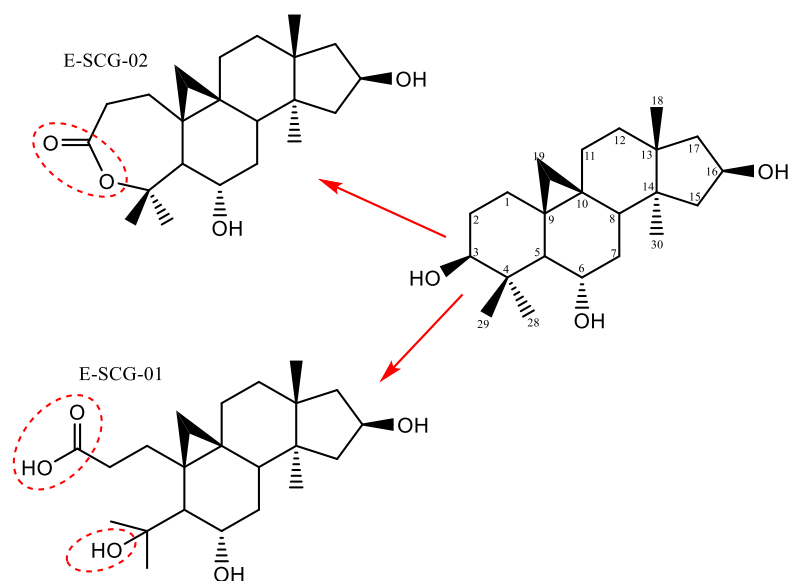


Figure 4.4 Metabolites derived from biotransformation of 20(27)-octanor cycloastragenol by *Camarosporium laburnicola*

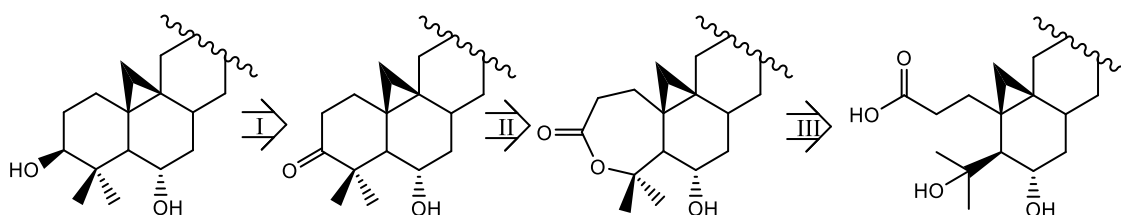


Figure 4.5 The proposed biochemical reaction chain for modifications occurring in the A ring I) Dehydrogenase enzyme, II) BVMO enzyme, III) Hydrolase enzyme

In this study, it has been realized that the hydroxylation reactions catalyzed by the P450 monooxygenase enzymes are predominant with the studied endophytes. As expected, the C-1 and C-11 positions were more susceptible to the monooxygenation due to the presence of cyclopropane ring giving allylic character to these methylene carbons. On the other hand, another active but sterically hindered C-5 position was subject to hydroxylation. A monooxygenation at C-5 position has been encountered for the first time in triterpenoid biotransformation studies. Moreover, C-7 monooxygenation reaction are being reported first time in cycloartane chemistry. In *Astragalus* cycloartane saponins, C-7 hydroxylated secondary metabolites have only been reported from *Astragalus oleifolius*; however, C-6/C-7 diol system is faced as a unique feature of **Neo-SCG-01**.

As mentioned above, oxidations of secondary alcohol groups to carbonyl are also significant for the substrate. Within the whole cell biotransformation studies, the

oxidation reactions to form aldehydes and ketones are frequently observed as undesirable continuation reactions after hydroxylations of C- H bonds. Some of the organisms oxidize the carbonyl compounds via BVMO reactions in fermentation conditions to give lactone metabolites. This leads to restriction for the usage of monooxygenases for preparative scale alcohol oxidation.⁸²

Screening the effects of fungal metabolites by means of telomerase activation was one of the major aims of this work. In parallel to biotransformation studies, the metabolites with sufficient amount and high purity were tested towards activation of telomerase versus DMSO control group on HEKN cell line.

The treatment dose range was set based on our previous studies (for **E-SCG-01** and **E-SCG-02**, 0.1-30 nM; for **A-SCG-01**, **A2-SCG-02**, **Neo-SCG-01**, **Neo-SCG-02** and **Neo-SCG-03**, 0.5-30 nM).

One of the potent molecules was the BVMO product **E-SCG-02**. This metabolite containing 7-membered lactone ring provided telomerase activation of 7.89 and 6.19 fold at 2 and 10 nM concentrations, respectively. From chemical point of view, the following issues are distinctive: i) the lactone formation eliminates a hydrogen bond donor [C-3(OH)]; ii) the polarity is relatively reduced compared to the lead compound; iii) the chair conformation in the A ring turns into a boat conformation; iv) higher electron density is present over the ring.

After lactone ring formation, a hydrolase enzyme catalyzes a further step to yield 3,4-seco metabolites (Figure 4.5). As a result, the C-3 is transformed to a carboxylic acid, whereas C-4/C-28/C-29 isopropyl cation forms that undergoes a nucleophilic attack by H₂O to afford a tertiary alcohol extending from C-4. The product of this biotransformation, namely **E-SCG-01**, found to be the most potent compound at the lowest test dose (12.4-fold activation at 0.1 nM) in our screening studies. Considering the general physicochemical properties of 3,4-seco, its more polar and ionizable nature due to the presence of a carboxylic acid is significant especially for water solubility and electrostatic interactions. However, ascribing the higher activity of **E-SCG-01** to its solubility property generates a contradiction in regard to high activity of lactone derivatives and some 3-oxo metabolites (unpublished data of 114Z958). Thus, it is supposed that the carboxylic acid formed in the A ring (C-3) and the hydroxylation at C-4 forming an electron rich region might be the key feature for molecular interactions with biological macromolecules (membrane/nuclear receptors and/or proteins) at cellular level.

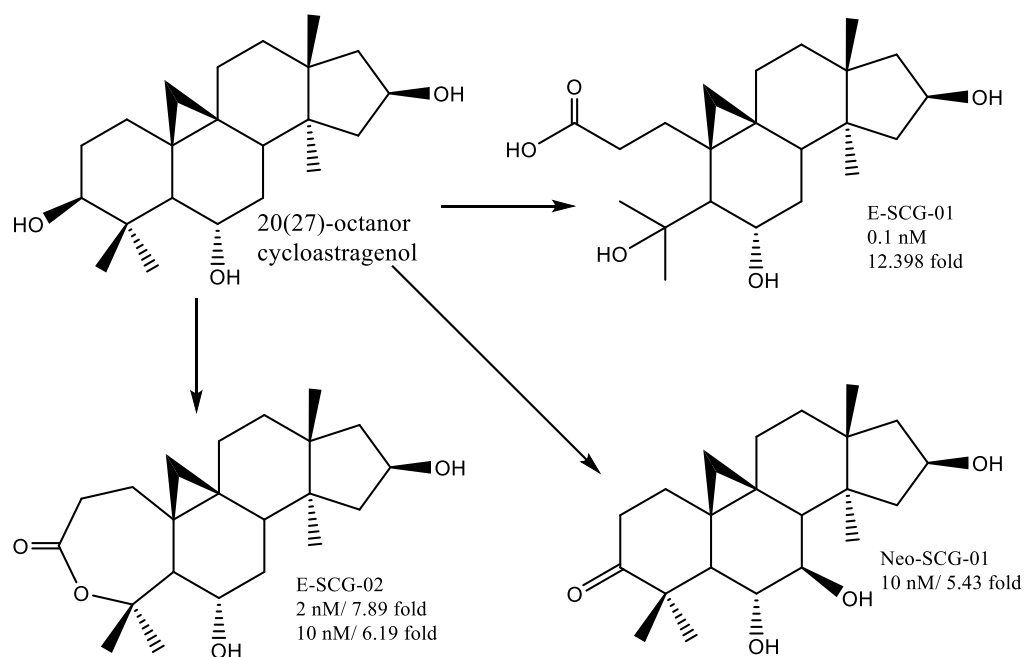


Figure 4.6 Chemical structures and active dosages of bioactive biotransformation products.

Consequently, further studies are warranted to establish structure-activity relationships confidently by preparing and testing new analogs of SCG and CA towards telomerase activation, to elucidate mechanism of action at molecular level, and to exploit catalytic capabilities of endophytic fungi from plants to obtain lead molecules with potent bioactivities and new mode of actions.

REFERENCES

1. I. Podolak, A. Galanty and D. Sobolewska, *Phytochemistry Reviews*, 2010, **9**, 425-474.
2. E. AKBEL and F. KARABAĞ, *Türk Bilimsel Derlemeler Dergisi*, 25-29.
3. J. M. Augustin, V. Kuzina, S. B. Andersen and S. Bak, *Phytochemistry*, 2011, **72**, 435-457.
4. H.-X. Sun, Y. Xie and Y.-P. Ye, *Vaccine*, 2009, **27**, 1787-1796.
5. J. Bruneton, *Journal*, 1995.
6. P. M. Dewick, *Medicinal natural products: a biosynthetic approach*, John Wiley & Sons, 2002.
7. J. Chappell, *Current opinion in plant biology*, 2002, **5**, 151-157.
8. S. Adesso, R. Russo, A. Quaroni, G. Autore and S. Marzocco, *International journal of molecular sciences*, 2018, **19**.
9. M. Ekici, H. Akan and Z. Aytac, *Turkish Journal of Botany*, 2015, **39**.
10. J. Fu, Z. Wang, L. Huang, S. Zheng, D. Wang, S. Chen, H. Zhang and S. Yang, *Phytotherapy Research*, 2014, **28**, 1275-1283.
11. J. Rios and P. Waterman, *Phytotherapy Research: An International Journal Devoted to Medical and Scientific Research on Plants and Plant Products*, 1997, **11**, 411-418.
12. I. Ionkova, A. Shkondrov, I. Krasteva and T. Ionkov, *Phytochemistry reviews*, 2014, **13**, 343-374.
13. X. Li, L. Qu, Y. Dong, L. Han, E. Liu, S. Fang, Y. Zhang and T. Wang, *Molecules*, 2014, **19**, 18850.
14. D. Gülcemal, PHD, Ege University, 2013.
15. E. Bedir, N. Pugh, I. Calis, D. S. PASCO and I. A. KHAN, *Biological and Pharmaceutical Bulletin*, 2000, **23**, 834-837.
16. R. Mamedova and M. Isaev, *Chemistry of natural compounds*, 2004, **40**, 303-357.
17. R. Abdallah, N. Ghazy, N. El-Sebakhy, A. Pirillo and L. Verotta, *Die Pharmazie*, 1993, **48**, 452-454.
18. D. Chu, J. Lin and W. Wong, *Zhonghua zhong liu za zhi [Chinese journal of oncology]*, 1994, **16**, 167-171.

19. W.-D. Zhang, H. Chen, C. Zhang, R.-H. Liu, H.-L. Li and H.-Z. Chen, *Planta medica*, 2006, **72**, 4-8.
20. Q. Du, Z. Chen, L.-f. Zhou, Q. Zhang, M. Huang and K.-s. Yin, *Canadian journal of physiology and pharmacology*, 2008, **86**, 449-457.
21. H. Liu, W. Wei, W.-y. Sun and X. Li, *Journal of ethnopharmacology*, 2009, **122**, 502-508.
22. C. B. Harley, A. C. Chin, A. Tsutomu, N. Y.-y. Ip, Y.-h. Wong and D. M. Miller-Martini, *United States Patent*, 2010, **US007846904B2**.
23. F. C. Ip, Y. P. Ng, H. An, Y. Dai, H. H. Pang, Y. Q. Hu, A. C. Chin, C. B. Harley, Y. H. Wong and N. Y. Ip, *Neurosignals*, 2014, **22**, 52-63.
24. I. H. Akgün, Msc, Ege Üniversitesi, 2006.
25. E. Polat, PhD, Ege University, 2009.
26. H. İ.K., PhD, Ege University, 2013.
27. E. H. Blackburn, *Cell*, 2001, **106**, 661-673.
28. R. C. Allsopp, H. Vaziri, C. Patterson, S. Goldstein, E. V. Younglai, A. B. Futcher, C. W. Greider and C. B. Harley, *Proceedings of the National Academy of Sciences*, 1992, **89**, 10114-10118.
29. T. De Lange, *Genes & development*, 2005, **19**, 2100-2110.
30. B. B. de Jesus, K. Schneeberger, E. Vera, A. Tejera, C. B. Harley and M. A. Blasco, *Aging cell*, 2011, **10**, 604-621.
31. M. Dagarag, T. Evazyan, N. Rao and R. B. Effros, *The Journal of Immunology*, 2004, **173**, 6303-6311.
32. B. Molgora, R. Bateman, G. Sweeney, D. Finger, T. Dimler, R. B. Effros and H. F. Valenzuela, *Cells*, 2013, **2**, 57-66.
33. W. D. Funk, C. K. Wang, D. N. Shelton, C. B. Harley, G. D. Pagon and W. K. Hoeffler, *Experimental cell research*, 2000, **258**, 270-278.
34. R. M. Cawthon, K. R. Smith, E. O'Brien, A. Sivatchenko and R. A. Kerber, *The Lancet*, 2003, **361**, 393-395.
35. N. P. Andrews, H. Fujii, J. J. Goronzy and C. M. Weyand, *Gerontology*, 2010, **56**, 390-403.
36. K. L. Rudolph, S. Chang, H.-W. Lee, M. Blasco, G. J. Gottlieb, C. Greider and R. A. DePinho, *Cell*, 1999, **96**, 701-712.
37. M. Thomas, L. Yang and P. J. Hornsby, *Nature biotechnology*, 2000, **18**, 39.

38. M. Kosmadaki and B. Gilchrest, *Micron*, 2004, **35**, 155-159.
39. M. Jaskelioff, F. L. Muller, J.-H. Paik, E. Thomas, S. Jiang, A. C. Adams, E. Sahin, M. Kost-Alimova, A. Protopopov and J. Cadinanos, *Nature*, 2011, **469**, 102.
40. W. d. S. Borges, K. B. Borges, P. S. Bonato, S. Said and M. T. Pupo, *Current Organic Chemistry*, 2009, **13**, 1137-1163.
41. L. Yan, H. Zhao, X. Zhao, X. Xu, Y. Di, C. Jiang, J. Shi, D. Shao, Q. Huang and H. Yang, *Applied microbiology and biotechnology*, 2018, 1-20.
42. H. Nisa, A. N. Kamili, I. A. Nawchoo, S. Shafi, N. Shameem and S. A. Bandh, *Microbial pathogenesis*, 2015, **82**, 50-59.
43. S. Kusari, C. Hertweck and M. Spiteller, *Chemistry & biology*, 2012, **19**, 792-798.
44. T. Suryanarayanan, N. Thirunavukkarasu, M. Govindarajulu, F. Sasse, R. Jansen and T. Murali, *Fungal biology reviews*, 2009, **23**, 9-19.
45. J. Ludwig-Müller, *Biotechnology letters*, 2015, **37**, 1325-1334.
46. R. Tan, *Nat Prod Rep*, 2006, **23**, 753771.
47. D. J. Newman, G. M. Cragg and D. G. Kingston, 2005.
48. Z. Yang, L. M. Rogers, Y. Song, W. Guo and P. Kolattukudy, *Proceedings of the National Academy of Sciences*, 2005, **102**, 4197-4202.
49. S. Kusari, S. Zühlke and M. Spiteller, *Journal of Natural Products*, 2009, **72**, 2-7.
50. S. Kusari, J. Košuth, E. Čellárová and M. Spiteller, *fungal ecology*, 2011, **4**, 219-223.
51. M. Baiping, F. Bing, H. Hongzhi and C. Yuwen, *World Science and Technology*, 2010, **12**, 150-154.
52. M. Doble, A. K. Kruthiventi and V. G. Gaikar, *Biotransformations and bioprocesses*, Marcel Dekker New York, NY, USA, 2004.
53. J. E. Leresche and H.-P. Meyer, *Organic process research & development*, 2006, **10**, 572-580.
54. K. B. Borges, W. de Souza Borges, R. Durán-Patrón, M. T. Pupo, P. S. Bonato and I. G. Collado, *Tetrahedron: Asymmetry*, 2009, **20**, 385-397.

55. M. R. Pimentel, G. Molina, A. P. Dionísio, M. R. Maróstica Junior and G. M. Pastore, *Biotechnology research international*, 2011, **2011**.
56. A. Illanes, A. Cauerhff, L. Wilson and G. R. Castro, *Bioresource technology*, 2012, **115**, 48-57.
57. M. A. Longo and M. A. Sanromán, *Food Technology and Biotechnology*, 2006, **44**, 335-353.
58. P. Fernandes, A. Cruz, B. Angelova, H. Pinheiro and J. Cabral, *Enzyme and microbial technology*, 2003, **32**, 688-705.
59. B. Suresh, T. Ritu and G. Ravishankar, in *Food biotechnology*, CRC Press, 2005, pp. 1641-1676.
60. C. C. De Carvalho, *Biotechnology advances*, 2011, **29**, 75-83.
61. J. Tao and J.-H. Xu, *Journal*, 2009, 1-19.
62. T. Hudlicky and J. W. Reed, *Chemical Society Reviews*, 2009, **38**, 3117-3132.
63. S. Sanchez and A. L. Demain, *Organic Process Research & Development*, 2010, **15**, 224-230.
64. D. M. Solano, P. Hoyos, M. Hernáiz, A. Alcántara and J. Sánchez-Montero, *Bioresource technology*, 2012, **115**, 196-207.
65. D. J. Pollard and J. M. Woodley, *TRENDS in Biotechnology*, 2007, **25**, 66-73.
66. Y. Wang and C.-C. Dai, *Annals of Microbiology*, 2011, **61**, 207-215.
67. S. L. Luo, L. Z. Dang, J. F. Li, C. G. Zou, K. Q. Zhang and G. H. Li, *Chemistry & biodiversity*, 2013, **10**, 2021-2031.
68. K. Srisilam and C. Veeresham, *Journal*, 2003.
69. R. Venisetty and V. Ciddi, *Current Pharmaceutical Biotechnology*, 2003, **4**, 153-167.
70. C. D. Murphy, *Biotechnology letters*, 2015, **37**, 19-28.
71. S. S Bhattacharya and J. S Yadav, *Current Protein and Peptide Science*, 2018, **19**, 75-86.
72. I. Parshikov, T. Heinze, J. Moody, J. Freeman, A. Williams and J. Sutherland, *Applied microbiology and biotechnology*, 2001, **56**, 474-477.
73. J. Carballeira, M. Quezada, P. Hoyos, Y. Simeó, M. Hernaiz, A. Alcantara and J. Sinisterra, *Biotechnology advances*, 2009, **27**, 686-714.

74. H. N. Bhatti and R. A. Khera, *Steroids*, 2012, **77**, 1267-1290.
75. S. Shah, H. Tan, S. Sultan, M. Faridz, M. Shah, S. Nurfazilah and M. Hussain, *International journal of molecular sciences*, 2014, **15**, 12027-12060.
76. M. Kuban, G. Öngen, I. A. Khan and E. Bedir, *Phytochemistry*, 2013, **88**, 99-104.
77. E. Bedir, C. Kula, Ö. Öner, M. Altaş, Ö. Tağ and G. Öngen, *Journal of Molecular Catalysis B: Enzymatic*, 2015, **115**, 29-34.
78. W. z. Yang, M. Ye, F. x. Huang, W. n. He and D. a. Guo, *Advanced Synthesis & Catalysis*, 2012, **354**, 527-539.
79. L. m. Feng, S. Ji, X. Qiao, Z. w. Li, X. h. Lin and M. Ye, *Advanced Synthesis & Catalysis*, 2015, **357**, 1928-1940.
80. G. Ekiz, Doctora, Ege Üniversitesi, 2016.
81. M. Kuban, G. Öngen and E. Bedir, *Organic letters*, 2010, **12**, 4252-4255.
82. W. Kroutil, H. Mang, K. Edegger and K. Faber, *Advanced Synthesis & Catalysis*, 2004, **346**, 125-142.
83. S. Tibpromma, K. D. Hyde, R. Jeewon, S. S. Maharachchikumbura, J.-K. Liu, D. J. Bhat, E. G. Jones, E. H. McKenzie, E. Camporesi and T. S. Bulgakov, *Fungal Diversity*, 2017, **83**, 1-261.